
# Analysis of *Saccharomyces cerevisiae* Mec1 and Rad9 functions in the DNA Damage Response

**Carla Manuela de Castro Abreu**

**Genome Stability Laboratory, Centre for Chromosome Biology,**
**Department of Biochemistry, School of Natural Sciences,**
**National University of Ireland Galway**

A thesis submitted to the National University of Ireland Galway for the degree of Doctor of Philosophy

Supervisor: Professor Noel F. Lowndes
Co-supervisor: Doctor Muriel Grenon

August 2012

# TABLE OF CONTENTS

# LIST OF FIGURES

# LIST OF TABLES

# ABBREVIATIONS

**4NQO:** 4-Nitroquinoline 1-Oxide
**5-FOA:** 5-Fluoroorotic Acid
**53BP1:** p53-binding protein 1
**aa:** amino acid
**AMP:** Adenosine Monophosphate
**APS:** Ammonium Persulphate
**ATM:** Ataxia Telangiectasia Mutated
**ATP:** Adenosine Triphosphate
**ATR:** Ataxia Telangiectasia and *RAD3* related
**BLM**: Bloom syndrome protein
**bp:** Base pair
**BRCA1**: breast cancer 1
**BRCT:** Breast cancer susceptibility protein
**BSA:** Bovine Serum Albumin
**CCE:** Cell crude extract
**CDC:** Cell Division Cycle
**CDK:** Cyclin-Dependent Kinase
**CHK**: Checkpoint Kinase
**CORE:** COunterselectable REporter
**CPT:** Camptothecin
**Crb2**: Cut5 repeat binding2
**CtIP**: CtBP-interacting protein
**Ctp1**: CtIP-related endonuclease
**DDC:** DNA Damage Checkpoint
**DDR:** DNA Damage Response
**dd$H_2O$:** double distilled water
**DDR:** DNA Damage Response
**DMSO:** Dimethyl Sulfoxide
**DNA:** Deoxyribonucleic Acid
**DNA-PKcs:** DNA-dependent Protein Kinase catalytic subunit
**dNTP:** Deoxynucleotide Triphosphate
**Dpb11:** DNA Polymerase B (II)
**DSB:** Double Strand Break
**dsDNA:** double stranded DNA
**DTT:** Dithiothreitol
**EDTA:** Ethylenediaminetetraacetic acid
**EGTA:** Ethylene-glycol tetraacetic acid
**ESR1:** Essential for Recombination 1
**Exo1:** Exonuclease 1
**FAT:** FRAP-ATM-TRRAP
**FATC:** FAT-C-terminal
**FHA:** Forkhead-associated domain
**FT:** Flow Through
**G1:** Gap phase 1
**G2:** Gap phase 2
**G418:** Geneticin
**gDNA:** genomic DNA
**GRC:** Gross Chromosomal Rearrangements
**HA:** Hemagglutinin
**HEAT:** Huntingtin, Elongation factor 3, A subunit of protein phosphatase 2A and TOR1
**HEPES:** 4-(2-hydroxyethyl)-1-piperazineethanesulfonic acid
**HR:** Homologous Recombination
**HU:** Hydroxyurea
**IR:** Ionising Radiation
**kb:** kilo base
**KD/KN:** kinase dead/Kinase negative
**kDa:** Kilodaltons
**KlURA3:***Kluyveromyces lactisURA3*
**LEU:** Leucine
**LSNE:** Large Scale Native Extract
**M:** Mitosis
**MCPH1**: Microcephalin
**MDC1**: Mediator of DNA damage checkpoint protein 1
**MEC:** Meiotic Entry Checkpoint
**mL:** Millilitre
**mM:** Millimolar
**MMS:** Methyl Methanesulfonate
**MN:** minimal medium
**MRC1:** Mediator of Replication Checkpoint 1
**MRX/MRN:** Mre11-Rad50-Xrs2/Nbs1
**mTOR:** mammalian Target Of Rapamycin
**NaOH:** Sodium Hydroxide
**NHEJ:** Non-Homologous End Joining
**nt:** nucleotide
**O/N:** Overnight
**ORC:** Origin Recognition Complex
**ORF:** Open Reading Frame
**PAGE:** Polyacrylamide Gel Electrophoresis
**PCNA:** Proliferating Cell Nuclear Antigen
**PCR:** Polymerase Chain Reaction
**PI3Ks:** Phosphatidylinositol-3-Kinases
**PIKK:** Phosphatidylinositol 3-Kinase like Kinase

**PP2A:** Protein phosphatase 2A
**PR65/A:** Protein phosphatase PP2A regulatory subunit A
**PRD:** PIKK Regulatory Domain
**RAD:** Radiosensitive
**Rfa**: Replication factor a
**RFC:** Replication Factor C
**Rmi1**: RecQ-mediated genome instability protein 1
**RNA:** Ribonucleic Acid
**RNR:** Ribonucleotide Reductase
**RPA:** Replication Protein A
**Rqh1**: RecQ type DNA helicase
**Sae2**: Sporulation in the absence of SPO11 protein2
**SCD:** S/TQ Cluster Domains
**Sgs1**: Slow Growth Suppressor 1
**SMG-1**: suppressor of morphogenesis in genitalia
**SML1**: Suppressor of Mec1 Lethality protein 1
**S-phase:** Synthesis phase
**SDS** Sodium Dodecyl Sulfate
**SMG-1:** Suppressor of Morphogenesis in Genitalia
**ssDNA:** single stranded DNA
**TAP:** Tandem affinity purification
**Tel1:** Telomere length regulation protein 1
**TELO2**: Telomere length regulation protein TEL2 homolog
**Tip60**: 60 kDa Tat-interactive protein
**TRAP:** Transformation/transcription domain-associated Protein
**TRP:** tryptophan
**Top3**: topoisomerase 3
**TopBP1:** Topoisomerase II binding protein 1
**URA:** uracil
**UV:** Ultraviolet
**YNB:** Yeast Nitrogen Base
**YPD:** Yeast Peptone and Dextrose media

# ACKNOWLEDGEMENTS

During the course of my Ph.D., many people have helped and supported me. Without them this thesis would not have been completed. I would like to sincerely thank all of them and show my appreciation for their understanding.

Firstly, I am thankful to the Fundação para a Ciência e a Tecnologia (FCT) for the doctoral fellowship award that supported this project and my stay in Ireland during the last four years, and the National University of Ireland, Galway for hosting me during this study.

I also wish to thank Dr. Michael P. Carty (Head of Discipline) and Dr. Heinz Peter Nasheuer (Head of School) for allowing me access to all the facilities available in the department of Biochemistry and to technical staff in Biochemistry who ensured our lab ran smoothly.

The development and execution of this project was only possible with the assistance and collaboration of a very special group of people. To begin with, I would like to thank my supervisors Prof. Noel Lowndes and Dr. Muriel Grenon for giving me this opportunity and for all their help, advice, valuable source of encouragement, support and friendship. I am very thankful for all that they have done for me.

I also owe a huge thanks and acknowledgement to all the members of the Lowndes group – I do not even know where and how to start to tell you what your company, friendship, and socializing nights out, meant to me. I will miss all of you a lot. Special thanks to Dr. Ramesh Kumar, a former PhD student, for our long collaboration and shared experiments in the study of Rad9 cell cycle phosphorylation in *S. cerevisiae*. I also want to express my gratitude to Marta Agost for our collaboration and shared experiments in the Mec1 structure-function studies in *S. cerevisiae* and also for her friendship. I am very grateful to Dr. John Eykelenboom for his guidance, practical advice and proofreading skills (particularly during the correction of this thesis). Thank you to Emma Harte, Sylvie Moureau, Mary Walsh, Dr. Silvia Maretto for their support, friendship and optimism and to other members of the laboratory that helped in any way during this project.

My deep appreciation to all the other members of the Chromosome Biology Laboratory, both former and present, especially: Dr. Karen Finn, Kevin Creavin, Sarah Eivers, Fabio Pessina, Danielle Hamilton, Martin Browne (for help in the purification of recombinant proteins), Dr. David Gaboriau (for help, support and

very good advice), Dr. Holger Stephan and Clara Sans (for her friendship and support). I am also grateful to Dr. Petra Werler, whose guidance and practical advices supported me in my first steps in the laboratory during my final project as a fourth year undergraduate student.

During this project and my stay in Galway, it was also of great importance the company of my fiancé Tiago Dantas. He knows how much I'm grateful for all that he has done for me. Even though, I take this opportunity to sincerely thank him for all his unconditional company, help and support in all moments that I needed. I would not still be here if was not because of him. I am delighted for the both of us that we managed to finish our PhD journey together.

Finally, but not less important, a special and sincere word of thanks to my parents and family for all their unconditional support, help, and understanding during this long period far away from home. I love you all very much and I am infinitively thankful for everything you have done for me. Without you I certainly would not be here today. *Aos meus pais e família, um obrigado muito especial pelo vosso apoio, ajuda e compreensão incondicionais durante este longo período longe de casa e por estarem sempre comigo em pensamento e coração. Amo-vos muito a todos e estou infinitamente grata por tudo o que têm feito por mim. Sem voçês nada disto tinha acontecido.*

Thank you to all of you and I apologise to those that I have forgotten to mention.

My stay in Galway, literally, has 'marked' my life forever. I will never forget all the people I have met and all the experiences I lived. To show my gratitude to all, I dedicate the following poem to all the people that made my life easier by helping me in any way during these last four years.

*"Thank you for what you did; You didn't have to do it.*
*I'm glad someone like you*
*Could help me to get through it.*
*I'll always think of you, with a glad and grateful heart;*
*You are very special;*
*I knew it from the start!*
*I want to tell you "Thank you",*
*But it doesn't seem enough.*
*Words don't seem sufficient*
*"Blah, blah" and all that stuff.*
*Please know I have deep feelings about your generous act.*
*I really appreciate you;*
*You're special, and that's a fact!"* *By Joanna Fuchs*

# THESIS STRUCTURE AND DECLARATION

**Thesis Structure**

A short summary is followed by a comprehensive introduction to the field (Chapter 1). There are two distinct results Chapters each written with short introductions specific to each topic, results, discussion, methodology and references. Chapter 2 is focused upon a structure-function analysis of Mec1, a kinase that is the central regulator of the DNA damage response. Chapter 3 is focused on the function of cell cycle phosphorylation of the Rad9 checkpoint mediator protein. This work, together with work from Dr. Ramesh Kumar, has undergone one round of review at the journal *Genes & Development* and will be resubmitted to this journal as soon as possible subsequent to submission of this thesis. The final Chapter 4 describes the main conclusions of this thesis work and directions that could be taken in future projects.

**Declaration of contributions**

I declare that I have not obtained a previous qualification from NUI Galway or elsewhere based upon any of the work contained in this thesis. I both conducted the experiments presented and wrote the thesis under the supervision of Professor Noel Lowndes and Dr. Muriel Grenon. There are a few exceptions, clearly indicated in the relevant Figure legends, included for clarity when appropriate. Specifically:

- Chapter 2: The experiments in Figure 2.5 were performed in collaboration with Marta Llorens Agost.
- Chapter 3: The experiments in Figure 3.1 was performed by Noel Lowndes, Karen Finn and Ramesh Kumar.
- Chapter 3: The experiments in Figures 3.2A & B, 3.4, 3.5A & B, 3.6B & C, S3.3 and S3.4A-D were performed in collaboration with Ramesh Kumar.
- Chapter 3: The experiments in Figure 3.3E were performed in collaboration with Ramesh Kumar and Kevin Creavin.
- Chapter 3: The experiments in Figure 3.7 were performed in collaboration with Sarah Eivers.

The above contributions have also been acknowledged on the title page of each Chapter.

## SUMMARY

The maintenance of genome integrity is critical for cell proliferation and survival of all organisms. Central to the DNA Damage Response are signal-transduction pathways, termed DNA damage checkpoints, conserved from yeast to human cells. Failure to respond properly to DNA damage, through the activation of these pathways, results in increased mutagenesis and genetic instability. In addition, in higher organisms, defects in the DNA damage checkpoints are frequently associated with cancer, ageing and several other pathologies. Clearly, to understand oncogenesis, and in particular its early stages, it will be important to fully understand the DNA damage response.

The phosphatidylinositol-3-kinase-like kinase Mec1, the ATR orthologue, is the master of the DNA damage checkpoints in *Saccharomyces cerevisiae* and is essetntial for cell viability. In chapter 2 of this thesis, we investigate the structure-function relationship of Mec1. In particular, we examine the role of tandem helical motifs, called HEAT repeats, that comprise the non-kinase portion of Mec1 and other PIKKs. In this study, we found that *mec1* mutants, expressing a Mec1 protein version where single/multiple HEATs were removed or replaced by equivalent HEATs from related PIKKs, behaved similarly to the null strain. This suggests that none of these mutants were proficient for Mec1's essential function. Our data indicates that the essential function of Mec1 is dependent on the integrity of its HEAT repeats.

Rad9, the prototypal checkpoint mediator, also plays a pivotal role in the DNA damage response in *S. cerevisiae*. In chapter 4 of this thesis we investigate the role of the cell cycle-dependent phosphorylation of Rad9 and we show that this process is dependent on B-type cyclin (Clbs) forms of Cdc28 (the single cyclin-dependent kinase in budding yeast). Based on this study, we propose that Cdc28 fine tunes Rad9 DNA damage response functions and we particularly focus on Rad9 regulatory functions in Chk1 activation. We found that the integrity of nine putative Cdc28 phosphorylation sites located in the N-terminal region of Rad9, especially T143, is required for Chk1 activation and Rad9-Chk1 interaction in the G2/M phase of the cell cycle. Our data suggests a novel PIKK- and Rad9-dependent model for Chk1 activation in response to DNA damage.

"In the middle of every difficulty

lies opportunity"

*by Albert Einstein*

# CHAPTER 1

## GENERAL INTRODUCTION

## Mec1/ATR – An essential PIKK in the DNA damage response

Carla Manuela Abreu, Muriel Grenon & Noel Francis Lowndes
Centre for Chromosome Biology, School of Natural Science, National University of Ireland Galway, University Road, Galway, Ireland

**Keywords**
ATR, Mec1, PIKK, DNA Damage Response, Checkpoint, HEAT

## 1.1. OVERVIEW

Maintenance of genome integrity is critical for cell proliferation and survival of all organisms. DNA (deoxyribonucleic acid) damage originating from exogenous sources (e.g. ionizing or ultraviolet radiation) is a constant threat to genome stability. Similarly, genome integrity can be challenged during normal cellular processes such as DNA replication, mitosis, biological metabolic reactions that generate free radicals or when chromosome ends (telomeres) become exposed (Lindahl, 1993). Unrepaired lesions can lead directly to mutations or, in the case of DNA strand-breaks or cross-links, they can interfere with processes such as DNA replication, gene transcription and chromosome segregation. A particularly cytotoxic form of DNA damage is the DNA double strand break (DSB) that can promote gross chromosomal rearrangements (GCRs) and loss of genetic information if not accurately repaired (Hanahan and Weinberg, 2011). Thus, eukaryotic cells have evolved safeguarding mechanisms to monitor genome integrity and initiate a coordinated cellular response, globally termed the DNA damage response (DDR). Central to the DDR are sophisticated surveilance signalling pathways known as DNA damage checkpoints that monitor the successful completion of particular cell cycle events and control a coordinated cellular response when DNA damage is detected. Activation of DNA damage checkpoints results in cell cycle arrest or slowdown, initiation of DNA repair, activation of transcriptional programmes or, if the damage is too severe, activation of senescence or apoptosis pathways (Harper and Elledge, 2007). Once repair is complete, the DNA damage checkpoint response is downregulated and cells re-enter the cell cycle in a process known as recovery. Alternatively, if the lesion is irreparable, cells may undergo adaptation and eventually re-enter the cell cycle in the continued presence of DNA damage (Clemenson and Marsolier-Kergoat, 2009).

## 1.2. DNA DAMAGE RESPONSE AND TUMORIGENESIS

Defects in the DNA damage checkpoints can allow cells to replicate and segregate damaged DNA molecules, resulting in increased genomic instability and mutagenesis. In higher organisms, these types of defect are frequently associated with cancer, premature ageing and several other pathologies (Bartkova et al., 2005; d'Adda di Fagagna et al., 2003; Gorgoulis et al., 2005; Kerzendorfer and O'Driscoll, 2009). For instance, studies of human cancers have shown that the deregulation of

the DNA damage response coupled with overactive cell division is an important contributing factor for tumorigenesis, even in the early precancerous stages (Bartkova et al., 2005; Gorgoulis et al., 2005). These studies suggest that both precancerous lesions and cancers are associated particularly with oncogene-induced DNA replication stress that leads to the accumulation of DSBs (Bartkova et al., 2005; Gorgoulis et al., 2005). In precancerous lesions, tumour suppressors, including DDR genes, are activated to promote the repair of the DSBs or, in case the damage is too severe, induce apoptosis or senescence, raising a barrier to tumour progression. On the other hand, the continuous formation and repair of DSBs may contribute to accumulation of genetic mutations and genomic instability, features that characterise most human cancers. In this environment, the selective pressure for inactivation of tumour suppressors and impaired DDR allows cancer to develop (Halazonetis et al., 2008). A schematic of the DNA damage model for oncogene-triggered progression and development of cancer is presented in the Figure 1.1. It is worth mentioning, that although this oncogene-induced DNA damage model for cancer development can help to understand many features of cancer, such as genomic instability and the key role of tumour suppressors in DNA damage checkpoint response to DSBs, some issues remain unclear. For example, it is not fully understood what the mechanisms and conditions are by which oncogenes induce DNA replication stress (Halazonetis et al., 2008). Most oncogenes deregulate entry into the cell cycle by enhancing the activities of the cyclin-dependent kinases (CDKs) that regulate the different phases of the cell cycle (Hartwell and Kastan, 1994). In yeast, deregulation of CDK activity compromises DNA replication and leads to formation of DNA DSBs and genomic instability (Lengronne and Schwob, 2002). By analogy, oncogenes could induce a state of DNA replication stress in human precancerous lesions leading to the formation of DNA DSBs (Halazonetis et al., 2008). In addition, there are other factors that can lead to genomic instability, like telomere erosion (Hansel et al., 2006; Maser and DePinho, 2002), and it is not clear how these can contribute to cancer. Consequently, the mechanisms underlying the DNA damage checkpoints are of considerable interest in understanding the molecular basis of cancer development. In this chapter we focus on the apical kinases that recognise damage and activate the DNA damage checkpoints and describe the current models for the activation of the DNA damage checkpoints in response to DSBs. Particularly, we will focus on the molecular mechanisms underlying the activation and downstream functions of the

Mec1 (meiotic entry checkpoint 1) kinase in *Saccharomyces cerevisiae*, most of which are highly conserved with its *Schizosaccharomyces pombe* and human homologues Rad3 (Radiosensitive protein 3) and ATR (Ataxia Telangiectasia and RAD3 related) respectively.

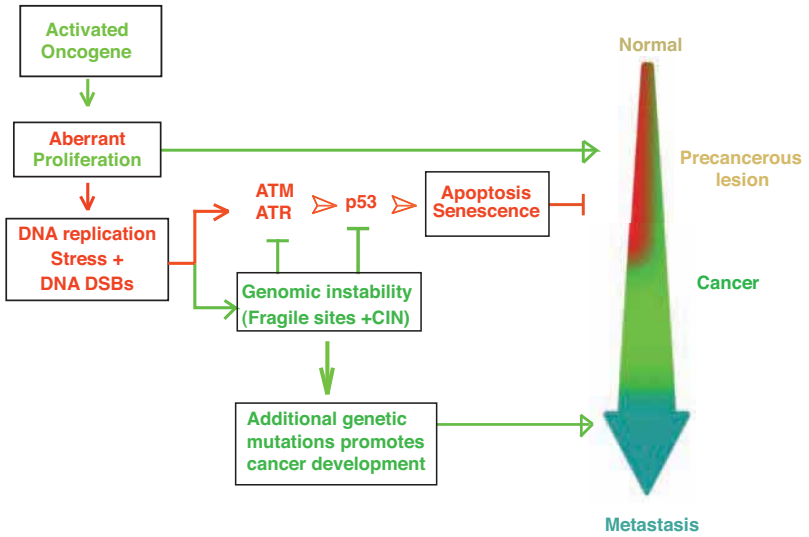


**Figure 1.1: Oncogene-triggered DNA damage model for the progression and development of cancer.** Oncogene-induced DNA replication stress leads to genomic instability and inhibition of tumour suppressors, features present from the beginning of cancer development, before the transition from precancerous lesion to cancer; Red – tumour suppressors (e.g. DDR genes) offer a barrier to tumor progression in precancerous lesion; Green - selective pressure for inactivation of tumour suppressors and impaired DDR allows cancer to develop; Blue – latest stages of cancer; CIN - chromosomal instability; Image adapted from Halazonetis et al., 2008.

### 1.3. ARCHITECTURE OF THE DNA DAMAGE CHECKPOINTS

In *S. cerevisiae*, the DNA damage checkpoints operate at three distinct stages of the cell cycle. The G1 (Gap phase 1) checkpoint arrests cells at the G1/S (Synthesis) transition prior to START (Fitz Gerald et al., 2002; Siede et al., 1994; Siede et al., 1993), before cells irreversibly commit to the next cell cycle. This transient arrest delays bud emergence, spindle pole body duplication, and S-phase entry, allowing time for DNA lesions to be repaired before the onset of DNA replication (Fitz Gerald et al., 2002). However, certain DNA aberrations, such as alkylated DNA, do not activate the G1 checkpoint and instead cells pass through START and elicit a checkpoint response during S-phase. This is because certain primary lesions need to be converted to secondary lesions, which occurs during DNA replication, before they can be recognised by the checkpoint machinery (reviewed in Longhese et al., 2003).

The intra-S phase checkpoint slows the rate of DNA replication in response to DNA damage (Paulovich and Hartwell, 1995), coordinates fork repair mechanisms and cell cycle progression, to ensure the fidelity and completion of DNA replication before cells enter mitosis (Branzei and Foiani, 2008). Finally, the G2/M (Gap phase 2/Mitosis) checkpoint arrests cells at the metaphase to anaphase transition (Weinert and Hartwell, 1988), preventing cells from progressing through mitosis in the presence of DNA damage.

The DNA damage checkpoints, like other signal transduction pathways, involves proteins that can be broadly classified as sensors, signal transducers, mediators, or effectors (Harper and Elledge, 2007). The 'central dogma' for the checkpoints states that the activation of the DNA damage checkpoints relies on the detection of the DNA damage by the sensors and this information is communicated through signal transducers to effectors *via* adaptor or mediator proteins, resulting in activation of effectors and the cellular responses to DNA damage. Accordingly with this concept, the checkpoints are simplified as unidirectional cascades; however this nomenclature exists merely to facilitate and simplify the comprehension of the DDR. Increasing studies have shown several proteins operating at several stages of the DDR pathway. For example, checkpoint proteins components of replication complexes are both sensors and transducers and might even be effectors (Putnam et al., 2009). Similarly, DNA repair proteins can act as both sensors and effectors (Putnam et al., 2009). Further complexity exists because checkpoint responses involve regulatory networks that combine both feedback loops and threshold responses (Putnam et al., 2009). Nonetheless, the different DNA damage and cell cycle checkpoint pathways share many components and their basic organization has been conserved during evolution as indicated by the similarity of most of the checkpoint proteins between yeast and human cells (Table 1.1; Lisby and Rothstein, 2009).

**Table 1.1: DNA damage checkpoint proteins in eukaryotes.** DNA damage checkpoint proteins and protein complexes involved in the early steps of DNA damage checkpoint activation in *S. cerevisiae*, and their structural or functional homologues in *S. pombe* and *Homo sapiens*.

| *S. cerevisiae* | *S. pombe*<br>*H. sapiens* | Step | Proposed function(s) |
|---|---|---|---|
| Mre11-Rad50-Xrs2 (MRX complex) | Rad32-Rad50-Nbs1<br>MRE11-RAD50-NBS1 (MRN complex) | Sensor | Sensing and processing DSBs. Involved in DSBs repair (NHEJ and HR), and telomere maintenance. |
| Tel1 (Telomere length regulation protein 1) | Tel1<br>ATM (Ataxia Telangiectasia Mutated) | Sensor | PIKK involved in signalling DSBs, has also some overlapping roles with Mec1 in DDR, and is involved in telomere maintenance. |
| Mec1 | Rad3<br>ATR | Sensor | Central PIKK in DDR, proposed to be involved in damage sensing and in signal transduction. |
| Ddc2 (DNA damage checkpoint protein 2) | Rad26<br>ATRIP (ATR-interacting protein) | Sensor/ Transducer | Mec1 regulatory subunit; Mediates Mec1 recruitment to sites of damage. |
| RPA (Replication protein A) | RPA | Initiation | Single-stranded DNA-binding heterotrimer protein complex formed by Rfa1 (Replication factor a 1), Rfa2 and Rfa3. Interacts physically with the Mec1-Ddc2 complex at the C-terminus of Mec1. |
| Rad24-Rfc2-5 (RFC (replication factor C)-like complex) | Rad17/Rfc2-5<br>RAD17/RFC2-5 | Sensor | Loading of 9-1-1 complex onto DNA. Role in the DNA damage signalling. |
| Ddc1-Rad17-Mec3 (PCNA (Proliferating cell nuclear antigen)-like or 9-1-1 complex) | Rad9-Rad1-Hus1<br>RAD9-RAD1-HUS1 | Sensor | Signal transduction and possibly involved in sensing and recruitment of other proteins onto DNA. Ddc1 directly activates Mec1 in *S. cerevisiae*. |
| Dpb11 (DNA Polymerase B (II) | Cut5/Rad4<br>TopBP1 (Topoisomerase II binding protein 1) | Sensor | Replication initiation protein; recruited by the 9-1-1 complex to sites of damage, where it activates Mec1/ATR; associates with DNA polymerase ε in the replisome. |
| Sae2 (Sporulation in the absence of SPO11 protein 2) | Ctp1 (CtIP-related endonuclease)<br>CtIP (CtBP-interacting protein) | DSB processing | Endonuclease that functions with MRX complex in the first step of DNA DSB resection. |
| Exo1 (Exonuclease 1) | Exo1<br>EXO1 | DSB processing | 5'-3' exonuclease involved in recombination and DNA repair. |
| Sgs1 (Slow Growth Suppressor 1) | Rqh1 (RecQ type DNA helicase)<br>BLM (Bloom syndrome protein) | DSB processing | RecQ-like helicase that functions with Dna2 to process DSBs. |
| Dna2 | Dna2<br>DNA2 | DSB processing | 5'-flap endonuclease/helicase that functions with Sgs1 to resect DSBs. |
| Rad9 | Crb2 (Cut5 repeat binding2)<br>53BP1 (p53-binding protein 1); MDC1 (Mediator of DNA damage checkpoint protein 1);<br>BRCA1 (breast cancer 1);<br>MCPH1 (Microcephalin) | Mediator | Involved in signal transduction as an adaptor and involved also in DSB repair; Facilitates Rad53 or Chk1 activation. |

| | | | |
|---|---|---|---|
| Mrc1 (Mediator of replication checkpoint 1) | Mrc1<br>Claspin | Mediator | Replication fork-associated scaffold; Involved in signal transduction as an adaptor for Rad53 activation in S-phase. |
| Rad53 | Cds1<br>CHK2 (Checkpoint Kinase 2) | Effector | Involved in signal transduction as effector kinase in the DNA damage and replication checkpoints. |
| Chk1 | Chk1<br>CHK1 | Effector | Involved in signal transduction as an effector kinase. |

### 1.3.1. PIK-like Kinases: Key early players

The master regulators of the DNA damage response are serine/threonine-kinases Tel1 (Telomere length regulation protein 1) and Mec1 (Mitosis Entry Checkpoint gene 1, also known as ESR1 (Essential for recombination 1) in *Saccharomyces cerevisiae*, Tel1 and Rad3 (RADiation sensitive 3) in *Saccharomyces pombe*, and ATM (Ataxia telangiectasia mutated) and ATR (Ataxia telangiectasia and Rad3-related) in mammalian cells (Lovejoy and Cortez, 2009; Zou and Elledge, 2003). In mammalian cells DNA-PKcs (DNA-dependent protein kinase catalytic subunit) also has DDR functions, although no homologue has been identified in *S. cerevisieae* and *S. pombe* (Critchlow and Jackson, 1998). These proteins function as both damage sensors and signal transducers and are members of the family of kinases known as phosphatidylinositol-3-kinase-like kinases (PIKKs). Mec1 is often considered to be the principal PIKK involved in detecting DNA damage in *S. cerevisiae* as *mec1* mutants are extremely sensitive to DNA damage (Harrison and Haber, 2006). However, the PIKK Tel1 has a more apparent function following the generation of several DSBs (Mantiero et al., 2007). In fact, Mec1 and Tel1 have key roles in DSB signalling very similar to their vertebrate homologues ATR and ATM, respectively. While ATM/Tel1 is required for checkpoint activation primarily in response to DSBs (Suzuki et al., 1999), ATR/Mec1 controls the response to a much broader spectrum of DNA damage including breaks, cross-links and base adducts and also has a clear role in the response to replication stress (Cimprich and Cortez, 2008). Both Mec1/ATR and Tel1/ATM are recruited to lesions early in the DDR, however the DNA damage signals that they recognise differ. ATM/Tel1 is recruited to DNA ends at sites of DSBs induced by IR (ionising radiation) or radiomimetic drugs while ATR/Mec1 is recruited to replication protein A-coated single stranded DNA (RPA-ssDNA), a common DNA structure found in normally replicating cells which

accumulates at stalled DNA replication forks and processed DNA lesions (Cortez et al., 2001; Falck et al., 2005; Smith et al., 1999; Suzuki et al., 1999). The processing of DNA lesions to a common DNA damage signal like RPA-ssDNA may explain the ability of the ATR signalling pathway to respond to such a diverse set of stimuli. In addition, unlike Tel1/ATM that is not required for cell survival, Mec1/ATR is essential for viability (Brown and Baltimore, 2000; Cortez et al., 2001; Desany et al., 1998; Zhao et al., 1998).

### 1.3.2. PIKK-dependent signaling to effector kinases

The DNA damage-dependent activation of the apical PIKK proteins leads to the phosphorylation of numerous substrates preferentially at serine or threonine residues that are followed by glutamine (SQ/TQ motifs) (Lovejoy and Cortez, 2009). Targets include the downstream checkpoint effector kinases (CHK). These serine/threonine kinases are Chk1 (Checkpoint kinase-1) and Rad53 (RADiation sensitive 53) in budding yeast, Chk1 and Cds1 in fission yeast, and the human orthologs CHK1 and CHK2 (Checkpoint kinase-2), respectively (Stracker et al., 2009). In *S. cerevisiae*, Mec1 activates both Rad53 and Chk1, while in mammalian cells ATM primarily activates CHK2 and ATR activates CHK1 (Stracker et al., 2009). The PIKK-dependent activation of the effector kinases is facilitated by mediator proteins that function as adaptors/catalysts that help localise these proteins to the vicinity of the PIKKs (Harper and Elledge, 2007). In budding yeast, Rad9 (RADiation sensitive 9) is the prototypal checkpoint mediator (Toh and Lowndes, 2003) and Crb2 (Cut5 repeat binding 2) is its homolog in *S. pombe*. In human cells an emerging group of proteins collectively execute the role of yeast Rad9, including BRCA1 (breast cancer 1), 53BP1 (p53-binding protein 1) and MDC1 (Mediator of DNA damage checkpoint protein 1; Harper and Elledge, 2007; Mohammad and Yaffe, 2009). The local recruitment of the CHK proteins and their subsequent activation allows amplification of the DNA damage signal from DNA lesions and stalled replication forks. The overall result is the activation of downstream targets to modulate the transcription level of repair genes and regulate cell cycle transitions by influencing the stability and/or localization of proteins involved in cell cycle progression or checkpoint maintenance (Branzei and Foiani, 2008; Stracker et al., 2009).

### 1.3.3. PIKKs and human disorders

Patients carrying inactivating mutations in ATM suffer from ataxia telangiectasia (A-T), a radiosensitivity and genome instability disorder with an estimated worldwide incidence between 1 in 40,000 and 1 in 100,000 people (Renwick et al., 2006; Shiloh and Kastan, 2001; Swift et al., 1986). This disorder is characterized by progressive cerebellar degeneration and predisposition to cancer (Bradbury and Jackson, 2003; Goodarzi et al., 2003; Renwick et al., 2006; Savitsky et al., 1995). Cells derived from A-T patients and from ATM-knockout mice display hypersensitivity to IR, chromosomal instability and defects in the G1/S, G2/M and intra S-phase checkpoints following DNA damage. These A-T cells however do not show sensitivity to UV (ultraviolet) light or to replication inhibitors and appear to grow with no obvious impairments in unperturbed conditions (Barlow et al., 1996; Kastan et al., 1992; Shiloh, 2006; Xu and Baltimore, 1996). In contrast, the early embryonic death of ATR knockout mice indicates that ATR is essential for cell growth and differentiation from an early stage of development (Brown and Baltimore, 2000; de Klein et al., 2000). In addition, deletion of ATR in adult mice leads to premature appearance of age-related phenotypes and stem cell loss (Ruzankina et al., 2007). Although complete inactivation of ATR is lethal, in humans a hypomorphic mutation in ATR is associated with the rare autosomal recessive disorder termed Seckel syndrome, which is characterised by growth retardation and microcephaly (O'Driscoll et al., 2003). This mutation affects ATR splicing which results in almost undetectable levels of the ATR protein, yet the remaining protein is sufficient for viability (O'Driscoll et al., 2003). Disruptions in the ATR pathway also result in genome instability and ATR is activated by most cancer chemotherapies. Furthermore, the ATR pathway is thought to be a promising target for cancer drug development (Collins and Kupfer, 2005; Kaelin, 2005).

### 1.3.4. Current model of checkpoint activation after DSB

The study of the DNA damage checkpoints in both higher cells and yeast model systems has led to the following model for checkpoint activation in response to a DNA double-strand break (Figure 1.2). It is remarkable that all steps of the checkpoint activation are highly conserved from yeast to human (reviewed in Lisby and Rothstein, 2009).

Following induction of a DSB (Figure 1.2A), chromatin structure is believed to be immediately remodelled at the site of DNA damage exposing, in an ill-understood manner, particular histone post-translational modifications (Figure 1.2B; (Huertas et al., 2009). For example, methylated lysine 79 of budding yeast histone H3 (H3K79me, constitutively methylated by the conserved histone methyltrasferase Dot1) or methylated lysine 20 of fission yeast histone H4 (H4K20), usually buried within compacted nucleosomes are exposed after DNA damage (Giannattasio et al., 2005; Sanders et al., 2004; van Leeuwen et al., 2002). These epigenetic marks provide docking sites for checkpoint proteins at the site of damage. It is possible that immediate remodelers of chromatin might also play other roles in checkpoint activation that remain to be determined.

In order to activate the DNA damage checkpoint a cell must first detect the damaged DNA. This was initially thought to be the role of the checkpoint proteins, however more recently specific DSB repair proteins have been found to be important sensors of the DNA damage, highlighting the overlapping role of these proteins. For example, in *S. cerevisiae*, the MRX (Mre11-Rad50-Xrs2; homologue of human MRE11-RAD50-NBS1) repair complex is the main sensor required for DSB-induced checkpoint activation (Figure 1.2C; Rupnik et al., 2009). This complex has a robust DNA end-bridging activity and facilitates the tethering of DSB ends via the zinc-hook motifs located in the coiled-coil region of the Rad50 subunit, similar to MRN in vertebrate cells (Hopfner et al., 2002; Lammens et al., 2011; Wiltzius et al., 2005). However, in vertebrate cells, the MRN complex functions together with the DNA-PK holoenzyme (Ku70-Ku80-DNA-PKcs) in tethering the DNA ends (Hiom, 2010). Importantly the MRX/MRN complex also controls the recruitment of Tel1/ATM signalling pathways via its interaction with the C-terminus of Xrs2/NBS1 protein thus providing an indirect mechanism for Tel1/ATM to detect damaged DNA (Figure 1.2C; Nakada et al., 2003). Tel1/ATM then begins the activation process by phosphorylating several targets including Xrs2/NBS1 and serine 129/139 of histone H2A/H2AX to create a region of γH2A /γH2AX. This region of γH2A/γH2AX provides amplification of the original DNA damage signal and facilitates recruitment of further checkpoint proteins (Lisby et al., 2004; Rogakou et al., 1998).

ATM, but not Tel1, has been reported to exist as an inactive dimer that undergoes DNA damage-induced in *trans* autophosphorylation to form partially active monomers that interact with NBS1 (Bakkenist and Kastan, 2003). The recruitment of the ATM monomers to DSBs by NBS1 also promotes ATM activation by the MRN complex bound to DNA (Falck et al., 2005; Lee and Paull, 2005; You et al., 2005), as well as early processing events induced by MRN (Jazayeri et al., 2008; Shiotani and Zou, 2009). It is proposed that full activation of ATM also requires prior acetylation of ATM by the acetyltransferase Tip60 (60 kDa Tat-interactive protein, Sun et al., 2005; Sun et al., 2007).

The DNA ends of the DSB are then processed via a two-step mechanism (Figure 1.2D; (Mimitou and Symington, 2008; Nimonkar et al., 2011; Zhu et al., 2008). The first step is initiated by the MRX/MRN and Sae2/CtIP (CtIP in vertebrate) that remove approximately 50-100 nucleotides from the 5' ends of the break, giving rise to short 3' ssDNA tails (Mimitou and Symington, 2008; Nimonkar et al., 2011; Zhu et al., 2008). The partially resected DNA ends serve as the substrate for more extensive nucleotide degradation carried out by two redundant pathways. In budding yeast, one pathway is dependent on the DNA exonuclease Exo1 (vertebrate EXO1) while the other is mediated by the helicase-topoisomerase complex Sgs1-Top3 (topoisomerase 3)-Rmi1 (RecQ-mediated genome instability protein 1) in collaboration with the 5'flap endonuclease Dna2 (vertebrate DNA2). This process leads then to the formation of long ssDNA regions with 3' overhangs (Gravel et al., 2008; Mimitou and Symington, 2008; Nakada et al., 2004; Nimonkar et al., 2011; Zhu et al., 2008). In vertebrate cells, recent *in vitro* studies have established that the BLM (ortholog of *S. cerevisiae* Sgs1) and DNA2 resect DNA via two pathways similar to that described for budding yeast (Nimonkar et al., 2011). In one pathway, BLM and DNA2 physically interact and function in the 5'-3' resection of DNA ends, a process dependent on the helicase and nuclease activity of BLM and DNA2, respectively (Nimonkar et al., 2011). In a second EXO1-dependent pathway, MRN, RPA and BLM stimulate resection by promoting the recruitment of EXO1 to DNA ends and, in the case of MRN, by enhancing the processivity of EXO1 (Nimonkar et al., 2011; Nimonkar et al., 2008).

Processive resection coincides with the dissociation of Sae2/CtIP, MRX/MRN and Tel1/ATM from the broken DNA end and concomitant binding of the ssDNA-binding protein RPA to the resultant 3'ssDNA tails (Figure 1.2E; Lisby et al., 2004). The generation of RPA-coated ssDNA provides a larger platform for the recruitment of other checkpoint complexes. This includes Mec1/ATR, recruited through the direct binding of its cofactor Ddc2/ATRIP to RPA-coated ssDNA (Figure 1.2F; (Zou and Elledge, 2003). Extensive resection of DSBs is then proposed to promote the transition from Tel1/ATM-dependent to robust Mec1/ATR-dependent checkpoint (Mantiero et al., 2007; Shiotani and Zou, 2009). Like Tel1, Mec1 can generate a region of γ-H2A around the DSB (Downs et al., 2000; Shroff et al., 2004). In addition to Mec1-Ddc2/ATR-ATRIP, the PCNA-like checkpoint complex (also known as 9-1-1 clamp, *S. cerevisiae* Ddc1-Rad17-Mec3; human RAD9-RAD1-HUS1) and the RFC-like checkpoint complex (*S. cerevisiae* Rad24-Rfc2-5; human RAD17-RFC2-5) are recruited at the site of damage, independently of the Mec1-Ddc2/ATR-ATRIP complex. Once the PCNA-like complex is loaded by the RFC-like complex at the junctions between ssDNA and dsDNA, the Ddc1 subunit of the 9-1-1 clamp directly interacts with Mec1-Ddc2 complex, contributing to the activation of the Mec1 kinase activity. This process has been only identified in *S. cerevisiae* to date (Navadgi-Patil and Burgers, 2009b). Mec1/ATR is also activated by the Dpb11/TopBp1 protein that interacts both with the Ddc1/RAD9 subunit of 9-1-1 complex and Mec1/ATR (Navadgi-Patil and Burgers, 2008; Navadgi-Patil et al., 2011). More details on this process will be given in the later sections.

Fully activated Mec1/ATR phosphorylates several checkpoints proteins, including subunits of RPA and 9-1-1 complexes and Dpb11/TopBP1 (Cimprich and Cortez, 2008). In *S. cerevisiae*, Mec1 also phosphorylates the mediator protein Rad9. In response to DNA damage, Rad9 is recruited onto chromatin by two independent pathways: one is via the two histone marks H3K79me and γH2A, the other is via interaction with Dpb11 (Figure 1.2G). Rad9 is able to mediate the activation of both effector kinases Rad53 and Chk1 following its hyperphosphorylation by Mec1 (Blankley and Lydall, 2004; Emili, 1998; Gilbert et al., 2001; Pellicioli and Foiani, 2005; Vialard et al., 1998). In *S. cerevisiae*, Rad53 is the principal effector kinase, whereas Chk1 plays a secondary role DNA damage and replication checkpoints (Stracker et al., 2009). The mechanism of Rad53 activation is well understood. In

summary, Rad9 serves as a scaffold protein facilitating the recruitment of multiple copies of the Rad53 protein. Effectively Rad9 acts as a "surface catalyst" upon which Rad53 can be phosphorylated either by Mec1 or by autophosphorylation before becoming fully activated (Pellicioli and Foiani, 2005). Once activated, Rad53 is released from Rad9 and phosphorylates different targets that mediate the appropriate response to DNA damage (Gilbert et al., 2001; Ma et al., 2006; Pellicioli and Foiani, 2005). Unlike Rad53, the mechanism of Chk1 activation is less well understood. Once activated, Chk1 phosphorylates the Pds1 kinase, whereas Rad53 phosphorylates kinases Cdc5 and Dun1, with either event contributing to the arrest of the cell cycle (Agarwal et al., 2003; Huang et al., 1998; Sanchez et al., 1999; Wang et al., 2001).

In higher eukaryotes, in contrast to *S. cerevisiae*, CHK1 is the primary effector of both the DNA damage and replication checkpoints in vertebrates, with CHK2 playing an auxiliary role (Stracker et al., 2009). The role of mediators in ATM-dependent activation of CHK2 is still unclear. On the other hand, it is well established that Claspin (homologue of *S. cerevisiae* Mrc1) functions as an adaptor protein for the ATR-dependent phosphorylation of CHK1 (Smith et al., 2010). In contrast to vertebrates, the yeast homologue Mrc1 regulates Rad53 activation specifically in response to replication stress as a molecular adaptor in a manner analogous to the role of Rad9 in response to DNA damage (Alcasabas et al., 2001; Osborn and Elledge, 2003). In vertebrates, CHK2 and CHK1 then phosphorylate many targets, including p53, Cdc25A, Cdc25C and Wee1, which are key regulators of the cell cycle (Smith et al., 2010).

It is worth pointing out that emerging evidence implicates previously unrelated kinases in regulating the functions of DDR proteins, in addition to the established PIKKs and effector kinases (Bensimon et al., 2011). For example, emerging evidence suggesting a role of serine-threonine kinases known as cyclin-dependent kinases (CDKs) in regulating DSB resection, checkpoint activation and DNA repair and this information has been a key milestone in the understanding of DDR activation and regulation (Enserink and Kolodner, 2010; Ira et al., 2004). Furthermore, although less well understood, the chromatin environment has been implicated in the activation of the DDR, where chromatin remodeling and post-

translational modifications (PTMs) other than phosphorylation are particularly important for its status (Polo and Jackson, 2011).

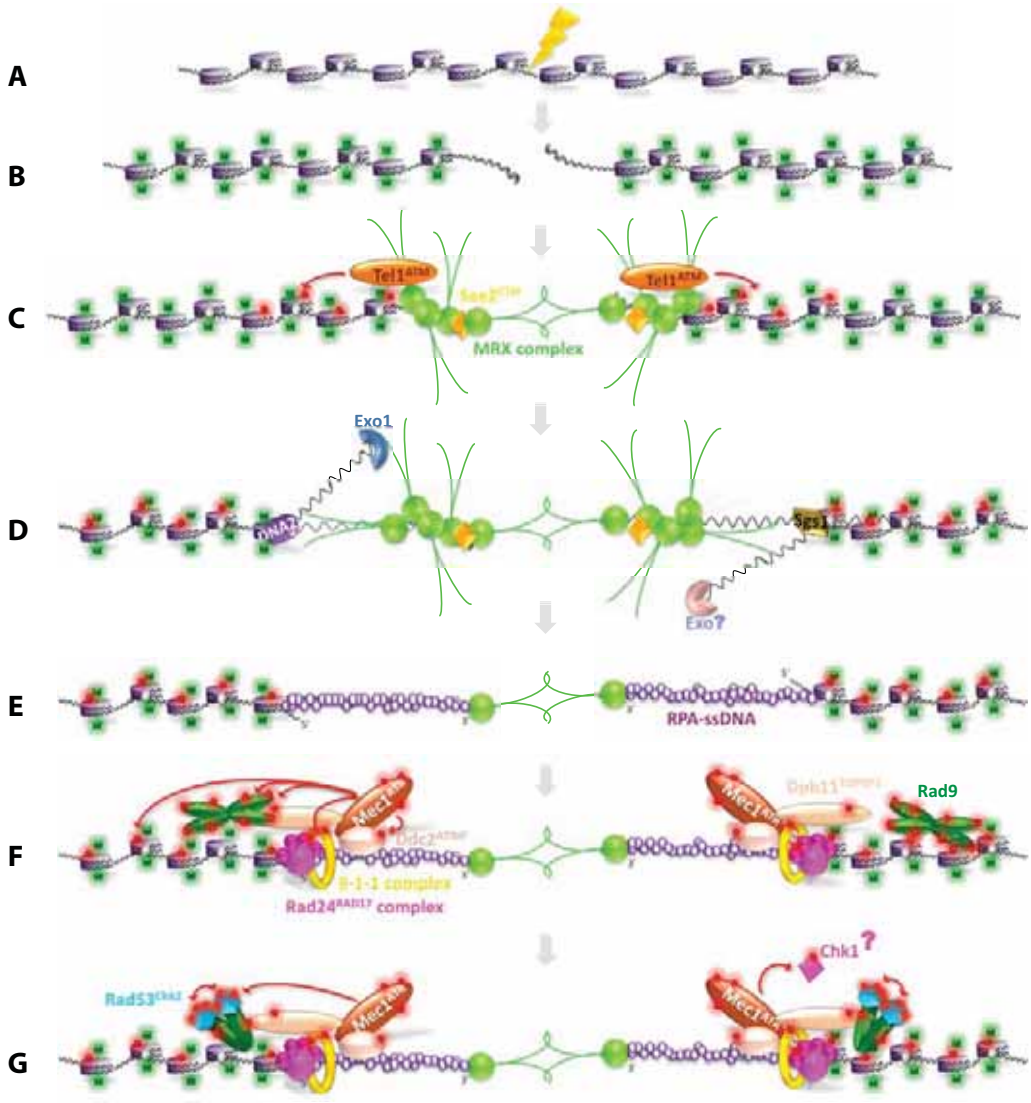


**Figure 1.2: Activation of the DNA damage checkpoints upon a DSB in *S. cerevisiae*.** After a DSB cells activate the DNA damage checkpoints through the Mec1-Ddc2 complex and its downstream targets Rad53 and Chk1, which trigger arrest in different cell cycle phases. This provides time for the cell to repair DNA lesions before entering mitosis, and induce the expression of DNA repair genes; green squares: Dot1-dependent methylation; red spots: phosphorylation; see text for more details.

## 1.4. MEC1/ATR: A MEMBER OF PHOSPHATIDYLINOSITOL-3 KINASE-LIKE KINASE FAMILY

Mec1/ATR belongs to a large superfamily of proteins known as the phosphatidylinositol-3-kinase-like kinases (PIKKs). The protein members of the PIKK family regulate a diverse array of cellular pathways. In human cells, the PIKK proteins ATR, ATM and DNA-PKcs are involved in the cellular response to DNA damage; mTOR (*m*ammalian *t*arget *o*f *r*apamycin) functions in the control of cell growth in response to nutrient depletion; SMG-1 (*s*uppressor of *m*orphogenesis in *g*enitalia) is a regulator of nonsense-mediated mRNA decay; and TRRAP (*tr*ansfo*r*mation/transcription domain-*a*ssociated *p*rotein) is involved in regulating chromatin structure (Abraham, 2004; Doyon and Cote, 2004; Martin and Hall, 2005). Only four of these proteins are conserved in budding yeast: Mec1, Tel1 (homologue of ATM), Tra1p (homologue of TRRAP) and Tor1 and Tor2 (homologues of mTOR) (Lempiainen and Halazonetis, 2009). Despite having very different biological functions at the cellular level, the structures of these kinases are well conserved.

### 1.4.1. Unique structural properties of PIKK family

#### *1.4.1.1. C-terminal regulatory domains*

The PIKK family comprises structurally unique proteins characterised by a large molecular size ranging from 300kDa to 500kDa and four conserved regulatory domains that distinguish them from other protein kinases (Figure 1.3). These distinct domains are present in the C-terminal half of the protein. In summary, these are the FRAP-ATM-TRRAP (FAT) domain, the kinase domain (KD) that contains the active site, the PIKK regulatory domain (PRD) and the FAT-C-terminal (FATC) domain (Keith and Schreiber, 1995; Bosotti et al, 2000; Mordes et al, 2008) (Abraham, 2004; Lempiainen and Halazonetis, 2009; Lovejoy and Cortez, 2009; Mordes and Cortez, 2008).

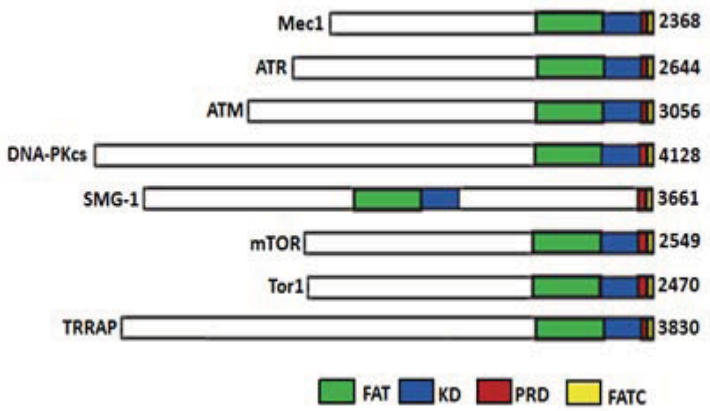


**Figure 1.3: Domain structure of PIKKs.** Schematic representation of the conserved protein domains characteristic of PIKKs, showing the number of amino acids; FAT - FRAP-ATM-TRRAP domain; KD – Kinase Domain; PRD - PIKK regulatory domain; FATC - FAT-C-terminal domain; Figure adapted from Lempiainen and Halazonetis, 2009.

The KDs of PIKKs is responsible for the catalytic activity of the protein and regulate the transfer of gamma phosphate from nucleotide triphosphates (ATP) to serine or threonine residues that are followed by a glutamine (Abraham, 2004; Lempiainen and Halazonetis, 2009). Note that TRRAP does not possess kinase activity due to lack in its kinase-like domain of the amino acids required for such activity (McMahon et al., 1998). The C-terminal KD of PIKKs counts for 5-10% of the total protein sequence and has low sequence similarity to classical eukaryotic protein kinases, which is the reason why PIKKs are considered atypical protein kinases (Abraham, 2004). In fact, sequences analysis of the PIKKs kinase domain demonstrates, as their name implies, a high sequence similarity with those of mammalian and yeast phosphoinositide 3-kinases (PI3Ks), lipid kinases that phosphorylate the 3-hydroxyl group of phosphoinositides to generate second messengers that induce cell proliferation (Cantley, 2002). Therefore, PI3Ks possibly can serve as a framework for understanding PIKK activity regulation.

Analysis of the three-dimentional structure of the PI3Ks shows that the C-terminus, considered to be equivalent to the PRD and FATC domains of PIKKs, is in close proximity to the activation loop of the KD. Considering that the PRD and FATC domains from PIKKs should adopt a similar 3D-structure to the C-terminus of PI3Ks due to their sequence similarity, it has been proposed that in PIKKs, the PRD and FATC domains might regulate their kinase activity by targeting the activation loop

of the kinase domain (Lempiainen and Halazonetis, 2009). Consistent with this possibility, analysis of the three-dimentional structure of DNA-PKcs revealed that the FAT and FATC domains are in direct contact with the catalytic PIKK core domain of this protein. Given that the DNA-PKcs interaction with Ku70-Ku86 heterodimer and DNA enhances its kinase activity it was then proposed that the FAT and FATC domains together act as a 'sensor' that couples conformational changes induced upon DNA binding to directly activate the catalytic center of the KD (Spagnolo et al., 2006).

The weakly conserved FAT domain is towards the N-terminus side of the protein with respect to the kinase domain and is about 500 amino acids in length. The role of this domain in PIKK function is still not fully understood but there is evidence suggesting that it might regulate indirectly PIKKs kinase activity (Bosotti et al., 2000). For example, the interaction between the NBS1 subunit of MRN complex with the ATM FAT domain stimulates ATM activity (Lempiainen and Halazonetis, 2009). Additionally, it has been proposed that the three-dimentional structure of the FAT domain of PIKKs might be similar to that of the helical domains of PI3Ks located before their KD that serve as a scaffold to which other proteins engage (Bosotti et al., 2000; Lempiainen and Halazonetis 2009).

The very C-terminal FATC domain of PIKKs, only found in combination with the FAT domain, is approximately 30 amino acids, and its sequence is highly conserved amongst all the family members (Bosotti et al, 2000). Due to this high sequence conservation, it is possible to substitute the FATC domain of ATM with the same from ATR, DNA-PKcs or TRRAP without disturbing its activity (Jiang et al., 2006), suggesting that the activity of these proteins is regulated similarly through the FATC domain. Noteworthy, however, is the loss of function when the FATC domains of ATR and mTOR are swapped with the same from ATM (Mordes et al., 2008a; Takahashi et al., 2000; You et al., 2005). This may indicate that ATR and mTOR FATC domains are involved in protein-protein interactions or other regulatory mechanisms (for example posttranslational modifications) that are not shared by that from ATM. In addition, several studies suggested that the FATC domain is essential for PIKK kinase activity and is very sensitive to mutagenesis. For example, deletion of even a single residue in the C-terminus of mTOR FATC region, abolishes mTOR

kinase activity, although does not affect its ability to bind ATP (Lempiainen and Halazonetis, 2009), suggesting that this domain blocks mTOR activity by some mechanism other than disruption of ATP binding. Moreover, single or double amino-acid substitutions in the FATC domain of several PIKKs drastically reduce their kinase activity (Morita et al., 2007; Nakada et al., 2005; Sun et al., 2005; Takahashi et al., 2000). These mutagenesis experiments have suggested that conserved hydrophobic amino acid residues in the FATC domain of PIKKs are critical for their function (Morita et al, 2007). Interestingly, naturally occurring mutations resulting in FATC truncations or additions to the human DNA-PK and ATM result in severe combined immune deficiency (Blunt et al., 1996) and A-T disorder phenotypes (Cavalieri et al., 2006), respectively. The current model for FATC function proposes that this domain mediates protein-protein interactions (Lempiainen and Halazonetis, 2009). Accordingly, the binding of Tip60 to the FATC domains of ATM and DNA-PKcs promotes their kinase activity in response to DNA damage. Furthermore, in ATM, this mechanism involves the Tip60-dependent acetylation of its PRD domain (K3016), which is then followed by ATM autophosphorylation and full activation (Jiang et al., 2006; Sun et al., 2005; Sun et al., 2007). Interestingly, another surprising mode of kinase regulation has been observed for ATM. This process involves the modification of cysteine residues at the FATC domain upon hydrogen peroxide treatment and is dependent on its DDR functions (Guo et al., 2010). It would be interesting to know if this new mechanism of ATM activation is shared with other PIKKs.

The PRD domain was delineated in the recent years as a small region, with varied length (from 16 to 82 amino acids, with the exception of SMG-1), located between the kinase and FATC domains (Mordes et al., 2008a). This region is not highly conserved between PIKKs. A deletion of this domain abolishes the kinase activity, although specific small deletions within the PRD of ATR (2430-2450 amino acids) or mTOR (2569-2576 amino acids) either do not compromise or enhances their catalytic activity respectively (Mordes et al., 2008a; Sekulic et al., 2000). These small deletions were in the N-terminal half of the PRD, which is poorly conserved among PIKKs (Lempiainen and Halazonetis, 2009). These studies suggest that the ability to differentially regulate the activity of various PIKKs might reside in this region. In contrast, the more conserved C-terminal half of the PRD is important for

the enzyme activity of PIKKs and seems to be site of posttranslational modifications or protein-protein interactions (Abraham, 2004; Lempiainen and Halazonetis, 2009; Lovejoy and Cortez, 2009; Mordes and Cortez, 2008). For example, the Lysine 3016 residue located at ATMs PRD becomes acetylated by Tip60 and alteration of this residue to an arginine compromises ATM activation after DNA damage, despite its normal basal activity (Sun et al., 2005; Sun et al., 2007). Furthermore, the PRD of ATR interacts with the activation domain of TopBP1, stimulating ATR kinase activity both *in vitro* and *in vivo* (Kumagai et al., 2006; Lovejoy and Cortez, 2009; Mordes et al., 2008a). Specific mutations in this ATR domain, such as Lysine 2589 to glutamic acid, although not affecting its basal activity, abolish TopBP1-dependent ATR activation (Mordes et al., 2008a).

#### *1.4.1.2. N-terminal tandem HEAT repeats*

Although the N-terminal regions of PIKKs have no apparent homology and vary considerably in size and sequence, deeper bioinformatic analyses has revealed that the non-kinase portions of the PIKK proteins (90-95% of the protein) are composed almost entirely of tandemly repeated α-helical motifs termed HEAT repeats (from 40 to ~54 units, (Perry and Kleckner, 2003). The divergence between one PIKK to another involves the addition or subtraction of one or few HEAT repeats, with some being specific to a particular subfamily (Brewerton et al., 2004; Perry and Kleckner, 2003). Their name derives from the four proteins in where these repeats were initially found: Huntingtin, Elongation factor 3, Alpha-regulatory subunit of protein phosphatase 2A and TOR1 (Andrade and Bork, 1995). A canonical single HEAT repeat is defined as a pair of interacting anti-parallel helices (hereafter called A and B) linked by a flexible intraloop, forming a helical hairpin (Figure 1.4A; (Andrade et al., 2001a; Andrade et al., 2001b). HEAT repeats, as well as their associated loops, are highly variable in length and amino acid composition ((Andrade et al., 2001a; Andrade et al., 2001b). Nevertheless, the helical regions of a HEAT unit have on average 10-20 amino acid residues, linked by 5-8 residues of intraunit loop and connected to a neighbouring unit by a $\geq 1$ residue in size corresponding to the interunit loop (Figure 1.4A and C; Perry and Kleckner, 2003). Additionally, the presence of two conserved motifs with specific amino acid sequence within each helical region confers specific structural characteristics to the HEAT repeats: a LLPXL motif, located within the central portion of helix A, sometimes introduces a

bend in the α-helical structure; and a VR motif, appears at the start of the helix B of the HEAT repeat (Perry and Kleckner, 2003).

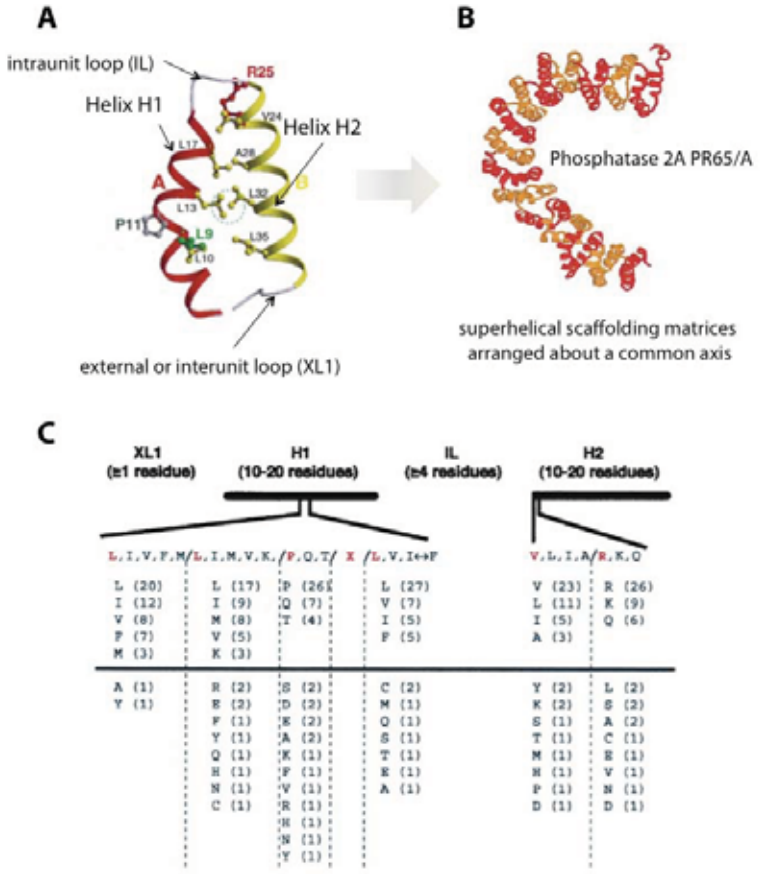


**Figure 1.4: HEAT repeats features.** (A) A typical HEAT repeat (HEAT tepeat 10 of importin-β); Residues shown in ball-and-stick represent key conserved residues (shown also in C); (B) Structure of the PR65/A subunit of human protein phosphatase 2A; (C) A structure based consensus sequence of HEAT repeats (see text for details). Figure adapted from Perry and Kleckner, 2003; Andrade et al., 2001a; Andrade et al., 2001b).

In HEAT-rich proteins, these repeats occur in a series with adjacent units piling together, linked by flexible interunit loops, to form elongated super-helical scaffolding matrices or 'solenoids', with a continuous hydrophobic core (Figure 1.4B; (Andrade et al., 2001a; Andrade et al., 2001b). When visualised by crystallography, solenoids form superhelical scaffold matrices often when engaged with other macromolecules (Chook and Blobel, 1999; Cingolani et al., 1999; Groves and Barford, 1999; Groves et al., 1999). The A helices, which have a bend of variable extent, form the convex surface of the superhelix and the B helices the concave surface. Accordingly, electron microscopy structure of the yeast Tor1

protein showed that its N-terminus creates a curved tubular-shaped structure to form a convex and a concave face similar to that adopted by proteins containing HEAT repeats (Adami et al., 2007; Llorca et al., 2003; Rivera-Calzada et al., 2005; Spagnolo et al., 2006). Additionally, electron microscopy (EM) studies proposing a model for the overall DNA-PKcs and ATM three-dimensional (3D) structures revealed similarities between DNA-PKcs and ATM, reflecting the probable structural homology within the PIKK family members (Boskovic et al., 2003; Chiu et al., 1998; Leuther et al., 1999; Llorca et al., 2003; Rivera-Calzada et al., 2005; Spagnolo et al., 2006). Each structure comprises two main regions: (1) a 'head-like' domain in which the KD has been located and from where extensions project corresponding to the FAT and FATC domains; (2) a curved and flattened tubular 'arm-like' domain where it was associated to the less conserved HEAT-rich N-terminus of the proteins (Llorca et al., 2003; Rivera-Calzada et al., 2005; Spagnolo et al., 2006).

The major differences amongst PIKKs are expected to be present in the HEAT-rich arm, due to the lack of homology between the different proteins at this region. Accordingly, the structural differences observed between ATM and DNA-PKcs occur within this region, reflecting possibly the differences in functions. Interestingly and in support of this idea, some of the HEAT repeats are only present in particular members of a subfamily (ATRs, ATMs, and TORs) but absent in the members of the other subfamilies (Andrade et al., 2001b).

Recently, the crystal structure of DNA-PKcs was obtained at reasonable resolution (6.6 A), and showed some features in common with the structures obtained by electron microscopy, but in which for the first time the overall fold is clearly visible as a ring-like structure (Figure 1.5; (Sibanda et al., 2010). The bending of this structure and the folding of the polypeptide chain into a hollow circular structure is facilitated by the many α-helical HEAT repeats, consisting of about 66 helices, that are located at the N-terminus of the protein. The C-terminus comprising the kinase, FAT and FATC domains, is located on the top of this structure and this region probably corresponds to the head/crown domain identified in previous electron microscopy structures (Boskovic et al., 2003; Chiu et al., 1998; Rivera-Calzada et al., 2005; Williams et al., 2008). It was proposed that conformational changes in the

ring-like structure leading the arms to swing could provide a mechanism for DNA-PKcs binding to DNA ends and/or its release of DNA after ligation. The conformational changes would probably be transmitted to the FAT, FATC and Kinase domains located in the head/crown, suggesting the arrangement of the ring structure is important to engage DNA-PKcs in the repair of damaged DNA (Sibanda et al, 2010). Interestingly, it was recently shown that PR65/A (Protein phosphatase PP2A regulatory subunit A), a subunit of the heterotrimeric PP2A (Protein phosphatase 2A) phosphatase which contains 15 HEAT repeats, undergoes (visco-)elastic deformations in response to forces promoting conformational changes in the regulatory and catalytic subunits of PP2A impacting on its activity (Grinthal et al., 2010).

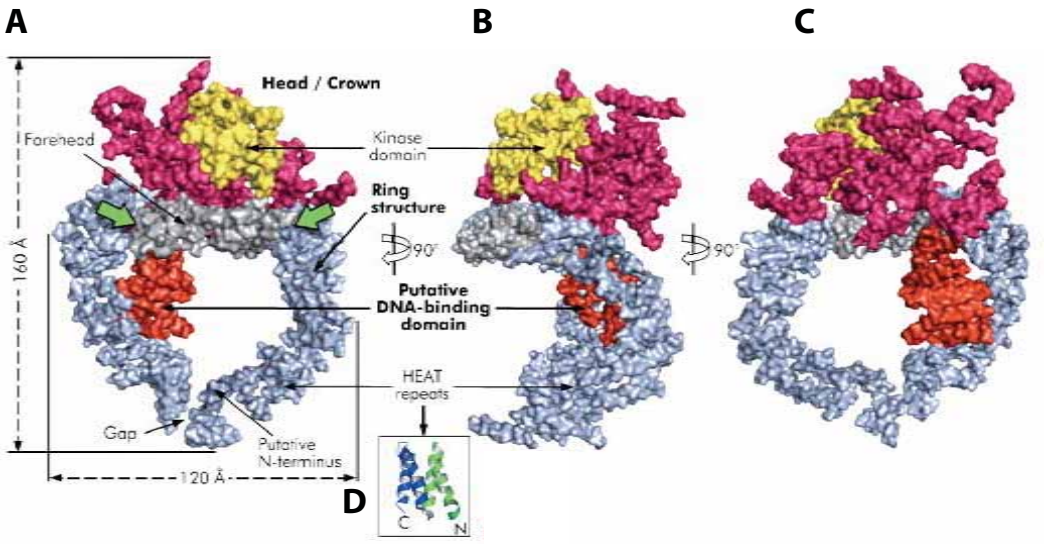


**Figure 1.5**: **Crystal structure of DNA-PKcs (6.6 A)**. The molecular surface of DNA-PKcs showing (A) front, with the potential conformationally variable regions denoted with green arrows, (B) side view, (C) back view, (D) a single HEAT repeat. The colour code of the molecule is as follows: ring structure in grey; the putative DNA binding domain in red; the larger head/crown domain in magenta and (for the kinase sub-domain) yellow. Adapted from Sibanda et al., 2010.

Although the presence of a common structural unit, conserved throughout the PIKKs suggests evolutionary conservation of their structure and mechanistic basis, relatively little is known about the importance of these HEAT repeats for the regulation of their activity, substrate specificity and specific interactions. Although HEAT repeat-containing proteins are involved in several cellular processes, a function common to many is that of mediating important protein-protein interactions.

For example, PR65/A interacts with several regulatory B subunits of PP2A. Moreover, importins β 1 and β 2, which contain 19 and 18 HEAT repeats respectively, bind to small GTPase Ran and to various protein substrates destined for nuclear import through two separate but closely spaced HEAT repeats (Bayliss et al., 2000; Groves et al., 1999). Consistent with this, there is also evidence suggesting that HEAT repeats mediate protein-protein interactions in PIKKs. In fact, recruitment of the PIKKs ATM/Tel1, ATR/Mec1 and DNA-PK to DNA lesions involves analogous mechanisms through the binding of their HEAT-containing N-terminal regions to their respective interacting partners NBS1/Xrs2, ATRIP/Ddc2 and Ku80/70 (Falck et al., 2005). As the domains in the proteins that interact with these PIKKs are functionally conserved and C-terminally related motifs (Falck et al., 2005), it is possible that ATR, ATM and DNA-PKcs have common interacting regions in their HEAT repeats with structural conservation. In *S. pombe*, four individual HEAT repeats (17-18 and 21-22) of Tel1 were identified to be required for the interaction between Tel1 and C-terminus of Nbs1 (You et al, 2005). Interestingly, the over-expression of a fragment encompassing these HEATs in mammalian cells resulted in a dominant negative effect, indicating that the function of this region may be evolutionary conserved (Chen et al., 2003; Morgan et al., 1997). Additionally, it has been shown in human cells that Tel2, a protein also involved in DDR, interacts with all PIKK proteins to control their stability, and specifically in ATM a subset of HEAT repeats (830-1290aa) mediate the interaction between these two proteins (Takai et al., 2007). It is then tempting to speculate that the HEAT repeats of PIKKs might act as platforms, which mediate protein-protein interactions. However, the major portion of the HEAT repeat-containing regions of these proteins still remains uncharacterised.

### 1.4.2. Mec1 structure-function relationship

The Mec1 kinase is the main regulator of the DDR in budding yeast where it plays a key role in the DNA damage network. Its function is critical for cellular responses to many types of DNA damage and defects in the Mec1 pathway result in hypersensitivity to genotoxins, loss of DNA damage checkpoints and genomic instability (Desany et al., 1998; Paulovich and Hartwell, 1995; Sanchez et al., 1996; Weinert et al., 1994). Mec1 is a 273kDa protein of 2368 amino acids and with similarity in its catalytic domain to other PIKKs (Figure 1.6). Due to its size and low

abundance it is a difficult protein to study and so far there are no reports on its purification. Most of the structure analysis of Mec1 is based on comparison with other protein members of the same family due to the high conservation among eukaryotes. Mec1 can be divided into three main regions. The carboxyl terminal is highly conserved between the ATR-family and is formed by the kinase domain, FAT, FATC and PRD domains. The amino terminal region, which is required for binding with Ddc2, does not have apparent homology with other PIKKs (Lempiainen and Halazonetis, 2009; Wakayama et al., 2001). In contrast, the central region shows significant homology with other ATR family members but has an unknown function. Mec1 also comprises ten putative PIKK phosphorylation sites and eight putative CDK phosphorylation sites. Proteome-wide analysis have identified two putative PIKK sites to be phosphorylated *in vivo* (Albuquerque et al., 2008; Smolka et al., 2007). However, the molecular mechanism and their role in Mec1 functions are unknown. In addition, the remainder of the putative PIKK and CDK sites are still uncharacterised.

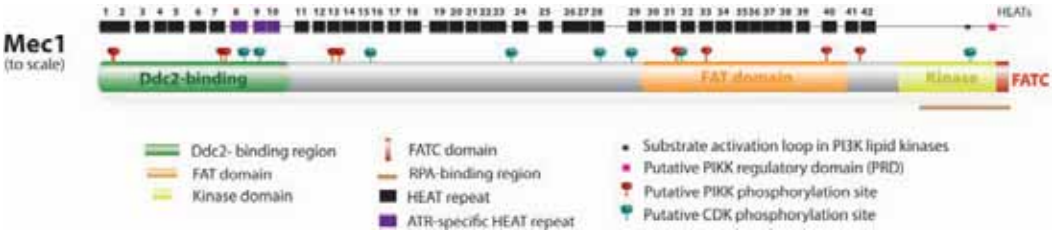


**Figure 1.6: Schematic representation of the Mec1 protein domains.** Structural motifs and interaction domains identified in the Mec1 protein, including the putative PIKK (S/T-Q) and Cdc28 (S/T-P) phosphorylation sites.

Mec1 Kinase domain contains the conserved motif DXXXXN (amino acids 2224 to 2229), which in conventional protein kinases plays a critical role in calalysis (Zakian, 1995). The mutation of this motif of Mec1 to SXXXXS, resulted in a Kinase-negative *mec1* mutant (MEC1-KN) with a null-like phenotype with respect to DNA damage sensitivity and cell lethality (Wakayama et al., 2001). In addition, *in vitro* Rad53 phosphorylation was shown to be abrogated with this mutant protein (Wakayama et al., 2001). In agreement, another study has shown that two *mec1* mutants (*mec1-kd1* and *mec1-kd2*), in which single amino acids are mutated in the Mec1 KD to give kinase-dead proteins (D2243E or D2224E, respectively), are also

indistinguishable from *mec1Δ* cells (Paciotti et al., 2001). These data indicate that the Mec1 kinase domain is required for all of its known functions (Mallory and Petes, 2000; Paciotti et al., 2001). Furthermore, the overexpression of the *mec1kd* variants caused dominant checkpoint defects when overexpressed in *MEC1* cells, especially in the checkpoint response in G1 and S-phase, but not in G2/M (Paciotti et al., 2001). This suggests that Mec1 functions required for response to DNA structures during specific cell cycle stages can be separated. Accordingly, two hypomorphic *mec1* mutants *mec1-100* (F1179S + N1700S) and *mec1-101* (V225G + S552P + L781S) generated by random mutagenesis are defective in the G1 and intra-S checkpoints but proficient in the G2/M checkpoint (Paciotti et al., 2001). In addition, the fact that the *mec1-101* mutant is also proficient in the replication checkpoint in the presence of HU (Hydroxyurea), further supports the hypothesis that the cellular response to DNA replication blocks or to DNA damage during DNA replication involves different Mec1 functions (Paciotti et al., 2001). In agreement with this, another *mec1* hypomorphic mutant (*mec1-21*), which results from a missense mutation in Mec1 (G882S), is defective in the S-phase checkpoint after UV and HU exposure but retains some G2 checkpoint function after IR (Desany et al., 1998; Sanchez et al., 1996; Sun and Fasullo, 2007). Althought the mutations in the *mec1-100*, *mec1-101* and *mec1-21* mutants are located outside the Mec1 kinase domain, we cannot exclude completely the possibility that they directly affect Mec1 kinase activity. However, it is also likely that these mutations might affect interactions between Mec1 and proteins or structures specifically involved in G1 and intra-S checkpoints.

Mutagenesis analysis of Mec1 also revealed that the C-terminal end of Mec1 (amino acids 2360 to 2368) is required for a direct interaction with RPA and for localization to sites of DNA damage (Nakada et al., 2005). Mec1 and its cofactor Ddc2 cooperate in interacting with RPA and thereby localise to sites of DNA damage in the form of a complex. In addition, the mutation of specific residues to alanine in this region (*mec1-85*, 2360-2362AAA) impairs Mec1-RPA interaction and affects Mec1 kinase activity, but does not affect the Mec1-Ddc2 complex formation. Note that kinase activity is dispensable for Mec1 localisation to damaged sites since Mec1-kinase negative proteins associate efficiently with DSBs. These results suggest that the FATC domain of Mec1 possesses two roles: it is required for the phosphorylation of

substrates and also for the association with sites of DNA damage (Nakada et al., 2005). Based on structural studies of DNA-PKcs (Rivera-Calzada et al., 2005; Sibanda et al.), it is possible that this domain might undergo conformational changes to promote Mec1 kinase activity upon binding to RPA, leading to phosphorylation of its downstream substrates.

Like other PIKKs, Mec1 is primarily composed of HEAT repeats, more precisely 42 HEATs in total. Multiple alignments of different PIKKs show that the Mec1 HEAT repeats numbers 8, 9 and 10 are specific to the ATR subfamily (Andrade et al., 2001b). However, the role of these HEAT repeats in Mec1/ATR functions is unknown. The only evidence reported attributing a function to the Mec1 HEAT repeat-containing region came from yeast-two hybrid assays showing a direct interaction between Mec1 and its cofactor Ddc2 that is dependent on the first 500 amino acids of Mec1 (Wakayama et al., 2001). Although, this process was not atributed to the involvement of HEAT repeats, it is possible that the HEATs number 1-10 comprised in the Ddc2-interacting region of Mec1 might be important to mediate this interaction. In addition, it is possible that not all the HEAT repeats within this region are required for the Mec1-Ddc2 interaction.

Taken together, emerging evidence suggests that PIKK activity is regulated by a complex relationship between protein conformational status, post-translational modifications, activator proteins and protein complex dynamics. Here, HEAT repeats are likely to have crucial functions whereby mediating different protein-protein interactions and conformational changes, to regulate different functions of the PIKK proteins. However, further experimental data on the structure and functions of these PIKK proteins is needed to clarify this matter. A true mechanistic understanding will require structural information. The large size of PIKKs might continue to challenge attempts at crystalising these proteins, but domain mapping and mutagenesis studies may enable the roles of smaller subdomain structures to be determined.

## 1.5. MEC1/ATR: AN ESSENTIAL REGULATOR OF GENOME STABILITY

### 1.5.1. A function essential for cell viability

#### *1.5.1.1. dNTPs regulation*

In *S. cerevisiae,* Mec1 was initially discovered by two independent groups for its role in preventing mitosis after DNA damage (Kato and Ogawa, 1994; Weinert et al., 1994). Subsequently, Zhao and collaborators also discovered that Mec1 has an essential role in cell viability. A function that is completely distinct from its involvement in the DNA damage checkpoint (Zhao et al., 1998).

The lethality brought about the *mec1* null mutation indicates the essential role of Mec1 during normal growth. *mec1* cells are defective for both chromosomal and mitochondrial DNA replication (Zhao et al., 1998). However, this defect can be supressed by either over-expression of Rnr3, one of the four subunits of the ribonucleotide reductase (RNR, the enzyme responsible for the catalysis of dNTPs (deoxynucleotides triphosphate) from ribonucleotides) or by deletion of the gene *SML1* (Suppressor of Mec1 Lethality protein 1), encoding an inhibitor of the Rnr1 subunit (Zhao et al., 1998). These findings indicate that Mec1 has a role in maintaining the correct level of dNTPs necessary for efficient DNA replication and normal S-phase progression (Figure 1.7). Mec1 regulates both the transcriptional induction of the *RNR* genes during S-phase, which also requires the Mbp1/Swi6 complex (a transcription factor that regulate gene expression during G1/S transition), and regulates the modulation of the Sml1-Rnr1 interaction (Zhao et al., 2000; Zhao et al., 1998). Note that Dun1 acts in both pathways in a Mec1-dependent manner, regulating *RNR* transcription during S-phase and phosphorylating Sml1, which directly leads to its degradation (Zhao and Rothstein, 2002). Moreover, the Mec1-dependent regulation of Sml1 is not only important for a normal S-phase but it is also important for the cellular response to DNA damage or replication blocks. Indeed, repair of DNA damage is a process that requires dNTPs. Therefore, RNR activity must be increased in order to synthesize a pool of dNTPs necessary for repairing DNA lesions (Zhao et al., 2000; Zhao et al., 1998).

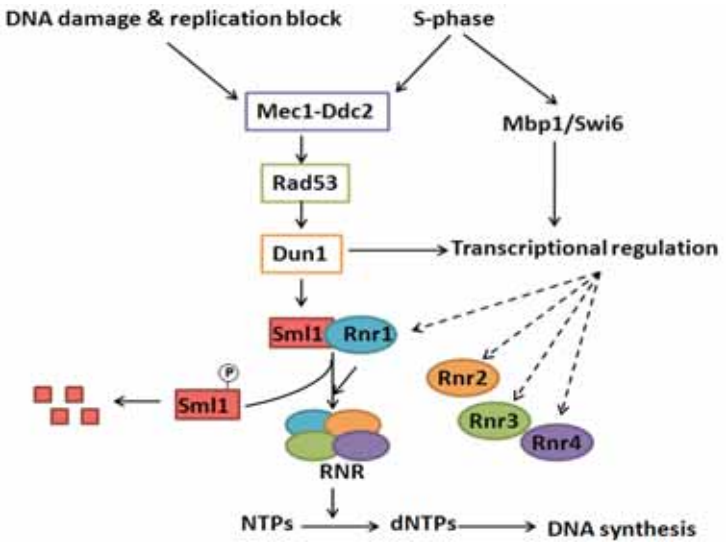


**Figure 1.7. Model for Mec1 function in RNR regulation.** The posttranslational regulation of RNR activity is mediated by removing the inhibitory effect of Sml1. This regulation can occur during S-phase or after DNA damage and replication block and this process is mediated by Dun1 preceded by the Mec1/Rad53 kinase. Thus, when there is requirement of DNA synthesis in the cell, Mec1 – through its downstream targets – phosphorylates either Sml1 or any of the RNR subunits removing the inhibitory effect of Sml1 on the RNR. As a result, Rnr1 is available to form an active RNR, which will be able to synthesize dNTPs; Adapted from Zhao et al., 1998; Zhao and Rothstein, 2002.

Similar to *mec1Δ* cells, *ddc2* and *rad53* null mutants are lethal and this lethality can be suppressed by the loss of Sml1 function. This reveals that both Ddc2 and Rad53 are necessary together with Mec1 for this essential function, as a cofactor and downstream kinase respectively. However, increasing dNTPs levels does not rescue the hypersensitivity to genotoxic or checkpoints defects in *mec1, ddc2* and *rad53* strains (Paciotti et al., 2000; Zhao et al., 1998). This demonstrates that the role of these genes in the DNA damage response and genome stability is independent from their essential role in controlling dNTPs cellular concentration.

#### *1.5.1.2. Replication checkpoint*

During S-phase, in addition to the intra-S phase checkpoint, which slows DNA replication and cell cycle progression in response to DNA damage, the replication checkpoint arrests cell cycle progression and inhibits firing of late replication origins in response to replication stress (Segurado and Tercero, 2009). The replication checkpoint is activated when replication forks stall due to replication perturbations or due to the depletion of dNTPs, for example as a result of ribonucleotide reductase (RNR) inhibition (Branzei and Foiani, 2009). Although genetically separable, the intra-S and replication checkpoints partially overlap as many checkpoint proteins

function in both pathways due to the occurrence of similar or common DNA structures (Zegerman and Diffley, 2009). Both checkpoints operate to maintain the integrity of the replication forks while facilitating replication completion and DNA repair and preventing entry into mitosis before DNA replication is complete (Segurado and Tercero, 2009).

As in the S-phase checkpoint, both Mec1 and Rad53 kinases also have critical roles in the replication checkpoint (Lopes et al., 2001; Segurado and Tercero, 2009; Tercero and Diffley, 2001). Mutagenic studies and chromatin immunoprecipitation assays suggest that Mec1 functions at the stalled forks to keep replication polymerases engaged and that this function is separable from its role in activating Rad53. The partial loss of function mutant, *mec1-100*, which compromises the S-phase checkpoint but not the G2/M checkpoint, shows partial loss of replicative polymerases at the stalled forks, but when combined with the mutation of the helicase Sgs1 this leads to complete fork collapse. In contrast, these observations are not observed in cells lacking Rad53, indicating that Rad53 is not involved in polymerase stability (Cobb et al., 2005). However, surprisingly, a recent study has shown that the replisome is stably associated with DNA replication forks following replication stress in the absence of Mec1 or Rad53 (De Piccoli et al., 2012). In addition, it was observed that Psf1, a subunit of the Cdc45-MCM-GINS helicase at forks, undergoes a Mec1-dependent phosphorylation upon replication. It was then proposed that the checkpoint kinases control replisome function rather than stability of DNA replication forks upon DNA replication stress (De Piccoli et al., 2012). Additional work will be needed to confirm this model and to identify the exact molecular mechanisms.

Recently, it has been also demonstrated that Rad53 can phosphorylate the nuclease Exo1, which might be implicated in generating ssDNA, and stabilise the DNA replication forks, at least in the presence of HU. However, the mechanism by which Exo1 affects DNA replication still remains unclear (Segurado and Diffley, 2008; Segurado and Tercero, 2009).

Unlike the intra-S phase checkpoint, Mrc1 (and not Rad9), is the mediator responsible for the activation of Rad53 in response to DNA replication inhibition

(Friedel et al., 2009; Osborn and Elledge, 2003; Pasero et al., 2003; Segurado and Tercero, 2009). Mrc1 associates with the replication fork under normal replication conditions, promoting efficient DNA replication during an unperturbed S-phase (Alcasabas et al., 2001; Hodgson et al., 2007; Osborn and Elledge, 2003; Szyjka et al., 2005; Tourriere et al., 2005). Upon encountering a replication block, Mrc1 forms a stable replication-pausing complex with the S-phase checkpoint protein complex Tof1-Csm3, preventing uncoupling of the replisome from the site of DNA synthesis (Katou et al., 2003). This complex promotes the recruitment of Mec1-Ddc2 to stalled replication forks, facilitating the phosphorylation of Mrc1 by Mec1 (Osborn and Elledge, 2003). Mec1-dependent phosphorylation of Mrc1 promotes the accumulation of Mec1-Ddc2 at stalled replication forks, leading to Rad53 activation (Naylor et al., 2009; Osborn and Elledge, 2003). It was proposed that Mrc1 mediates the Mec1-dependent phosphorylation of Rad53 by acting as a molecular adaptor in a manner analogous to the role of Rad9 in responding to DNA damage (Osborn and Elledge, 2003). However, a physical interaction between Mrc1 and Rad53 has yet to be demonstrated. In the absence of Mrc1, Rad9 can fulfil this role, indicating that the replication stress signal can be converted into a DNA damage signal (Alcasabas et al., 2001; Foss, 2001), leading to Rad9-mediated activation of Rad53 and Chk1 (Alcasabas et al., 2001). Faithful replication of the genome is paramount to the maintenance of genomic stability, thus it is not surprising that the multiple checkpoint and repair pathways that act in S-phase display considerable complexity and redundancy (Myung and Kolodner, 2002).

ATR is essential for the viability of replicating human and mouse cells even without any external genomic threaten (Brown and Baltimore, 2000, 2003; Cortez et al., 2001; de Klein et al., 2000). However, it is still unclear whether the essential role of ATR reflects a conserved role in fork stabilization and/or RNR regulation. To date, no evidence exists to show a role of ATR in regulating the dNTPs levels. On the other hand, several line of evidence indicate that ATR has a critical role in the replication checkpoint to maintain replication fork integrity, similar to its Mec1 homologue in *S. cerevisiae* (Friedel et al., 2009). In addition, CHK1 also appears to be involved in regulation of replication initiation and fork progression (Maya-Mendoza et al., 2007; Wilsker et al., 2008). Accordingly, conditional deletion of ATR in mouse embryonic fibroblasts (MEFs) leads to accumulation of DNA DSBs

during S-phase (Brown and Baltimore, 2000). In addition, inhibition of ATR or CHK1 in the presence of low levels of DNA replication stress, results in increased DNA breaks specifically located at structurally distinct DNA regions known as fragile sites, which are thought to represent chromosomal regions that are particularly difficult to replicate and characterized by a higher incidence of replication forks stalling (Casper et al., 2002; Durkin et al., 2006). Furthermore, CHK1-deficient cells fail to maintain viable replication forks when DNA polymerase is inhibited (Zachos et al., 2003). Thus, all evidence to date supports a crucial role of ATR-CHK1 signalling in the stabilization of DNA replication forks. In this process the replication fork-associated protein Claspin (scMrc1) functions as an adaptor protein to recruit CHK1 to stalled replication forks, facilitating ATR-dependent phosphorylation and activation of CHK1 (Friedel et al., 2009). Activated CHK1 then dissociates from chromatin to phosphorylate its substrates (Smits et al., 2006).

### 1.5.2. Regulation of Mec1/ATR-dependent DDR functions

#### *1.5.2.1. RPA-coated ssDNA: key structure for Mec1/ATR localisation to DNA damage*

The activation of Mec1/ATR upon DNA damage or replication stress occurs not by sensing the DNA damage or replication stress directly but by interacting with factors that either bind directly to DNA lesions or to processed intermediates. In the past decade, studies using yeast, *Xenopus laevis* and mammalian cells have provided strong evidence that single-stranded DNA (ssDNA) is the key structure required for Mec1/ATR activation (Zou and Elledge, 2003; Lisby and Rothstein, 2004). The ssDNA structure is commonly induced either by the functional uncoupling of replicative helicases and polymerases during fork stalling or multiple DNA repair pathways that lead to resection of DSBs (Friedel et al., 2009). Once generated in cells, ssDNA is rapidly coated by the single-stranded binding complex RPA (replication protein A).

***1.5.2.2. Ddc2/ATRIP: an obligate partner of Mec1/ATR***

However, Mec1/Rad3/ATR recognition of RPA-coated ssDNA also depends on its regulatory subunit protein, Ddc2 (homologue of *S. pombe* Rad26 and *human* ATRIP) (Ball et al., 2007; Nakada et al., 2005; Rouse and Jackson, 2002; Zou and Elledge, 2003). In fact, Ddc2/ATRIP is considered an obligate subunit of Mec1/ATR and mutation of either Mec1/ATR or Ddc2/ATRIP causes the same phenotypes (Ball et al., 2007; Cortez et al., 2001; Rouse and Jackson, 2000; Wakayama et al., 2001). However, although Ddc2/ATRIP is required for the phosphorylation of Mec1/ATR targets, this protein does not appear to regulate Mec1/ATR kinase activity directly in yeast or human cells (Mordes et al., 2008a; Wakayama et al., 2001). Accordingly, purified Mec1-Ddc2/ATR-ATRIP shows a very low protein kinase activity (Majka and Burgers, 2007). This indicates that Mec1/ATR kinase activity is specifically regulated and activated during checkpoint activation, in which the Ddc2/ATRIP-dependent localisation of Mec1/ATR to sites of damage is an essential step.

In human cells, ATR and ATRIP regulate each other's stability, indicating that these proteins are mutually dependent partners in cell cycle checkpoint pathways (Cortez et al., 2001). Their mutual dependency for expression suggests that the relative levels of ATR and ATRIP protein in cells is tightly regulated and that these proteins need to bind each other at a fixed stoichiometry to be stable. Elsewhere, it has also been observed that ATR and ATRIP associate in a tight complex (Kumagai et al., 2004). Hydrodynamic analysis of the ATR-ATRIP complex in human cells, however, revealed that the elution profile of ATR and ATRIP from a gel filtration column does not overlap fully under relatively mild conditions, suggesting that an equilibrium may exist between free ATR and ATRIP and ATR and ATRIP in the form of the ATR-ATRIP complex in cells (Unsal-Kacmaz and Sancar, 2004). Similarly immunodepletion studies in *Xenopus* egg extracts also revealed that approximately 30% of the total *Xenopus* ATR (XATR) was not bound to *Xenopus* ATRIP (XATRIP) (Kumagai et al., 2004).

The Ddc2-Mec1/ATR-ATRIP interaction domains were identified in both budding yeast and human cells (Ball et al., 2005). The N-terminal region of Mec1/ATR has been shown to be required for the interaction with its cofactor. Althought this region has low sequence conservation among ATR ortologues, this suggests that it might

adapt a similar conformation in these proteins (Falck et al., 2005). This is supported by the fact that the Ddc2-/ATRIP-interacting region in Mec1/ATR are composed of HEAT repeats (Perry and Kleckner, 2003). For instance, yeast two-hybrid screens have shown that Ddc2-interacting region in Mec1 is comprised of the first 500 amino acids (HEATs 1-10) in budding yeast (Paciotti et al., 2000; Wakayama et al., 2001) while in human cells, the N-terminal region within 30-346 amino acids (HEATs 1-7) is involved in ATR binding to ATRIP (Ball et al., 2005; Perry and Kleckner, 2001). In addition, ATRIP residues 641 – 726 were found to be sufficient to interact with the N-terminus of ATR (Ball et al., 2005). However, a study in human cells has revealed that additional ATRIP domains may also be necessary in order to stabilise this interaction (Cortez et al., 2001). In *S. cerevisiae*, immunoprecipitation experiments also revealed that the C-terminus of Ddc2 is required for interaction with Mec1 (Wakayama et al., 2001).

Mec1/ATR interacts constitutively with its cofactor Ddc2/ATRIP to form a complex that is recruited to RPA-coated ssDNA upon DNA damage or replication stress (Ball et al., 2005; Paciotti et al., 2000; Rouse and Jackson, 2000; Wakayama et al., 2001; Unsal-Kacmaz and Sancar, 2004). In both yeast and human cells, Ddc2/ATRIP binding to RPA is required for Mec1-Ddc2/ATR-ATRIP recruitment to RPA-coated ssDNA. In fact, biochemical studies indicate that the binding of Ddc2/ATRIP to RPA occurs through evolutionary conserved binding surfaces (Ball et al., 2007). The primary interaction involves an acidic α-helix in Ddc2/ATRIP that binds to the basic cleft of the N-terminal oligonucleotide/oligosaccharide binding (OB)-fold domain of the large RPA subunit (Ball et al., 2007). In *S. cerevisiae*, the *rfa1-t11* mutation causes a charge reversal in this basic cleft and impairs the binding and recruitment of Ddc2 to DSBs (Zou and Elledge, 2003). Furthermore, in budding yeast, localisation of the Mec1-Ddc2 complex to RPA-coated ssDNA is mediated through both Ddc2-RPA and Mec1-RPA interdependent interactions (Ball et al., 2007; Nakada et al., 2005; Rouse and Jackson, 2002; Zou and Elledge, 2003), the latter being mediated by Mec1 C-terminus. In higher cells, evidence suggests that a similar interdependency between ATR and ATRIP exists. It has been shown that ATR can interact with RPA-coated ssDNA (Bomgarden et al., 2004), suggesting that ATR might contribute to localisation of the ATR-ATRIP complex to sites of damage, as observed in budding yeast. Additionally, a splice variant of ATRIP that cannot bind

to ATR revealed that ATR association is also essential for proper ATRIP localization (Ball et al., 2005). Interestingly, biochemical and electron microscopy analyses have also shown that ATR purified from mammalian cells can interact with duplex DNA and UV-damage DNA (Unsal-Kacmaz et al., 2002). In addition, linearised plasmid stimulates ATR activity *in vitro*, and this stimulation increases when the DNA is damaged by UV or benzo[a]pyrene diol epoxide (Choi et al., 2009; Unsal-Kacmaz et al., 2002). This suggests that ATR can also bind to damaged DNA independently of RPA-ssDNA. However, to date, no DNA-binding domain or region has been identified in ATR (Unsal-Kacmaz et al., 2002). A hint may come from recent research on the HEAT repeat-containing AlkD glycosylase protein from *Bacillus cereus*, where it was shown that this glycosylase binds alkylated and abasic DNA via its HEAT repeats (Rubinson et al., 2010). In this process, the HEATs create a concave surface lined with positively charged residues that mediate electrostatic interactions with the phosphoribose DNA backbone. The AlkD glycosylase does not recognise the DNA lesion directly, rather this protein senses helical distortion created when the damaged base is flipped out into solution. Furthermore, DNA-PK structural studies have shown that HEAT repeats can bind DNA (Sibanda et al., 2010; Williams et al., 2008). Together this evidence could provide a mechanism by which ATR may bind to damaged DNA through its HEAT repeats. This could explain how multiple types of DNA lesion would be recognised by ATR.

#### *1.5.2.3. Kinase activity regulation: Cell cycle activators of Mec1/ATR*

#### *An important role for the dsDNA-ssDNA junctions*

Although RPA-coated ssDNA might be sufficient to localise the Mec1-Ddc2/ATR-ATRIP complex, it is not sufficient for Mec1/ATR activation. In addition, dsDNA-ssDNA junction also has an important role in Mec1/ATR activation. *In vitro* studies using both purified yeast proteins and *Xenopus* egg extracts show that ssDNA annealed with primers, but not ssDNA alone, triggers the activation of Mec1 and its *Xenopus* homologue Xatr (MacDougall et al., 2007; Majka et al., 2006). In yeast, one or more Mec1 activators are independently recruited to these ssDNA-dsDNA junction sites promoting Mec1 kinase activity and phosphorylation of a large number of proteins, including Rfa1 and Rfa2 subunits of RPA, the activators themselves and the downstream effector kinase Rad53 (Navadgi-Patil and Burgers, 2009a). Recent

evidence has shown that these Mec1 activators differ depending on the stage of the cell cycle. The 9-1-1 checkpoint clamp (Ddc1-Rad17-Mec3 in *S. cerevisiae* and Rad9-Rad1-Hus1 in human cells) and the essential replication initiation factor Dpb11 (a BRCA1 C-terminal (BRCT)-domain containing protein homologue to Cut5 in *S. pombe* and TopBp1 in human cells) are two known activators of Mec1 (Figure 1.8). The proper loading of the 9-1-1 complex onto the 5'-ssDNA/dsDNA junctions by the Rad24-RFC complex is required for the activation of the G1 and G2 checkpoints, but its employment differs between these two phases of the cell cycle (Majka et al., 2006; Navadgi-Patil and Burgers, 2009b; Puddu et al., 2011). On the other hand, Dpb11/Cut5/TopBP1, an essential protein for replisome assembly and for the DNA replication checkpoint (Garcia et al., 2005), is only required for *S. cerevisiae* Mec1 activation in G2-phase (Navadgi-Patil and Burgers, 2009b). In contrast, the activation of ATR in *S. pombe* and higher eukaryotes appears to require a single pathway in all cell cycle phases involving both the 9-1-1 complex and the TopBP1/Cut5 protein, a process analogous to *S. cerevisiae* Mec1 activation in G2 phase (Navaddi-Patil and Burgers, 2011).

***Direct activation of Mec1 by the 9-1-1 complex in G1-phase***

Upon DNA damage, RPA restricts the loading of the clamp-like 9-1-1 complex onto the 5'-ss/dsDNA junctions by the loader complex in an ATP-driven reaction (Ellison and Stillman, 2003; Majka and Burgers, 2003; Majka et al., 2006). Although earlier studies in *S. cerevisiae* reported that 9-1-1 complex loading occurs independently of the Mec1-Ddc2 recruitment to RPA-coated ssDNA (Kondo et al., 2001; Majka et al., 2006; Melo et al., 2001; Wu et al., 2005), other studies suggest that the 9-1-1 complex may participate in recruiting Mec1-Ddc2 complex to DSBs (Barlow et al., 2008; Dubrana et al., 2007). This could partly be due to a proposed function of 9-1-1 in recruiting a 5'-exonuclease involved in the generation of 5' junctions at DSBs (Zubko et al., 2004). Multiple nucleases such as Exo1, Dna2, Sae2 and Mre11-Rad50-Xrs2 seem to play a role in this process, however it remains to be determined if any of these nucleases, or perhaps an additional nuclease, are regulated by the 9-1-1 clamp (Mimitou and Symington, 2008; Zhu et al., 2008). In addition, recent evidence in higher cells suggests that the ATR-phosphorylation of the RAD17 Ser635 and Ser645 residues promotes accumulation of 9-1-1 at damaged DNA (Medhurst et al., 2008). Co-localization of the Mec1-Ddc2 and 9-1-1 complexes at

sites of damage facilitate a stable association between Mec1-Ddc2 and Ddc1 subunit, which directly stimulates Mec1 kinase activity *in vitro* and activates the G1 checkpoint *in vivo*. This process has been identified only in *S. cerevisiae* (Bonilla et al., 2008; Majka et al., 2006; Navadgi-Patil and Burgers, 2011). Using physiologically relevant salt concentrations, *in vitro* activation of Mec1 critically depends on the loading of 9-1-1 by Rad24-RFC onto the appropriate DNA substrate. However, at low salt-concentrations, the Ddc1 subunit of the 9-1-1 complex is able to interact with Mec1 and activates its kinase activity even in the absence of DNA, clamp loader or any other clamp subunits, suggesting that the critical motifs for activating Mec1 reside in Ddc1 (Majka et al., 2006). In fact, this was confirmed by the artificial co-localisation of Ddc1 with Mec1 via its Ddc2 subunit by fusing the Ddc1 and Ddc2 to the LacI protein in a strain harbouring a large array of Lac operator sequences. In this system, checkpoint activation even in undamaged conditions was observed (Bonilla et al., 2008). These studies suggested that the minimal requirement for the checkpoint activation is the interaction between Ddc1 and Mec1-Ddc2 complex. Consistent with this, the unstructured C-terminal tail of Ddc1 has a bipartite domain required for Mec1 activation *in vitro* and G1 checkpoint function *in vivo* (Navadgi-Patil and Burgers, 2009b). This bipartite Mec1 activation domain comprises two motifs characterised by a tryptophan residue surrounded by 1 or 2 hydrophobic amino acids. Interestingly, mutation of these two key aromatic residues (W352 and W544) at the C-terminus of Ddc1 abolishes Mec1 activation *in vitro* and G1 checkpoint *in vivo* (Navadgi-Patil and Burgers, 2009b). Remarkably, a small 30-mer peptide comprising the two motifs of Ddc1 was sufficient to activate Mec1 *in vitro*, and the mutation of either tryptophan residue completely abolished this process (Navadgi-Patil and Burgers, 2009b). Interestingly, although the Ddc1 homologues (Rad9 in both *S. pombe* and human cells) have C-terminal tails of various lengths and little sequence conservation, *S. cerevisiae* Mec1 can also be activated by a similar peptide comprising the putative Mec1 activation motifs from *S. pombe* Rad9. This indicates that both the activation motifs and the activation mechanisms for Mec1 might be evolutionarily conserved (Navadgi-Patil and Burgers, 2011). However, the molecular mechanism by which Ddc1 directly activates Mec1 kinase activity is unknown.

***Mec1 activation by both the 9-1-1 complex and Dpb11 in G2-phase***

In the G2/M phase, the 9-1-1 complex activates Mec1 by two mechanisms. One mechanism involves the direct activation of Mec1 by the unstructured C-terminal tail of Ddc1, analogous to G1 phase. The second mechanism involves the recruitment of Dpb11 to sites of damage through an interaction between its C-terminal BRCT domains III and IV with Mec1-dependent phosphorylated Ddc1-T602 (Navadgi-Patil and Burgers, 2008, 2009b). Accordingly, mutational analysis of the Mec1 activation motifs in the Ddc1 subunit of the 9-1-1 complex (*ddc1-2W2A* mutant) which completely abrogates G1 checkpoint activation, revealed that Rad53 phosphorylation was still detected in G2-phase upon DNA damage, although two-fold reduced (Navadgi-Patil and Burgers, 2009b). On the other hand, the same reduction in Rad53 phosphorylation was observed when the T602 residue of Ddc1 was mutated to alanine (T602A). Consistently, a *ddc1-2W2A, T602A* double mutant, defective in both Ddc1-dependent Mec1 activation and Dpb11 recruitment, has defective G2 checkpoint activation, similar to a *ddc1-2W2A dpb11-1* double mutant in which both Mec1 activation domains from Ddc1 and Dpb11 are defective (Navadgi-Patil and Burgers, 2009b).

The Ddc1-dependent recruitment of Dpb11 facilitates the association of the C-terminal AAD (ATR-activating domain) of Dpb11 with the Mec1-Ddc2 complex, a process that is dependent on Dpb11-interacting regions in both Mec1 and Ddc2 and is highly conserved in higher cells (Mordes et al., 2008b). This process then promotes Mec1 kinase activity towards its substrates, including Dpb11 at its T731 residue (Mordes et al., 2008b). This phosphorylated form of Dpb11 serves then as a potent Mec1 activator to further amplify Mec1 kinase activity toward its substrates (Mordes et al., 2008b). Recently, it has been shown that activation of Mec1 by Dpb11 requires its unstructured C-terminal tail, similarly to Ddc1. Moreover, two specific residues in this unstructured tail of Dpb11 (W700 and W735) are important for both interaction with and *in vitro* activation of Mec1 in G2/M phase, similar to the AAD in *Xenopus* TopBP1 (Dpb11 homologue) (Kumagai et al., 2006; Navadgi-Patil et al., 2011). These biochemical studies indicate that 9-1-1 complex and Dpb11 share an analogous mode for Mec1 activation by the intrinsic disordered C-terminal tail of each activator. In addition, it is speculated that the flexible and bipartite features of these Mec1-activating motifs might enable them to make two critical

contacts with Mec1-Ddc2 inducing a conformational change of the kinase complex thereby enhancing its activity (Zou, 2009). However, evidence for such a mechanism is missing. In addition, it is not fully understood why different mechanisms for Mec1 activation exist in different stages of the cell cycle. Most of what is known about regulation of Mec1 activity in G1 and G2 was obtained by *in vitro* studies and it is still unclear if the same modes for Mec1 activation occur *in vivo*.

***The activator in S-phase: still a question mark***

In *S. cerevisiae* it is unclear whether the 9-1-1 complex and Dpb11 are absolutely required for checkpoint activation during S-phase due to the existence of conflicting studies (Berens and Toczyski, 2012; Navadgi-Patil and Burgers, 2009b; Puddu et al., 2011). For instance, it has been shown that *ddc1Δ* cells are sensitive to MMS (methyl methanesulfonate) and UV but not to the replication inhibitor HU (hydroxyurea) (Longhese et al., 1997). This suggests that the 9-1-1 complex is involved in response to DNA damage but not replication stress, although it appears to be required for slowing of S-phase in response to MMS (Paulovich et al., 1997). On the other hand, in a *dpb11-1* mutant (truncated at amino acid 583, lacking almost all the domain required for Mec1 activation), Rad53 is still phosphorylated upon HU treatment (Navadgi-Patil and Burgers, 2009b). This suggests that Dpb11 is dispensible for Mec1 activation in response to replication stress. Furthermore, in the *ddc1Δdpb11-1* double mutant, where the activation functions of both Ddc1 and Dpb11 are eliminated, Rad53 can still be phosphorylated after replication stress. These results suggest the existence of another activator of Mec1 in S-phase, possibly involved in response to replication stress (Navadgi-Patil and Burgers, 2009b). However, recent *in vivo* evidence suggests that the 9-1-1 complex and Dpb11 are required to activate Mec1 independently from each other in S-phase and that the DNA polymerase ε complex together with the replication factor Sld2 are required to establish the Dpb11-dependent branch of Mec1 activation (Puddu et al., 2011).

A possible explanation for the contradictory evidence might come from the fact that Dpb11 has an essential role in replication initiation in addition to its Mec1 activation function as a checkpoint protein (Navadgi-Patil and Burgers, 2011). This makes it difficult to examine the contributions made directly by Dpb11 through Mec1 activation from those made indirectly through its role in the assembly of replication

forks. In fact, the classical and often used *dpb11-1* mutant has defective replication initiation at the permissive and restrictive temperatures (Kamimura et al., 1998). Remarkably, a separation of function *dpb11-601* mutant (truncated at amino acid 601) which has unaffected replication functions and is proficient in activating Mec1, shows an intact replication checkpoint but a compromised G2/M DNA damage checkpoint (Navadgi-Patil et al., 2011). This suggests that the checkpoint function of Dpb11 in activating Mec1 is not essential for a functional replication checkpoint. Therefore, the replication checkpoint defect observed in *dpb11-1* is not a result of a failure by the mutant to activate Mec1 but is likely caused by the replication initiation defect of this allele. Altogether, these data suggest that additional activator(s) of Mec1 exist in the replication checkpoint, but without excluding a role for Ddc1 and Dpb11 in this process, although it is likely to be redundant with additional activator(s).

A recent *in vivo* study using a replication-checkpoint mimic array by artificially co-localising Ddc2 and Mrc1 on chromatin showed that Mec1 can act merely through Mrc1 to phosphorylate Rad53 after acute replication stress even in a *ddc1Δdpb11-1* mutant (Berens and Toczyski, 2012). This suggests that the known Mec1 activators are dispensable in S-phase and that the localization of Mrc1 and Mec1 is the minimal signal required to activate the replication checkpoint. However, this study still does not exclude that an undiscovered, replication-specific Mec1 activator could operate at the stalled replication forks. Therefore, further studies are required to clarify this matter.

***Conservation of mechanisms in S. pombe and higher eukaryotes***

Although Mec1 is activated by various means in yeast, the mechanism behind ATR activation is still obscure in other organisms. In fission and mammalian cells, the 9-1-1 complex and Cut5/TopBP1 protein are required for Rad3/ATR activation through out the cell cycle (Delacroix et al., 2007; Furuya et al., 2004; Kumagai et al., 2006; Lee et al., 2007). However, unlike *S. cerevisiae*, evidence to demonstrate a direct role for Rad9 (Ddc1 homologous) in ATR activation is still lacking, despite the fact that this would be structurally possible (Navadgi-Patil and Burgers, 2009a). Instead, in *S. pombe* and higher eukaryotes, activation of ATR by 9-1-1-recruited TopBP1 appears to be the dominant mechanism, which is highly conserved with that

of Dpb11 in *S. cerevisiae* (Choi et al., 2007; Navadgi-Patil and Burgers, 2008b, Mordes et al., 2008b). For instance, in human cells, TopBP1 interacts with the Rad9 subunit of the 9-1-1 complex (Kumagai et al, 2006), in a process that is mediated by the interaction between phosphorylated S387 residue at the C-terminus of Rad9 (equivalent to the T602 of Ddc1) and the BRCT domains I and II of human TopBP1 (Delacroix et al, 2007; Lee et al, 2007; St Onge et al., 2003). In contrast to budding yeast, S387 of Rad9 is not phosphorylated by ATR in higher cells (St. Onge et al, 2003). It is possible that this residue is constitutively phosphorylated and binds TopBP1 at all cell cycle stages. Interestingly, casein kinase 2 (CK2) has been shown to phosphorylate Rad9, mediating the interaction between the 9-1-1 complex and TopBP1 (Delacroix et al., 2007; Rappas et al., 2011; Takeishi et al, 2010). TopBP1 subsequently binds and activates the ATR-ATRIP complex through its bipartite AAD located between BRCT domains VI and VII (Kumagai et al, 2006). The tryptophan residue in one of the conserved regions is also critical for this process (Kumagai et al., 2006). However, how exactly TopBP1 activates ATR is still unclear. Evidence suggests that TopBP1 binds primarily to a region within ATRIP (301-338 amino acids), but also to ATR. The TopBP1-interacting region in ATR is located in its C-terminus (2483-2597 amino acids) spaning the C-terminal end of the KD and an undefined region between the kinase and FATC domains, which was termed the PIKK regulatory domain (PRD; Mordes et al, 2008b). Mutations in either ATRIP or ATR regions prevent ATR activation (Mordes et al, 2008b). In addition, although initial studies in *Xenopus* and yeast failed to establish a DNA dependence of this Mec1/ATR activation mechanism, studies using purified human checkpoint proteins show that the presence of RPA-coated ssDNA significantly stimulates TopBP1 in the activation of ATR. Moreover, this stimulation is dependent on the interaction between TopBP1 and RPA (Choi et al., 2010). It is important to note that the C-terminus of TopBP1 also lacks a well-defined sructure similar to that of the C-terminal tail in Rad9. This may support an idea that the flexible nature of these protein domains may be important to mediate the respective protein-protein interactions critical for ATR activation. Furthermore, the activation of *S. cerevisiae* Mec1 by the AAD of *Xenopus* TopBP1 supports a strong evolutionary conservation of the mechanisms required for Mec1/ATR activation (Navadgi-Patil and Burgers, 2011).

Interestingly, a recent study has proposed that ATR activation in human cells also involves ATR autophosphorylation after DNA damage (Liu et al., 2011; Nam et al., 2011). Accordingly, ATR autophosphorylation at the Thr1989 residue within the FAT domain is dependent on RPA, ATRIP and ATR kinase activity but surprisingly not on TopBP1 (Liu et al., 2011). The first RPA-ssDNA-dependent step results in accumulation of ATR-ATRIP complexes onto the DNA lesions, promoting *in trans* ATR autophophorylation at Thr1989. Then TopBP1, previously recruited by the 9-1-1 complex, directly recognizes phosphorylated Thr1989 residue via its BRCT domains 7 and 8, leading to stably engage the ATR-ATRIP complex and stimulate the ATR kinase activity (Liu et al., 2011).

In *S. cerevisiae*, a large-scale analysis of all yeast protein kinases activity (Zhu et al., 2000) also showed that Mec1 undergoes auto-phosphorylation, resulting in a four-fold increase in the phosphate content of the protein (Zhu et al., 2000), however the role for this process is still ill defined. It is possible that Mec1 autophosphorylation is also involved in engaging Dpb11 to allow its full activation, analogous to mammalian cells. Unpublished data from the Lowndes laboratory suggested that Mec1 is phosphorylated during a normal cell cycle and further phosphorylated in response to DNA damage (Steffano Maffini, *unpublished results*). Thus, the phosphorylation status of Mec1/ATR seems to be an important factor for the regulation of its kinase activity.

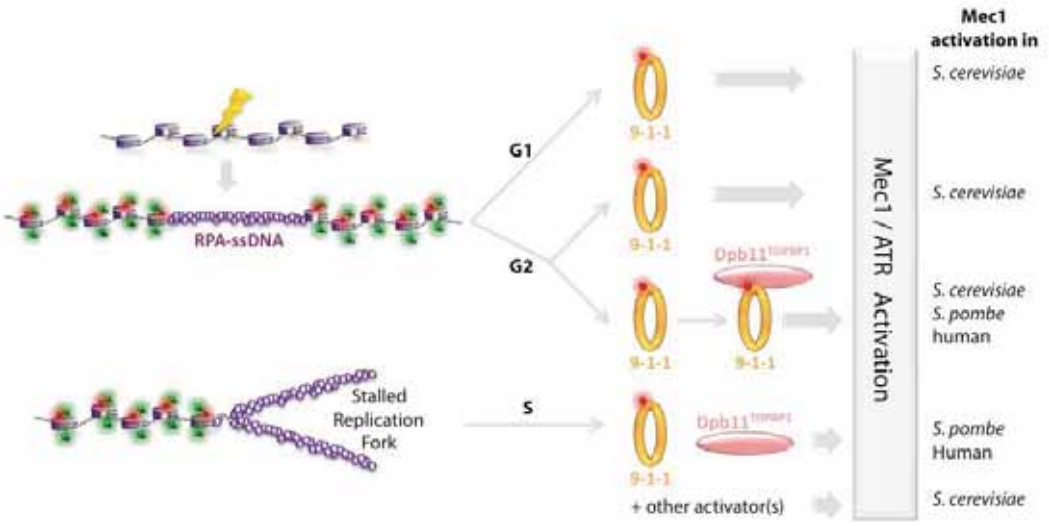


**Figure 1.8: Cell cycle-dependent activation of Mec1/ATR pathways in *S. cerevisiae,* in *S. pombe* and human cells**; different types of signals on DNA are shown dependent on the cell cycle stage (upon DNA damage RPA-ssDNA is commonly formed onto DNA in G1 and G2 phases, while

replication forks stall in the presence of DNA damage in S-phase); 9-1-1 complex and Dpb11$^{TopBP1}$ function in the different checkpoints as shown; Red dot – phosphorylation; Figure adapted from Navadgi-Patil and Burgers, 2011.

### 1.5.3. Mec1-/ATR-dependent checkpoint

#### *1.5.3.1. BRCT-Containing Proteins: Mediating PIKKs signals to the effector checkpoint kinases*

Upon DNA damage or replication stress Mec1/ATR activates the downstream checkpoint effectors. In *S. cerevisiae*, Rad9 mediates the Mec1-dependent phosphorylation of both Rad53 and Chk1 effector kinases after DNA damage in all cell cycle phases, playing an integral role in G1 and G2/M checkpoints and a relatively minor role in the intra-S phase checkpoint (Gilbert et al., 2001; Sanchez et al., 1999; Siede et al., 1993; Sweeney et al., 2005; Weinert and Hartwell, 1988). Note that Rad53 can also be phosphorylated by Tel1, while no evidence exists for Tel1-mediated Chk1 activation (Sanchez et al, 2006). In contrast to *S. cerevisiae*, the role of Rad9's structural and functional homologues BRCA1, 53BP1 and MDC1 proteins in mediating the PIKK-dependent activation of CHK1 and CHK2 in vertebrate cells in still unclear. These mediator proteins comprise a complex and unique family characterized by the presence of C-terminal tandem motifs that were initially identified in BRCA1, thus known as BRCA1 Carboxyl Terminus (BRCT) motifs (Garcia et al., 2005). These domains are highly conserved and function as phosphoprotein-binding domains involved in recruitment to chromatin by interacting with modified histone residues, protein–protein interactions and oligomerization (Manke et al., 2003; Rodriguez et al., 2003; Yu et al., 2003).

Mediators are typically phosphoproteins, phosphorylated by multiple kinases, especially PIKKs upon DNA damage (Cortez et al., 1999; Emili, 1998; Lou et al., 2003; Rappold et al., 2001; Saka et al., 1997; Vialard et al., 1998; Xia et al., 2001; Xu and Stern, 2003). In *S. cerevisiae*, the DNA damage-induced and PIKK-dependent phosphorylation of budding yeast Rad9 is required for its activation and correlates with the remodeling of a large ≥850 kDa Rad9 complex into a smaller 560 kDa complex, containing the DNA damage induced hyperphosphorylated form of Rad9, which mediates the activation of Rad53 (Gilbert et al. 2001; Gilbert et al. 2003) and Rad9 oligomerisation (Usui et al., 2009). In contrast, in vertebrates the

role of PIKK-dependent phosphorylation of mediator proteins has not been elucidated to date.

DNA damage mediators are also frequently phosphorylated during cell cycle progression in the absence of exogenous DNA damage (Esashi and Yanagida, 1999; Jullien et al., 2002; Rappold et al., 2001; Ruffner et al., 1999; Ruffner and Verma, 1997; Usui et al., 2009; Vialard et al., 1998). The 'Rad9-like' mediators share a high number of consensus motifs for phosphorylation by CDKs (S/T-P-x-K/R, where x can be any amino acids, or minimal S/T-P sites) but their functions remain unknown. In *S. cerevisiae*, Rad9 contains an exceptionally high density of such motifs compared to the rest of the yeast proteome (twenty S/T-P sites of which nine conform to the full CDK consensus) (Moses et al., 2007; Ubersax et al., 2003). The mobility of Rad9 during electrophoresis suggests that it is a heavily modified protein and phosphatase-sensitive isoforms of slower mobility have been observed in the S and M phases (Vialard et al., 1998). Note that the Rad9 cell cycle-phosphorylated forms are collectively termed hypophosphorylated Rad9, in order to distinguish them from the DNA damage-inducible hyperphosphorylated form of Rad9 (Vialard et al, 1998; Emili, 1998). Not surprisingly, Rad9 has been identified as an *in vitro* substrate of Cdk1 or Cdc28, the single cyclin-dependent kinase in yeast (Loog and Morgan, 2005; Ubersax et al., 2003). Mass spectrometric studies have supported the *in vivo* phosphorylation of 15 of these CDK consensus sites (Albuquerque et al., 2008; Holt et al., 2009; Smolka et al., 2005). However, the biological role of CDK-dependent phosphorylation of Rad9 remains to be characterised. The function of Rad9 in inhibiting DSBs resection suggests that this protein might be phosphorylated by CDK to control DSB processing. Recent evidence also showed that the recruitment of Rad9 to chromatin through its interaction with Dpb11 requires the CDK-dependent phosphorylation of two CDK sites (S462 and T474) at the central region of Rad9 (Pfander and Diffley, 2011). In addition, phosphorylation of the most N-terminal CDK site of Rad9 (S11) has also been implicated in this process (Granata et al., 2010). Therefore, it is attempting to speculate that CDK phosphorylation of different residues on Rad9 might regulate distinct functions of this protein, however this still needs to be confirmed.

#### *1.5.3.2. PIKK-dependent activation of effector checkpoint kinases*

#### *Rad53/CHK2 activation*

In *S. cerevisiae*, the mechanism of Rad53 activation mediated by Rad9 as described below has been partially reconstituted *in vitro* (Sweeney et al, 2005) and is the best characterised function of Rad9 (Figure 1.9). Following DNA damage, Rad9 is recruited to chromatin via binding of its Tudor and BRCT domains to methylated H3K79 and γ-H2A, respectively (Grenon et al., 2007; Hammet et al., 2007; Huyen et al., 2004). In G2/M phase, an alternative mechanism, dependent on an interaction between the Ddc1 subunit of the 9-1-1 complex and the replication factor Dpb11, can mediate the recruitment of Rad9 to sites of damage in the absence of H3K79me and γ-H2A (Figure 1.9A; (Puddu et al., 2008). Once recruited to sites of damage via one of these two pathways, Rad9 undergoes PIKK-dependent hyperphosphorylation on several residues, including the SQ/TQ sites in its Serine Cluster Domain (SCD) (Emili, 1998; Schwartz et al., 2002; Vialard et al., 1998). This DNA-induced process subsequently promotes the remodeling of a large hypophosphorylated complex (≥850KDa), containing various Rad9 molecules associated with Ssa1/2, into a smaller complex (560KDa) containing hyperphosphorylated Rad9, Ssa1/2 as well as the Rad53 kinase (Figure 1.9B; (Blankley and Lydall, 2004; Emili, 1998; Gilbert et al., 2001; Pellicioli and Foiani, 2005; Sanchez et al., 1999; Sanchez et al., 1996; Schwartz et al., 2002; Sun et al., 1996; Sweeney et al., 2005). It is proposed that Ssa1/Ssa2 proteins facilitate the Mec1-dependent remodelling of the hypophosphorylated Rad9 complex following DNA damage, although this remains to be proven (Gilbert et al., 2003). Mec1-phosphorylated SCD of Rad9 provides a docking site for Rad53, which associates with its two FHA (forkhead-associated) domains (Durocher et al., 1999; Schwartz et al., 2002; Sun et al., 1998; Sweeney et al., 2005). Hyperphosphorylated Rad9 then acts as an adaptor checkpoint protein by bringing Rad53 in close proximity of Mec1 facilitating its Mec1-dependent phosphorylation for its pre-activation (Figure 1.9C; Ma et al., 2006; Sweeney et al, 2005). In addition, Rad9 functions as a catalyst by facilitating the increase of the local concentration of Rad53 molecules allowing its in trans autophosphorylation and full activation (Figure 1.9D; Gilbert et al., 2001; Pellicioli and Foiani, 2005). Rad53 phosphorylation is a key step in the signal transduction cascade and it is generally used as a marker to monitor full checkpoint activation (Pellicioli et al., 1999). Once activated, Rad53 is released from Rad9 through an ATP-dependent

mechanism after which it is able to phosphorylate the nuclear targets responsible for the numerous responses to DNA damage (Figure 1.9E; Gilbert et al., 2001; Pellicioli and Foiani, 2005). As well as mediating the interaction between Rad9 and Rad53, PIKK-dependent phosphorylation of the Rad9 SCD promotes Rad9 oligomerisation at sites of damage via an interaction between the BRCT domains of Rad9 and the phosphorylated SCD (Usui et al., 2009). Although Rad9 oligomerisation appears to be dispensable for initial Rad53 activation, it is required for the maintenance of Rad53 activation and the checkpoint-induced cell cycle arrest (Usui et al., 2009). DNA damage-induced Rad9 oligomerisation promotes its accumulation at sites of damage, allowing amplification of the DNA damage signal and sustained activation of Rad53 (Usui et al., 2009). It is proposed that a feedback loop, in which fully activated Rad53 phosphorylates the Rad9 tandem BRCT domains to attenuate the BRCT-SCD interaction, mediates the turnover of hyperphosphorylated Rad9 by promoting its dissociation from sites of damage (Usui et al., 2009). Interestingly, in vertebrates, CHK2 is also known to undergo ATM-dependent activation by a two-step mechanism involving dimerization and trans-autophosphorylation, but a molecular role for DNA damage mediators in this activation remains to be investigated (Smith et al., 2010).

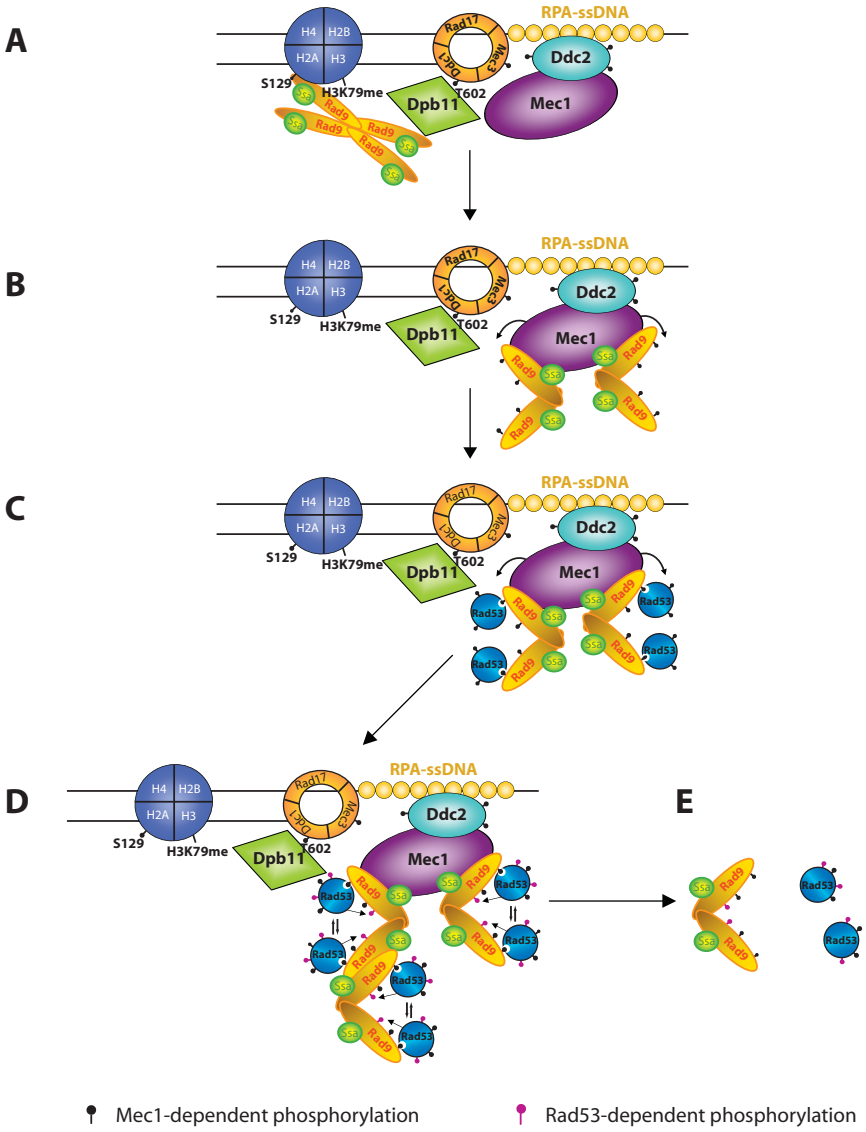


**Figure 1.9: Rad9 complex remodelling and Rad53 activation.** (A) Following DSB creation, the Mec1-Ddc2 and hypophosphorylated Rad9 complexes are recruited to the site of damage. (B) Mec1-dependent hyperphosphorylation of Rad9 mediates a conformational change in the Rad9 complex, which facilitates Rad53 binding. (C) The Rad9 complex acts as a molecular adaptor bringing Rad53 into close proximity to Mec1, thus facilitating Mec1-dependent Rad53 phosphorylation. (D) The Rad9 complex also functions as a molecular scaffold, bringing "primed" Rad53 molecules into close proximity, facilitating Rad53 in trans autophosphorylation. (E) Activated Rad53 is then released from the Rad9 complex in an ATP-dependent manner, and phosphorylates Rad9 to inhibit further oligomerisation. Figure adapted from Gilbert et al., 2001.

***Chk1 activation***

Activation of Chk1 appears well conserved from yeast to human, requiring phosphorylation by the ATR kinase that in turn depends upon various DNA damage mediators, which bring Chk1 into close proximity of ATR (Stracker et al., 2009). In addition, in contrast to Rad53/CHK2, Chk1/CHK1 seems to autophosphorylate *in cis* upon DNA damage (Chen et al., 2009). In vertebrates, it is well established that the ATR-dependent activation of CHK1 is mediated by the adaptor protein Claspin (scMrc1) and occurs primarily in response to replication stress and UV-induced DNA damage (Chen and Sanchez, 2004; Smits et al., 2010). Claspin is recruited to the ATR-phosphorylated Rad17 subunit of the RAD17-RFC complex, an interaction important for sustaining Chk1 phosphorylation (Wang et al., 2006). The association of Claspin with Chk1 is then regulated by the phosphorylation of at least two residues (T817 and S819) within two conserved and repeated phosphopeptide motifs of Claspin by ATR, the basal activity of Chk1 itself and perhaps by other ATR-dependent kinases (Chini and Chen, 2003, 2004, 2006; Kumagai et al., 2004; Yoo et al., 2006). The DNA damage dependent Claspin-Chk1 interaction brings ATR and Chk1 into proximity, promoting ATR-dependent phosphorylation of Chk1 (Chini and Chen, 2003; Kumagai and Dunphy, 2000; Osborn and Elledge, 2003). ATR-dependent phosphorylation of Chk1 at multiple sites, including serines 317, 345 and 366, within its C-terminal regulatory domain, promotes CHK1 activaton by inducing a conformational change that relieves the inhibition of the N-terminal kinase domain by the C-terminal regulatory domain (Kumagai et al., 2004; Liu et al., 2000; Walker et al., 2009; Walworth and Bernards, 1996; Zhao and Piwnica-Worms, 2001). In *S. pombe* the equivalent S345 mutant (S345A) was found to be damage sensitive and DNA damage checkpoint defective (Jiang et al., 2003; Lopez-Girona et al., 2001). ATR-dependent Chk1 phosphorylation also directs Chk1 dissociation from chromatin, a process shown to be required for efficient DNA-damage induced checkpoint activation (Smits et al., 2006).

In addition to Claspin, BRCA1 and MDC1 adaptor proteins have been implicated in Chk1 activation, since deficiency in these proteins impacts upon Chk1 phosphorylation after DNA damage (Lin et al., 2004; Smits et al., 2010; Stewart et al., 2003; Stracker et al., 2009; Yamane et al., 2003). However, the mechanisms behind this process are still unclear.

In *S. cerevisiae*, Mrc1, the Claspin orthologue, seems to mainly control Rad53 activation in the DNA replication checkpoint (Tanaka, 2010) and a role in Chk1 activation remains to be reported. Chk1 only becomes activated under replication stress when Mrc1 is absent and the replication stress signal is converted into a DNA damage signal (Alcasabas et al., 2001; Foss, 2001), leading to Rad9-mediated activation of both Rad53 and Chk1 (Alcasabas et al., 2001). Accordingly, in both budding and fission yeasts the prototypical mediator, Rad9/Crb2, has also been implicated in Chk1 activation after DNA damage (Blankley and Lydall, 2004). However, the mechanism underlying this process is poorly understood. In *S. pombe*, the N-terminal region of Crb2 comprises a domain required for Chk1 activation, the so called Chk1 activation domain (CAD), and that shares sequence homology to the same region of Rad9 in budding yeast. Moreover, Chk1 activation seems to be dependent on the cell cycle phosphorylation of Crb2 CAD, as well as on the interaction with Cut5 (Dpb11/TopBP1 homologue) (Mochida et al., 2004; Saka et al., 1997). Interestingly, it has been shown that the CAD of Rad9 (mapped to the first 231 amino acids in its N-terminus) is also required for Chk1 activation (Saka et al., 1997, Blankly and Lydall 2004). In addition, a yeast-two hybrid interaction between Rad9 and Chk1 has been reported (Uetz et al., 2000) and this interaction appears to be distinctly regulated by the Rad9-Rad53 interaction since it is independent of the Rad9 SCD (Schwartz et al., 2002). However, mechanistic evidence supporting this mode of Chk1 activation mediated by Rad9 are still missing since these studies have not been corroborated by other biochemical assays to date.

Overall, in all organisms, the apical PIK kinases together with DDR mediator proteins have important roles in the regulation of Chk1, although the molecular mechanisms of this regulation require further exploration.

### 1.6. WORKING HYPOTHESIS / AIM OF THIS WORK

Mec1, the ATR ortologue, is the master regulator of the DNA damage checkpoints in *Saccharomyces cerevisiae*. This kinase is a member of the PIKK family due to the presence of conserved kinase, FAT and FATC domains in its C-terminus. In addition, tandem helical motifs, called HEAT repeats, make up most of the non-kinase portion of Mec1 and other PIKKs. However, the role of these HEAT repeats in PIKK functions is ill understood. Furthermore, although many studies have been carried out to understand the regulation of Mec1 kinase activity *in vitro*, not a lot is known about its regulation *in vivo*, substrate specificity and specific interactions. Based on studies in other HEAT-rich proteins, we hypothesise that HEAT repeats mediate PIKK-protein interactions. In one part of this study, we are interested in the structure-function relationship of Mec1 protein (Chapter 2). The aim of this project was to investigate which HEAT repeats are required for protein-protein interactions involved in the essential and DDR functions of Mec1 and assign specific functions to specific HEATs of Mec1. In order to do so, we have used the genetically tractable *S. cerevisiae* system to generate six internal deletions of *MEC1*, termed 'window deletion' mutants, where a single or multiple HEATs spanning most of the primary sequence of the protein are missing. To investigate the role of the deleted HEAT repeats in Mec1 functions, we used cellular and biochemical techniques to examine the DNA damage checkpoint activation, DNA repair and dNTP homeostasis in the window deletion mutants. Furthermore, to determine if specific HEATs of Mec1 share specific functions or structural features with other PIKKs, we generated hybrid *mec1* mutants by replacing the deleted Mec1 regions with the equivalent HEATs from the homologous and related PIKKs, ATR and Tel1 respectively. To examine if HEAT-replacements sustain Mec1 DDR and essential functions, DNA damage sensitivity assay and dNTP regulation analysis were performed in the hybrid mutants. The understanding of Mec1 molecular and biochemical functions and its activity regulation is fundamental to enlighten the regulation of the PIKK-dependent DNA Damage Response in higher cells.

The Rad9 checkpoint protein also plays a pivotal role in the DNA damage response. Although the PIK kinase- and Rad9-dependent mechanism of Rad53 activation has been well described ((Blankley and Lydall, 2004; Gilbert et al., 2001; Schwartz et al., 2002), the mechanism of activation of Chk1 is not well understood. Thus,

another major objective of this project was to address the question of how Chk1 is activated in budding yeast (Chapter 3). Rad9 is extensively phosphorylated in a CDK-dependent manner during a normal cell cycle, and hyperphosphorylated in a Mec1/Tel1-dependent manner following DNA damage (Emili, 1998; Vialard et al., 1998; N. Lowndes, *unpublished data*). Rad9 contains 20 putative sites for phosphorylation by Cdc28, and is a CDK substrate (Ubersax et al., 2003). Furthermore, the N-terminal CAD region, corresponding to the first 231 amino acids, is known to be required for Chk1-specific checkpoint (Blankley and Lydall, 2004). A mechanistic clue as to how Chk1 is activated comes from the reported interaction between Rad9 and Chk1 using a single technique; yeast two-hybrid analysis, and is only reported as "*data not shown*" (Sanchez et al., 1999). Additionally, we noticed that almost half of the putative CDK sites in Rad9 are concentrated in the N-terminal CAD accounting for less than a fifth of the Rad9 protein. Based on these data and on studies from *S. pombe*, we hypothesise that the CDK-dependent phosphorylation of the CAD region of Rad9 is required for Chk1 activation. To test this, biochemical and molecular techniques were employed to examine cell cycle progression, DNA damage checkpoint activation, and DNA damage sensitivity in $rad9^{CDK}$ mutant strains. To determine which cyclin-Cdc28 complex preferentially phosphorylates Rad9 CAD, phosphorylation of this region was also examined by *in vitro* kinase assays. We also examined whether Cdc28-dependent phosphorylation of the Rad9 CAD regulates a physical interaction between Rad9 and Chk1 and if all CDK sites or only one site in this region is required for this interaction. Biochemical and molecular techniques, including yeast two-hybrid and immunoprecipitation analyses were employed to address these questions.

## 1.7. REFERENCES


Abraham, R.T. (2004). PI 3-kinase related kinases: 'big' players in stress-induced signaling pathways. DNA Repair (Amst) *3*, 883-887.

Albuquerque, C.P., Smolka, M.B., Payne, S.H., Bafna, V., Eng, J., and Zhou, H. (2008). A multidimensional chromatography technology for in-depth phosphoproteome analysis. Mol Cell Proteomics *7*, 1389-1396.

Alcasabas, A.A., Osborn, A.J., Bachant, J., Hu, F., Werler, P.J., Bousset, K., Furuya, K., Diffley, J.F., Carr, A.M., and Elledge, S.J. (2001). Mrc1 transduces signals of DNA replication stress to activate Rad53. Nat Cell Biol *3*, 958-965.

Andrade, M.A., and Bork, P. (1995). HEAT repeats in the Huntington's disease protein. Nat Genet *11*, 115-116.

Andrade, M.A., Perez-Iratxeta, C., and Ponting, C.P. (2001a). Protein repeats: structures, functions, and evolution. J Struct Biol *134*, 117-131.

Andrade, M.A., Petosa, C., O'Donoghue, S.I., Muller, C.W., and Bork, P. (2001b). Comparison of ARM and HEAT protein repeats. J Mol Biol *309*, 1-18.

Ball, H.L., Myers, J.S., and Cortez, D. (2005). ATRIP binding to replication protein A-single-stranded DNA promotes ATR-ATRIP localization but is dispensable for Chk1 phosphorylation. Mol Biol Cell *16*, 2372-2381.

Bartkova, J., Bakkenist, C.J., Rajpert-De Meyts, E., Skakkebaek, N.E., Sehested, M., Lukas, J., Kastan, M.B., and Bartek, J. (2005). ATM activation in normal human tissues and testicular cancer. Cell Cycle *4*, 838-845.

Bayliss, R., Littlewood, T., and Stewart, M. (2000). Structural basis for the interaction between FxFG nucleoporin repeats and importin-beta in nuclear trafficking. Cell *102*, 99-108.

Bensimon, A., Aebersold, R., and Shiloh, Y. (2011). Beyond ATM: the protein kinase landscape of the DNA damage response. FEBS Lett *585*, 1625-1639.

Berens, T.J., and Toczyski, D.P. (2012). Colocalization of Mec1 and Mrc1 is sufficient for Rad53 phosphorylation in vivo. Mol Biol Cell *23*, 1058-1067.

Blankley, R.T., and Lydall, D. (2004). A domain of Rad9 specifically required for activation of Chk1 in budding yeast. J Cell Sci *117*, 601-608.

Blunt, T., Gell, D., Fox, M., Taccioli, G.E., Lehmann, A.R., Jackson, S.P., and Jeggo, P.A. (1996). Identification of a nonsense mutation in the carboxyl-terminal region of DNA-dependent protein kinase catalytic subunit in the scid mouse. Proc Natl Acad Sci U S A *93*, 10285-10290.

Bomgarden, R.D., Yean, D., Yee, M.C., and Cimprich, K.A. (2004). A novel protein activity mediates DNA binding of an ATR-ATRIP complex. J Biol Chem *279*, 13346-13353.

Boskovic, J., Rivera-Calzada, A., Maman, J.D., Chacon, P., Willison, K.R., Pearl, L.H., and Llorca, O. (2003). Visualization of DNA-induced conformational changes in the DNA repair kinase DNA-PKcs. EMBO J *22*, 5875-5882.

Bosotti, R., Isacchi, A., and Sonnhammer, E.L. (2000). FAT: a novel domain in PIK-related kinases. Trends Biochem Sci *25*, 225-227.

Branzei, D., and Foiani, M. (2008). Regulation of DNA repair throughout the cell cycle. Nat Rev Mol Cell Biol *9*, 297-308.

Brewerton, S.C., Dore, A.S., Drake, A.C., Leuther, K.K., and Blundell, T.L. (2004). Structural analysis of DNA-PKcs: modelling of the repeat units and insights into the detailed molecular architecture. J Struct Biol *145*, 295-306.

Casper, A.M., Nghiem, P., Arlt, M.F., and Glover, T.W. (2002). ATR regulates fragile site stability. Cell *111*, 779-789.

Cavalieri, S., Funaro, A., Porcedda, P., Turinetto, V., Migone, N., Gatti, R.A., and Brusco, A. (2006). ATM mutations in Italian families with ataxia telangiectasia include two distinct large genomic deletions. Hum Mutat *27*, 1061.

Chen, S., Paul, P., and Price, B.D. (2003). ATM's leucine-rich domain and adjacent sequences are essential for ATM to regulate the DNA damage response. Oncogene *22*, 6332-6339.

Chen, Y., Caldwell, J.M., Pereira, E., Baker, R.W., and Sanchez, Y. (2009). ATRMec1 phosphorylation-independent activation of Chk1 in vivo. J Biol Chem *284*, 182-190.

Chen, Y., and Sanchez, Y. (2004). Chk1 in the DNA damage response: conserved roles from yeasts to mammals. DNA Repair (Amst) *3*, 1025-1032.

Chini, C.C., and Chen, J. (2003). Human claspin is required for replication checkpoint control. J Biol Chem *278*, 30057-30062.

Chini, C.C., and Chen, J. (2004). Claspin, a regulator of Chk1 in DNA replication stress pathway. DNA Repair (Amst) *3*, 1033-1037.

Chini, C.C., and Chen, J. (2006). Repeated phosphopeptide motifs in human Claspin are phosphorylated by Chk1 and mediate Claspin function. J Biol Chem *281*, 33276-33282.

Chiu, C.Y., Cary, R.B., Chen, D.J., Peterson, S.R., and Stewart, P.L. (1998). Cryo-EM imaging of the catalytic subunit of the DNA-dependent protein kinase. J Mol Biol *284*, 1075-1081.

Choi, J.H., Lindsey-Boltz, L.A., and Sancar, A. (2009). Cooperative activation of the ATR checkpoint kinase by TopBP1 and damaged DNA. Nucleic Acids Res *37*, 1501-1509.

Chook, Y.M., and Blobel, G. (1999). Structure of the nuclear transport complex karyopherin-beta2-Ran x GppNHp. Nature *399*, 230-237.

Cimprich, K.A., and Cortez, D. (2008). ATR: an essential regulator of genome integrity. Nat Rev Mol Cell Biol *9*, 616-627.

Cingolani, G., Petosa, C., Weis, K., and Muller, C.W. (1999). Structure of importin-beta bound to the IBB domain of importin-alpha. Nature *399*, 221-229.

Clemenson, C., and Marsolier-Kergoat, M.C. (2009). DNA damage checkpoint inactivation: adaptation and recovery. DNA Repair (Amst) *8*, 1101-1109.

Cobb, J.A., Schleker, T., Rojas, V., Bjergbaek, L., Tercero, J.A., and Gasser, S.M. (2005). Replisome instability, fork collapse, and gross chromosomal rearrangements arise synergistically from Mec1 kinase and RecQ helicase mutations. Genes Dev *19*, 3055-3069.

Cortez, D., Wang, Y., Qin, J., and Elledge, S.J. (1999). Requirement of ATM-dependent phosphorylation of brca1 in the DNA damage response to double-strand breaks. Science *286*, 1162-1166.

Cortez, D., Guntuku, S., Qin, J., and Elledge, S.J. (2001). ATR and ATRIP: partners in checkpoint signaling. Science *294*, 1713-1716.

Critchlow, S.E., and Jackson, S.P. (1998). DNA end-joining: from yeast to man. Trends Biochem Sci *23*, 394-398.

d'Adda di Fagagna, F., Reaper, P.M., Clay-Farrace, L., Fiegler, H., Carr, P., Von Zglinicki, T., Saretzki, G., Carter, N.P., and Jackson, S.P. (2003). A DNA damage checkpoint response in telomere-initiated senescence. Nature *426*, 194-198.

De Piccoli, G., Katou, Y., Itoh, T., Nakato, R., Shirahige, K., and Labib, K. (2012). Replisome stability at defective DNA replication forks is independent of s phase checkpoint kinases. Mol Cell *45*, 696-704.

Downs, J.A., Lowndes, N.F., and Jackson, S.P. (2000). A role for Saccharomyces cerevisiae histone H2A in DNA repair. Nature *408*, 1001-1004.

Doyon, Y., and Cote, J. (2004). The highly conserved and multifunctional NuA4 HAT complex. Curr Opin Genet Dev *14*, 147-154.

Durkin, S.G., Arlt, M.F., Howlett, N.G., and Glover, T.W. (2006). Depletion of CHK1, but not CHK2, induces chromosomal instability and breaks at common fragile sites. Oncogene *25*, 4381-4388.

Durocher, D., Henckel, J., Fersht, A.R., and Jackson, S.P. (1999). The FHA domain is a modular phosphopeptide recognition motif. Mol Cell *4*, 387-394.

Emili, A. (1998). MEC1-dependent phosphorylation of Rad9p in response to DNA damage. Mol Cell *2*, 183-189.

Esashi, F., and Yanagida, M. (1999). Cdc2 phosphorylation of Crb2 is required for reestablishing cell cycle progression after the damage checkpoint. Mol Cell *4*, 167-174.

Fitz Gerald, J.N., Benjamin, J.M., and Kron, S.J. (2002). Robust G1 checkpoint arrest in budding yeast: dependence on DNA damage signaling and repair. J Cell Sci *115*, 1749-1757.

Foss, E.J. (2001). Tof1p regulates DNA damage responses during S phase in Saccharomyces cerevisiae. Genetics *157*, 567-577.

Friedel, A.M., Pike, B.L., and Gasser, S.M. (2009). ATR/Mec1: coordinating fork stability and repair. Curr Opin Cell Biol *21*, 237-244.

Garcia, V., Furuya, K., and Carr, A.M. (2005). Identification and functional analysis of TopBP1 and its homologs. DNA Repair (Amst) *4*, 1227-1239.

Gilbert, C.S., Green, C.M., and Lowndes, N.F. (2001). Budding yeast Rad9 is an ATP-dependent Rad53 activating machine. Mol Cell *8*, 129-136.

Gorgoulis, V.G., Vassiliou, L.V., Karakaidos, P., Zacharatos, P., Kotsinas, A., Liloglou, T., Venere, M., Ditullio, R.A., Jr., Kastrinakis, N.G., Levy, B*., et al.* (2005). Activation of the DNA damage checkpoint and genomic instability in human precancerous lesions. Nature *434*, 907-913.

Granata, M., Lazzaro, F., Novarina, D., Panigada, D., Puddu, F., Abreu, C.M., Kumar, R., Grenon, M., Lowndes, N.F., Plevani, P.*, et al.* (2010). Dynamics of Rad9 Chromatin Binding and Checkpoint Function Are Mediated by Its Dimerization and Are Cell Cycle-Regulated by CDK1 Activity. PLoS Genet *6*.

Grenon, M., Costelloe, T., Jimeno, S., O'Shaughnessy, A., Fitzgerald, J., Zgheib, O., Degerth, L., and Lowndes, N.F. (2007). Docking onto chromatin via the Saccharomyces cerevisiae Rad9 Tudor domain. Yeast *24*, 105-119.

Grinthal, A., Adamovic, I., Weiner, B., Karplus, M., and Kleckner, N. (2010). PR65, the HEAT-repeat scaffold of phosphatase PP2A, is an elastic connector that links force and catalysis. Proc Natl Acad Sci U S A *107*, 2467-2472.

Groves, M.R., and Barford, D. (1999). Topological characteristics of helical repeat proteins. Curr Opin Struct Biol *9*, 383-389.

Groves, M.R., Hanlon, N., Turowski, P., Hemmings, B.A., and Barford, D. (1999). The structure of the protein phosphatase 2A PR65/A subunit reveals the conformation of its 15 tandemly repeated HEAT motifs. Cell *96*, 99-110.

Guo, Z., Deshpande, R., and Paull, T.T. (2010). ATM activation in the presence of oxidative stress. Cell Cycle *9*, 4805-4811.

Halazonetis, T.D., Gorgoulis, V.G., and Bartek, J. (2008). An oncogene-induced DNA damage model for cancer development. Science *319*, 1352-1355.

Hammet, A., Magill, C., Heierhorst, J., and Jackson, S.P. (2007). Rad9 BRCT domain interaction with phosphorylated H2AX regulates the G1 checkpoint in budding yeast. EMBO Rep *8*, 851-857.

Hanahan, D., and Weinberg, R.A. (2011). Hallmarks of cancer: the next generation. Cell *144*, 646-674.

Hansel, D.E., Meeker, A.K., Hicks, J., De Marzo, A.M., Lillemoe, K.D., Schulick, R., Hruban, R.H., Maitra, A., and Argani, P. (2006). Telomere length variation in biliary tract metaplasia, dysplasia, and carcinoma. Mod Pathol *19*, 772-779.

Harper, J.W., and Elledge, S.J. (2007). The DNA damage response: ten years after. Mol Cell *28*, 739-745.

Harrison, J.C., and Haber, J.E. (2006). Surviving the breakup: the DNA damage checkpoint. Annu Rev Genet *40*, 209-235.

Hartwell, L.H., and Kastan, M.B. (1994). Cell cycle control and cancer. Science *266*, 1821-1828.

Hiom, K. (2010). Coping with DNA double strand breaks. DNA Repair (Amst) *9*, 1256-1263.

Holt, L.J., Tuch, B.B., Villen, J., Johnson, A.D., Gygi, S.P., and Morgan, D.O. (2009). Global analysis of Cdk1 substrate phosphorylation sites provides insights into evolution. Science *325*, 1682-1686.

Huertas, D., Sendra, R., and Munoz, P. (2009). Chromatin dynamics coupled to DNA repair. Epigenetics *4*, 31-42.

Huyen, Y., Zgheib, O., Ditullio, R.A., Jr., Gorgoulis, V.G., Zacharatos, P., Petty, T.J., Sheston, E.A., Mellert, H.S., Stavridi, E.S., and Halazonetis, T.D. (2004). Methylated lysine 79 of histone H3 targets 53BP1 to DNA double-strand breaks. Nature *432*, 406-411.

Jiang, K., Pereira, E., Maxfield, M., Russell, B., Goudelock, D.M., and Sanchez, Y. (2003). Regulation of Chk1 includes chromatin association and 14-3-3 binding following phosphorylation on Ser345. J Biol Chem.

Jiang, X., Sun, Y., Chen, S., Roy, K., and Price, B.D. (2006). The FATC domains of PIKK proteins are functionally equivalent and participate in the Tip60-dependent activation of DNA-PKcs and ATM. J Biol Chem *281*, 15741-15746.

Jullien, D., Vagnarelli, P., Earnshaw, W.C., and Adachi, Y. (2002). Kinetochore localisation of the DNA damage response component 53BP1 during mitosis. J Cell Sci *115*, 71-79.

Kamimura, Y., Masumoto, H., Sugino, A., and Araki, H. (1998). Sld2, which interacts with Dpb11 in Saccharomyces cerevisiae, is required for chromosomal DNA replication. Mol Cell Biol *18*, 6102-6109.

Kerzendorfer, C., and O'Driscoll, M. (2009). Human DNA damage response and repair deficiency syndromes: linking genomic instability and cell cycle checkpoint proficiency. DNA Repair (Amst) *8*, 1139-1152.

Kumagai, A., and Dunphy, W.G. (2000). Claspin, a novel protein required for the activation of Chk1 during a DNA replication checkpoint response in Xenopus egg extracts. Mol Cell *6*, 839-849.

Kumagai, A., Kim, S.M., and Dunphy, W.G. (2004). Claspin and the activated form of ATR-ATRIP collaborate in the activation of Chk1. J Biol Chem *279*, 49599-49608.

Lempiainen, H., and Halazonetis, T.D. (2009). Emerging common themes in regulation of PIKKs and PI3Ks. EMBO J *28*, 3067-3073.

Lengronne, A., and Schwob, E. (2002). The yeast CDK inhibitor Sic1 prevents genomic instability by promoting replication origin licensing in late G(1). Mol Cell *9*, 1067-1078.

Lin, S.Y., Li, K., Stewart, G.S., and Elledge, S.J. (2004). Human Claspin works with BRCA1 to both positively and negatively regulate cell proliferation. Proc Natl Acad Sci U S A *101*, 6484-6489.

Lindahl, T. (1993). Instability and decay of the primary structure of DNA. Nature *362*, 709-715.

Lisby, M., and Rothstein, R. (2009). Choreography of recombination proteins during the DNA damage response. DNA Repair (Amst) *8*, 1068-1076.

Liu, Q., Guntuku, S., Cui, X.S., Matsuoka, S., Cortez, D., Tamai, K., Luo, G., Carattini-Rivera, S., DeMayo, F., Bradley, A.*, et al.* (2000). Chk1 is an essential kinase that is regulated by Atr and required for the G(2)/M DNA damage checkpoint. Genes Dev *14*, 1448-1459.

Liu, S., Shiotani, B., Lahiri, M., Marechal, A., Tse, A., Leung, C.C., Glover, J.N., Yang, X.H., and Zou, L. (2011). ATR autophosphorylation as a molecular switch for checkpoint activation. Mol Cell *43*, 192-202.

Longhese, M.P., Clerici, M., and Lucchini, G. (2003). The S-phase checkpoint and its regulation in Saccharomyces cerevisiae. Mutat Res *532*, 41-58.

Longhese, M.P., Paciotti, V., Fraschini, R., Zaccarini, R., Plevani, P., and Lucchini, G. (1997). The novel DNA damage checkpoint protein ddc1p is phosphorylated periodically during the cell cycle and in response to DNA damage in budding yeast. Embo J *16*, 5216-5226.

Loog, M., and Morgan, D.O. (2005). Cyclin specificity in the phosphorylation of cyclin-dependent kinase substrates. Nature *434*, 104-108.

Lopez-Girona, A., Tanaka, K., Chen, X.B., Baber, B.A., McGowan, C.H., and Russell, P. (2001). Serine-345 is required for Rad3-dependent phosphorylation and function of checkpoint kinase Chk1 in fission yeast. Proc Natl Acad Sci U S A *98*, 11289-11294.

Lou, Z., Chini, C.C., Minter-Dykhouse, K., and Chen, J. (2003). Mediator of DNA damage checkpoint protein 1 regulates BRCA1 localization and phosphorylation in DNA damage checkpoint control. J Biol Chem *278*, 13599-13602.

Lovejoy, C.A., and Cortez, D. (2009). Common mechanisms of PIKK regulation. DNA Repair (Amst) *8*, 1004-1008.

Majka, J., and Burgers, P.M. (2007). Clamping the Mec1/ATR checkpoint kinase into action. Cell Cycle *6*, 1157-1160.

Manke, I.A., Lowery, D.M., Nguyen, A., and Yaffe, M.B. (2003). BRCT repeats as phosphopeptide-binding modules involved in protein targeting. Science *302*, 636-639.

Mantiero, D., Clerici, M., Lucchini, G., and Longhese, M.P. (2007). Dual role for Saccharomyces cerevisiae Tel1 in the checkpoint response to double-strand breaks. EMBO Rep *8*, 380-387.

Martin, D.E., and Hall, M.N. (2005). The expanding TOR signaling network. Curr Opin Cell Biol *17*, 158-166.

Maser, R.S., and DePinho, R.A. (2002). Keeping telomerase in its place. Nat Med *8*, 934-936.

Maya-Mendoza, A., Petermann, E., Gillespie, D.A., Caldecott, K.W., and Jackson, D.A. (2007). Chk1 regulates the density of active replication origins during the vertebrate S phase. EMBO J *26*, 2719-2731.

Medhurst, A.L., Warmerdam, D.O., Akerman, I., Verwayen, E.H., Kanaar, R., Smits, V.A., and Lakin, N.D. (2008). ATR and Rad17 collaborate in modulating Rad9 localisation at sites of DNA damage. J Cell Sci *121*, 3933-3940.

Mochida, S., Esashi, F., Aono, N., Tamai, K., O'Connell, M.J., and Yanagida, M. (2004). Regulation of checkpoint kinases through dynamic interaction with Crb2. Embo J *23*, 418-428.

Mordes, D.A., Glick, G.G., Zhao, R., and Cortez, D. (2008a). TopBP1 activates ATR through ATRIP and a PIKK regulatory domain. Genes Dev *22*, 1478-1489.

Mordes, D.A., Nam, E.A., and Cortez, D. (2008b). Dpb11 activates the Mec1-Ddc2 complex. Proc Natl Acad Sci U S A *105*, 18730-18734.

Morgan, S.E., Lovly, C., Pandita, T.K., Shiloh, Y., and Kastan, M.B. (1997). Fragments of ATM which have dominant-negative or complementing activity. Mol Cell Biol *17*, 2020-2029.

Moses, A.M., Heriche, J.K., and Durbin, R. (2007). Clustering of phosphorylation site recognition motifs can be exploited to predict the targets of cyclin-dependent kinase. Genome Biol *8*, R23.

Myung, K., and Kolodner, R.D. (2002). Suppression of genome instability by redundant S-phase checkpoint pathways in Saccharomyces cerevisiae. Proc Natl Acad Sci U S A *99*, 4500-4507.

Nakada, D., Hirano, Y., Tanaka, Y., and Sugimoto, K. (2005). Role of the C terminus of Mec1 checkpoint kinase in its localization to sites of DNA damage. Mol Biol Cell *16*, 5227-5235.

Nakada, D., Matsumoto, K., and Sugimoto, K. (2003). ATM-related Tel1 associates with double-strand breaks through an Xrs2-dependent mechanism. Genes Dev *17*, 1957-1962.

Nam, E.A., Zhao, R., Glick, G.G., Bansbach, C.E., Friedman, D.B., and Cortez, D. (2011). Thr-1989 phosphorylation is a marker of active ataxia telangiectasia-mutated and Rad3-related (ATR) kinase. J Biol Chem *286*, 28707-28714.

Navadgi-Patil, V.M., and Burgers, P.M. (2009a). A tale of two tails: activation of DNA damage checkpoint kinase Mec1/ATR by the 9-1-1 clamp and by Dpb11/TopBP1. DNA Repair (Amst) *8*, 996-1003.

Navadgi-Patil, V.M., and Burgers, P.M. (2009b). The unstructured C-terminal tail of the 9-1-1 clamp subunit Ddc1 activates Mec1/ATR via two distinct mechanisms. Mol Cell *36*, 743-753.

Navadgi-Patil, V.M., and Burgers, P.M. (2011). Cell-cycle-specific activators of the Mec1/ATR checkpoint kinase. Biochem Soc Trans *39*, 600-605.

Osborn, A.J., and Elledge, S.J. (2003). Mrc1 is a replication fork component whose phosphorylation in response to DNA replication stress activates Rad53. Genes Dev *17*, 1755-1767.

Paulovich, A.G., and Hartwell, L.H. (1995). A checkpoint regulates the rate of progression through S phase in S. cerevisiae in response to DNA damage. Cell *82*, 841-847.

Pellicioli, A., and Foiani, M. (2005). Signal transduction: how rad53 kinase is activated. Curr Biol *15*, R769-771.

Pellicioli, A., Lucca, C., Liberi, G., Marini, F., Lopes, M., Plevani, P., Romano, A., Di Fiore, P.P., and Foiani, M. (1999). Activation of Rad53 kinase in response to DNA damage and its effect in modulating phosphorylation of the lagging strand DNA polymerase. Embo J *18*, 6561-6572.

Perry, J., and Kleckner, N. (2003). The ATRs, ATMs, and TORs are giant HEAT repeat proteins. Cell *112*, 151-155.

Pfander, B., and Diffley, J.F. (2011). Dpb11 coordinates Mec1 kinase activation with cell cycle-regulated Rad9 recruitment. Embo J *30*, 4897-4907.

Polo, S.E., and Jackson, S.P. (2011). Dynamics of DNA damage response proteins at DNA breaks: a focus on protein modifications. Genes Dev *25*, 409-433.

Puddu, F., Granata, M., Di Nola, L., Balestrini, A., Piergiovanni, G., Lazzaro, F., Giannattasio, M., Plevani, P., and Muzi-Falconi, M. (2008). Phosphorylation of the budding yeast 9-1-1 complex is required for Dpb11 function in the full activation of the UV-induced DNA damage checkpoint. Mol Cell Biol *28*, 4782-4793.

Putnam, C.D., Jaehnig, E.J., and Kolodner, R.D. (2009). Perspectives on the DNA damage and replication checkpoint responses in Saccharomyces cerevisiae. DNA Repair (Amst) *8*, 974-982.

Rappas, M., Oliver, A.W., and Pearl, L.H. (2011). Structure and function of the Rad9-binding region of the DNA-damage checkpoint adaptor TopBP1. Nucleic Acids Res *39*, 313-324.

Rappold, I., Iwabuchi, K., Date, T., and Chen, J. (2001). Tumor suppressor p53 binding protein 1 (53BP1) is involved in DNA damage-signaling pathways. J Cell Biol *153*, 613-620.

Rivera-Calzada, A., Maman, J.D., Spagnolo, L., Pearl, L.H., and Llorca, O. (2005). Three-dimensional structure and regulation of the DNA-dependent protein kinase catalytic subunit (DNA-PKcs). Structure *13*, 243-255.

Rodriguez, M., Yu, X., Chen, J., and Songyang, Z. (2003). Phosphopeptide binding specificities of BRCA1 COOH-terminal (BRCT) domains. J Biol Chem *278*, 52914-52918.

Rubinson, E.H., Gowda, A.S., Spratt, T.E., Gold, B., and Eichman, B.F. (2010). An unprecedented nucleic acid capture mechanism for excision of DNA damage. Nature *468*, 406-411.

Ruffner, H., Jiang, W., Craig, A.G., Hunter, T., and Verma, I.M. (1999). BRCA1 is phosphorylated at serine 1497 in vivo at a cyclin-dependent kinase 2 phosphorylation site. Mol Cell Biol *19*, 4843-4854.

Ruffner, H., and Verma, I.M. (1997). BRCA1 is a cell cycle-regulated nuclear phosphoprotein. Proc Natl Acad Sci U S A *94*, 7138-7143.

Rupnik, A., Lowndes, N.F., and Grenon, M. (2009). MRN and the race to the break. Chromosoma *119*, 115-135.

Ruzankina, Y., Pinzon-Guzman, C., Asare, A., Ong, T., Pontano, L., Cotsarelis, G., Zediak, V.P., Velez, M., Bhandoola, A., and Brown, E.J. (2007). Deletion of the developmentally essential gene ATR in adult mice leads to age-related phenotypes and stem cell loss. Cell Stem Cell *1*, 113-126.

Saka, Y., Esashi, F., Matsusaka, T., Mochida, S., and Yanagida, M. (1997). Damage and replication checkpoint control in fission yeast is ensured by interactions of Crb2, a protein with BRCT motif, with Cut5 and Chk1. Genes Dev *11*, 3387-3400.

Sanchez, Y., Bachant, J., Wang, H., Hu, F., Liu, D., Tetzlaff, M., and Elledge, S.J. (1999). Control of the DNA damage checkpoint by chk1 and rad53 protein kinases through distinct mechanisms. Science *286*, 1166-1171.

Sanchez, Y., Desany, B.A., Jones, W.J., Liu, Q., Wang, B., and Elledge, S.J. (1996). Regulation of RAD53 by the ATM-like kinases MEC1 and TEL1 in yeast cell cycle checkpoint pathways. Science *271*, 357-360.

Schwartz, M.F., Duong, J.K., Sun, Z., Morrow, J.S., Pradhan, D., and Stern, D.F. (2002). Rad9 phosphorylation sites couple Rad53 to the Saccharomyces cerevisiae DNA damage checkpoint. Mol Cell *9*, 1055-1065.

Shroff, R., Arbel-Eden, A., Pilch, D., Ira, G., Bonner, W.M., Petrini, J.H., Haber, J.E., and Lichten, M. (2004). Distribution and dynamics of chromatin modification induced by a defined DNA double-strand break. Curr Biol *14*, 1703-1711.

Sibanda, B.L., Chirgadze, D.Y., and Blundell, T.L. Crystal structure of DNA-PKcs reveals a large open-ring cradle comprised of HEAT repeats. Nature *463*, 118-121.

Sibanda, B.L., Chirgadze, D.Y., and Blundell, T.L. (2010). Crystal structure of DNA-PKcs reveals a large open-ring cradle comprised of HEAT repeats. Nature *463*, 118-121.

Siede, W., Friedberg, A.S., and Friedberg, E.C. (1993). RAD9-dependent G1 arrest defines a second checkpoint for damaged DNA in the cell cycle of Saccharomyces cerevisiae. Proc Natl Acad Sci U S A *90*, 7985-7989.

Siede, W., Friedberg, A.S., Dianova, I., and Friedberg, E.C. (1994). Characterization of G1 checkpoint control in the yeast Saccharomyces cerevisiae following exposure to DNA-damaging agents. Genetics *138*, 271-281.

Smith, J., Tho, L.M., Xu, N., and Gillespie, D.A. (2010). The ATM-Chk2 and ATR-Chk1 pathways in DNA damage signaling and cancer. Adv Cancer Res *108*, 73-112.

Smits, V.A., Reaper, P.M., and Jackson, S.P. (2006). Rapid PIKK-dependent release of Chk1 from chromatin promotes the DNA-damage checkpoint response. Curr Biol *16*, 150-159.

Smits, V.A., Warmerdam, D.O., Martin, Y., and Freire, R. (2010). Mechanisms of ATR-mediated checkpoint signalling. Front Biosci *15*, 840-853.

Smolka, M.B., Albuquerque, C.P., Chen, S.H., Schmidt, K.H., Wei, X.X., Kolodner, R.D., and Zhou, H. (2005). Dynamic changes in protein-protein interaction and protein phosphorylation probed with amine-reactive isotope tag. Mol Cell Proteomics *4*, 1358-1369.

Spagnolo, L., Rivera-Calzada, A., Pearl, L.H., and Llorca, O. (2006). Three-dimensional structure of the human DNA-PKcs/Ku70/Ku80 complex assembled on DNA and its implications for DNA DSB repair. Mol Cell *22*, 511-519.

St Onge, R.P., Besley, B.D., Pelley, J.L., and Davey, S. (2003). A role for the phosphorylation of hRad9 in checkpoint signaling. J Biol Chem *278*, 26620-26628.

Stewart, G.S., Wang, B., Bignell, C.R., Taylor, A.M., and Elledge, S.J. (2003). MDC1 is a mediator of the mammalian DNA damage checkpoint. Nature *421*, 961-966.

Stracker, T.H., Usui, T., and Petrini, J.H. (2009). Taking the time to make important decisions: the checkpoint effector kinases Chk1 and Chk2 and the DNA damage response. DNA Repair (Amst) *8*, 1047-1054.

Sun, Z., Fay, D.S., Marini, F., Foiani, M., and Stern, D.F. (1996). Spk1/Rad53 is regulated by Mec1-dependent protein phosphorylation in DNA replication and damage checkpoint pathways. Genes Dev *10*, 395-406.

Sun, Z., Hsiao, J., Fay, D.S., and Stern, D.F. (1998). Rad53 FHA domain associated with phosphorylated Rad9 in the DNA damage checkpoint. Science *281*, 272-274.

Suzuki, K., Kodama, S., and Watanabe, M. (1999). Recruitment of ATM protein to double strand DNA irradiated with ionizing radiation. J Biol Chem *274*, 25571-25575.

Sweeney, F.D., Yang, F., Chi, A., Shabanowitz, J., Hunt, D.F., and Durocher, D. (2005). Saccharomyces cerevisiae Rad9 acts as a Mec1 adaptor to allow Rad53 activation. Curr Biol *15*, 1364-1375.

Takai, H., Wang, R.C., Takai, K.K., Yang, H., and de Lange, T. (2007). Tel2 regulates the stability of PI3K-related protein kinases. Cell *131*, 1248-1259.

Tanaka, K. (2010). Multiple functions of the S-phase checkpoint mediator. Biosci Biotechnol Biochem *74*, 2367-2373.

Toh, G.W., and Lowndes, N.F. (2003). Role of the Saccharomyces cerevisiae Rad9 protein in sensing and responding to DNA damage. Biochem Soc Trans *31*, 242-246.

Ubersax, J.A., Woodbury, E.L., Quang, P.N., Paraz, M., Blethrow, J.D., Shah, K., Shokat, K.M., and Morgan, D.O. (2003). Targets of the cyclin-dependent kinase Cdk1. Nature *425*, 859-864.

Uetz, P., Giot, L., Cagney, G., Mansfield, T.A., Judson, R.S., Knight, J.R., Lockshon, D., Narayan, V., Srinivasan, M., Pochart, P.*, et al.* (2000). A comprehensive analysis of protein-protein interactions in Saccharomyces cerevisiae. Nature *403*, 623-627.

Unsal-Kacmaz, K., Makhov, A.M., Griffith, J.D., and Sancar, A. (2002). Preferential binding of ATR protein to UV-damaged DNA. Proc Natl Acad Sci U S A *99*, 6673-6678.

Unsal-Kacmaz, K., and Sancar, A. (2004). Quaternary structure of ATR and effects of ATRIP and replication protein A on its DNA binding and kinase activities. Mol Cell Biol *24*, 1292-1300.

Usui, T., Foster, S.S., and Petrini, J.H. (2009). Maintenance of the DNA-damage checkpoint requires DNA-damage-induced mediator protein oligomerization. Mol Cell *33*, 147-159.

Vialard, J.E., Gilbert, C.S., Green, C.M., and Lowndes, N.F. (1998). The budding yeast Rad9 checkpoint protein is subjected to Mec1/Tel1-dependent hyperphosphorylation and interacts with Rad53 after DNA damage. Embo J *17*, 5679-5688.

Wakayama, T., Kondo, T., Ando, S., Matsumoto, K., and Sugimoto, K. (2001). Pie1, a protein interacting with Mec1, controls cell growth and checkpoint responses in Saccharomyces cerevisiae. Mol Cell Biol *21*, 755-764.

Walker, M., Black, E.J., Oehler, V., Gillespie, D.A., and Scott, M.T. (2009). Chk1 C-terminal regulatory phosphorylation mediates checkpoint activation by de-repression of Chk1 catalytic activity. Oncogene *28*, 2314-2323.

Walworth, N.C., and Bernards, R. (1996). rad-dependent response of the chk1-encoded protein kinase at the DNA damage checkpoint. Science *271*, 353-356.

Wang, X., Zou, L., Lu, T., Bao, S., Hurov, K.E., Hittelman, W.N., Elledge, S.J., and Li, L. (2006). Rad17 phosphorylation is required for claspin recruitment and Chk1 activation in response to replication stress. Mol Cell *23*, 331-341.

Weinert, T.A., and Hartwell, L.H. (1988). The RAD9 gene controls the cell cycle response to DNA damage in Saccharomyces cerevisiae. Science *241*, 317-322.

Williams, D.R., Lee, K.J., Shi, J., Chen, D.J., and Stewart, P.L. (2008). Cryo-EM structure of the DNA-dependent protein kinase catalytic subunit at subnanometer resolution reveals alpha helices and insight into DNA binding. Structure *16*, 468-477.

Wilsker, D., Petermann, E., Helleday, T., and Bunz, F. (2008). Essential function of Chk1 can be uncoupled from DNA damage checkpoint and replication control. Proc Natl Acad Sci U S A *105*, 20752-20757.

Xia, Z., Morales, J.C., Dunphy, W.G., and Carpenter, P.B. (2001). Negative cell cycle regulation and DNA damage-inducible phosphorylation of the BRCT protein 53BP1. J Biol Chem *276*, 2708-2718.

Xu, X., and Stern, D.F. (2003). NFBD1/MDC1 regulates ionizing radiation-induced focus formation by DNA checkpoint signaling and repair factors. Faseb J *17*, 1842-1848.

Yamane, K., Chen, J., and Kinsella, T.J. (2003). Both DNA topoisomerase II-binding protein 1 and BRCA1 regulate the G2-M cell cycle checkpoint. Cancer Res *63*, 3049-3053.

Yoo, H.Y., Jeong, S.Y., and Dunphy, W.G. (2006). Site-specific phosphorylation of a checkpoint mediator protein controls its responses to different DNA structures. Genes Dev *20*, 772-783.

Yu, X., Chini, C.C., He, M., Mer, G., and Chen, J. (2003). The BRCT domain is a phospho-protein binding domain. Science *302*, 639-642.

Zachos, G., Rainey, M.D., and Gillespie, D.A. (2003). Chk1-deficient tumour cells are viable but exhibit multiple checkpoint and survival defects. EMBO J *22*, 713-723.

Zakian, V.A. (1995). ATM-related genes: what do they tell us about functions of the human gene? Cell *82*, 685-687.

Zegerman, P., and Diffley, J.F. (2009). DNA replication as a target of the DNA damage checkpoint. DNA Repair (Amst) *8*, 1077-1088.

Zhao, H., and Piwnica-Worms, H. (2001). ATR-mediated checkpoint pathways regulate phosphorylation and activation of human Chk1. Mol Cell Biol *21*, 4129-4139.

Zhao, X., Georgieva, B., Chabes, A., Domkin, V., Ippel, J.H., Schleucher, J., Wijmenga, S., Thelander, L., and Rothstein, R. (2000). Mutational and structural analyses of the ribonucleotide reductase inhibitor Sml1 define its Rnr1 interaction domain whose inactivation allows suppression of mec1 and rad53 lethality. Mol Cell Biol *20*, 9076-9083.

Zhao, X., Muller, E.G., and Rothstein, R. (1998). A suppressor of two essential checkpoint genes identifies a novel protein that negatively affects dNTP pools. Mol Cell *2*, 329-340.

Zou, L. (2009). Checkpoint Mec-tivation comes in many flavors. Mol Cell *36*, 734-735.

Zou, L., and Elledge, S.J. (2003). Sensing DNA damage through ATRIP recognition of RPA-ssDNA complexes. Science *300*, 1542-1548.

Zubko, M.K., Guillard, S., and Lydall, D. (2004). Exo1 and Rad24 differentially regulate generation of ssDNA at telomeres of Saccharomyces cerevisiae cdc13-1 mutants. Genetics *168*, 103-115.

# CHAPTER 2

## Structure-function studies of Mec1$^{ATR}$ uncover a tight dependency between its functions and intact HEAT repeats

Carla Manuela Abreu, Marta Llorens, Muriel Grenon, John Eykelenboom & Noel Francis Lowndes

Centre for Chromosome Biology, School of Natural Science, National University of Ireland Galway, University Road, Galway, Ireland

*Running title*: Role of HEAT repeats in Mec1 functions.

*Key words*: Mec1, ATR, PIKK, HEAT, DNA damage.

## 2.1. SUMMARY

Mec1, the ATR orthologue, is the master of the DNA damage checkpoints in *Saccharomyces cerevisiae*. This kinase is a member of the PIKK family due to the presence of a conserved Kinase, FAT and FATC domains in the C-terminus of the protein. In addition, tandem helical motifs, called HEAT repeats, comprise the non-kinase portion of Mec1 and other PIKKs. However, the role of these HEAT repeats in PIKK functions is unknown. Here, we have used the genetically tractable *S. cerevisiae* system and developed a strategy to generate *mec1* mutant strains carrying mutations at any location within the *MEC1* gene. In this study, we generated six internal deletions of *MEC1*, termed 'window deletions' mutants, where a single or multiple HEATs spanning most of the primary sequence of the protein are removed. We found that all six window deletion mutants behaved similarly to the null strain, indicating that none of these mutants were proficient for the Mec1 essential function despite being normally expressed and produced. Additionally, we investigated whether the null-like phenotype of these window deletion mutants resulted from a compromised protein structure. We attempted to restore structure and function of the Mec1 mutant proteins by replacing the deleted regions with the equivalent HEATs from the homologous and related PIKKs, ATR and Tel1 respectively. Analysis of the replacement mutants revealed unsuccessful rescue of Mec1 essential function, indicating that either the region of Mec1 replaced is involved with the essential function of Mec1, or that the structure of the protein is still compromised in these mutants. Taking together, we concluded that Mec1 essential function is tightly dependent on the integrity of its HEAT repeats.

## 2.2. HIGHLIGHTS

- Strategy developed to create any *mec1* mutant
- HEAT repeats are required for Mec1 essential function
- Equivalent HEAT repeats from ATR and Tel1 do not complement *mec1* window deletion mutants
- HEAT repeats impact on essential protein-protein interactions or structure of Mec1
- Mec1 essential function is dependent on the integrity of its HEAT repeats

## 2.3. INTRODUCTION

Eukaryotic cells have evolved sophisticated surveillance mechanisms, termed the DNA damage checkpoints, to maintain genome integrity. The checkpoint machinery is highly conserved from yeast to human cells and monitors the genome for the presence of damaged or incomplete replicated DNA. Defects in this machinery lead to damage-sensitivity in yeast and cancer-susceptibility in humans. In *Saccharomyces cerevisiae*, the master regulator of the DNA damage checkpoints is Mec1, the mammalian ATR orthologue, which controls the appropriate cellular responses to genotoxic stress such as cell-cycle progression, transcription and DNA repair. Mec1 activity is also essential for cell growth by maintaining the correct level of dNTPs necessary for efficient DNA replication in a normal cell cycle or in the presence of genotoxic stress. The lethality of the *mec1Δ* mutation can be suppressed by either over-expression of *RNR3*, coding for one of the four subunits of the ribonucleotide reductase (RNR, the enzyme responsible of the formation of dNTPs from ribonucleotides) or by deletion of the gene *SML1*, coding for an inhibitor of the Rnr1 subunit (Zhao et al., 1998).

Upon DNA damage or replication stress, the activation of Mec1 occurs not by sensing directly the DNA lesions, but is regulated by interacting with factors that either bind directly to DNA lesions or to processed intermediates. Mec1 constitutively associates with its regulatory subunit Ddc2 via its N-terminus to form a heterodimer (Paciotti et al., 2000; Wakayama et al., 2001). The generation of single-stranded DNA (ssDNA) coated with the single-stranded binding protein RPA at stalled replication forks or resected DSBs is a critical step in the recruitment of Mec1 to sites of damage, which is mediated through both Ddc2-RPA and Mec1-RPA interdependent interactions (Ball et al., 2007; Nakada et al., 2005; Rouse and Jackson, 2002; Zou and Elledge, 2003). In addition, one or more Mec1 activators are independently recruited to these sites promoting Mec1 kinase activity and phosphorylation of a large number of proteins, including Rfa1 and Rfa2 subunits of RPA, the activators themselves and the downstream effector kinase Rad53 (Navadgi-Patil and Burgers, 2009a).

Recent evidence has shown that these Mec1 activators differ at the various stages of the cell cycle. The PCNA-like Ddc1-Rad17-Mec3 complex (the 9-1-1 complex) and the replication protein Dpb11 are the two known activators of Mec1 in budding yeast. The proper loading of the 9-1-1 complex onto the 5'-ssDNA/dsDNA junctions by the Rad24-RFC complex is required for stimulating Mec1 kinase activity and activation of the G1 and G2 checkpoints, although its employment differs between these two phases of the cell cycle (Majka et al., 2006; Navadgi-Patil and Burgers, 2009b; Puddu et al., 2011). The Ddc1 subunit of the 9-1-1 complex directly interacts with Mec1-Ddc2 complex and stimulates Mec1 activity in G1 phase, a process identified only in *S. cerevisiae* so far (Bonilla et al., 2008; Majka et al., 2006; Navadgi-Patil and Burgers, 2011). Moreover, in G2/M phase, 9-1-1 complex activates Mec1 by two mechanisms. One mechanism involves direct activation of Mec1 by the Ddc1 subunit. In the second mechanism, the 9-1-1 complex recruits Dpb11 to sites of damage, which then interacts with the Mec1-Ddc2 complex promoting Mec1 kinase activity (Mordes et al., 2008b). This mode of Mec1 activation is highly conserved and also functions in the replication checkpoint in higher cells (Navadgi-Patil and Burgers, 2011). However, in *S. cerevisiae*, it is not fully understood why different mechanisms for Mec1 activation exist during the cell cycle. In addition, most observation on the regulation of Mec1 activity were made *in vitro* and it still remains to be determined if these modes of Mec1 activation occur *in vivo*.

With respect to checkpoint activation in *S. cerevisiae* during S-phase it is not even certain whether the 9-1-1 complex and Dpb11 are absolutely required (Berens and Toczyski, 2012; Navadgi-Patil and Burgers, 2009a; Puddu et al., 2011). Rad53 phosphorylation is still detected upon replication stress in the *ddc1Δdpb11-1* double mutant, where the activation functions of both Ddc1 and Dpb11 are eliminated, indicating that an additional mode for activating Mec1 must exist for the replication checkpoint (Navadgi-Patil and Burgers, 2011). Further studies will be required to clarify this matter.

Mec1/ATR belongs to a large superfamily of proteins known as the phosphoinositide 3 kinase-related kinases (PIKKs). In human cells, the PIKK family also includes ATM (ataxia-telangiectasia mutated), DNA-PKcs (DNA-dependent protein kinase

catalytic subunit), mTOR (mammalian target of rapamycin), SMG-1 (suppressor of morphogenesis in genitalia), and TRRAP (transformation/transcription domain-associated protein). Only four of these proteins are conserved in budding yeast: Mec1, Tel1 (homologue of ATM), Tra1p (homologue of TRRAP) and Tor1 and Tor2 (homologues of FRAP) (Lempiainen and Halazonetis, 2009). The PIKK family comprises structurally unique proteins characterised by a large molecular size ranging from 300kDa to 500kDa and four conserved domains that distinguish them from other protein kinases. From the N-terminus to the C-terminus these are: i) the FAT (FRAP-ATM-TRRAP) domain; ii) the kinase domain (KD, 5-10% of the total sequence), highly conserved with those of mammalian and yeast phosphoinositide 3-kinases (PIK3s) (Cantley, 2002; Hunter 1995; Tibbetts and Abraham 2000); iii) PIKK regulatory domain (PRD); and iv) the FAT-C-terminal (FATC) domain (Abraham, 2004; Keith and Schreiber, 1995; Lempiainen and Halazonetis, 2009; Lovejoy and Cortez, 2009; Mordes and Cortez, 2008; Mordes et al., 2008a). The FAT, PRD and FATC domains are critical for the calatytic activity of PIKKs and are very sensitive to mutagenesis (Mordes and Cortez, 2008) (Jiang et al., 2006) (Morita et al., 2007; Nakada et al., 2005; Sun et al., 2005; Takahashi et al., 2000). Some studies suggest that the FAT, PRD and FATC domains may regulate the PIKK kinase activity possibly by acting as a structural scaffold or protein-binding domains for PIKK activators (Bosotti et al., 2000). In addition, posttranslational modifications within the PIKK regulatory domains also seem to modulate PIKK proteins activity (Liu et al., 2011).

Examination of the PIKKs primary and higher order structures indicates potentially important features that may also control their activity and functions. Three-way alignments show that the non-kinase portions of PIKKs (90-95% of the proteins) comprise analogous structures dominated by helical HEAT repeat domains ranging from 40 to 54 units. The divergent sequences between one PIKK to another involve the addition /subtraction of one or few HEAT repeats, some of which are specific to each subfamily (Brewerton et al., 2004; Perry and Kleckner, 2003). The name of these repeats derives from the four proteins where they were initially found: Huntingtin, Elongation factor 3, Alpha-regulatory subunit of protein phosphatase 2A and TOR1 (Andrade and Bork, 1995). A canonical single HEAT repeat is defined as a pair of interacting anti-parallel helices linked by a flexible intra-unit loop, forming

a helical hairpin (Perry and Kleckner, 2003). HEAT repeats, as well as the associated loops, are highly variable in length and amino acid composition (Andrade et al., 2001a; Andrade et al., 2001b). Nonetheless, on average a typical HEAT unit has 10-20 amino acids, linked by 5-8 residues of an intra-unit loop and connected to a neighbouring unit by an inter-unit loop with ≥1 residues (Perry and Kleckner, 2003). In HEAT repeat-containing proteins, adjacent repeats pile together to form a twisted single domain, with a continuous hydrophobic core, forming an elongated super-helix or 'solenoid'. When visualised by crystallography, solenoids form superhelical scaffold matrices often when engaged with other macromolecules (Chook and Blobel, 1999; Cingolani et al., 1999; Groves and Barford, 1999; Groves et al., 1999). Accordingly, electron microscopy structures of yeast Tor1 as well as the ATM and DNA-PKcs human proteins showed that their N-terminus create a curved tubular-shaped structure to form a convex and a concave face similar to that adopted by other proteins containing HEAT repeats (Adami et al., 2007; Llorca et al., 2003; Rivera-Calzada et al., 2005; Spagnolo et al., 2006). Additionally, the crystal structure of DNA-PKcs revealed that its HEAT repeat-containing N-terminus forms a ring-like structure that undergoes conformational changes upon binding to DNA and enhances its kinase activity (Sibanda et al., 2010).

Although HEAT repeat-containing proteins are involved in several cellular processes, a function common to many is that of mediating important protein-protein interactions. For example, PR65/A, a subunit of the heterotrimeric PP2A phosphatase containing 15 HEAT repeats, interacts with several regulatory B subunits of PP2A. Moreover, importins β1 and β2, which contain 19 and 18 HEAT repeats respectively, bind to small GTPase Ran and to various protein substrates destined for nuclear import through two separate but closely spaced HEAT repeats (Bayliss et al., 2000; Groves et al., 1999). Consistent with this, there is also emerging evidence suggesting that HEAT repeats mediate protein-protein interactions in PIKKs. For instance in *S. pombe*, it was shown that the recruitment of Tel1 (ATM homologue) to DNA lesions was regulated by the interaction between the C-terminus of Nbs1 and HEATs 17-18 and 21-22 in Tel1, resembling the two separate but closely spaced HEAT repeat domains in importins (You et al., 2005). Furthermore, it was proposed that the recruitment of the PIKKs ATM/Tel1, ATR/Mec1 and DNA-PK to DNA lesions involves analogous mechanisms through

the binding of their HEAT-containing N-terminal regions to their respective interacting partners NBS1/Xrs2, ATRIP/Ddc2 and Ku80/70 (Falck et al., 2005). In human ATR, the region containing 30-346 amino acids is required for its interaction with ATRIP (Ball et al., 2005), and this domain is evolutionary conserved in Mec1 (1-500 amino acids), which is involved with Ddc2 interaction (Wakayama et al., 2001). However detailed analysis to identify the specific HEAT repeats involved in these processes has not yet been reported. Additionally, it has been shown in human cells that the TELO2 (telomere length regulation protein TEL2 homolog) protein also involved in the DNA damage response, interacts with all PIKK proteins to control their stability, and with respect to ATM specifically, a subset of HEAT repeats (830-1290aa) mediate the interaction between these two proteins (Takai et al., 2007). Taken together, we speculate that the HEAT repeats of PIKKs may act like platforms that mediate protein-protein interactions. However, the major portions of the HEAT repeat-containing regions of these proteins still remain uncharacterised.

Recently, an alternative function for the HEAT repeats has been proposed. Molecular dynamics simulations of PR65, the HEAT repeat-containing subunit of the heterotrimeric PP2A enzyme, suggested that scaffold HEAT repeats are susceptible to elastic behavior and responsive to force. Indeed, deformations in the HEAT repeat structure of PR65 dominate reversible conformational fluctuations in the regulatory and catalytic subunits of PP2A, modulating its substrate binding and catalysis (Grinthal et al., 2010). Accordingly, analogous to PR65, HEAT repeat proteins, rather then being a rigid structural scaffold, are predicted to be a dynamic and (visco-)elastic molecules whose activity and functions can be modulated by external forces or spontaneous fluctuations in their structure (Grinthal et al., 2010). It is possible that ATM, DNA-PK and ATR, through their HEAT repeats and alterations in their higher order structure upon binding to damaged DNA or accessory proteins, may all be similarly stimulated and regulated to phosphorylate substrate proteins.

Here, we have focused in studying the PIKK protein Mec1, the *S. cerevisiae* orthologue of human ATR. In this study, we investigated which HEAT repeats are required for the essential and DDR functions of Mec1. We have used the genetically tractable *S. cerevisiae* model system to generate six internal deletions of *MEC1*,

termed '*window deletions'* mutants, where a single or multiple HEATs spanning most of the primary sequence of the protein are missing. We found that all the six window deletion mutants behaved similarly to the null strain, indicating that none of these mutants were proficient for the essential function of Mec1. Additionally, we investigated whether the null-like phenotype of these window deletion mutants resulted from a compromised protein function. We further attempted to restore structure and function of the Mec1 mutant proteins by replacing the deleted regions with the equivalent HEATs from the homologous and related PIKKs, ATR and Tel1 respectively. The analysis of these new mutants revealed that the replacements could not rescue the essential function(s) of Mec1, indicating that either protein-protein interactions required for Mec1 essential function are distributed throughout the entire protein length, or, more likely, a structural property required for Mec1 function is still affected in these mutants. Taken together, we conclude that Mec1 functions are tightly dependent upon the structural integrity of the HEAT repeat region of this protein.

## 2.4. RESULTS

### 2.4.1 Similarity between ATR and Mec1

We set out to define the roles of HEAT repeats in PIKK function by studying Mec1, the ATR homologue of *S. cerevisiae*. The HEAT repeats in Mec1 were defined accordingly with Perry and Kleckner bioinformatic analyses (Perry and Kleckner, 2003). As shown in Figure 2.1A the overall amino acid sequence of *sc*Mec1 and *h*ATR share 18% of similarity. In agreement with the presence of the regulatory domains of the PIKK family in the C-terminus of its member proteins, this region is more conserved between Mec1 and ATR (KD and FATC share 35% and 51% of similarity, respectively) than the N-terminus (the ATRIP or Ddc2 partner-binding domains only share 8.7% of similarity). In accord with a previous bioinformatic analysis (Perry and Kleckner, 2003), ATR contains of 45 HEAT repeats while Mec1 contains of 42 HEAT repeats (the equivalent to ATR HEAT repeats number 6, 7 and 8 are missing in Mec1). These are distributed almost throughout the entire length of both proteins, the exception being the C-terminal Kinase, PRD and FATC domains, which do not contain any HEAT-repeats (Figure 2.1B and C). In both ATR and Mec1 the HEAT repeats vary in size from 30 to 47 amino acids, with the inter-unit

loops also varying from 1-87 amino acids in ATR and 1-63 amino acids in Mec1. We have compared the amino acid sequence within each repeat between ATR and Mec1 (Figure 2.1D). Although the similarity within each HEAT repeat is relatively low, the C-terminal HEAT repeats have slightly greater conservation (reaching up to 35% similarity within the FAT domain, with the greatest similarity closest to the kinase domain). Note that HEAT repeats number 6, 7 and 8 of ATR are absent in Mec1, and also that HEATs 11-13 are known as ATR-specific HEAT repeats as they are shared specifically between ATR orthologues (Perry and Kleckner, 2003). The presence of the same repeating structural unit among all PIKKs indicates that these HEAT repeats are not only important for PIKK function, but perhaps the fundamental mechanisms by which they modulate the activity of these proteins might be conserved between all PIKKs. On the other hand, the presence of some HEAT motifs in some PIKK proteins that are missing in others might be indicative of distinctive functions.

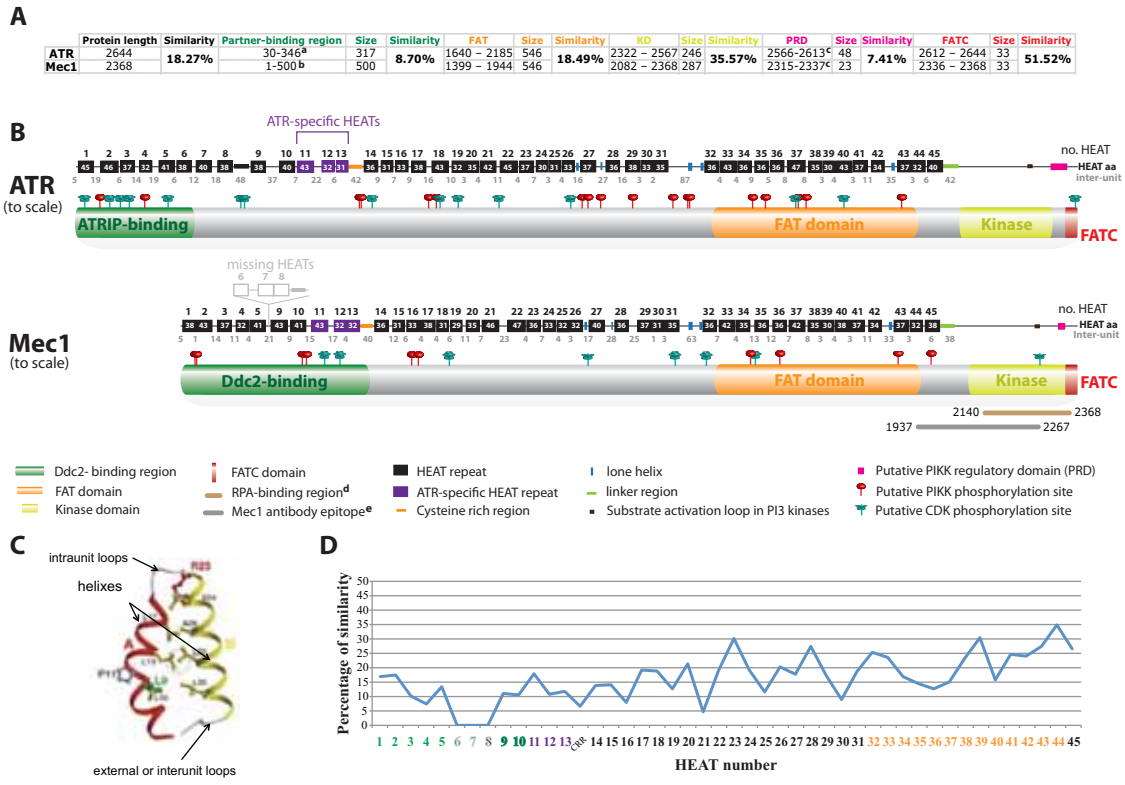


**Figure 2.1: Domains, HEAT repeat organisation and Amino acids similarity between human ATR and *S. cerevisiae* Mec1.** (A) Amino acids similarity between ATR and Mec1 entire proteins and within known conserved regions or domains; Regions or domains were defined accordingly with UniProt, apart from the partner-binding region of ATR and Mec1 (accordingly with [a]Ball et al., 2005 and [b]Wakayama et al., 2001, respectively); PRD of ATR and Mec1 (accordingly with [c]Lempiainen

and Halazonetis, 2009); colours as in B; (B) Domain structure of ATR and Mec1; HEAT repeats, including the number of amino acids (aa) in each HEAT (white numbers) and in each inter-unit loop (grey numbers) are also shown accordingly with Perry and Kleckner, 2003; colours as shown in legend; The RPA-binding region in Mec1 is defined accordingly with [d]Nakada et al., 2005; Epitope of Mec1 antibody ([c]Downs et al., 2000) used in this study is also shown; (C) Structure of a typical HEAT repeat; Colours show antiparallel helices; Key amino acids are also shown (Adapted from Andrade et al., 2001); (D) Graph of amino acids similarity between ATR and Mec1 within each HEAT repeat, excluding inter-unit loops; colours as in B; All similarities obtained using the algorithm ClustalO.

### 2.4.2. Generation of novel *mec1* structure-function mutants

To understand the role of HEAT repeats in Mec1 functions we sought to initially generate a unique set of *mec1* structure-function mutants at the endogenous *MEC1* locus, wherein each mutant corresponded to loss of a single or multiple HEAT repeats spanning most of the primary sequence of Mec1. Note that the C-terminal portion of Mec1 corresponding to the kinase and FATC domains were not disrupted. For this purpose, we adapted the break-mediated version of the *delitto perfetto* approach (Storici et al., 2003; Storici et al., 2001; Storici and Resnick, 2003, 2006) and combined it with fusion PCR methodology. This methodology takes advantage of a COunterselectable REporter (hereafter termed CORE) cassette, which allows the selection of mutants that have lost the CORE and express the truncated version of the protein with no extra sequences in its *locus*. Importantly, because Mec1 has a documented essential role in the synthesis of dNTPs and *mec1* mutants are unviable (Zhao et al., 1998), all the strains constructed in this study were generated in *sml1Δ* background in order to suppress any lethality from possible *mec1* mutants (*SML1* encodes an inhibitor of the Rnr1 subunit of ribonucleotide reductase, RNR; Zhao et al., 1998). Mec1 regulates RNR through both regulating the induced the transcription of *RNR* genes during S-phase and, most importantly, the inhibitory phosphorylation (mediated by Rad53 and Dun1) of the Sml1 inhibitor of RNR. Loss of the Sml1 inhibitor of RNR obviates the requirement for Mec1-dependent inhibition of Sml1, allowing active RNR to synthesize dNTPs. Indeed, *sml1*Δ cells show increased dNTP levels, raising the efficiency of DNA replication and allowing the survival of cells when *MEC1* is mutated for its essential function (Zhao et al., 1998).

Among the CORE cassettes available, we opted for the *CORE-I-SceI* comprising the *Kluveromyces lactis URA3 (KlURA3)* counter-selectable marker, the *kanMX4* selectable reporter gene and the *I-SceI* gene, encoding the I-Sce1 endonuclease, under the control of the *GAL1* promoter (the *CORE-I-SceI* cassette was kindly

provided by Dr. F. Storici, see Storici and Resnick, 2006). This genetic system allows the generation of a DSB downstream of the cassette in a galactose-inducible manner and significantly increases, by more than 1000-fold, the homologous recombination efficiency. Briefly, to generate the *mec1* mutants (for detailed protocol see Material and Methods), we firstly transformed *sml1Δ* cells with the *CORE-I-SceI*, fused at its 5' and 3' ends with sequences homologous to four different sites within the *MEC1* ORF (Figure 2.2A and 2.2C). This resulted in the creation of four distinct *mec1::CORE-I-SceI* insertion mutants (named *mec1:CORE1, mec1::CORE2, mec1::CORE3*, and *mec1::CORE4*), which differ in the location of the cassette within the *MEC1* genomic *locus* (Figure 2.2B). The successful integration of the CORE cassette was confirmed by genomic PCR as well as phenotypic and genotypic analyses (Figure 2.2D and 2.2E). The CORE-containing strains were able to grow on media either containing G418 (Geneticin) or lacking URA (uracil) due to the presence of the *kanMX4* and *KlURA3* markers within the CORE but missing from wild type control cells. Given that Mec1 has a role in homologous recombination, a process required for the subsequent steps of the generation of *mec1* structure-function mutants (Flott et al., 2011; Ullal et al., 2011), we have also performed DNA damage sensitivity analysis in the CORE-containing strains to examine if Mec1 DDR functions are affected in these cells (Figure 2.2E). Unlike wild type, the *mec1::CORE2*, *mec1::CORE3* and *mec1::CORE4* insertion mutants were, similarly to *mec1Δ* cells, highly sensitive to ionizing and ultra-violet radiation. In contrast, *mec1::*CORE1 insertion mutant was resistant to ionizing and ultra-violet radiation similarly to wild type cells. We then complemented the three *mec1::CORE2*, *mec1::CORE3* and *mec1::CORE4* insertion mutants with a centromeric plasmid carrying $MEC1^{+}$ (pML227, kindly provided by Prof. Maria Pia Longhese, (Paciotti et al., 2001, see Table S2.2 for plasmids). The DNA damage sensitivity after IR and UV treatments of the CORE-containing strains (see Table S2.1 for strains) was rescued by the *MEC1* centromeric plasmid (*mec1::CORE2* + $pMEC1^{+}$, *mec1::CORE3* + $pMEC1^{+}$, *mec1::CORE4* + $pMEC1^{+}$) to resistance level comparable to wild type cells.

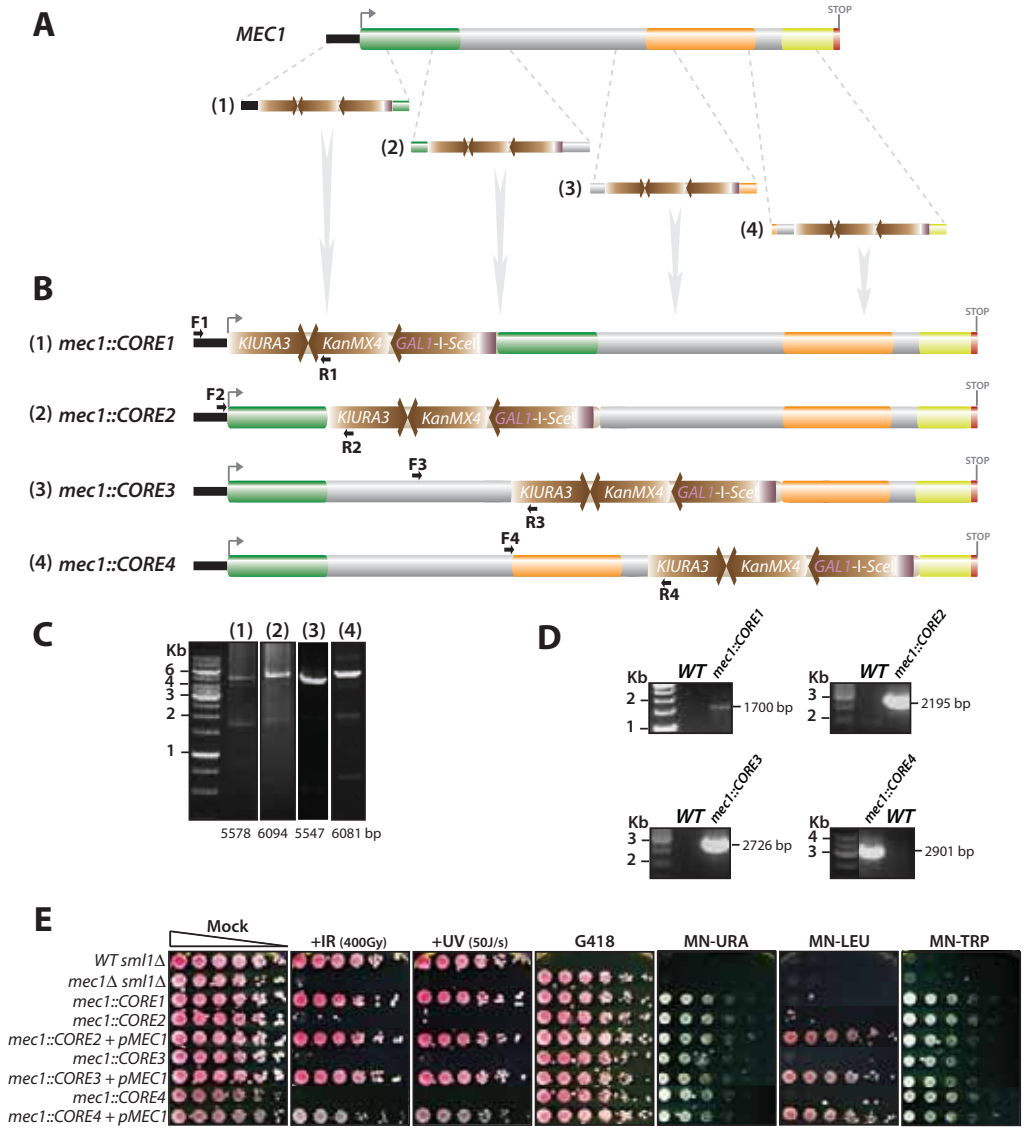


**Figure 2.2: Generation of the CORE-containing strains.** Note that cassettes shown in A, B and C have been numbered from (1) to (4). (A) Schematic of the independent integration of four different fusion PCR fragments of the CORE-I-SceI into four different positions at *MEC1*; Regions of homology within the arms of the fusion PCR fragments and *MEC1* are shown in similar color; black – *MEC1* endogenous promoter; green – Ddc2-binding region (DBR); orange – FAT domain; yellow – KD; red – FATC domain; grey – regions of unknown function; arrow – ORF; STOP – stop codon. (B) CORE-containing strains resulting from the independent integration at the *MEC1* genomic location shown in A; Primers used in diagnostic PCR in D are shown; F1=T1, R1=N517-KanRev, F2=Mec1-1, R2=KlURA-3', F3=T14, R3=KlURA-3', F4=T13, R4=KlURA-3' (see Table 2.3 for primers); (C) Fusion PCR fragments illustrated in A; (D) Diagnostic PCR of CORE-containing strains using primers shown in B; (E) Strains phenotypical analyses to the indicated treatment; Mock – YPD (Yeast Peptone Dextrose) medium (complete medium); IR and UV treatments are done on YPD media; MN – Minimal medium lacking the indicated amino acid (URA – uracil; LEU – leucine; TRP – tryptophan); G418 (Geneticin) – YPD containing 200µg/µl of G418; wild type cells (WT), *mec1Δ*, *mec1::CORE1*, *mec1::CORE2*, *mec1::CORE2 + pMEC1*, *mec1::CORE3*, *mec1::CORE3 + pMEC1*, *mec1::CORE4*, *mec1::CORE4 + pMEC1* (all strains in *sml1Δ* background, see Table S2.1 for strains); *pMEC1* - *MEC1* centromeric plasmid (pML227, see Table S2.2 for plasmids).

We then transformed the relevant CORE-containing strains with six DNA fragments prepared by fusion PCR from yeast genomic DNA and corresponding to fusions of the *MEC1* genomic sequence flanking the sequence to be deleted (Figure 2.3A-C, for detailed protocol see material and methods). Homologous recombination-dependent integration at the *MEC1* locus of these targeting fragments resulted in the loss of the *CORE-I-SceI* cassette and the generation of the desired in-frame deletion of the genomic region of the *MEC1* ORF (which was absent in the transforming fragment generated by fusion PCR, see Figure 2.3B and C). Note that the prior galactose-dependent induction of single DSBs downstream to the *CORE-I-SceI* was critical for high efficiency gene targeting during this step (see Material and Methods). As shown in Figure 2.3B, the final window deletion mutants generated were *mec1-W1*, *mec1-W2*, *mec1-W3*, *mec1-W4*, *mec1-W5* and *mec1-W6* lacking respectively the HEAT repeats (1) 1-10 (comprised in the Ddc2 binding region of Mec1), (2) 11-13 (ATR-specific HEAT repeats), (3) 14-21, (4) 22-31, (5) 32-44 (comprised in the FAT domain) and (6) 45 (single HEAT repeat between the FAT and the Kinase domains). Note that all these mutants are in the *sml1Δ* background. The final window deletions mutants were then selected for loss of the *MEC1* centromeric plasmid required for homologous recombination in cells at intermediate steps that lacked functional MEC1 (*data not shown*). We confirmed the successful targeting by genomic PCR along with sequencing of the entire *MEC1* gene for each of the final strains generated (Figure 2.3D and *data not shown*).

We then confirmed the genotype of the strains generated by performing phenotypic analyses of two independent clones for each *MEC1* window deletion mutant generated both before and after the loss of the *MEC1* centromeric plasmid (Figure 2.3E and *data not shown*). Complete loss of the *CORE-I-SceI* in all analysed *MEC1* window deletion mutants and the absence of the cassette elsewhere in the genome was confirmed as the strains were able to grow on media containing 5-FOA but not on media either containing G418 or lacking uracil, unlike the parental CORE-containing strains. The loss of the *MEC1* centromeric plasmid (*LEU2*$^{+}$) was also confirmed by the inability of the final *mec1* deletion mutants to grow on media lacking leucine. Note that all the *mec1* deletion mutants are still in the *sml1Δ* background (*SML1* has been replaced by the *TRP1* marker), as shown by their survival on media lacking tryptophan.

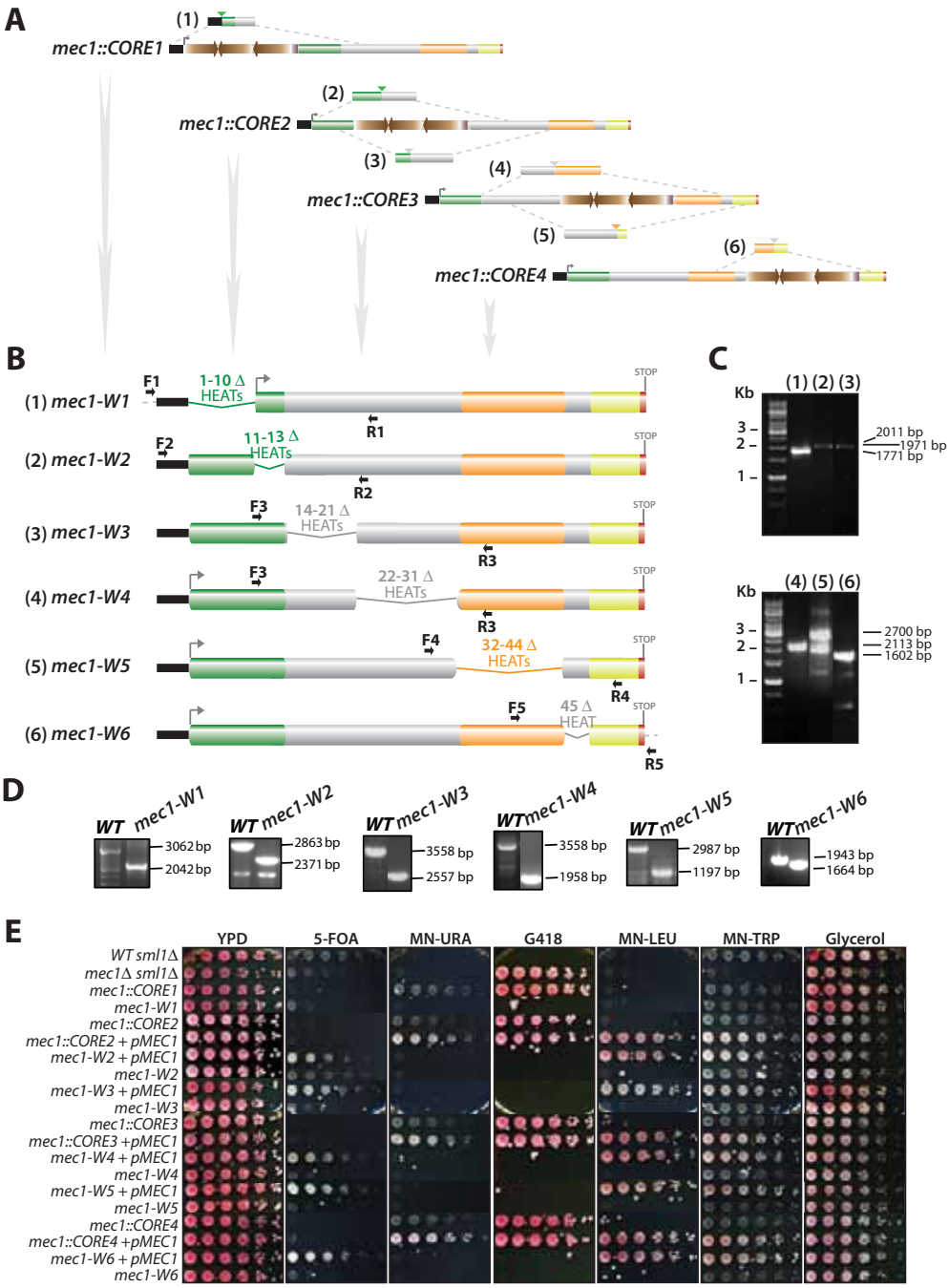


**Figure 2.3: Generation of the final *mec1* window deletion strains.** (A) Schematic of the independent integration of six different fusion PCR fragments containing the desired deletion (triangle) into different positions at *MEC1* in the respective CORE-containing strain; each CORE-containing strain is complemented with *cpMEC1* and was used to generate one or two independent window deletion mutants; Final window deletion mutants are: *mec1-w1, mec1-w2, mec1-w3, mec1-W4, mec1-W5 and mec1-W6,* corresponding to deletion of HEAT repeats 1-10, 11-13, 14-21, 22-31, 32-44 and 45, respectively; color of homology arms in fusion PCR fragments are shown accordingly with the homologous region at *MEC1*; black – *MEC1* endogenous promoter; green – Ddc2-binding region (DBR); orange – FAT domain; yellow – KD; red – FATC domain; grey – unknown regions; arrow – ORF; STOP – stop codon; numbers correspond to numbers in B, C and D; (B) Final window deletion strains resulting from the independent integration at the *MEC1* genomic location shown in A; Primers used in diagnostic PCR are shown in B; F1=LCD96, R1=B12, F2=T1, R2=B3, F3=T4,

R3=B11, F4=T10, R4=B17, F5=T16, R5=Mec1-2; (C) Fusion PCR fragments illustrated in A; (D) Diagnostic PCR of final window deletion strains using primers shown in B (for details see Material and Methods); (E) Cell growth analysis of mutants in B under selective media as indicated; YPD – Yeast Peptone Dextrose medium (complete medium); MN – Minimal medium lacking the indicated amino acid (URA – uracil; LEU – leucine; TRP – tryptophan); 5-FOA (5-Fluoroorotic Acid): Minimal media containing 1mg/ml of 5-FOA; G418 (Geneticin) – YPD containing 200µg/µl of G418; Glycerol – YPD containing 3% of ethanol and 3% of glycerol; *pMEC1* - *MEC1* centromeric plasmid; all strains in *sml1Δ* background.

We next monitored the expression of the Mec1 truncated protein version in all generated window deletion mutants by western blotting. We used the only available Mec1-specific antibody (polyclonal antiserum NL33, generated at Cancer Research UK by the Lowndes' group, see Downs et al., 2000), which recognizes a region of Mec1 comprising the last HEAT repeat of the FAT domain and the approximately 66% N-terminal portion of the Kinase domain (1937-2267 amino acids, Figure 2.1B). We were able to detect all Mec1 truncated forms with the expected size and expression levels comparable with wild type (Figure 2.4A and B). Note that although in Mec1-W6 protein the window deletion coincides partially with the epitope of the antibody, the remaining sequence in the kinase domain seems to be sufficient for the detection of Mec1 band in the *mec1-W6* mutant. These results suggest that the generated deletions had no significant impact on Mec1 expression and stability.

### 2.4.3. HEAT repeats are required for all Mec1 functions

To test whether the regions of Mec1 removed in the *MEC1* window deletions have a role in the DNA damage checkpoints and repair, we performed a DNA damage sensitivity assay to examine the survival of the *mec1* deletion mutants upon different types and doses of DNA damaging agents or replicative stress. As shown in Figure 2.4C, all *mec1* mutant strains, like *mec1Δ* but unlike wild type cells, were sensitive to agents inducing DNA single- and double-strand breaks: IR, Zeocin and Bleocin, which primarily cause DNA double-stranded breaks, as well as to UV (promotes mainly the formation of pyrimidine dimers, where covalent cross-links occur in cytosine and thymine residues) and 4-Nitroquinoline 1-oxide (4NQO, UV mimetic agent that reacts mainly with guanine and to a lesser extent with adenine, leading to formation of DNA adducts), both of which cause lesions that are primarily repaired by nucleotide excision repair. In addition, all *mec1* mutants were sensitive to replicative stress upon treatment with three different agents that perturb DNA synthesis, hydroxyurea (HU, inhibits the ribonucleotide reductase, an enzyme

required for *de novo* dNTP synthesis, resulting in depletion of the dNTPs pool and the slow down of DNA synthesis), methyl methanesulfonate (MMS, methylates DNA on $N^7$-deoxyguanine and $N^3$-deoxyadenine leading to replication forks stalling; Lundin et al., 2005) and camptothecin (CPT, a cytotoxic quinoline alkaloid which inhibits the enzyme DNA topoisomerase I). Importantly, this sensitivity was rescued and comparable to wild type cells when all *mec1* mutants harbored the *MEC1* centromeric plasmid. Our data indicate that Mec1 checkpoint and repair functions are perturbed in all *mec1* window deletion mutants.

Due to the similarity of the phenotypes of the window deletions to *mec1Δ* cells, we examined if the window deletions we generated in Mec1 are involved in its essential function, which has been by-passed in these strains by the *sml1* mutation. To test this hypothesis we transformed all *mec1* mutant cells (*sml1Δ* background) with a centromeric plasmid carrying *SML1* (pWJ739, kindly provided by Rodney Rothstein; Zhao et al., 1998) and compared to wild type and *mec1Δ* cells. If the window deletions generated (*mec1-W1*, *mec1-W2*, *mec1-W3*, *mec1-W4*, *mec1-W5* and *mec1-W6* cells, all in the *sml1Δ* background) do not affect the essential function of Mec1, we would expect these mutants to be viable when complemented with the *SML1* centromeric plasmid (p*SML1*). However, all six *mec1* deletion mutant cells, similarly to *mec1Δ* cells, were not viable in the presence of *SML1* (Figure 2.4D). Note that all strains had similar transformation efficiency (*data not shown*).

In support of the above observations, the equivalent window deletions introduced into ATR using the chicken DT40 model system, also resulted in null phenotypes despite normal expression of the truncated ATR proteins (Eykelenboom J and Agost LM, *unpublished data*). Thus, despite completely different strategies and model systems used to generate the equivalent window deletions in the Mec1 and ATR proteins, these two studies are consistent with similar mechanisms underlying the regulation, and possibly ultra-structure, of Mec1 and ATR that are evolutionary conserved. In short, as null phenotypes were observed with all Mec1 and ATR window deletions we conclude that the essential function of these two proteins must be distributed along the entire length of the proteins that corresponds to repeated HEAT motifs.

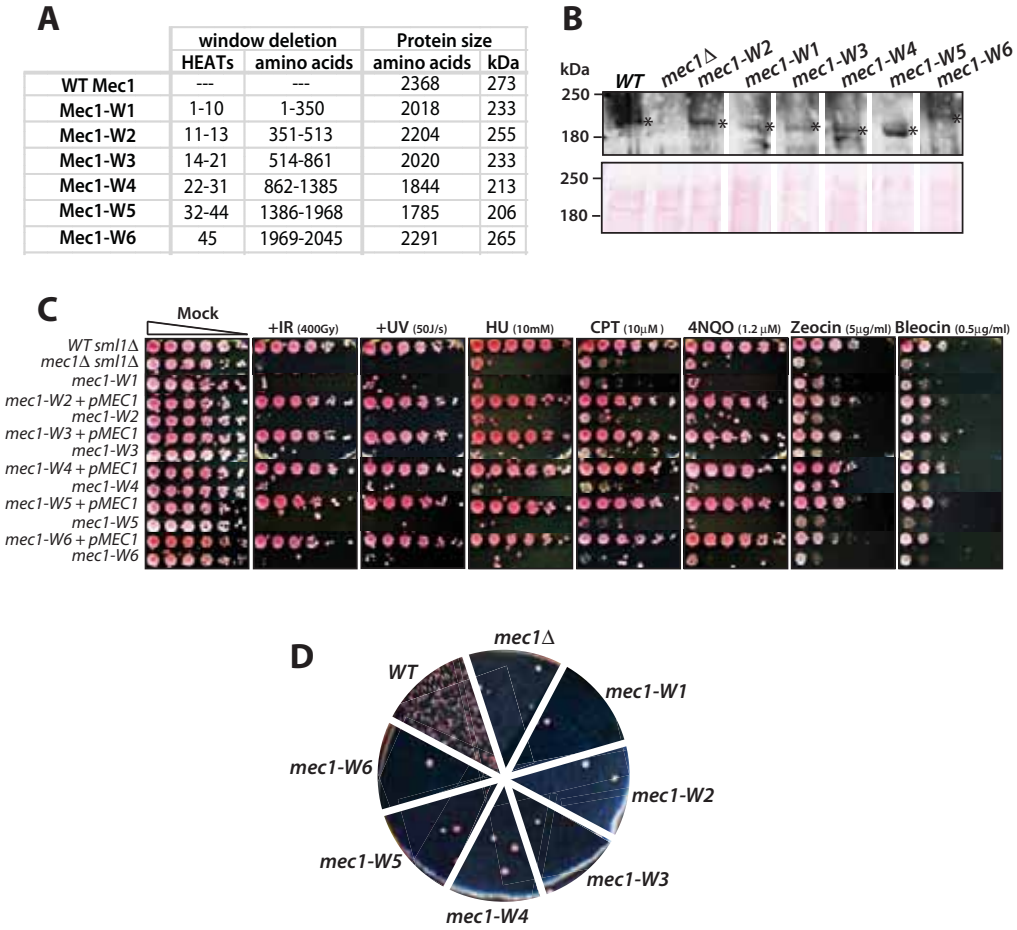


| | window deletion | | Protein size | |
|---|---|---|---|---|
| | HEATs | amino acids | amino acids | kDa |
| WT Mec1 | --- | --- | 2368 | 273 |
| Mec1-W1 | 1-10 | 1-350 | 2018 | 233 |
| Mec1-W2 | 11-13 | 351-513 | 2204 | 255 |
| Mec1-W3 | 14-21 | 514-861 | 2020 | 233 |
| Mec1-W4 | 22-31 | 862-1385 | 1844 | 213 |
| Mec1-W5 | 32-44 | 1386-1968 | 1785 | 206 |
| Mec1-W6 | 45 | 1969-2045 | 2291 | 265 |

**Figure 2.4: Analyses of Mec1 protein and functions in the *mec1* window deletion mutants.** (A) Analysis of size of Mec1 protein in the final *mec1* window deletion mutants. (B) Western blotting of Mec1 in final *mec1* window deletion mutants as indicated; Expected size as shown in A; asterisk (*) showing the respective Mec1 protein band; Ponceau is also shown as a loading control; (C) DNA damage sensitivity analysis of strains under genotoxic treatment as indicated; Mock – Yeast Peptone and Dextrose medium (complete medium); IR, UV, HU, CPT, 4NQO (4-Nitroquinoline 1-oxide), Zeocin and Bleocin treatments are done on YPD media radiated or containing the indicated dose, respectively; all strains are in *sml1Δ* background; *pMEC1* - *MEC1* centromeric plasmid; (D) Viability analysis of indicated strains transformed with *SML1* centromeric plasmid; Minimal medium lacking leucine was used in this assay (for details see Material and Methods).

### 2.4.4. Generation of novel *mec1* hybrid mutants

We sought to take a more conservative strategy in an attempt to restore structure and function of Mec1 mutant proteins. We replaced the regions removed in the window deletions with the equivalent HEAT repeats from hATR (human) and *sc*Tel1 (*S. cerevisiae*), homologous and related PIKKs respectively (Figure 2.5A). Since HEAT repeats 11-13 from Mec1 are present only in ATR orthologues and have been termed ATR-specific HEAT repeats (Perry and Kleckner, 2003), we hypothesized that the

role of these repeats might have been conserved between human and budding yeast. To test this, we replaced the HEAT repeats 11-13 from Mec1 with HEAT repeats 11-13 from human ATR. In addition, we independently replaced HEATs 11-13 from Mec1 with the equivalent region, HEAT repeats 13-14, from the budding yeast Tel1 protein (an orthologue of ATM) which, based on reported alignment data, are located at the same position in Tel1 protein to that of Mec1 (Perry and Kleckner, 2003). In this mutant we did not expect to rescue the essential function of Mec1, but perhaps might be able to restore some DNA damage specific phenotypes.

To test if the window deletions are compromising Mec1 structure, thus affecting its activity and functions we prepared some additional substitution mutants. These substitutions could possibly result in separation of function mutations and/or the acquisition of novel functions. Specifically, we replaced HEAT repeats 14-21 from Mec1 with the corresponding HEATs 17-23 from budding yeast Tel1. Whereas a role for HEAT repeats 14-21 of Mec1 has not been reported to date, HEAT repeats 17-18 and 21-22 of fission yeast Tel1 were shown to be required for its interaction with Nbs1 (You et al., 2005). Successful rescue of the essential function of Mec1 in these hybrid mutants might indicate that the replacing region not only rescues the structural integrity of Mec1, but that the region of Mec1 lost in the replacement mutant must not be involved in its essential function. In addition to being compromised in a specific function(s), the replacing region might also bring with it proficiency in new functions. It is important to mention that the size of the inter-unit loops was maintained in all the replacements in order to make the substitution mutation as conservative as possible.

The replacement mutants (named *mec1-W2::ATR*$^{H11\text{-}13}$, *mec1-W2::tel1*$^{H13\text{-}14\ 3ATR\text{-}HEATs\text{-}R}$ and *mec1-W3::tel1*$^{H17\text{-}21}$) were generated as described above using the parental *mec1::CORE2* strain complemented with the *MEC1* centromeric plasmid (Figure 2.5B and 2.5C, *for details see Material and Methods*). Note that once more the final mutants are in the *sml1Δ* background. The *MEC1* centromeric plasmid was then lost to generate the final replacement mutants (*data not shown*). We confirmed the successful targeting by genomic PCR and by sequencing the entire *MEC1* gene in the final strain (Figure 2.5D and *data not shown*).

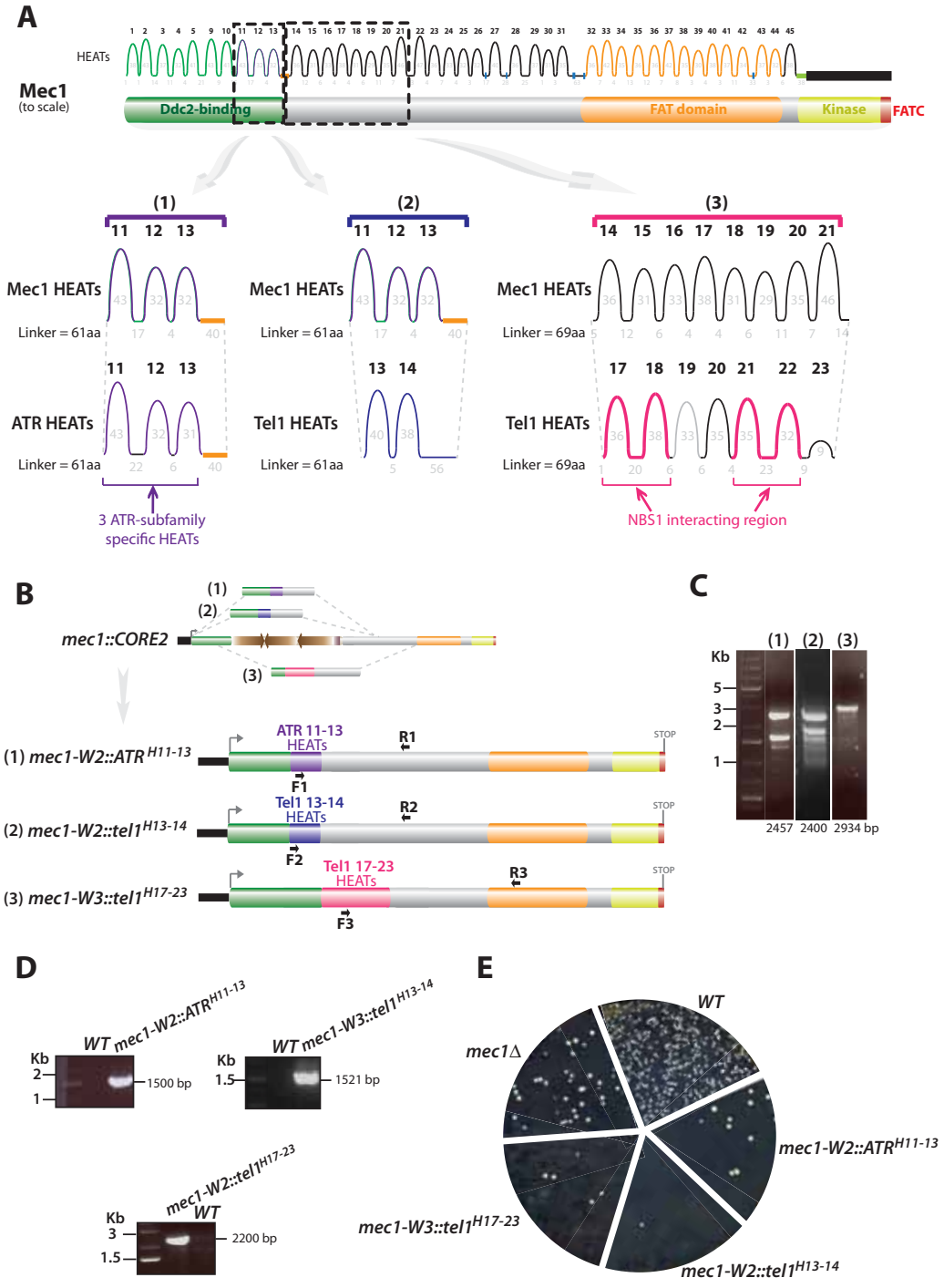


**Figure 2.5: Generation of strains expressing Mec1/ATR/Tel1 hybrid proteins.** (A) Schematic of Mec1 protein structure and corresponding HEAT repeats; the three independent replacements in Mec1 are also shown; numbers correspond to numbers in B and C; (B) Schematic of independent integrations of three different fusion PCR fragments containing the desired replacement in the respective CORE-containing strain; color of homology arms in fusion PCR fragments are shown accordingly with the homologous region at *MEC1*; Final replacement strains, named *mec1-W2::ATR*$^{H11-13}$, *mec1-W2::tel1*$^{H13-14}$ and *mec1-W3::tel1*$^{H17-24}$ are also shown; black – *MEC1* endogenous promoter; green – Ddc2-binding region (DBR); orange – FAT domain; yellow – KD; red – FATC domain; grey – unknown regions; arrow – ORF; STOP – stop codon; (C) Fusion PCR

fragments illustrated in B; (D) Diagnostic PCR of final replacement strains from the independent integration at the *MEC1* genomic location shown in A and B; Primers used in diagnostic PCR are shown B; F1=5'-SpecFw, R1=B5, F2=R1-tel1-5', R2=B5, F3=5'-DIAG-R2.1-2.2replac, R3=B11; (E) Viability analysis of indicated strains transformed with *SML1* centromeric plasmid; Minimal medium lacking leucine was used in this assay (for details see Material and Methods); all strains are in the *sml1Δ* background; Experiments done in collaboration with Marta Llorens.

### 2.4.5. ATR or Tel1 HEATs cannot rescue the lethality of *mec1* mutants

We then tested if Mec1 essential function was rescued in the *mec1-W2::ATR*$^{H11\text{-}13}$, *mec1-W2::Tel1*$^{H13\text{-}14}$ and *mec1-W3::tel1*$^{H17\text{-}21}$ mutants. To do this, all *mec1* replacement strains together with wild type and *mec1Δ* strains (all in *sml1Δ* background) were transformed with a centromeric plasmid carrying *SML1* as described above. Similar to *mec1Δ* cells, the three *mec1/ATR/tel1* replacement mutants were unviable in the presence of *SML1* (Figure 2.5E). Thus, none of the substitution mutations resulting in Mec1-ATR or Mec1-Tel1 fusion proteins were able to support the essential function of the Mec1 kinase. These data could be explained by either an inability of any of the substituted HEAT repeats to function in budding yeast cells, likely due to the phylogenetic distances involved, or could be consistent with failure of the substitution mutants to rescue an overall structural property dependent upon the specific HEAT repeats found in Mec1.

## 2.5. DISCUSSION

The Mec1 kinase of budding yeast, an orthologue of human ATR, is an essential regulator of both dNTPs homeostasis and genome integrity (Cimprich and Cortez, 2008; Zhao et al., 1998). In this study, we examined the roles of HEAT repeats in mediating the function of Mec1 for both normal cellular proliferation and the DDR. We showed that six mutants that result is sequential loss of internal amino acids spanning the 90% of the protein corresponding to the 42 HEAT repeats of Mec1 behaved similarly to a *mec1* deleted strain. In particular, our results indicate that none of these mutants are proficient for the essential function of Mec1. Furthermore, *mec1/ATR/tel1* hybrid mutants corresponding to replacement of two Mec1 window deletion with the equivalent regions from either ATR or Tel1 also did not rescue of the essential function of Mec1. Possible explanations for the loss of Mec1 functions in our *mec1* window deletion mutants are discussed in detail below.

### 2.5.1. Development of a *mec1::CORE* strain collection to facilitate Mec1 structure-function studies

Multiple different genome manipulation methods can be used to manipulate the budding yeast genome at any given locus (Erdeniz et al., 1997; Moerschell et al., 1988; Scherer and Davis, 1979). All are based on the efficient homologous recombination of this model system. In this study we decided to adapt the break-mediated version of the *delitto perfetto* approach developed by Storici and colleagues (Figure 2.2 and 2.3; (Storici et al., 2003; Storici et al., 2001; Storici and Resnick, 2003, 2006) and combine it with fusion PCR methodology in order to facilitate the generation of *mec1* structure-function mutants. The *delitto perfetto* approach, besides being a clone-free system, takes advantage of a CORE cassette that comprises a *KanMX* reporter gene, which monitors the insertion of the cassette, and a *URA3* counter-selectable marker that allows selection of cells that have lost the cassette. The use of the CORE harboring a dual selection allows an efficient screening of transformants that result from correct gene targeting. As such transformants can be rare, they can be difficult to identify if using a conventional single selectable marker where spontaneous inactivation of the single marker can occur. Importantly, the cassette that we used in this study, termed *CORE-I-SceI*, includes an additional gene encoding for the site-specific endonuclease I-*Sce*I under the control of the galactose inducible *GAL1,10* promoter (Storici and Resnick, 2006) as well as a single *I-SceI* site included in the 3' primer used to amplify the cassette. This additional feature greatly facilitates gene targeting as the induction of a *I-SceI* DSB has been shown to increase the targeting efficiency via recombinational repair more than 1000-fold in other studies (Storici et al., 2003; Storici and Resnick, 2006). In this work we have generated *mec1::CORE1*, *mec1::CORE2*, *mec1::CORE3* and *mec1::CORE4* parental strains. These strains can then be transformed with the appropriate DNA fragments that allow in one-step transformation the generation of a large choice of mutations ranging from point mutation to large deletions and insertions at precise position within the *MEC1* ORF. This approach also offers the opportunity of multiple rounds of mutation.

Testing the survival of the *mec1::CORE1*, *mec1::CORE2*, *mec1::CORE3* and *mec1::CORE4* parental strains after DNA damage, we observed that one of these strains (*mec1::CORE1*) was viable in these conditions contrasting with the

remaining strains (*mec1::CORE2*, *mec1::CORE3*, *mec1::CORE4*). In this strain, it is possible that one of the promoters of the *CORE-I-SceI* genes (likely to be the *GAL1,10* promoter, which is a strong and bidirectional promoter) may serve for Mec1 expression. Apart from the *mec1::CORE1* which is proficient in homologous recombination, the other three CORE-containing strains needed to be complemented by a plasmid harboring wild type *MEC1*. This step restored the homologous recombination defect of *MEC1* mutants, thereby allowing efficient gene targeting and the episomal *MEC1* can be easily cured to allow phenotypic characterization of the final strain.

It is important to note that the generation of novel *mec1* mutants in a haploid background is also facilitated by the prior deletion of *SML1*, which encodes an inhibitor of the Rnr1 subunit of ribonucleotide reductase, RNR (Zhao et al., 1998). Thus, *mec1* mutants that would otherwise be lethal can be generated. Mec1 regulates RNR through both regulating the induced the transcription of *RNR* genes during S-phase and, most importantly, the inhibitory phosphorylation (mediated by Rad53 and Dun1) of the Sml1 inhibitor of RNR. Loss of the Sml1 inhibitor of RNR obviates the requirement for Mec1-dependent inhibition of Sml1, allowing active RNR to synthesize dNTPs. Indeed, *sml1*Δ cells show increased dNTP levels, raising the efficiency of DNA replication and allowing the survival of cells when *MEC1* is mutated for its essential function (Zhao et al., 1998).

In this study we have here generated a collection of four strains that together constitute a unique tool for the generation of novel *mec1* mutants throughout the entire *MEC1* ORF of use for activity, structure and functional studies.

### 2.5.2. Putative roles of HEAT repeats in Mec1 functions

The role of the HEAT repeats of the Mec1 kinase in its activity, substrate specificity and specific interactions are unknown. Therefore, we began a structure-function study of Mec1 by generating *mec1* mutants in which different sets of N-terminal or internal HEAT repeats were individually deleted. The α-helical repeat nature of the N-terminal 90% of Mec1 and other PIKK proteins results from evolutionarily adaptable structural units that have been shown to act like platforms for protein-protein interactions in many systems (Groves and Barford, 1999). Consistent with

this, the presence of multiple HEAT repeats throughout the large PIKK proteins clearly suggests the possibility of roles in assembling and regulating multiprotein complexes. Here, we have shown that six different window deletions spanning the entire HEAT repeat region of Mec1 mutants are functionally null. Given that the deletions we generated varied from a single to multiple HEAT repeats in different regions of Mec1, this was an unexpected result. Our prediction had been that we would be able to observe different phenotypes with the different deletion mutants, consistent with the involvement of the different HEAT repeats in distinctive protein-protein interactions. However, given their *null* phenotype upon treatment with different types of DNA damage and replicative stress, as well as with their inability to grow in the presence of *SML1*, the window HEAT repeat deletions generated in this study seem to impact on all Mec1 functions, although they do not affect the protein expression levels.

Remarkably, other studies in our laboratory using equivalent mutants in ATR, generated in the chicken DT40 cell line, resulted in similar null phenotypes (Marta Llorens and John Eyekelboom, *unpublished data*). Thus the equivalent window deletions of both Mec1 and ATR behave similarly indicating the evolutionary conservation of our results. Our current data indicate that either all the window deletions in both Mec1 and ATR regulate the essential function(s) of these proteins or, alternatively, that for unknown structural reasons Mec1 and ATR cannot tolerate deletions anywhere within their HEAT repeat regions.

#### *2.5.2.1. HEAT repeats as scaffolds for protein-protein interactions*

The hypothesis that all the window deletions disrupt molecular interactions required for regulating essential function(s) implies that such molecular interactions, e.g. protein-protein interactions, required for the essential function of Mec1 and ATR are distributed through out the entire length of the HEAT repeat region of these proteins. Support for this hypothesis comes from the involvement of the N-terminal region of Mec1/ATR, Tel1/ATM and DNA-PKcs in their partner-dependent recruitment to DNA lesions or replication structures, steps thought to be critical for their activation and function (Falck et al., 2005). Consistent with this, it was shown that the first 500 amino acids in the N-terminus of Mec1 mediate Mec1 binding to its cofactor Ddc2 (Wakayama et al., 2001). However, these studies were obtained using fragments of

Mec1 and Ddc2 in yeast two-hybrid analysis and no supporting data was obtained using full-length proteins. Genetic experiments have shown that the Ddc2 protein is necessary for all known Mec1 functions, thus *ddc2Δ* mutants behaves identically to *mec1Δ* cells (Paciotti et al., 2000; Rouse and Jackson, 2000; Wakayama et al., 2001). Interestingly, the Ddc2-binding region previously described comprises the first N-terminal 13 HEAT repeats of Mec1, whereas our *mec1-W1* mutant is missing just the first 10 HEATs repeats and was functionally null. Thus our data suggests that a smaller region of Mec1 containing HEAT repeats 1-10 might mediate *in vivo* the binding of Mec1 to Ddc2. HEAT repeats 11-13 correspond to the three ATR-specific HEAT repeats. It is likely that these HEAT repeats are not necessary for interacting with Ddc2, but with other unknown protein(s). Accordingly, the equivalent ATRIP-binding region in ATR comprises HEATs 1-8, excluding the three ATR-specific HEAT repeats. Since these HEATs are specific for the ATR sub-family members (Perry and Kleckner, 2003) it is then attempting to speculate that they might be involved in the essential function of these proteins. Consistent with this, *mec1-W2* behaved like a *mec1* null strain. Further experiments are required to clarify this matter.

It is possible that the HEAT repeats mediate essential protein-protein interactions important to regulate the kinase activity of PIKK proteins. Consistent with this, in *S. pombe* the interaction between Nbs1 with Tel1 17-18 and 21-22 HEATs stimulates Tel1 kinase activity (You et al., 2005). Moreover, a recent study also showed that ATR autophosphorylation in the T1989 residue within its FAT domain mediates TopBP1 interaction to stimulate ATR kinase activity (Liu et al., 2011). Interestingly and in agreement with all these studies, our *mec1-W5* mutant behaved like a *mec1Δ* strain under DNA damaging growth conditions and was unable to grow when complemented with *SML1*. It is possible that the HEAT repeats comprised in the FAT domain are involved in critical interactions between Mec1 and regulator proteins that modulate its kinase activity, similarly to its homologue ATR.

Activation of Mec1 activity is mediated by the Ddc1 subunit of the 9-1-1 complex and the replication protein Dpb11. It is though that these two proteins share an analogous mode for Mec1 activation using the intrinsically disordered C-terminal

tails of each activator (Navadgi-Patil and Burgers, 2009b). In addition, it is speculated that the flexible and bipartite features of these Mec1-activating motifs might enable them to make two critical contacts with Mec1-Ddc2 inducing a conformational change of the kinase complex thereby enhancing its activity (Zou, 2009). However, molecular evidences for such mechanism are missing. It is possible that the HEAT repeats within the regulatory FAT domain of Mec1 might be involved in this process, promoting Mec1 kinase activity through interaction with its activator proteins and/or conformational changes.

In this study we also showed that *mec1-W6* mutant cells, where the single HEAT repeat between the FAT and Kinase domain is missing, behaved like a *mec1* null strain under the same conditions, indicating that this HEAT is required for Mec1 essential function. It is possible that this single HEAT repeat is involved, together with the FAT domain, in critical interactions between Mec1 and regulator proteins that modulate its kinase activity. Alternatively, due to its proximity to the KD its deletion can affect directly Mec1 catalytic activity. It would be interesting to examine if the window deletions generated in all our *mec1* mutants affect Mec1 kinase activity. We would expect that all the Mec1 mutant proteins are kinase-defective, since the window deletion mutants are indistinguishable from *mec1Δ* cells, similarly to previously reported kinase-negative *mec1* strains (Wakayama et al., 2001; Paciotti et al., 2001; Mallory and Petes, 2000). Noteworthy, in our study we did not include the Kinase domain since it is well established that this domain is required for Mec1 enzymatic activity and alterations within this domain result in kinase defective *mec1* mutants (Mallory and Petes, 2000; Nakada et al., 2005; Paciotti et al., 2001).

#### *2.5.2.2. HEAT repeats as spacers/springs*

To date, no function has been attributed to the large central region of Mec1. Our data suggests that this portion of Mec1 protein may be also involved in its essential function, since both *mec1-W3* and *mec1-W4* behaved similarly to *mec1Δ* in all the assays tested. These results could indicate that the HEAT repeats 14-31 might interact with a protein crucial for the activity and functions of Mec1. Alternatively, it is possible that the deletions generated in these regions are too large and therefore compromise the molecular architecture of Mec1. In this context, the overall size of

Mec1 protein might also be important for its functions. However, no ultra-structure has been solved either for Mec1 or for its orthologue ATR in order to clarify this issue. However, since the amino-acid sequences between the PIKK family members are similar especially at their C-terminus, a prediction is that their overall molecular architecture might be similar. Indeed, there are structural data available for the related ATM and DNA-PKcs kinases that indicate analogous EM-structures composed by a large head domain, believed to correspond to the kinase, FAT and FATC domains, and a protruding curved and flattened arm comprising the HEAT-containing N-terminal part of these proteins (Llorca et al., 2003; Rivera-Calzada et al., 2005; Spagnolo et al., 2006; Williams et al., 2008).

More recently, the crystal structure of DNA-PKcs with a resolution of 6.6 A was reported and shares some features in common with the previously reported electron microscopy models (Figure S2.1). Importantly, the DNA-PKcs crystal structure displays for the first time the overall architecture of this protein to be clearly a ring-like structure (Sibanda et al., 2010). The bending of this structure and the folding of the polypeptide chain into a hollow circular structure is facilitated by the many α-helical HEAT repeats, about 66 helices, that locate at the N-terminus of the protein. The C-terminus comprising the FAT, kinase and FATC domains is located on the top of this structure and this region probably corresponds to the head/crown domain identified in previous electron microscopy structures (Boskovic et al., 2003; Chiu et al., 1998; Rivera-Calzada et al., 2005; Williams et al., 2008). A small HEAT repeat domain that is likely to be the DNA binding domain shown in other EM studies (Williams et al., 2008) was also observed inside of this structure. In the circular arrangement of the HEAT repeats a small gap and two points of irregularity that flank a portion of the structure on the opposite site of the gap was also observed. Therefore, it was proposed that conformational changes in the static ring-like structure observed by crystallography might result in the arms swinging apart to provide a mechanism for DNA-PKcs binding to DSBs and/or release after DNA ends ligation. The conformational changes would probably be transmitted to the FAT, FATC and Kinase domains located in the head/crown, suggesting the arrangement and the size of the ring structure is important to engage DNA-PKcs in the repair of damaged DNA (Sibanda et al., 2010).

Accordingly, we speculate that other PIKKs such as Mec1 might have a similar highly ordered structure, including long, convex arms composed of HEATs that interact to generate a circular structure, the dimensions of which might be required to enclose DNA-protein structures for its proper recruitment to DNA lesions and activation. Interestingly, it was recently shown that PR65, the HEAT repeat-containing subunit of the protein phosphatase 2 (PP2A), undergoes (visco-)elastic deformations in response to forces promoting conformational changes in the regulatory and catalytic subunits of PP2A impacting in its activity (Grinthal et al., 2010). Analogously, it is then possible that the helical nature of HEAT repeats provides some flexibility to the structure of PIKKs allowing them to undergo conformational changes that result in a structurally more active form of these proteins.

### 2.5.3. *MEC1* mutants in which HEAT repeats are replaced by equivalent ATR or Tel1 HEAT repeats are inviable

In an attempt to restore structure and function of the Mec1 mutant proteins we took a more conservative strategy to deletion of HEAT repeats, we replaced some of the previous deleted Mec1 regions with the equivalent HEATs from the orthologous ATR kinase or the related Tel1 kinase. However, these replacement mutations were also phenotypically *null* with respect the essential function of Mec1. Our prediction was that this strategy might conserve structural features by introducing similar protein motifs from another PIKK protein (e.g. the ATR-related repeats of human ATR) and allow the successful rescue of Mec1's essential function. Additionally, it was also possible that substitution mutants might gain additional functions associated with the PIKK from which the substitutions were obtained (e.g. in case of the HEATs 14-22 from Tel1 that are involved in Tel1-Nbs1 interaction; (You et al., 2005)). Given that the three replacing mutants generated were unviable, it is possible that the replaced Mec1 HEAT repeats are either required for essential protein-protein interactions not conserved in ATR or Tel1, or they convey a structural arrangement to Mec1 protein that is incompatible with Mec1 function. Note that western blot analyses remain to be carried out in these hybrid mutants to exclude the possibility that the replacing HEATs are affecting Mec1 expression. Analysis of the molecular architecture of the Mec1-ATR and Mec1-Tel1 hybrid proteins relative to the WT

Mec1 (for example, by cryoelectron microscopy) would be critical to support/disprove the possibility of structural abnormalities in these hybrid proteins.

Taken together, it is clear that Mec1/ATR functions are tightly dependent on its HEAT repeats. Importantly, although the separation of discrete functions could not be achieved by the structure function studies conducted in this work, it is remarkable that Mec1 and ATR, and possibly all other PIKKs, are so sensitive to changes in their primary amino structure. This perhaps indicates that Mec1 and ATR have structures that are exquisitely sensitive to even subtle perturbations.

## 2.6. MATERIAL AND METHODS

### 2.6.1. Media and Growth conditions

Yeast cells were grown in YPD liquid (1% (w/v) yeast extract (Difco), 2% (w/v) bactopeptone (Difco), 2% (w/v) glucose (Difco)) or solid media containing a plus of 2% (w/v) agar (Difco). Cells were grown in conical flasks with liquid media at 30ºC in a shaker incubator at 170 rpm. The volume of culture did not exceed one quarter of the conical flask volume to ensure adequate aeration. Cells that were grown in plates of YPD solid media were incubated at 30ºC, and generally after 40h yeast colonies were obtained.

The synthetic complete media used in transformation for generating DSB is based in YNB medium (Yeast Nitrogen Base without amino acids, Difco) with 2% glucose (w/v, Difco) or 2% galactose (w/v) as desired, in which all amino acids required in this study (histidine, adenine, uracil, leucine and tryptophan) were added to have a final concentration of 20µl/ml.

### 2.6.2. Selective media and Genotoxic treatments

The minimal media is based in YNB medium (Yeast Nitrogen Base without amino acids, Difco) with 2% agar (w/v) (Difco) and 2% glucose (w/v, Difco) in which the required amino acids were added to have a final concentration of 20µl/ml (histidine, adenine, uracil, leucine and tryptophan to grow). The 5-FOA (5-Fluoroorotic Acid) media contain extra uracil to a final concentration of 50µl/ml and 5-FOA at 1mg/ml. The G418 media consist on YPD solid media containing geneticin at a final

concentration of 200µg/ml. The glycerol media consist on YPD media with 3% ethanol and 3% glycerol instead of using glucose.

The genotoxic treatment for sensitivity analysis was performed by the drop test methodology using media with different genotoxic agents: 1) MMS (Sigma-Aldrich) was added to YPD media to a final concentration of 0.015%. 2) CPT (Sigma) was added to YPD media to a final concentration of 10µM. 3) 4NQO (Sigma) was added to YPD to a final concentration of 0,625µM. 4) HU (Sigma) was added to YPD to a final concentration of 5mM. 5) Cells were irradiated with UV using Philips 254nm UV-C lamp (Ultra Violet Products). The UV irradiation rate ($J/m^2/s$) from the lamp was measured before each irradiation, using a UV dosimeter, and the time of exposure was calculated, (time = desired dose (50J) / UV intensity ($J/m^2/s$)). 6) γ-irradiation (200 or 400 Gy) was carried out using a $^{137}Cs$ source at a dose-rate of 12.10 Gy/min (Mainance Engineering, UK).

### 2.6.3. Yeast strains and Plasmids

All yeast strains used in this study are made in the W303-1a background and are listed in Table S1. All mutant alleles used were integrated on the chromosome. Yeast Strain and plasmid constructions are described below. Plasmids and oligonucleotides used in this study are listed in Tables S2 and S3 respectively.

### 2.6.4. *mec1* mutants construction

A 5-step strategy was developed to construct all *mec1* mutant strains and is described below. In this strategy we combined the *Delitto Perfetto* (adapted from (Storici and Resnick, 2006) and fusion PCR approaches to generate all *mec1* window deletion mutants in *sml1Δ* background.

#### *2.6.4.1. SML1 deletion*

To delete *SML1*, a 1130 bp *TRP1* selectable marker was amplified from plasmid pRS304 (Sikorski and Philip, 1989) using primers SML1-URA5' and SML1-URA3' containing at their 5' ends 40 and 45 bp homologous to the regions upstream and downstream of the *SML1* locus, respectively. The PCR construct was then transformed into W303-1a cells. After selecting the candidates on media lacking tryptophan, deletion of *SML1* was confirmed by genomic PCR, using primers

SML1-1 and SML1-2, and their wild type-like phenotype in the presence of several genotoxic agents was confirmed by droptest analysis (*data not shown* and Figure 2).

#### *2.6.4.2. CORE-containing mec1 mutants*

CORE-containing mutants were obtained by independently transforming the *sml1::TRP1* strain with four CORE-I-*Sce*I-targeting constructs (CORE-H1; CORE-H2; CORE-H3; CORE-H4) generated by fusion PCR as follow. A 4.6 Kb CORE-I-*Sce*I cassette was PCR amplified four times from the plasmid pGSKU (Storici and Resnick, 2006) using the following set of primers: CORE-H1-fw with CORE-H1-rev, CORE-H2-fw with CORE-H2-rev, CORE-H3-fw with CORE-H3-rev, and CORE-H4-fw with CORE-H4-rev, respectively. Note that the 3' primers of each set contained an I-*Sce*I restriction site at their 5' ends where a DSB is generated after galactose induction in a subsequent step (described below).

The 5' and 3' targeting arms for each construct ranging size from 500 bp to 2 Kb were amplified from the genomic DNA regions upstream and downstream to the place for integration of the CORE cassette using the following set of primers: T1 with B1 (-500aa to -1aa) and T2 with B2 (+1aa to +500aa) for CORE-H1; T4 with B4 (+1051aa to +1539aa) and T5 with B5 (+1540aa to +2583aa) for CORE-H2; T10 with B10 (+3668aa to +4155aa) and T11 with B11 (+4156aa to +4653aa) for CORE-H3; and T16 with B16 (+5188aa to +6135aa) and T17 with B17 (+6136aa to +6694aa) for CORE-H4, respectively. The CORE cassettes contained overlapping sequences at both 5' and 3' extremities to their respective targeting arms allowing their fusion by a 2-step PCR reaction. For instance, the fragments to be fused were joined into a single molecule in the first step of the fusion PCR, and amplified in a second step using the extreme primers T1 and B2, T4 and B5, T10 and B11, and T16 and B17 for each targeting construct respectively.

The fused targeting DNA was then transformed into *W303 sml1::TRP1* strain as previously described (Storici and Resnick, 2006). The CORE-I-SceI cassettes were integrated by HR at four different regions of *MEC1* immediately upstream or downstream to the region to be deleted/replaced, generating *mec1::CORE1*, *mec1::CORE2*, *mec1::CORE3* and *mec1::CORE4* strains (Figure 2A). Whenever the yield from the fusion PCR between the CORE-I-SceI cassette and both 5' and 3'

arms was low, cells were co-transformed with two fragments, each corresponding to the fusion of the cassette to only one of the arms. Due to the high efficiency of HR in yeast cells, concurrent recombination events between both CORE cassettes of the two fragments and the targeting arms with the homologous genomic region allow the integration of the CORE cassette at the desired *locus* (Storici and Resnick, 2006). Colonies growing on selective media (either containing G418 or lacking uracil) were tested by diagnostic PCR using primers LCD96 with KlURA-3' for *mec1::CORE1*; Mec1-1 with KlURA-3' for *mec1::CORE2*; T14 with KlURA-3' for *mec1::CORE3*; and T13 with KlURA-3' for *mec1::CORE4*, respectively. This diagnostic PCR discriminated wild type cells, and cells that would have integrated the CORE cassette in the correct *locus* from cells that would have integrated elsewhere in the genome. Strains in which targeted integration occurred were isolated.

#### *2.6.4.3. Complementation of CORE-containing mec1 mutants with MEC1 centromeric plasmid*

*mec1::CORE2*, *mec1::CORE3* and *mec1::CORE4* were complemented with a centromeric plasmid containing *MEC1* (pML227, kindly provided by Longhese MP; (Paciotti et al., 2001) by transforming cells with 300 ng of plasmid DNA as described before (lithium acetate method; (Wach et al., 1994).

#### *2.6.4.4. mec1 window deletion / replacement mutants*

To generate the window deletion mutants *mec1-W1*, *mec1-W2*, *mec1-W3*, *mec1-W4*, *mec1-W5* and *mec1-W6*, six targeting constructs containing the deletion were prepared by fusion PCR (termed W1, W2, W3, W4, W5, W6, respectively). For each construct, two DNA fragments ranging size from 500 bp to 2 Kb and flanking the *MEC1* region to be deleted, were amplified from yeast genomic DNA using primers T1 with B1 (-500aa to -1aa) and T3 with B3 (+1051aa to +2402aa) for W1; T2 with B6 (+1a to +1050aa) and T7 with B5 (+1540aa to +2583aa) for W2; T4 with B8 (+1051aa to +1539aa) and T9 with B9 (+2584aa to +4155aa) for W3; T5 with B12 (+1540aa to +2583aa) and T13 with B13 (+4156aa to +5904aa) for W4; T14 with B14 (+2584aa to +4155aa) and T15 with B15 (+5905aa to +6531aa) for W5; and T16 with B18 (+5188aa to +5904aa) and T19 with B19 (+6136aa to +7104aa) for W6, respectively. These fragments contained overlapping sequences at their 3' or 5' extremities, correspondingly, that allowed their fusion during a 2-step fusion PCR

reaction by using the extreme primers: T1 with B3 for W1; T2 with B5 for W2; T4 with B9 for W3; T5 with B13 for W4; T14 with B15 for W5; and T16 with B19 for W6, respectively. The fusion PCR constructs were transformed into the *CORE*-containing strains as previously described (Storici and Resnick, 2006). For instance, *mec1::CORE1* was transformed with W1 construct to generate *mec1-W1* mutant; *mec1::CORE2* was independently transformed with W2 and W3 constructs to generate *mec1-W2* and *mec1-W3*, respectively; *mec1::CORE3* was independently transformed with W4 and W5 constructs to generate *mec1-W4* and *mec1-W5* mutants; and *mec1::CORE4* was transformed with W6 construct to generate *mec1-W6* mutant. Importantly, for transformation of these *mec1::CORE-I-SceI* strains the induction of a DSB was needed prior to the integration of the DNA fragments in order to stimulate homologous recombination and increase the efficiency of genome targeting (Storici and Resnick, 2006). Briefly, cells were grown in media containing galactose for 4 hours to induce the expression of the endonuclease I-SceI and to generate a DSB at 3' end of the CORE-I-SceI cassette as previously described (Storici and Resnick, 2006).

To generate the replacement mutants *mec1-W2::ATR*$^{H11\text{-}13}$, *mec1-W2::tel1*$^{H13\text{-}14}$ and *mec1-W3*$^{H17\text{-}23}$, three targeting constructs containing the replacing region were prepared by fusion PCR (termed W2::R1, W2::R2 and W3::R1, respectively). Replacing PCR fragments of 501bp, 418bp and 914bp to generate W2::R1, W2::R2 and W3::R1 constructs were amplified from human cDNA and yeast genomic DNA using primers R1.2ATR-5' with R1.2ATR-3' (+1744aa to +2244aa), R1.1tel1-5' with R1.1tel1-3' (+2005aa to +2421aa) and R2.2tel1-5' with R2.2tel1-3' (+2683aa to +3528aa), respectively. The 5' and 3' targeting arms for each construct ranging size from 500 bp to 1.5 Kb were amplified from the genomic DNA regions flanking the *MEC1* region to be replaced using primers T2 with B6R1 (+1aa to +1050aa) and T5 with B3 (+1540aa to +2402aa) for W2::R1 and W2::R2; and T4 with B4 (+1051aa to +1539aa) and T14 with B9 (+2584aa to +4155aa) for W3::R1. The replacing PCR fragments contained overlapping sequences at both 5' and 3' extremities to their respective targeting arms allowing their fusion by a 2-step PCR reaction. For instance, the fragments to be fused were joined into a single molecule in the first step of the fusion PCR, and amplified in a second step using the extreme

primers T2 with B3 for both W2::R1 and W2::R2 constructs, and T4 with B9 for W3::R1 targeting construct respectively.

The fusion PCR constructs were transformed into the *CORE*-containing strains previously cultured in media containing galactose for the induction of a DSB at 3' end of the CORE-I-SceI cassette as described before (Storici and Resnick, 2006). For instance, *mec1::CORE2* was independently transformed with W2::R1 and W2::R2 constructs to generate *mec1-W2::ATR*$^{H11\text{-}13}$ and *mec1-W2::tel1*$^{H13\text{-}14}$, respectively; while *mec1::CORE3* was transformed with W3::R1 targeting construct to generate *mec1-W3::tel1*$^{H17\text{-}23}$ mutant.

Upon transformation, different dilutions of transformant cells (1/10 and 9/10) were then plated on YPD media and incubated for 24 hours at 30°C. After two sets of replica-plating on 5-FOA plates to decrease the background resulted from false positive transformants, colonies were replica-plated on selective media (containing either G418, 5-FOA or lacking uracil). Colonies were allowed to grow for approximately 3 days and the selection steps were repeated one more time. Multiple independent colonies were obtained for each of the deletion/replacement strains generated and were used in strain 91haracterization studies (*data not shown*). Diagnostic PCR was performed on the genomic DNA of the selected clones and was designed to amplify a fragment that would allow to discriminate between wild-type, mutant cells that would have loss the CORE-I-SceI cassette from cells that would have only lost parts of the cassette, and cells that would have integrated the targeting construct in the correct *locus* from others that would have integrated it elsewhere in the genome. Primers (or at least one of them) selected outside of the region that was integrated by homologous recombination were used to confirm the insertion of the DNA change for each *mec1* window deletion mutant: LCD96 and B12 for *mec1-W1*; T1 with B3 for *mec1-W2*, T4 with B11 for *mec1-W3* and *mec1-W4*, T10 with B17 for *mec1-W5* and T16 with Mec1-2 for *mec1-W6*. A primer specific for the replacement together with a primer outside of the integrated region were used to confirm the correct replacement mutants: 5'-SpecFw with B5 for *mec1-W2::ATR*$^{H11\text{-}13}$, R1tel1-5' with B5 for *mec1-W2::tel1*$^{H13\text{-}14}$; and 5'-DIAG_R2.1-2.2replac with B11 for *mec1-W3*$^{H17\text{-}23}$.

#### *2.6.4.5. Selection for the loss of MEC1 centromeric plasmid*

*mec1* mutants were allowed to grow overnight in rich medium to promote the loss of the *MEC1* centromeric plasmid. Approximately 500 cells were then plated on YPD and after two days of growth at 30°C were replica plated on selective media lacking leucine (MN-LEU). Few colonies of each clone not able to grow on MN-LEU were picked and plated on YPD.

### 2.6.5. Western blotting and Antibodies

Sodium hydroxide protein extracts (Kushnirov, 2000) were separated by sodium dodecyl sulphate-polyacrylamide gel electrophoresis (SDS-PAGE). Western blotting was performed as previously described (O'Shaughnessy et al., 2006; Vialard et al., 1998). Mec1 was resolved in 6.5%, 80/1 acrylamide/bis-acrylamide, SDS-PAGE gel and probed with NL33 (Noel F. Lowndes; (Downs et al., 2000)) antibody at 1:500 dilution in PBS containing 0.1% Tween-20.

### 2.6.6. Drop test methodology

DNA damage sensitivity analysis was performed by spotting five-fold serial dilutions ($5x10^6$ to $1x10^4$ cells/ml) of exponentially growing cultures of the indicated strains on plates containing the indicated genotoxic agents or treated as indicated. Plates were incubated in the 30ºC incubator unless otherwise specified for two days before scanning.

### 2.6.7. Viability assay

Viability assay was performed by transforming exponentially growing cells with 300 ng of *SML1* centromeric plasmid (kindly provided by R. Rothstein, (Zhao et al., 1998), using the Lithium Acetate method described previously (Wach et al., 1994). $1x10^8$ cells were plated onto selective medium lacking leucine. Plates were then incubated at 30°C for two days or until colonies were formed.

### 2.6.8. Yeast native extracts

0.5-1.5 liter cultures of yeast strains expressing a Mec1 mutant protein under the control of their own endogenous promoters were grown in YPD medium at a cell density of $1x10^7$ cells/ml. Cells were then collected by centrifugation and washed twice with pre-cooled dd$H_2O$ and once in 2x lysis buffer (300 mM KCl, 100mM

Hepes pH 7.5, 20% glycerol, 8mM β -mercaptoethanol, 2 mM EDTA, 0.1% Tween20, 0.01% NP-40). Cells were extruded into liquid nitrogen through a syringe and the frozen 'noodles' stored at -80ºC until required. Noodles were manually ground in a mortar in liquid nitrogen. One volume (relative to cells) of 2x lysis buffer, containing a protein inhibitor cocktail (2.8 μM leupeptin, 8 μM pepstatin A, 4 mM PMSF, 8 mM benzamidine, 8 μM antipain, 4 μM chymostatin in ethanol) and phosphatase inhibitors (2 mM sodium fluoride, 1.2mM β-glycerophosphate, 0.04 μM sodium vanadate, 2 mM EGTA, 10 mM sodium pyrophosphate), was added. Cell extract was clarified by a low speed centrifugation followed by additional centrifugation for 1 hour at 42000 rpm in a Beckman Sw55Ti rotor.

## 2.7. REFERENCES


Abraham, R.T. (2004). PI 3-kinase related kinases: 'big' players in stress-induced signaling pathways. DNA Repair (Amst) *3*, 883-887.

Adami, A., Garcia-Alvarez, B., Arias-Palomo, E., Barford, D., and Llorca, O. (2007). Structure of TOR and its complex with KOG1. Mol Cell *27*, 509-516.

Andrade, M.A., and Bork, P. (1995). HEAT repeats in the Huntington's disease protein. Nat Genet *11*, 115-116.

Andrade, M.A., Perez-Iratxeta, C., and Ponting, C.P. (2001a). Protein repeats: structures, functions, and evolution. J Struct Biol *134*, 117-131.

Andrade, M.A., Petosa, C., O'Donoghue, S.I., Muller, C.W., and Bork, P. (2001b). Comparison of ARM and HEAT protein repeats. J Mol Biol *309*, 1-18.

Ball, H.L., Ehrhardt, M.R., Mordes, D.A., Glick, G.G., Chazin, W.J., and Cortez, D. (2007). Function of a conserved checkpoint recruitment domain in ATRIP proteins. Mol Cell Biol *27*, 3367-3377.

Ball, H.L., Myers, J.S., and Cortez, D. (2005). ATRIP binding to replication protein A-single-stranded DNA promotes ATR-ATRIP localization but is dispensable for Chk1 phosphorylation. Mol Biol Cell *16*, 2372-2381.

Bayliss, R., Littlewood, T., and Stewart, M. (2000). Structural basis for the interaction between FxFG nucleoporin repeats and importin-beta in nuclear trafficking. Cell *102*, 99-108.

Berens, T.J., and Toczyski, D.P. (2012). Colocalization of Mec1 and Mrc1 is sufficient for Rad53 phosphorylation in vivo. Mol Biol Cell *23*, 1058-1067.

Bonilla, C.Y., Melo, J.A., and Toczyski, D.P. (2008). Colocalization of sensors is sufficient to activate the DNA damage checkpoint in the absence of damage. Mol Cell *30*, 267-276.

Boskovic, J., Rivera-Calzada, A., Maman, J.D., Chacon, P., Willison, K.R., Pearl, L.H., and Llorca, O. (2003). Visualization of DNA-induced conformational changes in the DNA repair kinase DNA-PKcs. EMBO J *22*, 5875-5882.

Bosotti, R., Isacchi, A., and Sonnhammer, E.L. (2000). FAT: a novel domain in PIK-related kinases. Trends Biochem Sci *25*, 225-227.

Brewerton, S.C., Dore, A.S., Drake, A.C., Leuther, K.K., and Blundell, T.L. (2004). Structural analysis of DNA-PKcs: modelling of the repeat units and insights into the detailed molecular architecture. J Struct Biol *145*, 295-306.

Chiu, C.Y., Cary, R.B., Chen, D.J., Peterson, S.R., and Stewart, P.L. (1998). Cryo-EM imaging of the catalytic subunit of the DNA-dependent protein kinase. J Mol Biol *284*, 1075-1081.

Chook, Y.M., and Blobel, G. (1999). Structure of the nuclear transport complex karyopherin-beta2-Ran x GppNHp. Nature *399*, 230-237.

Cimprich, K.A., and Cortez, D. (2008). ATR: an essential regulator of genome integrity. Nat Rev Mol Cell Biol *9*, 616-627.

Cingolani, G., Petosa, C., Weis, K., and Muller, C.W. (1999). Structure of importin-beta bound to the IBB domain of importin-alpha. Nature *399*, 221-229.

Downs, J.A., Lowndes, N.F., and Jackson, S.P. (2000). A role for Saccharomyces cerevisiae histone H2A in DNA repair. Nature *408*, 1001-1004.

Erdeniz, N., Mortensen, U.H., and Rothstein, R. (1997). Cloning-free PCR-based allele replacement methods. Genome Res *7*, 1174-1183.

Falck, J., Coates, J., and Jackson, S.P. (2005). Conserved modes of recruitment of ATM, ATR and DNA-PKcs to sites of DNA damage. Nature *434*, 605-611.

Flott, S., Kwon, Y., Pigli, Y.Z., Rice, P.A., Sung, P., and Jackson, S.P. (2011). Regulation of Rad51 function by phosphorylation. EMBO Rep *12*, 833-839.

Grinthal, A., Adamovic, I., Weiner, B., Karplus, M., and Kleckner, N. (2010). PR65, the HEAT-repeat scaffold of phosphatase PP2A, is an elastic connector that links force and catalysis. Proc Natl Acad Sci U S A *107*, 2467-2472.

Groves, M.R., and Barford, D. (1999). Topological characteristics of helical repeat proteins. Curr Opin Struct Biol *9*, 383-389.

Groves, M.R., Hanlon, N., Turowski, P., Hemmings, B.A., and Barford, D. (1999). The structure of the protein phosphatase 2A PR65/A subunit reveals the conformation of its 15 tandemly repeated HEAT motifs. Cell *96*, 99-110.

Jiang, X., Sun, Y., Chen, S., Roy, K., and Price, B.D. (2006). The FATC domains of PIKK proteins are functionally equivalent and participate in the Tip60-dependent activation of DNA-PKcs and ATM. J Biol Chem *281*, 15741-15746.

Keith, C.T., and Schreiber, S.L. (1995). PIK-related kinases: DNA repair, recombination, and cell cycle checkpoints. Science *270*, 50-51.

Kushnirov, V.V. (2000). Rapid and reliable protein extraction from yeast. Yeast *16*, 857-860.

Lempiainen, H., and Halazonetis, T.D. (2009). Emerging common themes in regulation of PIKKs and PI3Ks. EMBO J *28*, 3067-3073.

Liu, S., Shiotani, B., Lahiri, M., Marechal, A., Tse, A., Leung, C.C., Glover, J.N., Yang, X.H., and Zou, L. (2011). ATR autophosphorylation as a molecular switch for checkpoint activation. Mol Cell *43*, 192-202.

Llorca, O., Rivera-Calzada, A., Grantham, J., and Willison, K.R. (2003). Electron microscopy and 3D reconstructions reveal that human ATM kinase uses an arm-like domain to clamp around double-stranded DNA. Oncogene *22*, 3867-3874.

Longhese, M.P., Paciotti, V., Neecke, H., and Lucchini, G. (2000). Checkpoint proteins influence telomeric silencing and length maintenance in budding yeast. Genetics *155*, 1577-1591.

Lovejoy, C.A., and Cortez, D. (2009). Common mechanisms of PIKK regulation. DNA Repair (Amst) *8*, 1004-1008.

Lundin, C., North, M., Erixon, K., Walters, K., Jenssen, D., Goldman, A.S., and Helleday, T. (2005). Methyl methanesulfonate (MMS) produces heat-labile DNA damage but no detectable in vivo DNA double-strand breaks. Nucleic Acids Res *33*, 3799-3811.

Majka, J., Niedziela-Majka, A., and Burgers, P.M. (2006). The checkpoint clamp activates Mec1 kinase during initiation of the DNA damage checkpoint. Mol Cell *24*, 891-901.

Mallory, J.C., and Petes, T.D. (2000). Protein kinase activity of Tel1p and Mec1p, two Saccharomyces cerevisiae proteins related to the human ATM protein kinase. Proc Natl Acad Sci U S A *97*, 13749-13754.

Moerschell, R.P., Tsunasawa, S., and Sherman, F. (1988). Transformation of yeast with synthetic oligonucleotides. Proc Natl Acad Sci U S A *85*, 524-528.

Mordes, D.A., and Cortez, D. (2008). Activation of ATR and related PIKKs. Cell Cycle *7*, 2809-2812.

Mordes, D.A., Glick, G.G., Zhao, R., and Cortez, D. (2008a). TopBP1 activates ATR through ATRIP and a PIKK regulatory domain. Genes Dev *22*, 1478-1489.

Mordes, D.A., Nam, E.A., and Cortez, D. (2008b). Dpb11 activates the Mec1-Ddc2 complex. Proc Natl Acad Sci U S A *105*, 18730-18734.

Morita, T., Yamashita, A., Kashima, I., Ogata, K., Ishiura, S., and Ohno, S. (2007). Distant N- and C-terminal domains are required for intrinsic kinase activity of SMG-1, a critical component of nonsense-mediated mRNA decay. J Biol Chem *282*, 7799-7808.

Nakada, D., Hirano, Y., Tanaka, Y., and Sugimoto, K. (2005). Role of the C terminus of Mec1 checkpoint kinase in its localization to sites of DNA damage. Mol Biol Cell *16*, 5227-5235.

Nasmyth, K., Adolf, G., Lydall, D., and Seddon, A. (1990). The identification of a second cell cycle control on the HO promoter in yeast: cell cycle regulation of SW15 nuclear entry. Cell *62*, 631-647.

Navadgi-Patil, V.M., and Burgers, P.M. (2009a). A tale of two tails: activation of DNA damage checkpoint kinase Mec1/ATR by the 9-1-1 clamp and by Dpb11/TopBP1. DNA Repair (Amst) *8*, 996-1003.

Navadgi-Patil, V.M., and Burgers, P.M. (2009b). The unstructured C-terminal tail of the 9-1-1 clamp subunit Ddc1 activates Mec1/ATR via two distinct mechanisms. Mol Cell *36*, 743-753.

Navadgi-Patil, V.M., and Burgers, P.M. (2011). Cell-cycle-specific activators of the Mec1/ATR checkpoint kinase. Biochem Soc Trans *39*, 600-605.

O'Shaughnessy, A.M., Grenon, M., Gilbert, C., Toh, G.W., Green, C.M., and Lowndes, N.F. (2006). Multiple approaches to study S. cerevisiae Rad9, a prototypical checkpoint protein. Methods Enzymol *409*, 131-150.

Paciotti, V., Clerici, M., Lucchini, G., and Longhese, M.P. (2000). The checkpoint protein Ddc2, functionally related to S. pombe Rad26, interacts with Mec1 and is regulated by Mec1-dependent phosphorylation in budding yeast. Genes Dev *14*, 2046-2059.

Paciotti, V., Clerici, M., Scotti, M., Lucchini, G., and Longhese, M.P. (2001). Characterization of mec1 kinase-deficient mutants and of new hypomorphic mec1 alleles impairing subsets of the DNA damage response pathway. Mol Cell Biol *21*, 3913-3925.

Perry, J., and Kleckner, N. (2003). The ATRs, ATMs, and TORs are giant HEAT repeat proteins. Cell *112*, 151-155.

Puddu, F., Piergiovanni, G., Plevani, P., and Muzi-Falconi, M. (2011). Sensing of replication stress and Mec1 activation act through two independent pathways involving the 9-1-1 complex and DNA polymerase epsilon. PLoS Genet *7*, e1002022.

Rivera-Calzada, A., Maman, J.D., Spagnolo, L., Pearl, L.H., and Llorca, O. (2005). Three-dimensional structure and regulation of the DNA-dependent protein kinase catalytic subunit (DNA-PKcs). Structure *13*, 243-255.

Rouse, J., and Jackson, S.P. (2000). LCD1: an essential gene involved in checkpoint control and regulation of the MEC1 signalling pathway in Saccharomyces cerevisiae. EMBO J *19*, 5801-5812.

Rouse, J., and Jackson, S.P. (2002). Lcd1p recruits Mec1p to DNA lesions in vitro and in vivo. Mol Cell *9*, 857-869.

Scherer, S., and Davis, R.W. (1979). Replacement of chromosome segments with altered DNA sequences constructed in vitro. Proc Natl Acad Sci U S A *76*, 4951-4955.

Sibanda, B.L., Chirgadze, D.Y., and Blundell, T.L. (2010). Crystal structure of DNA-PKcs reveals a large open-ring cradle comprised of HEAT repeats. Nature *463*, 118-121.

Spagnolo, L., Rivera-Calzada, A., Pearl, L.H., and Llorca, O. (2006). Three-dimensional structure of the human DNA-PKcs/Ku70/Ku80 complex assembled on DNA and its implications for DNA DSB repair. Mol Cell *22*, 511-519.

Storici, F., Durham, C.L., Gordenin, D.A., and Resnick, M.A. (2003). Chromosomal site-specific double-strand breaks are efficiently targeted for repair by oligonucleotides in yeast. Proc Natl Acad Sci U S A *100*, 14994-14999.

Storici, F., Lewis, L.K., and Resnick, M.A. (2001). In vivo site-directed mutagenesis using oligonucleotides. Nat Biotechnol *19*, 773-776.

Storici, F., and Resnick, M.A. (2003). Delitto perfetto targeted mutagenesis in yeast with oligonucleotides. Genet Eng (N Y) *25*, 189-207.

Storici, F., and Resnick, M.A. (2006). The delitto perfetto approach to in vivo site-directed mutagenesis and chromosome rearrangements with synthetic oligonucleotides in yeast. Methods Enzymol *409*, 329-345.

Sun, Y., Jiang, X., Chen, S., Fernandes, N., and Price, B.D. (2005). A role for the Tip60 histone acetyltransferase in the acetylation and activation of ATM. Proc Natl Acad Sci U S A *102*, 13182-13187.

Takahashi, T., Hara, K., Inoue, H., Kawa, Y., Tokunaga, C., Hidayat, S., Yoshino, K., Kuroda, Y., and Yonezawa, K. (2000). Carboxyl-terminal region conserved among phosphoinositide-kinase-related kinases is indispensable for mTOR function in vivo and in vitro. Genes Cells *5*, 765-775.

Takai, H., Wang, R.C., Takai, K.K., Yang, H., and de Lange, T. (2007). Tel2 regulates the stability of PI3K-related protein kinases. Cell *131*, 1248-1259.

Ullal, P., Vilella-Mitjana, F., Jarmuz, A., and Aragon, L. (2011). Rtt107 phosphorylation promotes localisation to DNA double-stranded breaks (DSBs) and recombinational repair between sister chromatids. PLoS One *6*, e20152.

Vialard, J.E., Gilbert, C.S., Green, C.M., and Lowndes, N.F. (1998). The budding yeast Rad9 checkpoint protein is subjected to Mec1/Tel1-dependent hyperphosphorylation and interacts with Rad53 after DNA damage. EMBO J *17*, 5679-5688.

Wach, A., Brachat, A., Pohlmann, R., and Philippsen, P. (1994). New heterologous modules for classical or PCR-based gene disruptions in Saccharomyces cerevisiae. Yeast *10*, 1793-1808.

Wakayama, T., Kondo, T., Ando, S., Matsumoto, K., and Sugimoto, K. (2001). Pie1, a protein interacting with Mec1, controls cell growth and checkpoint responses in Saccharomyces cerevisiae. Mol Cell Biol *21*, 755-764.

Williams, D.R., Lee, K.J., Shi, J., Chen, D.J., and Stewart, P.L. (2008). Cryo-EM structure of the DNA-dependent protein kinase catalytic subunit at subnanometer resolution reveals alpha helices and insight into DNA binding. Structure *16*, 468-477.

You, Z., Chahwan, C., Bailis, J., Hunter, T., and Russell, P. (2005). ATM activation and its recruitment to damaged DNA require binding to the C terminus of Nbs1. Mol Cell Biol *25*, 5363-5379.

Zhao, X., Muller, E.G., and Rothstein, R. (1998). A suppressor of two essential checkpoint genes identifies a novel protein that negatively affects dNTP pools. Mol Cell *2*, 329-340.

Zou, L. (2009). Checkpoint Mec-tivation comes in many flavors. Mol Cell *36*, 734-735.

Zou, L., and Elledge, S.J. (2003). Sensing DNA damage through ATRIP recognition of RPA-ssDNA complexes. Science *300*, 1542-1548.

## 2.8. SUPPLEMENTAL INFORMATION

### 2.8.1. Inventory

**Supplemental Figures (page 97)**



**Supplemental Tables (pages 98-101)**

## 2.8.2. Supplemental Figures

### *Figure S2.1*

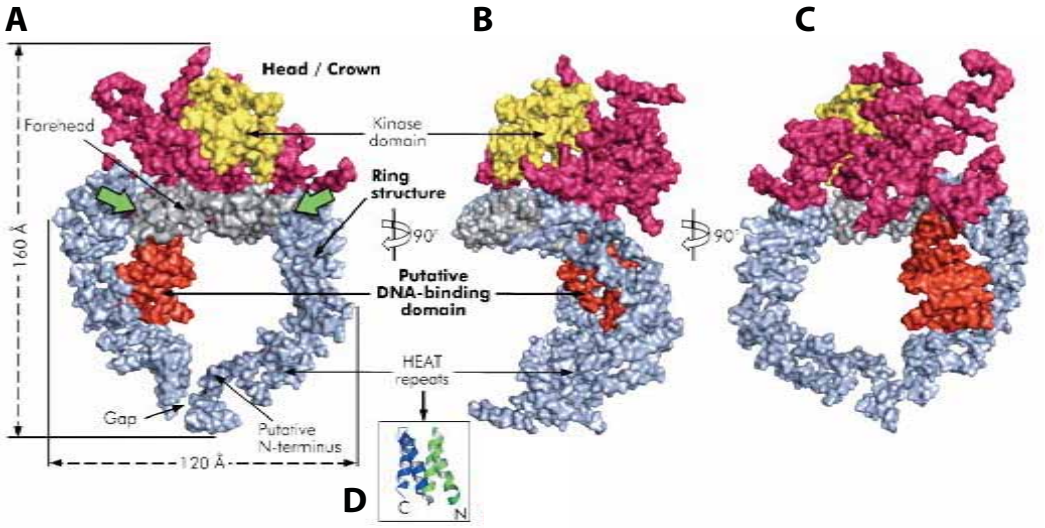


**Figure S2.1**: **Crystal structure of DNA-PKcs (6.6 A)**. The molecular surface of DNA-PKcs showing (A) front, with the potential conformationally variable regions denoted with green arrows, (B) side view, (C) back view, (D) a single HEAT repeat. The colour code of the molecule is as follows: ring structure in grey; the putative DNA binding domain in red; the larger head/crown domain in magenta and (for the kinase sub-domain) yellow. Adapted from Sibanda et al., 2010.

### 2.8.3. Supplemental Tables

**Table S2.1: Strains used in this study.**

| Strain | Genotype | Reference |
|---|---|---|
| W303-1a | *MATa ade2-1; his3-11,15; leu2-3,112; trp1-1; ura3; can1-100* | (Nasmyth et al., 1990) |
| *sml1Δ* | *MATa sml1::TRP1* | This study |
| *mec1::CORE1* | *MATa sml1::TRP1 mec1:: KlURA, kanMX4,GAL1,I-SceI* | This study |
| *mec1::CORE2* | *MATa sml1::TRP1 mec1:: KlURA, kanMX4,GAL1,I-SceI* | This study |
| *mec1::CORE3* | *MATa sml1::TRP1 mec1:: KlURA, kanMX4,GAL1,I-SceI* | This study |
| *mec1::CORE4* | *MATa sml1::TRP1 mec1:: KlURA, kanMX4,GAL1,I-SceI* | This study |
| *mec1Δ sml1Δ* | *MATa mec1::HIS3 sml1::kanMX4* | (Longhese et al., 2000) |
| *mec1::CORE2 + cpMEC1* | *MATa sml1::TRP1 mec1:: KlURA, kanMX4,GAL1,I-SceI MEC1*$^{+}$ | This study |
| *mec1::CORE3 + cpMEC1* | *MATa sml1::TRP1 mec1:: KlURA, kanMX4,GAL1,I-SceI MEC1*$^{+}$ | This study |
| *mec1::CORE4 + cpMEC1* | *MATa sml1::TRP1 mec1:: KlURA, kanMX4,GAL1,I-SceI MEC1*$^{+}$ | This study |
| *mec1-W1* + cp*MEC1* | *MATa sml1::TRP1 mec1-W1 MEC1*$^{+}$ | This study |
| *mec1-W2* + cp*MEC1* | *MATa sml1::TRP1 mec1-W2 MEC1*$^{+}$ | This study |
| *mec1-W3* + cp*MEC1* | *MATa sml1::TRP1 mec1-W3 MEC1*$^{+}$ | This study |
| *mec1-W4* + cp*MEC1* | *MATa sml1::TRP1 mec1-W4 MEC1*$^{+}$ | This study |
| *mec1-W5* + cp*MEC1* | *MATa sml1::TRP1 mec1-W5 MEC1*$^{+}$ | This study |
| *mec1-W6* + cp*MEC1* | *MATa sml1::TRP1 mec1-W6 MEC1*$^{+}$ | This study |
| *mec1-W1* | *MATa sml1::TRP1 mec1-W1* | This study |
| *mec1-W2* | *MATa sml1::TRP1 mec1-W2* | This study |
| *mec1-W3* | *MATa sml1::TRP1 mec1-W3* | This study |
| *mec1-W4* | *MATa sml1::TRP1 mec1-W4* | This study |
| *mec1-W5* | *MATa sml1::TRP1 mec1-W5* | This study |
| *mec1-W6* | *MATa sml1::TRP1 mec1-W6* | This study |
| *mec1-W2::ATR*$^{H11\text{-}13}$ + cp*MEC1* | *MATa sml1::TRP1 mec1-W2::ATR*$^{H11\text{-}13\ \Delta}$ *SML1*$^{+}$ | This study |
| *mec1-W2::tel1*$^{H13\text{-}14}$ + cp*MEC1* | *MATa sml1::TRP1 mec1-W2::tel1*$^{H13\text{-}14}$ *SML1*$^{+}$ | This study |
| *mec1-W3tel1*$^{H17\text{-}23}$ + cp*MEC1* | *MATa sml1::TRP1 mec1-W3tel1*$^{H17\text{-}23}$ *SML1*$^{+}$ | This study |
| *mec1-W2::ATR*$^{H11\text{-}13}$ | *MATa sml1::TRP1 mec1-W2::ATR*$^{H11\text{-}13}$ | This study |
| *mec1-W2::tel1*$^{H13\text{-}14}$ | *MATa sml1::TRP1 mec1-W2::tel1*$^{H13\text{-}14}$ | This study |
| *mec1-W3tel1*$^{H17\text{-}23}$ | *MATa sml1::TRP1 mec1-W3tel1*$^{H17\text{-}23}$ | This study |

**Table S2.2: Plasmids used in this study.**

| Plasmid | Reference | Usage |
|---|---|---|
| pRS304 | Sikorski and Hieter, 1989 | To delete *SML1* |
| pGSKU | (Storici and Resnick, 2006) | Amplify CORE-I-SceI |
| pML227 (*LEU2 CEN4 MEC1*) | (Paciotti et al., 2001) | *MEC1* centromeric plasmid for complementation during generation of *mec1* mutants |
| pWJ739 (*LEU2 CEN4 SML1*) | (Zhao et al., 1998) | *SML1* centromeric plasmid for viability assay |

**Table S2.3: Primers used in this study.**

| Primer | Sequence (5' → 3') | Usage |
|---|---|---|
| SML1-URA5' | TTGTGATCTTACGGTCTCACTAACCTCTCTTCAACTGCTCGATTGTACTGAGAGTGCACC | To delete *SML1* |
| SML1-URA3' | GAAGGGTATCTAAGAGAAGAAAAGAACAGAACTAGTGGGAAATGGCTGTGCGGTATTTCACACCG | |
| SML1-1 | GCCATAACATATCGTTACTG | diagnostic PCR for *sml1::TRP1* |
| SML1-2 | GGACAATGTTGGCGCTAGCG | diagnostic PCR for *sml1::TRP1* |
| CORE-H1-fw | CCGCGTAAAGGCCCACAAGACTGCTTCGTACGCTGCAGGTCGAC | To amplify CORE-I-SceI for CORE-H1 |
| CORE-H1-rev | GATATTTGACGTGTGATTCCATTAGGGATAACAGGGTAATCCGCGCGTTGGCCG | |
| CORE-H2-fw | CAAATAGACCAGAGGCTGCGTTCGTACGCTGCAGGTCGAC | To amplify CORE-I-SceI for CORE-H2 |
| CORE-H2-rev | CCTGTAGATTTCTGATTTACCCCGCGCGTTGGCCGATTCAT | |
| CORE-H3-fw | GATACGAAAACAACTAACATGCTTTTCGTACGCTGCAGGTCGAC | To amplify CORE-I-SceI for CORE-H3 |
| CORE-H3-rev | CGCAAAAACTCATCTATTCTCAACCGCGCGTTGGCCGATTCAT | |
| CORE-H4-fw | CCATTTAGGCCGGTTGTTTCTTTCGTACGCTGCAGGTCGAC | To amplify CORE-I-SceI for CORE-H4 |
| CORE-H4-rev | GATGATCCGAATCTAATTATCCGCGCGTTGGCCGATTCAT | |
| T1 | CTACGAGGCCGAGCTGAGGG | To amplify homology arm and for fusion PCR for CORE-H1 and W1; Diagnostic PCR for *mec1-W2* |
| B1 | GCAGTCTTGTGGGCCTTTAC | To amplify homology arm for CORE-H1 and W1 |
| T2 | ATGGAATCACACGTCAAATA | To amplify homology arm for CORE-H1, W2, W2::R1 and W2::R2; Fusion PCR for W2, W2::R1 and W2::R2 |
| B2 | CCCAACAAGACTTCAGTCAA | To amplify homology arm and for fusion PCR for CORE-H1 |
| T4 | AAAAGAAGGTCCCTACCTGTTGAAGC | To amplify homology arm and for fusion PCR for CORE-H2, W3 and W3::R1; Diagnostic PCR of *mec1-W3 and mec1-W4* |

| | | |
|---|---|---|
| B4 | CGCAGCCTCTGGTCTATTTGG | To amplify homology arm for CORE-H2 and W3::R1 |
| T5 | GGTAAATCAGAAATCTTCAGG | To amplify homology arm for CORE-H2, W4, W2::R1 and W2::R2; Fusion PCR for W4 |
| B5 | GATATTTTTGTACTTCGAACCATG | To amplify homology arm and for fusion PCR for CORE-H2 and W2; Diagnostic PCR of *mec1-W2::ATR*$^{H11\text{-}13}$ and *mec1-W2::tel1*$^{H13\text{-}14}$ |
| T10 | CCATCTATCCGCTTTTATCTTCC | To amplify homology arm and for fusion PCR for CORE-H3; Diagnostic PCR of *mec1-W5* |
| B10 | AAGCATGTTAGTTGTTTTCGTATC | To amplify homology arm for CORE-H3 |
| T11 | TTGAGAATAGATGAGTTTTTGCG | To amplify homology arm for CORE-H3 |
| B11 | CAAAGTTTGAACATTGCCTTC | To amplify homology arm and for fusion PCR for CORE-H3; Diagnostic PCR of *mec1-W3 and mec1-W4* and *mec1-W3::tel1*$^{H17\text{-}23}$ |
| T16 | TGGAAGCAAGGTGAGAATG | To amplify homology arm and for fusion PCR for CORE-H4 and W6; Diagnostic PCR of *mec1-W6* |
| B16 | AGAAACAACCGGCCTAAATG | To amplify homology arm for CORE-H4 |
| T17 | ATAATTAGATTCGGATCATC | To amplify homology arm for CORE-H4 |
| B17 | GTAATATGTTTTCACAGTG | To amplify homology arm and for fusion PCR for CORE-H4; Diagnostic PCR of *mec1-W5* |
| LCD96 | CTATTCAAAAGGCCGCTG | Diagnostic PCR of *mec1::CORE1* and *mec1-W1* |
| N517-KanRev | GTATGGGCTAAATGTACGG | Diagnostic PCR of *mec1::CORE1* |
| KlURA3-3' | GAGCAATGAACCCAATAACGAAATC | Diagnostic PCR of *mec1::CORE2, mec1::CORE3, mec1::CORE4* |
| Mec1-1 | GTGAGGCTGACAACAAGAACG | Diagnostic PCR of *mec1::CORE2* |
| T14 | AATAACTGGACGGATGATCAG | Diagnostic PCR of *mec1::CORE3*; To amplify homology arm for W5 and W3::R1; Fusion PCR for W5 |
| T13 | CATGGTTCGAAGTACAAAAATATCTTGAGAATAGATGAGTTTTTGCG | Diagnostic PCR of *mec1::CORE4*; To amplify homology arm for W4 |
| T3 | GTAAAGGCCCACAAGACTGCAAAAGAAGGTCCCTACCTGTTG | To amplify homology arm for W1 |
| B3 | CCTTTGTCAAAAGTTGGAGCC | To amplify homology arm and for fusion PCR for W1, W2::R1 and W2::R2; Dianostic PCR of *mec1-W2* |
| B6 | CCTGTAGATTTCTGATTTACCCAAATCAAAATATACAATCG | To amplify homology arm for W2 |
| T7 | CGATTGTATATTTTGATTTGGGTAAATCAGAAATCTTCAGG | To amplify homology arm for W2 |
| B8 | CTGATCATCCGTCCAGTTATTCGCAGCCTCTGGTCTATTTGG | To amplify homology arm for W3 |

| | | |
|---|---|---|
| T9 | CCAAATAGACCAGAGGCTGCGAATA ACTGGACGGATGATCAG | To amplify homology arm for W3 |
| B9 | AAGCATGTTAGTTGTTTTCGTATC | To amplify homology arm and for fusion PCR for W3 and W3::R1 |
| B12 | CGCAAAAACTCATCTATTCTCAAGAT ATTTTTGTACTTCGAACCATG | To amplify homology arm for W4; Diagnostic PCR of *mec1-W1* |
| B13 | ATGAGGATTTTGCGAATGTTG | To amplify homology arm and fusion PCR for W4 |
| B14 | CCAATGCACTAGAAACTAGATCAAGC ATGTTAGTTGTTTTCGTATC | To amplify homology arm for W5 |
| T15 | GATACGAAAACAACTAACATGCTTGA TCTAGTTTCTAGTGCATTGG | To amplify homology arm for W5 |
| B15 | CTGTTCCATGTAAAACTCGAG | To amplify homology arm and fusion PCR for W5 |
| B18 | GATGATCCGAATCTAATTATATGAGG ATTTTGCGAATGTTG | To amplify homology arm for W6 |
| T19 | CAACATTCGCAAAATCCTCATATAAT TAGATTCGGATCATCTTATAAAG | To amplify homology arm for W6 |
| B19 | CCAAAATGGAAGCCAACC | To amplify homology arm fusion PCR for W6 |
| R1.2ATR-5’ | GACTAATAAAGCTCTCTCGATTGTAT ATTTTGATTTGTTTGAAGATCATATCC TGGAAG | To amplify the replacing PCR fragment for W2::R1 |
| R1.2ATR-3’ | GTTTGAATGAAGTATCCTGAAGATTT CTGATTTACCAGTGGCTTTCAAGTTCC TAC | |
| R1.1tel1-5’ | GACTAATAAAGCTCTCTCGATTGTAT ATTTTGATTTGCTCACACGTTATAATG AAATTC | To amplify the replacing PCR fragment for W2::R2; Diagnostic PCR of *mec1-W3::tel1*$^{H13-14}$ |
| R1.1tel1-3’ | GTTTGAATGAAGTATCCTGAAGATTT CTGATTTACCTCCAATTGTGTACGGA CTATTATTC | To amplify the replacing PCR fragment for W2::R2 |
| R2.2tel1-5’ | CGTGCGAATAAATCCAAATAGACCAG AGGCTGCGAGTTCTTCCAATCAAGCT ATG | To amplify the replacing PCR fragment for W3::R1 |
| R2.2tel1-3’ | GGAACGCTTGTTCCTGATCATCCGTC CAGTTATTAATACACAAGTAATAGCT GTTATC | |
| B6R1 | CAAATCAAAATATACAATCG | To amplify homology arm for W2::R1 and W2::R1 |
| Mec1-2 | CACCTGCAGTGATGGTTAGATC | Diagnostic PCR of *mec1-W6* |
| 5’-SpecFw | TTTGAAGATCATATCCTGGAAGATTT ATGTGG | Diagnostic PCR of *mec1-W2::ATR*$^{H11-13}$ |
| 5’-DIAG_R2.1-2.2replac | CTCTTCGAATATTGTAAGTTTG | Diagnostic PCR of *mec1-W3::tel1*$^{H17-23}$ |

# CHAPTER 3

## Phosphorylation of the DNA damage mediator Rad9 by cyclin-dependent kinases regulates activation of Checkpoint kinase 1

Ramesh Kumar*, Carla Manuela Abreu*, Karen Finn, Kevin Creavin, Sarah Eivers Muriel Grenon•# & Noel Francis Lowndes•#
Centre for Chromosome Biology, School of Natural Science, National University of Ireland Galway, University Road, Galway, Ireland

* *These authors contributed equally to this work*
• *These authors contributed equally to this work*
# *Corresponding authors*: muriel.grenon@nuigalway.ie and noel.lowndes@nuigalway.ie

*Running title*: CDK regulates Rad9-Chk1 interaction
*Key words*: Rad9, Chk1, Cdk1/Cdc28, phosphorylation, cell cycle, DNA damage.

## 3.1. SUMMARY

Extensive cell cycle-dependent phosphorylation is characteristic of DNA damage response mediators but is of unknown function. Here, we show that cell cycle phosphorylation of the Rad9 DNA damage mediator depends on B-type cyclin (Clbs) forms of the major cyclin-dependent kinase Cdc28 (Cdk1) in budding yeast. This phosphorylation does not inhibit Rad9 checkpoint activity in response to normal replication structures. Instead, we propose that Cdk1 fine tunes Rad9 DNA damage related functions. In particular, we have found that the integrity of nine putative Cdk1 phosphorylation sites located in the N-terminal region of Rad9 is required for Chk1 activation, specifically in the G2/M phase of the cell cycle. Phosphorylation of Rad9 T143 at its N-terminus by Clb-forms of Cdk1 regulates Rad9 interaction with Chk1, independently of the recently reported Rad9-Dpb11 interaction. Our data suggests a model where Rad9 and Chk1 interact constitutively, with remodelling of this complex in response to DNA damage requiring Mec1-dependent phosphorylation.

## 3.2. HIGHLIGHTS

- Cell cycle phosphorylation of Rad9 is Cdk1-dependent.
- N-terminal CDK phosphorylation of Rad9 regulate Chk1 activation in G2/M cells.
- N-terminal CDK phosphorylation sites in Rad9 regulate its constitutive interaction with Chk1.
- Cdk1 regulates distinct Rad9-Chk1 and Rad9-Dpb11 interactions.

## 3.3. INTRODUCTION

Cells have evolved sophisticated surveillance mechanisms to monitor for the presence of DNA damage collectively termed DNA Damage Response (DDR). Central to this are signal-transduction pathways, termed DNA damage checkpoints, conserved from yeast to human cells. The factors involved in these pathways constantly survey the genome for DNA damage, and control the appropriate biological responses to genomic damage: DNA repair, cell cycle arrests or slowdown, specific transcriptional genes induction, senescence and apoptosis

(Alderton et al., 2006; Harper and Elledge, 2007). Collectively these biological responses are important to suppress mutagenesis and genetic instability that can lead to the formation of tumours in higher cells, primarily due to defective induction of apoptosis and senescence (Halazonetis et al., 2008).

Activation of critical players in the DNA damage checkpoints is often mediated by phosphorylation events, which modulates their stability or activity (Finn et al., 2011). The apical kinases of these pathways are members of a family of Phosphatidyl-Inositol-3-kinase-like kinases (PIKKs), which include Tel1 and Mec1 in *Saccharomyces cerevisiae*, as well as their respective homologues Tel1 and Rad3 in *Schizosaccharomyces pombe*, and ATM (ataxia telangiectasia mutated), ATR (ATM and Rad3-related) and DNA-PKcs (DNA-dependent protein kinase catalytic subunit, no homologue has been identified in both yeast) in vertebrates (Critchlow and Jackson, 1998; Lovejoy and Cortez, 2009; Zhou and Elledge, 2000). Once activated by DNA-protein structures generated in response to lesions, PIKKs regulate numerous DDR proteins, including the downstream 'checkpoint' or CHK kinases, Chk1 (in all three species) and Chk2 (Rad53 or Cds1, in budding and fission yeast respectively). These two 'effector' kinases in turn phosphorylate target proteins leading to the downstream biological consequences of DDR activation (Stracker et al., 2009a).

DDR induction, particularly in response to DSBs, involves additional serine/threonine kinases, known as cyclin-dependent kinases (CDK) (Wohlbold and Fisher, 2009). Initially, CDK activity was known only for its role at the end of the DNA damage checkpoint, where CDK activity is inhibited, resulting in cell cycle arrest and providing time for DNA repair (Li and Cai, 1997). More recently, regulatory roles of CDK have been shown to be required further upstream in the DNA damage transduction cascade. The best described role of CDK is in DSB processing leading to the amplification of the checkpoint signal by stimulating the switch from ATM to ATR-dependent checkpoint signaling. This also regulates the choice of the DSB repair mechanisms (NHEJ or HR) accordingly with the cell cycle phase (Stracker et al., 2009b; Wohlbold and Fisher, 2009). Evidence also suggests that CDK activity might regulate other DDR proteins not necessarily involved at the DSB processing step. For example, CDK activity regulates multiple steps of the

homologous recombination process (Wohlbold and Fisher, 2009). Recently, it was also shown in higher cells that Chk1 is also subject to CDK-mediated phosphorylation at serines 286 and 301 required for efficient Chk1 activation and multiple checkpoint proficiency (Xu et al., 2012; Xu et al., 2011). Our growing understanding of the role of CDKs in the early events of the DDR suggests that other non-inducible protein kinases (e.g. DDK or casein kinase 2) may also be regulated after DNA damage to become key components of the DDR.

DNA damage mediators, molecular adaptors that facilitate protein-protein interactions at sites of DNA damage, contribute to the PIKK-dependent activation of CHK kinases (FitzGerald et al., 2009; Jungmichel and Stucki, 2010; O'Donovan and Livingston, 2010). In budding yeast, Rad9, the first checkpoint protein identified (Weinert and Hartwell, 1988), is the prototypal checkpoint mediator (Toh and Lowndes, 2003). This 148 kDa protein is required for the DNA damage checkpoints in all cell cycle phases (O'Shaughnessy et al., 2006), DNA repair (Barbour et al., 2006; de la Torre-Ruiz and Lowndes, 2000; Murakami-Sekimata et al., 2010; Toh et al., 2006) and DSBs resection (Barlow et al., 2008; Lazzaro et al., 2008; Lydall and Weinert, 1997). Rad9 is homologous to Crb2 from *S. pombe*, while, in human cells shares functional and structural similarities to three mediator proteins, 53BP1, MDC1 and BRCA1 (FitzGerald et al., 2009; Jungmichel and Stucki, 2010; O'Donovan and Livingston, 2010).

The mechanism of Rad53 activation mediated by Rad9 as described below has been partially reconstituted *in vitro* (Sweeney et al., 2005) and is its best understood biological function. Upon DNA damage, Mec1-hyperphosphorylated Rad9 acts as an adaptor protein by interacting through its SCD (serine clustral domain) with the FHA domains of Rad53 bringing the latter in close proximity to Mec1 for its pre-activation. At the same time, Rad9 acts as a scaffold protein by facilitating the increase of the local concentration of Rad53 molecules allowing its *in trans* autophosphorylation and fully activation to occur (Gilbert et al., 2001; Pellicioli and Foiani, 2005). Once activated, Rad53 is released from Rad9 through an ATP-dependent mechanism after which is able to phosphorylate the nuclear targets responsible for the numerous responses to DNA damage (Gilbert et al., 2001; Pellicioli and Foiani, 2005).

In contrast, Chk1 seems to autophosphorylate *in cis* upon DNA damage (Chen et al., 2009). Activation of Chk1 appears well conserved from yeast to human, requiring phosphorylation by the Mec1/ATR kinase. Chk1 phosphorylation is then a state for Chk1 activation. This mechanism in turn makes Chk1 activation depend upon various DNA damage mediators, to bring Chk1 into close proximity to ATR (Stracker et al., 2009a). However, the mechanism underlying this process is poorly understood. In higher cells it is well established a Claspin-dependent activation of CHK1, involving PIK kinase-dependent phosphorylation of Claspin itself (Lindsey-Boltz et al., 2009).

In both budding and fission yeast, Mrc1 is the Claspin ortologue. Interestingly, budding yeast Mrc1 share a conserved domain to the Chk1-binding domain (CKBD) of Claspin, both of which are sufficient to stimulate ATR-dependent phosphorylation of Chk1 in an *in vitro* system using purified human proteins (Lindsey-Boltz et al., 2009). However, no other evidences exist for a role of Mrc1 in mediating Chk1 activation in both budding and fission yeasts. In fact, Mrc1 seems to be specifically required in the DNA replication checkpoint to mediate the activation of Cds1 and Rad53, the Chk2 ortologues in fission and budding yeasts respectively (Tanaka, 2010). Interestingly, in *S. pombe* there are *in vitro* evidences showing that Crb2 (ortholog of *S. cerevisiae* Rad9 and human BRCA1, 53BP1, MDC1 and MCPH1) interacts with Chk1 in a two-hybrid system. In addition, it was identified a N-terminal region of Crb2 required for Chk1 activation, so called Chk1 activation domain (CAD), which shares sequence homology to the same region of Rad9 in budding yeast as well as to 53BP1 and BRCA1 in human cells (Saka et al., 1997). Accordingly, it has been shown that the CAD of Rad9 is also required for Chk1 activation (Blankley and Lydall, 2004), and this mechanism appears to be distinctively regulated from the Rad9-Rad53 branch since it is independent of the Rad9 SCD (Schwartz et al., 2002). Moreover, in fission yeast, Chk1 activation seems to be dependent on the cell cycle phosphorylation of Crb2 CAD, as well as on the interaction with Cut5 (Dpb11 homologue, (Mochida et al., 2004; Saka et al., 1997). Altogether, these data suggest that the mediator Rad9 in budding yeast may be also involved in Chk1 activation through a direct interaction with the later (Chen et al., 2009; Saka et al., 1997; Sanchez et al., 1999). However, biochemical evidences supporting this mode of Chk1 activation mediated by Rad9 are still missing. In

higher cells, Rad9-like mediator proteins, including BRCA1 and MDC1, play a complex role, which require further mechanistic characterization (Smits et al., 2010; Stracker et al., 2009a). Overall, in all organisms, the apical PIK kinases together with DDR mediator proteins have important roles in the regulation of Chk1 that still need to be investigated.

Mediators are typically phosphoproteins, phosphorylated by multiple kinases. It is well established that Rad9, and the mediators in higher cells, are extensively phosphorylated on several residues after DNA damage in a PIKK-dependent manner for their activation to occur (Cortez et al., 1999; Emili, 1998; Goldberg et al., 2003; Lou et al., 2003; Rappold et al., 2001; Saka et al., 1997; Vialard et al., 1998; Xia et al., 2001; Xu and Stern, 2003). In budding yeast, Rad9 activation correlates with the remodeling a large hypophosphorylated complex (≥850KDa), containing various Rad9 molecules associated with Ssa1/2 complex, into a smaller complex (560KDa) containing hyperphosphorylated Rad9, Ssa1/2 and Rad53 kinase, mediating the activation of the latter as well as Rad9 oligomerisation (Blankley and Lydall, 2004; Gilbert et al., 2001; Gilbert et al., 2003; Sanchez et al., 1999; Sanchez et al., 1996; Schwartz et al., 2002; Sun et al., 1996; Sweeney et al., 2005; Usui et al., 2009).

It has also been shown that the DDR mediator proteins are frequently phosphorylated during cell cycle progression in the absence of exogenous DNA damage (Esashi and Yanagida, 1999; Jullien et al., 2002; Rappold et al., 2001; Ruffner et al., 1999; Ruffner and Verma, 1997; Vialard et al., 1998). Consistent with this, these proteins comprise a high number of consensus sites for CDK phosphorylation (S/T-P-x-K/R, where x can be any amino acids, or minimal S/T-P sites). However, the impact of this phosphorylation in their functions remains undefined. In particular, among the yeast proteome, Rad9 stands with an exceptionally high density of such motifs, twenty S/T-P sites of which nine rigorously resemble the complete consensus sequence ([S/T]-P-X-[R/K]) characteristic of these sites (Moses et al., 2007; Ubersax et al., 2003). Interestingly, the mobility profile of Rad9 protein during electrophoresis suggests that it endures considerable protein modifications and phosphatase-sensitive isoforms of slower mobility have been observed in the S and M phases of the cell cycle (Vialard et al., 1998). Not surprisingly, Rad9 has been identified as an *in vitro* substrate of Clb2-

Cdc28 and Clb5-Cdc28 complexes (Loog and Morgan, 2005; Ubersax et al., 2003) and, in fact, fifteen of the twenty consensus CDK residues have been confirmed to be phosphorylated *in vivo* by mass spectrometric studies (Albuquerque et al., 2008; Holt et al., 2009; Smolka et al., 2005). However, the biological importance of CDK-dependent phosphorylation of Rad9 remains uncharacterised.

Here, we show that phosphorylation of Rad9 during the S, G2 and M phases of the cell cycle depends on B-type cyclin (Clbs) forms of the unique cyclin-dependent kinase Cdc28 (also termed Cdk1) in budding yeast. We propose that the cell cycle phosphorylation of Rad9 is not required for its checkpoint activity in response to normal replication structures generated during S-phase, but rather it modulates the activity of the various Rad9 functions during the DDR. We describe the role of this phosphorylation in the PIKK-dependent activation of Chk1. We show here that the Cdc28-dependent *in vivo* phosphorylation of nine particular consensus CDK phosphorylation sites located within the N-terminal 231 amino acids of Rad9 is specifically required for the phosphorylation and maintenance of Chk1-dependent, but Rad53-independent, signalling after DNA damage. In addition, we demonstrate that this process involves the direct physical interaction between Rad9 and Chk1, independently of the recently reported Rad9-Dpb11 interaction, where, among the nine CDK sites, CDK7 (T143) is the residue mainly contributing for the interaction in a Cdc28-dependent manner. We propose a model in which the CDK-dependent phosphorylation of the Rad9 N-terminus during S, G2 and M phases, allows a constitutive interaction between Chk1 and Rad9. PIK kinase-dependent phosphorylation of these proteins at the sites of damage is then followed by release of Rad9 in association with activated Chk1 to phosphorylate its substrates.

## 3.4. RESULTS

### 3.4.1. Cdc28/Clb activity is required for DNA damage-independent phosphorylation of Rad9 during S, G2 and M phases of the cell cycle

Rad9 is a peculiar protein due to its protein size varies from 180 to 220 kDa when analysed on a SDS-PAGE gel (Vialard et al., 1998). This fluctuation in Rad9 mobility mirrors its phosphorylation. A well-known mechanism for Rad9 phosphorylation that occurs after DNA damage is dependent on Mec1/Tel1, and

results in a slower migrating form termed hyperphosphorylated Rad9 (Emili, 1998; Grenon et al., 2001; O'Shaughnessy et al., 2006; Vialard et al., 1998). Phosphorylation of Rad9 is also detected as a small mobility shift, previously termed hypophosphorylated Rad9, in S- and G2-arrested cells in a normal cell cycle, but not observed in G1-arrested cells (Vialard et al., 1998). In addition, these cell cycle-specific forms of Rad9 are lost after λ-phosphatase treatment in cell extracts from either asynchronously growing or arrested cells, suggesting a cell cycle stage-dependent phosphorylation of Rad9 (Vialard et al., 1998). To simplify the distinction between the different phospho-forms of Rad9, hereafter we use C-Rad9 for the cell cycle-dependent forms and D-Rad9 for the DNA damage-dependent hyper-phosphorylated Rad9.

To further investigate the role of the cell cycle phosphorylation of Rad9, we analysed the mobility of this protein by SDS-PAGE and western blot analyses using whole cell extracts from cells that were initially arrested in G1 and subsequently synchronously released in the cell cycle under normal growth conditions (Figure 3.1A). Initially Rad9 is detected as a smaller form in G1 phase as previously demonstrated (Grenon et al., 2001). As cells progress through S and G2/M phases, distinct slower migrating forms of Rad9 are detected, which disappear towards the end of mitosis, and subsequently the fastest migrating form of Rad9 reappears in the new G1 phase. We conclude that Rad9 is increasingly phosphorylated during progression through S, G2 and M phases of the cell cycle.

We next wanted to investigate the kinase that is responsible for the cell cycle profile of Rad9 *in vivo* phosphorylation. Interestingly, the cyclic pattern of Rad9 phosphorylation fits precisely with the cell cycle activity of the single kinase in budding yeast that regulates cell cycle progression, known as Cdc28 or Cdk1 (Enserink and Kolodner, 2010). Moreover, Rad9 has been identified as an *in vitro* substrate of Cdc28-Clb2 and Cdc28-Clb5 complexes (Loog and Morgan, 2005; Ubersax et al., 2003). To test if the cell cycle phosphorylation profile of Rad9 is dependent on Cdc28 activity, we took advantage of cells expressing Cdc28-as1, an analogue sensitive (as) version of Cdc28. Cdc28-as1 comprises an enlarged ATP-binding pocket that, although does not impact in the ATP binding, allows to have a higher affinity to the bulky nonhydrolyzable ATP analogue, 1-NMPP1, that fits into

the mutant-binding pocket but cannot bind to wild-type kinases. As a result, it is possible to inhibit much of the cell's Cdk1 activity within 5–10 min by addition of high concentrations (5–25 mM) of 1-NMPP1. Importantly, the mutation in Cdc28-as1 (Phe88Cly) is deep in the ATP-binding pocket, far from the protein substrate-binding site, and is not expected to alter the protein substrate specificity of the protein kinase (Bishop et al., 2000; Ubersax et al., 2003). The dephosphorylation of the Cdc28 downstream substrates relies then on the activity of counteracting phosphatases (Bishop et al., 2000). The dephosphorylation of Orc6, a known Cdc28 target (Liang and Stillman, 1997), was analysed by western blotting to follow Cdc28-as1 activity (Ubersax et al., 2003). Cell extracts from asynchronous, G1- and G2-arrested *cdc28as-1* cells growing in the presence or absence of 1-NMPP1 were prepared and analysed by western blotting. Upon Cdc28-as1 inactivation, the migration of Rad9 in G1-arrested cells was not affected. In contrast, Rad9 slower migrating forms were absent in asynchronous and G2-arrested cells (Figure 3.1B). Therefore, the cell cycle phosphorylation profile of Rad9 as cells progress through S, G2 and M phase is dependent upon Cdc28 activity.

Clb1 to 6 are obvious candidates for the cyclin partners of Cdc28 required for Rad9 cell cycle phosphorylation *in vivo*. We therefore examined Rad9 migration in conditional CDC mutants with different levels of Cdc28/Clb activity at non-permissive temperature and investigated Rad9 mobility profile by SDS-PAGE and western blot analyses (Figure 3.1C). Cdc4 (a protein from the SCF complex) is required for destruction of Sic1, a potent and specific inhibitor of B-type cyclin CDK complexes (Enserink and Kolodner, 2010). G1 cells with high levels of the Cdc28-Clb inhibitor, Sic1, can be generated by arresting *cdc4-1* cells with a factor and shifting to the restrictive temperature (Nash et al., 2001; Piatti et al., 1996; Schwob et al., 1994). Upon release from the α-factor block, cell cycle-dependent phosphorylation of Rad9 was severely abrogated in *cdc4-1* cells, whereas this did not occur with *cdc7-1* cells, which also block cell cycle progression prior to S phase but with high CDK activity (Figure 3.1C). This abrogation of Rad9 cell cycle phosphorylation is dependent upon Sic1, as cell cycle phosphorylation of Rad9 is restored in similarly treated *cdc4-1 sic1Δ* cells. In fact, in the absence of Sic1, Rad9 is phosphorylated even during α-factor arrest as a consequence of residual Cdc28-Clb activity. Additionally, by manipulation of the levels of the Cdc6 protein we

could establish that Rad9 can be normally phosphorylated irrespective of whether DNA synthesis takes place or not (Figure S3.1B). Together, our data indicate that Rad9 cell cycle phosphorylation is dependent upon B-type cyclin forms of the major CDK of budding yeast and independent of the generation of S phase structures.

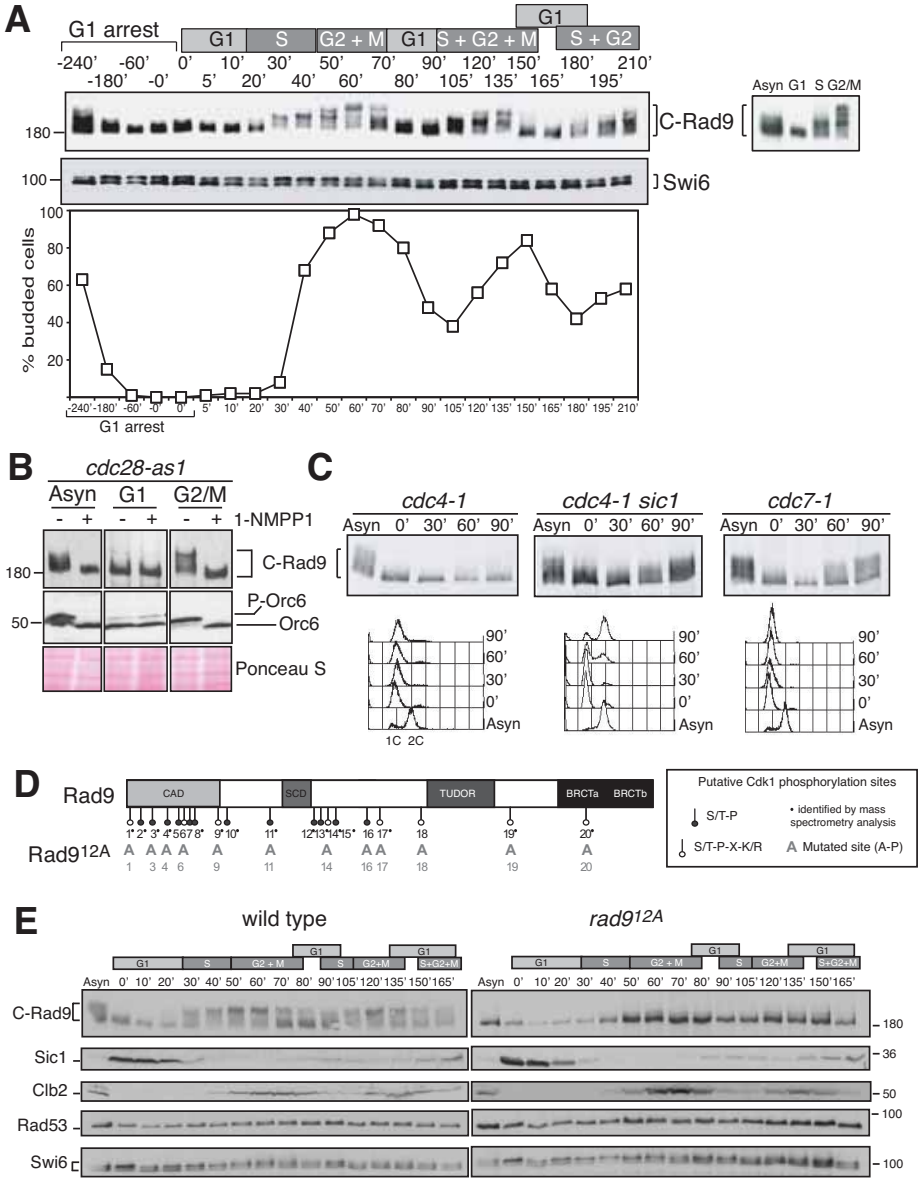


**Figure 3.1: Rad9 is phosphorylated by Cdk1 in the absence of DNA damage.**
(A) Cell cycle regulation of Rad9 phosphoforms. An α-factor block and release experiment with yeast strain CG378. Rad9 phospho-forms were identified in protein extracts by western blotting. The phospho-protein Swi6 serves as a loading control. The cell cycle phases of synchronously cycling cells determined by budding analysis are indicated above the blots. The insert in the graph shows Rad9 from asynchronous cells or cells arrested with α-factor, HU or nocodazole. (B) Rad9 phosphorylation is dependent on Cdc28 activity. Rad9 and Orc6 western blots shown are prepared from asynchronously growing and α-factor or nocodazole arrested *cdc28-as1* cells either mock or 1-NMPP1 treated. (C) Rad9 phosphorylation is dependent on Cdc28/Clb activity. The indicated cells

were arrested with α-factor, shifted to 30°C and samples were taken at the indicated times for Rad9 western and FACS analysis. (D) Schematic representation of Rad9 showing the 20 consensus sites for phosphorylation by Cdc28 and those mutated to alanine in *rad9*$^{12A}$ cells. (E) Rad9$^{12A}$ is severely defective in cell cycle-dependent phosphorylation and *rad9*$^{12A}$ cells cycle normally without detectable checkpoint activation. Western analysis of the indicated proteins from WT and isogenic *rad9*$^{12A}$ cells. Experiments done mostly by Noel Lowndes, Karen Finn and Ramesh Kumar. Also see Figure S3.1.

### 3.4.2. Abrogation of Rad9 cell cycle phosphorylation does not affect cell proliferation

We sought out to determine whether consensus CDK sites in Rad9 contribute to its cell cycle-phosphorylation profile *in vivo*. We generated a strain in which twelve of the twenty putative CDK phosphorylation sites, including all nine conforming to the strict S/T-P-X-K/R consensus were mutated into alanine to generate a *rad9*$^{12A}$ allele (Figure 3.1D). Phosphorylation of Rad9 and Rad9$^{12A}$ during cell cycle progression was investigated by western blot (Figure 3.1E), in addition to budding and DNA content (Figure S3.1C) analyses. Rad9 cell cycle phosphorylation was severely abolished in the *rad9*$^{12A}$ mutant indicating that the twelve CDK sites mutated represent the majority of the sites in Rad9 that are phosphorylated *in vivo*.

The presence of a S-phase threshold that allows cells to tolerate damage-like DNA structures that are normally generated at the replication forks has been proposed (Cobb et al., 2004; Shimada et al., 2002). Therefore, we hypothesise that a possible role for Rad9 phosphorylation by Cdc28 is to decrease Rad9 activity upon entry into S phase in order to prevent inappropriate signaling from commonly occurring DNA replication structures. However, cell cycle progression of the *rad9*$^{12A}$ mutant was not detectably different from wild type cells. In particular, major cell cycle transitions and the extent of S phase, as judged by FACS analysis and budding index (Figure S3.1C), as well as the Sic1 and Clb2 cell cycle markers (Figure 3.1E), were not detectably perturbed. Consistent with this data, in proliferating *rad9*$^{12A}$ cells without exogenous damaging treatments, no increased number of large budded cells was observed (Figure S3.1C) neither Rad53 nor Rad9 were activated (Figure S3.1D), indicating that the DNA damage checkpoints are not activated in undamaged mutant cells. Importantly, after ionizing radiation, *rad9*$^{12A}$ cells largely retain normal checkpoint regulation and hyper-phosphorylated Rad9$^{12A}$ can be detected with wild type kinetics (Figure S3.1D and E). This data clearly demonstrates that Cdc28-

dependent phosphorylation of Rad9 in the 12 consensus CDK motifs is unlikely to be required to prevent inappropriate sensing of structures generated in S phase.

It is important to mention that David Toczyski's group has reported a similar Rad9 mutant where 18 consensus CDK sites in Rad9 were mutated into alanine to generate a *rad9-18A* allele (Bonilla et al., 2008). Interestingly, in this mutant the DNA damaged-induced phosphorylation of Rad9 was completely abolished in addition to its CDK-dependent phosphorylation. This data suggests that some of these specific residues that are mutated in *rad9-18A* but not in our $rad9^{12A}$ mutant might be needed to fine tune Rad9 functions in checkpoint activation. This data led us to hypothesise that the CDK-dependent phosphorylation of specific subsets of consensus CDK sites serves to modulate Rad9 activity in order to perform specific DNA damage checkpoint functions. Several studies in our laboratory have supported this hypothesis (Granata et al., 2010) *and our unpublished data*) and here we focus in one of them.

### 3.4.3. CDK phosphorylation sites in the CAD region of Rad9 are required for Chk1 activation

A region in the N-terminus of Rad9 is required for damage-induced Chk1 phosphorylation, so termed Chk1 Activating Domain or CAD (Blankley and Lydall, 2004). However the mechanisms behind this process are unknown. We hypothesised that the nine putative CDK phosphorylation sites within CAD region of Rad9 are required for Chk1 phosphorylation. To test this hypothesis we generated a *RAD9* mutant where the four serines and the five threonines corresponding to CDK sites 1-9 were mutated to alanines, termed $rad9^{CDK1\text{-}9A}$ (Figure 3.2A), and compared it to a $rad9^{CAD\Delta}$ strain expressing a Rad9 truncated version lacking the CAD region. Survival analysis have shown that $rad9^{CDK1\text{-}9A}$ and $rad9^{CAD\Delta}$, similar to wild type but unlike *rad9*Δ cells, are not sensitive to IR (which primarily causes DNA strand breaks) and 4-NQO (4-nitroquinoline 1-oxide, which causes single strand breaks and DNA adducts that can be repaired by nucleotide excision repair) treatments, indicating that these mutants are largely functional (Figure 3.2B). Interestingly, contrasting with wild type, $rad9^{CDK1\text{-}9A}$ and $rad9^{CAD\Delta}$ cells, *chk1Δ* cells displayed pronounced sensitivity, equivalent to *rad9Δ*, when plated on bleocin. Nevertheless,

this sensitivity to bleocin that can be indicative of a Chk1 role in surviving bleocin-induced lesions during S phase seems to be independent of Rad9 CAD region since *rad9*$^{CDK1\text{-}9A}$ and *rad9*$^{CAD\Delta}$ cells behaved like wild type cells in the same conditions. Importantly, when *chk1Δ* cells were spotted on medium containing bleocin together with nocodazole for an extended arrest in G2/M, the bleocin sensitivity was rescued.

We investigated the profile of Rad9 cell cycle phosphorylation in *rad9*$^{CDK1\text{-}9A}$ by western blot analysis (Figure 3.2C). In both asynchronous and G2-arrested cells, Rad9$^{CDK1\text{-}9A}$ migrated faster than Rad9 but to a reproducibly lesser extent than Rad9$^{12A}$, consistent with mutation of additional CDK sites in Rad9$^{12A}$. Nonetheless, the phospho-mobility shift of Rad9 is abrogated when Cdc28 is inactivated in the presence of 1-NMPP1. With this data we conclude that at least some of the CDK sites mutated in Rad9$^{CDK1\text{-}9A}$ and Rad9$^{12A}$ are phosphorylated *in vivo*.

We also examined whether a specific cyclin-Cdc28 complex preferentially phosphorylates the CAD region of Rad9 by *in vitro* kinase assays. Using TAP-purified Cln2-, Clb5-, Clb3- and Clb2-Cdc28 complexes as previously (Figure 3.2D; (Koivomagi et al., 2011; Loog and Morgan, 2005), we tested their ability to phosphorylate a recombinant CAD protein relative to the standard histone H1 substrate used in Cdc28 kinase assays (Figure 3.2E). Although less well phosphorylated than histone H1, we observed that the Rad9 CAD region had a similar phosphorylation profile as histone H1, both being preferentially phosphorylated by the Cdc28/Clb2 kinase. Strikingly, no phosphorylation of CAD was observed when the recombinant CAD$^{CDK1\text{-}9A}$ mutant protein was used as a substrate (Figure 3.2E), indicating that the sites targeted by the Cdc28/Clb2 complex in vitro are among the 9 CDK putative sites in the CAD region.

If the CDK1-9 sites within Rad9 CAD are required for Chk1 activation, we predict that Chk1 phosphorylation upon DNA damage is abolished in the *rad9*$^{CDK1\text{-}9A}$ cells. We used western blot analysis to investigated the damage-induced Chk1 phosphorylation in *rad9*$^{CDK1\text{-}9A}$ cells expressing Chk1-3HA and compared it with *rad9*$^{CAD\Delta}$, as previously described (Figure 3.2E; (Sanchez et al., 1999). The higher mobility Chk1 phospho-form that rapidly appears in asynchronously growing wild

type cells upon 4-NQO treatment is absent in *rad9Δ* and *rad9*$^{CAD\Delta}$ cells (Blankley and Lydall, 2004; Sanchez et al., 1999). Interestingly, the damage-induced Chk1 phospho-shift was also mostly dependent on the integrity of the CDK1-9 sites. It is important to mention that the defect of the respective cells in activating Chk1 cannot be explained by the absence of the DNA damage-induced phosphorylation of Rad9$^{CDK1\text{-}9A}$ or Rad9$^{CAD\Delta}$, since hyperphosphorylated Rad9 is detected in both *rad9*$^{CDK1\text{-}9A}$ and *rad9*$^{CAD\Delta}$ cells upon IR and 4NQO treatments (Figure S3.2B). Interestingly, western blot analysis of Rad53 (parallel transducer kinase to Chk1) revealed that the *rad9*$^{CDK1\text{-}9A}$ cells are still able to activate Rad53 analogous to *rad9*$^{CAD\Delta}$ and wild type cells (Blankley and Lydall, 2004). Similar results were obtained in response to IR, bleocin, UV and 4-NQO, indicating that the CDK1-9 sites are not required for Rad53 activation (Figure S3.2A). Our data suggest that the role of the nine putative CDK phosphorylation sites in the Rad9 CAD is to specifically regulate DNA damage induced-Chk1 phosphorylation.

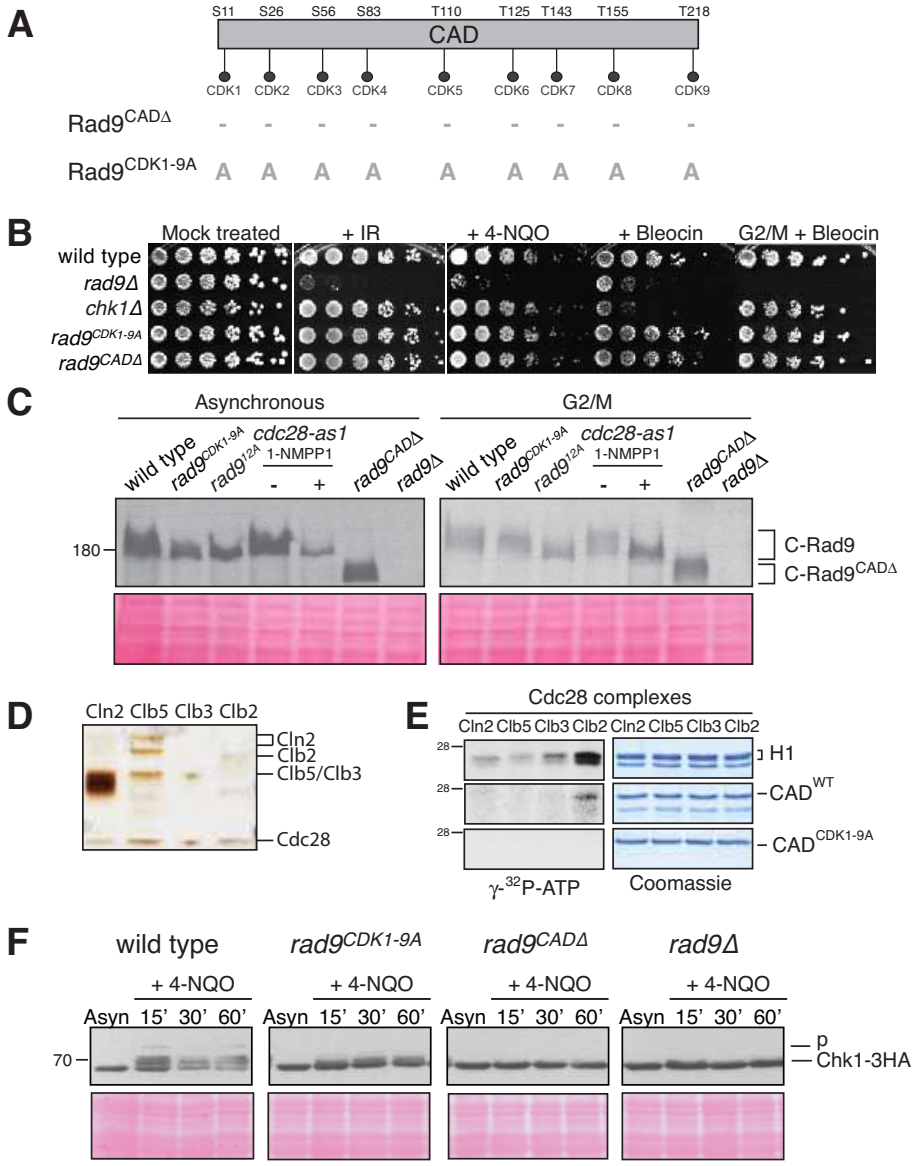


**Figure 3.2: The nine N-terminal CDK consensus sites contribute to Cdc28-dependent phosphorylation of Rad9 *in vitro* and *in vivo* and are required for phosphorylation of Chk1.** (A) Schematic representation of the Rad9$^{CDK1-9A}$ mutant protein. (B) Cells expressing Rad9$^{CDK1-9A}$ as their only Rad9 protein are not sensitive to the indicated DNA damaging treatments. Drop test were performed in the indicated strains. Mock – YPD (Yeast Peptone Dextrose) medium (complete medium); IR (400Gy), 4-NQO (1.25µM), Bleocin (0.25µg/ml) and G2/M+Bleocin (10µg/ml Nocodazole + 0.25µg/ml Bleocin) treatments are done on YPD media radiated or containing the specific drug at the mentioned dose; MN – Minimal medium lacking the indicated amino acid (URA – uracil; LEU – leucine; TRP – tryptophan); G418 (Geneticin) – YPD containing 200µg/µl of G418; Experiments A and B done in collaboration with Ramesh Kumar. (C) Rad9$^{CDK1-9A}$ displays defective cell cycle and Cdc28-dependent phosphorylation *in vivo*. Rad9 western blot prepared from the indicated strains. 1-NMPP1 treatment of *cdc28-as1* cells was used to indicate Cdc28-dependent phosphorylation. (D) Silver staining of the indicated TAP-purified cyclin-Cdc28 complexes. (E) CDK1-9 sites within CAD region of Rad9 are preferentially phosphorylated *in vitro* by Clb2-Cdc28 complex, followed by Clb2-Cdc28. Kinase assays were performed in CAD$^{WT}$ and CAD$^{1-9A}$ using the indicated cyclin-Cdc28 complexes. The corresponding Coomassie gels are shown as a loading control. (F) DNA damage induced Chk1 phosphorylation is defective in *rad9$^{CDK1-9A}$*, *rad9$^{CADΔ}$* and *rad9Δ* cells. Asynchronously growing cells were treated with 4-NQO for the indicated times and Chk1 phosphorylation analysed by western blotting.

### 3.4.4. CDK sites in the Rad9 CAD are specifically required for Chk1 activation in G2/M phase

Comparison of G1 and G2/M arrested cells reveals that Chk1 phosphorylation is drastically affected in *rad9*$^{CDK1\text{-}9A}$ when arrested in G2/M, while is still activated when these cells are in G1 (Figure 3.3A and B). In both arrest conditions, the damage-induced Rad9 and Rad53 phosphorylations in the *rad9*$^{CAD\Delta}$ and *rad9*$^{CDK1\text{-}9A}$ cells are also comparable with wild type cells either upon IR or 4NQO treatments (Figure 3.3 and Figure S3.2A). Taking together, the role of the CDK sites within CAD region of Rad9 is to specifically regulate DNA damage induced-Chk1 phosphorylation in G2/M, stage of the cell cycle when CDK activity and Rad9 cell cycle phosphorylation are elevated.

To confirm if the CDK1-9 sites function exclusively in the Chk1 activation pathway or are also required for Rad53 activation. We performed an epistasis analysis using the G2 cell cycle checkpoint assay that we previously reported (O'Shaughnessy et al., 2006). The G2/M delay in this assay requires Rad9-dependent regulation of two additive branches involving both checkpoint kinases, Chk1 and Rad53/Chk2 (Gardner et al., 1999; Sanchez et al., 1999). In this analysis, *rad9*$^{CDK1\text{-}9A}$ cells displayed a partially defective G2/M checkpoint similarly to single deletion of *chk1Δ* or *rad53Δ* (Figure 3.3E). A similar partial defect was observed in *rad9*$^{CDK1\text{-}9A}$ *chk1Δ* cells, whereas *rad9*$^{CDK1\text{-}9A}$ *rad53Δ* cells were completely defective in this G2 checkpoint assay. The epistatic relationship between *rad9*$^{CDK1\text{-}9A}$ and *chk1Δ*, as well as the additive relationship between *rad9*$^{CDK1\text{-}9A}$ and *rad53Δ*, strongly indicate that the CDK1-9 sites of Rad9 function specifically to regulate Chk1 activation in response to DNA damage.

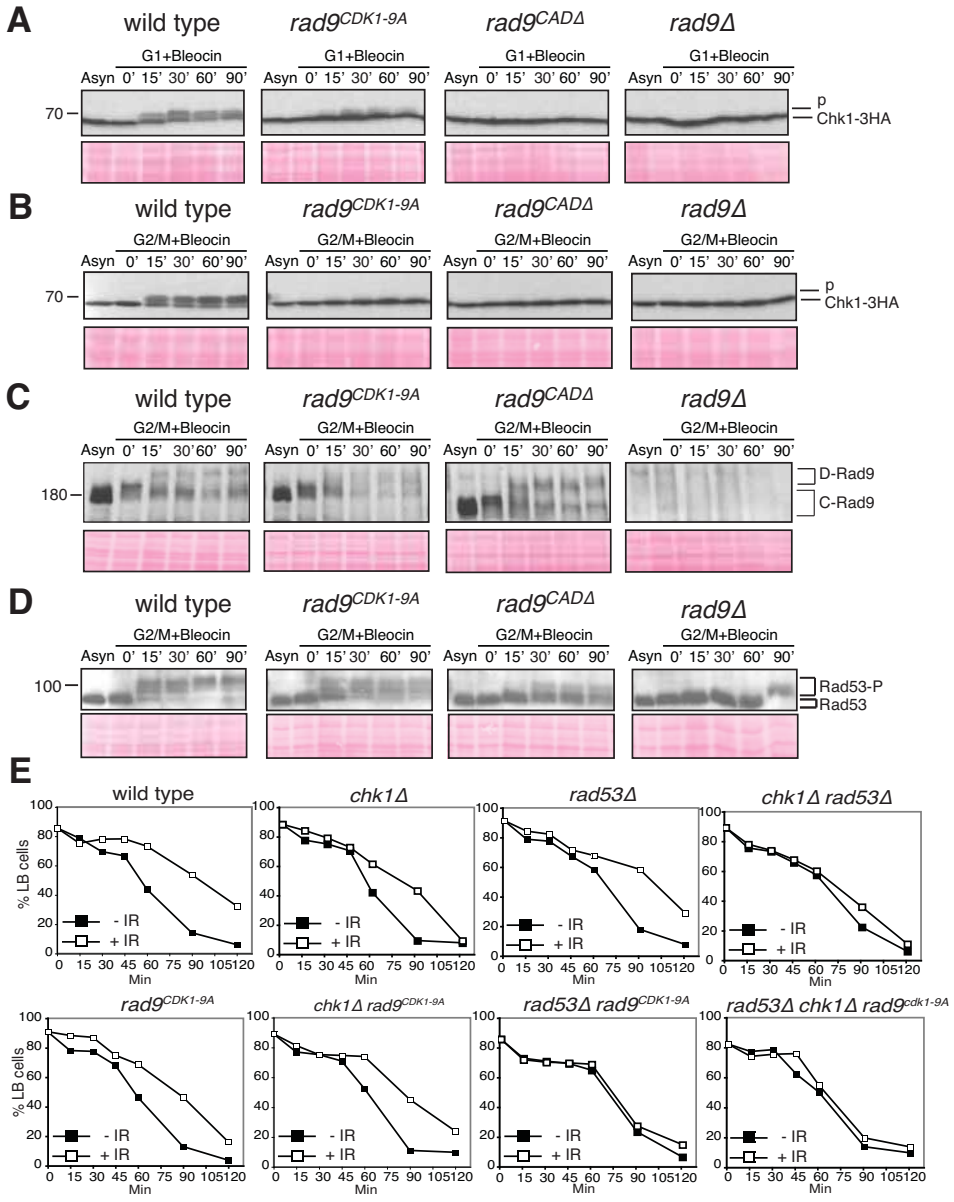


**Figure 3.3: The CDK1-9 sites specifically act in the Chk1 branch of the G2/M checkpoint.** Cells were grown and arrested in the cell cycle as indicated with either α-factor or nocodazole and treated with Bleocin (5µg/ml) for the indicated times. Extracts prepared for western blotting of Chk1-3HA (A & B), Rad9 (C) or Rad53 (D). (E) The CDK1-9 sites of Rad9 function specifically in the Chk1 branch and not the Rad53 branch of the G2/M checkpoint. The indicated strains were examined for epistatic relationships using the G2/M checkpoint assay. All strains contained the *sml1Δ* mutation necessary for the viability of *rad53Δ* cells. Experiments done in collaboration with Ramesh Kumar and Kevin Creavin. Also see Figure S3.2.

### 3.4.5. Cdc28 activity is required for initiation and maintenance of Chk1 activation upon DNA damage

Activation of Rad53 is well known to be cell cycle regulated and dependent on Cdc28 activity exclusively in response to a HO-induced DSB, but not to single strand breaks and DNA adducts that are repaired by NER. This is due to a key role for Cdc28 in controlling DSB resection (Enserink and Kolodner, 2010; Ira et al., 2004). However, Chk1 activation is less understood. To investigate whether Cdc28-dependent activation of Chk1 is specific to DSB-inducing agents, we have inhibited Cdc28 activity by adding 1-NMPP1 to G2/M-arrested *cdc28-as1* cells and treated them with bleocin and 4-NQO (Figure 3.4A), as well as IR (Figure S3.3). Interestingly, in the absence of Cdc28 activity, Chk1 activation was affected either post treatment with bleocin, IR or 4-NQO (Figure 3.4A). This is contrasting with both Rad53 and Rad9 that were not activated after bleocin and IR treatments, whereas their activation was only delayed after treatment with 4-NQO. These results indicate that Chk1 phosphorylation upon DNA damage is absolutely dependent upon Cdc28 activity, rather than a downstream consequence of the Cdc28-dependent resection at DSBs.

In *cdc28-as1* cells where Chk1 phosphorylation has been induced by bleocin, the addition of 1-NMPP1 to abrogate Cdc28 activity rapidly resulted in the loss of the active phospho-form of Chk1 (Figure 3.4B, note that while C-Rad9 also requires continuous Cdc28 activity, D-Rad9 does not), indicating that Cdc28 activity is continuously required for maintenance of Chk1 signalling, similarly to Rad53 (Ira et al., 2004). Together our data indicate that Cdc28 activity is absolutely required for initiation and maintenance of Chk1 phosphorylation under any of the DNA damaging conditions tested. This is consistent with a Cdc28 role in controlling Chk1 activation by regulating cell cycle-dependent phosphorylation of CDK sites in the N-terminus of Rad9, regardless of the type of DNA damage.

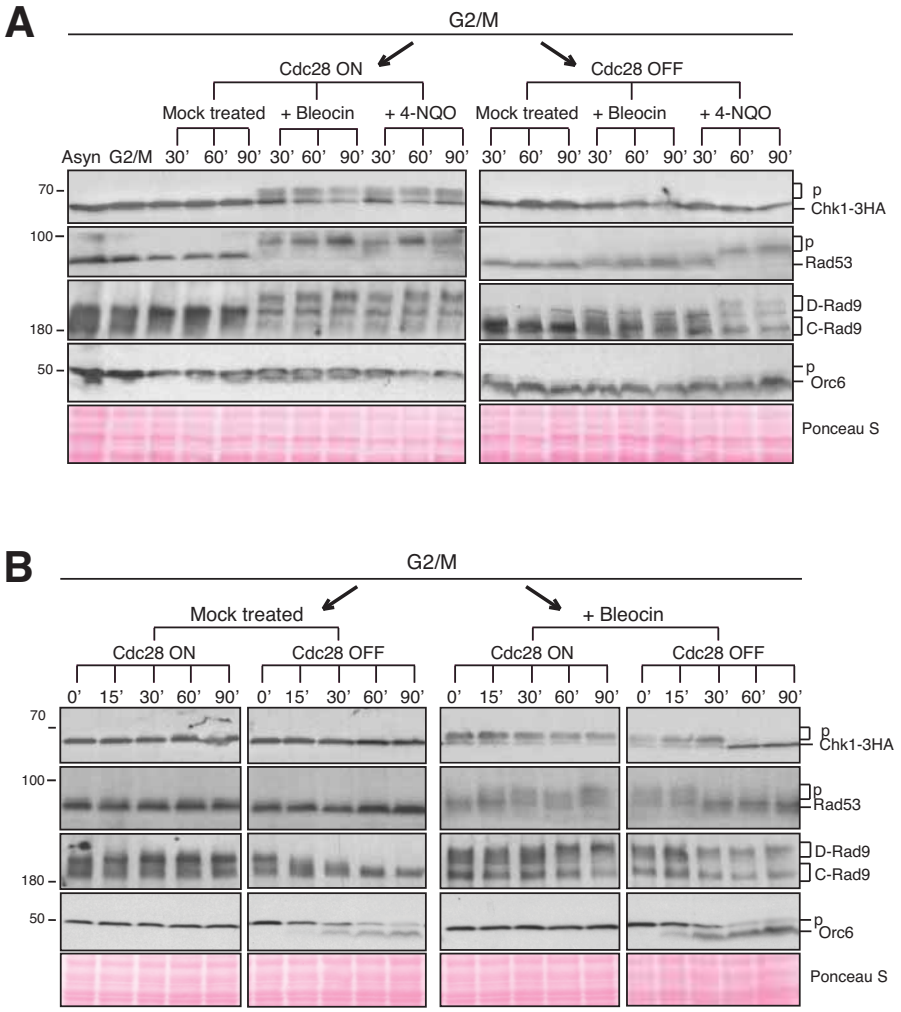


**Figure 3.4: CDK is required for the activation and maintenance of Chk1-dependent signaling.** Cdc28 activity was regulated using the 1-NMPP1 inhibitor in G2/M arrested cdc28-as1 cells treated with bleocin (5µg/ml) or 4-NQO (5µM) to examine the activation of Chk1 signaling (A) and the maintenance of Chk1 signaling (B). Rad9 and Rad53 were followed as markers of checkpoint activation, while Ocr6 phosphorylation serves as a marker for Cdk1 inactivation. Experiments done in collaboration with Ramesh Kumar. Also see Figure S3.3.

### 3.4.6. Both CDK1-9 sites and Cdc28 activity are required for physical interaction between Rad9 and Chk1

First evidences for the mechanism behind Chk1 activation were previously obtained by yeast 2-hybrid (Y2H) assays demonstrating an *in vitro* interaction between Rad9 and Chk1 (Sanchez et al., 1999). We then hypothesised that the CAD region might facilitate the physical interaction between Rad9 and Chk1 since it is required for Chk1 phosphorylation. Since multiple potential CDK phosphorylation sites within

Rad9 CAD regulate Chk1 activation, these nine sites or a subset of these sites might be sufficient to mediate the Rad9 interaction with Chk1. By Y2H assay, we were able to independently confirm the Y2H interaction between Rad9 and Chk1 (Figure 3.5A). In addition, we demonstrated that the N-terminal CAD region of Rad9 alone is sufficient for this interaction. Most importantly, in cells harbouring Rad9$^{CDK1\text{-}9A}$ and Chk1 the interaction is lost, indicating that the integrity of the CDK1-9 sites is required for the interaction between full length Rad9 and Chk1. It is important to mention that no galactosidase activity was observed when the bait and prey proteins were expressed on their own, excluding the possibility of the individual proteins initiate transcription of the galactosidase reporter gene even in the absence of a protein-protein interaction (Figure S3.4A). In addition, the level of expression was found to be equal in all fusion proteins (Figure S3.4B).

We assayed the ability of Cdc28 to control the interaction between Rad9 and Chk1. Using a triple plasmid based Y2H assay, we observed that the Rad9-Chk1 interaction in G2/M cells was significantly reduced in the absence of Cdc28 activity (Figure 3.5B and Figure S3.4C), analogously to our previously reported Dpb11-Rad9 interaction (Granata et al., 2010). Interestingly, the Y2H interaction between Rad9 and Chk1 is still detected in G1-arrested cells (Figure 3.5B), consistent with a slight Rad9-dependent defect in Chk1 phosphorylation after DNA damage in this cell cycle phase (Figure 3.3A). However, unlike G2/M phase, the Rad9-Chk1 interaction in G1-arrested cells clearly was Cdc28-independent, suggesting the existence in G1 of another regulatory mechanism for this interaction independent of Cdc28 activity. Note that the interaction between Rad9 and Chk1 in G1 is still dependent on the integrity of the CDK1-9 sites (Figure S3.4D), results that also support the decreased Chk1 phosphorylation observed in G1-arrested *rad9*$^{CDK1\text{-}9A}$ cells (Figure 3.3A). Taking together, we conclude that the interaction between Rad9 and Chk1 is absolutely dependent on the CAD region of Rad9, the nine CDK sites within this region and the activity of Cdc28 during G2/M phase of the cell cycle.

Given that additional data to support Rad9-Chk1 interaction has not been reported to date, we have performed co-immunoprecipitation (co-IP) experiments to independently support our yeast two-hybrid analysis (Figure 3.5C-F). Note that the cells used for these experiments expressed Chk1 tagged with 3FLAG (Figure S3.4E).

Surprisingly, in Chk1-3FLAG immunoprecipitates from G2/M-arrested wild type cell extracts, Rad9 can be clearly detected either in normal or damaging conditions. Notably, Chk1 preferentially associated with Mec1/Tel1-phosphorylated D-Rad9 after DNA damage, even though C-Rad9, the phosphoform dependent upon Cdc28, was the major form detected in the cell native extracts. The Rad9-Chk1 interaction can also be observed in reciprocal co-immunoprecipitation experiments in which Rad9-9MYC was immunoprecipitated from G2/M arrested cells treated with bleocin (Figure 3.5E). In parallel and similar experiments using *rad9*$^{CDK1\text{-}9A}$ mutant cells, we were able to confirm that the Chk1-Rad9 interaction detected in Chk1 immunoprecipitates from mock- or bleocin-treated cell extracts was lost when the nine putative sites in the CAD region are mutated in unphosphorylatable residues (Figure 3.5D). These data are in agreement with the defect of Chk1 phosphorylation in *rad9*$^{CDK1\text{-}9A}$ cells and indicate that the integrity of the CDK1-9 sites in the CAD region of Rad9 is required for a constitutive interaction between Rad9 and Chk1.

We have recently reported an interaction between Dpb11 and Rad9 (Granata et al., 2010) and here we examined the presence of Dpb11 in the Rad9-Chk1 interaction by co-immunoprecipitation experiments. Interestingly, the amount of Rad9 interacting with Dpb11 is less when compared to the same interacting with Chk1, either in the presence or absence of DNA damage. Additionally, interaction between Dpb11 and C-Rad9 is still detected in extracts from bleocin-treated wild type cells, distinct from the Chk1-Rad9 interaction (Figure 3.5C). Surprisingly, although the Dpb11-Rad9 interaction detected in Dpb11 immunoprecipitates from *rad9*$^{CDK1\text{-}9A}$ cells after DNA damage was lost, this interaction could still be detected in extracts from mock-treated *rad9*$^{CDK1\text{-}9A}$ cells. Importantly, Dpb11 and Chk1 were reproducibly undetectable in the Chk1 and Dpb11 immunoprecipitates respectively. Our data suggests that Rad9 constitutively forms two distinct sub-complexes in our native cell crude extracts that either contain Chk1 or Dpb11. CDK1-9 sites seem to have an important role specially in response to DNA damage only for the regulation of the Dpb11 interaction as shown previously (Granata et al., 2010), whereas the interaction with Chk1 is strictly dependent on their integrity even in undamaged conditions.

We also performed co-immunoprecipitation experiments using *cdc28-as1* cells in the presence or absence of 1-NMPP1 in order to confirm the requirement of Cdc28 activity for the Rad9-Chk1 interaction (Figure S3.4F). Native cell crude extracts used in these experiments were prepared from *cdc28-as1* cells that were arrested in G2 and treated with 1-NMPP1 prior to bleocin addition or mock treatment. In the absence of 1-NMPP1, the damage-induced form of Rad9 can be detected in Chk1 immunoprecipitates from G2/M-arrested *cdc28-as1* cells treated with bleocin, although to a less extent of wild type cells. Interestingly, in the presence of 1-NMPP1, the D-Rad9 is lost in Chk1 immunoprecipitates from G2/M-arrested *cdc28as1* cells treated with bleocin. However, it is important to mention that in cell crude extracts from 1-NMPP1-treated *cdc28-as1* cells Rad9 protein levels, as well as Chk1, Dpb11 and Orc6, are strikingly lower when comparing with extracts from wild type cells and *cdc28-as1* mock-treated for 1-NMPP1. Note that the decrease in Rad9 protein levels are not observed in denaturing total protein extracts (Figure S3.4G), excluding the possibility of protein degradation when Cdc28 is inactive. This suggests that Rad9 soluble levels might be altered in the native cell crude extracts from 1-NMPP1-treated *cdc28-as1* cells comparative to wild type cells, difference that is masked in the denaturing whole cell extracts. Interestingly, C-Rad9 form was still detected in Dpb11 immunoprecipitates in G2-arrested *cdc28-as1* cells after 1-NMPP1 treatment as in G2-arrested *cdc28-as1* cells when mock-treated for 1-NMPP1. This suggests that even though the protein levels are lower, Rad9 can still be detected in the immunoprecipitates. To reinforce this, we carried out a similar immunoprecipitation experiment using twice the amount of total protein (20mgs, *data not shown*) and we were still not able to detect any interaction between D-Rad9 and Chk1 after 1-NMPP1, suggesting that the absence of Rad9 in Chk1 immunoprecipitates is due to the loss of the interaction and not to the lower levels of Rad9 when Cdc28 is inactive. Taken together our results indicate that CDK-dependent phosphorylation of the nine sites located in the N-terminus of Rad9 regulate a constitutive interaction between Chk1 and Rad9 both in the presence and in the absence of DNA damage.

### 3.4.7. *In vitro* ATP-dependent release of Rad53 but not Chk1 from Rad9 complexes

We previously reported a Rad9-Rad53 interaction and demonstrated *in vitro* that Rad53 could be released from Rad9 in an ATP-dependent manner (Gilbert et al., 2001; Gilbert et al., 2003; O'Shaughnessy et al., 2006). We therefore tested whether Chk1 could be released from the Rad9 by the same mechanism. As previously observed (Gilbert et al., 2001), after Rad9 immunuprecipitates were washed and incubated with either ATP, γS-ATP (a non-hydrolysable ATP analogue) or simply mock treated, Rad53 became further phosphorylated and was released into the supernatant in a manner dependent upon ATP hydrolysis (Figure 3.5F). In contrast, further phosphorylation of Chk1 and its realease from the beads was not detected in the presence of ATP. This *in vitro* data is consistent with the existence of distinct molecular mechanisms regulating the activity of the two distinct checkpoint kinases, Chk1 and Rad53.

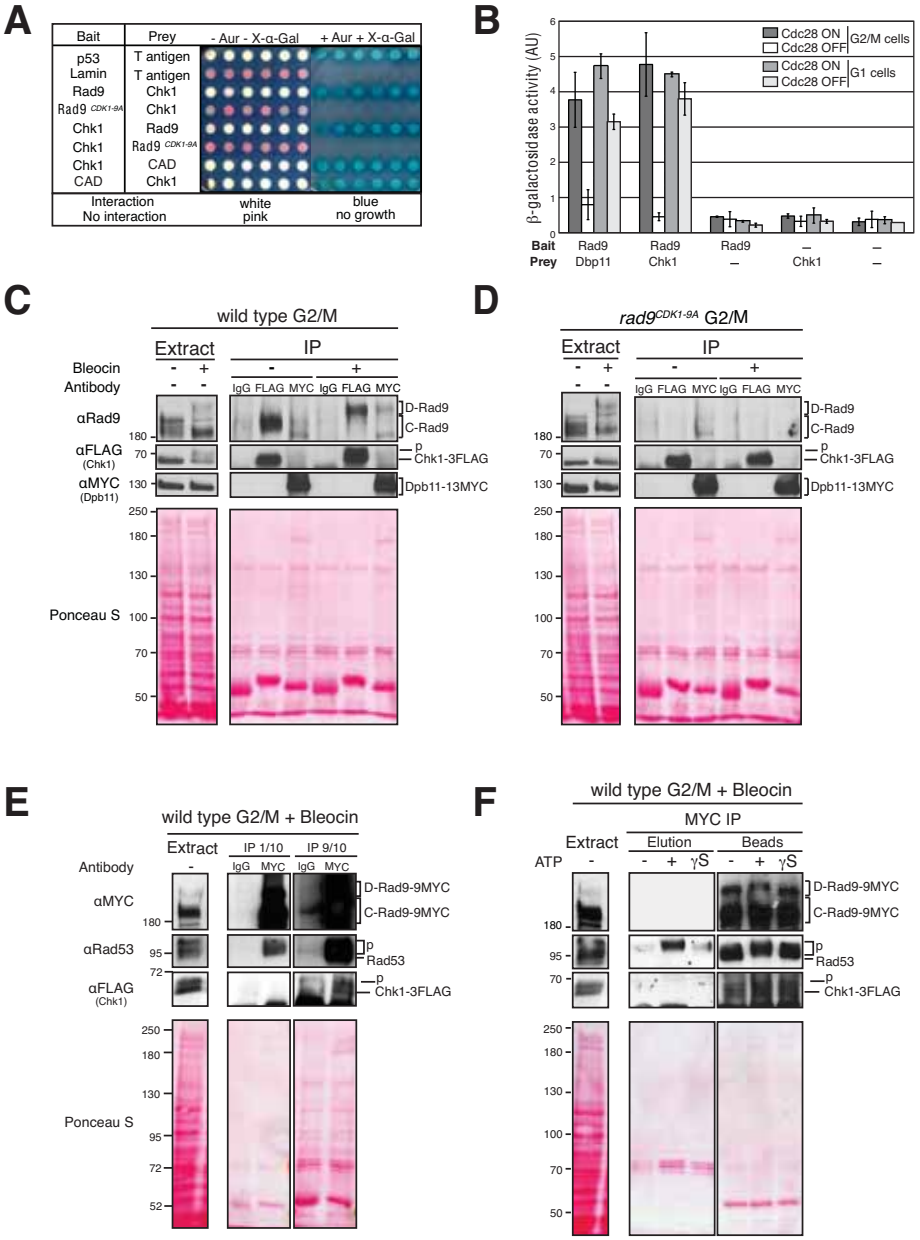


**Figure 3.5: CDK-dependent phosphorylation of the nine N-terminal CDK sites in Rad9 regulates the Rad9-Chk1 interaction.** (A) Rad9 and Chk1 interaction measured *in vitro* using a yeast two-hybrid (Y2H) assay is dependent on the CDK1-9 sites. Y2H interaction of specific bait and prey plasmids shown on the left is indicated by the white color of the otherwise red cells, their resistance to Aureobasidin A and their blue color on media containing the X-alpha-gal substrate, as for the p53/T antigen interaction. (B) The Y2H interaction between Rad9 and Chk1 is dependent on CDK activity in G2/M cells. The indicated bait and prey plasmids were introduced into *cdc28-as1* cells treated or not with 1-NMPP1 1h after synchronization of cells with either nocodazole or α-factor and prior to induction of bait expression. CDK-dependent Rad9-Dpb11 interaction was used as a control. Experiments A and B done in collaboration with Ramesh Kumar. (C) The Rad9 and Chk1 interaction measured using immunoprecipitation (IP) occurs both in the absence and presence of DNA damage. IPs were performed as indicated on extracts prepared from nocodazole-arrested cells, expressing both Chk1-3FLAG and Dpb11-13MYC, and either mock treated or treated with 20μg/ml of bleocin for 45 min. Mock (IgG) or MYC IPs were performed as controls. Rad9, Chk1-3FLAG and Dpb11-13MYC specific bands were detected in western blots. Lower exposures of the extracts are shown to facilitate their visualization. (D) Chk1 interaction with Rad9 is dependent on the CDK1-9

sites. As in panel C, except *rad9*$^{CDK1\text{-}9A}$ cells were used. (E) Western analysis of the indicated proteins in a reciprocal IP using Rad9-9MYC and Chk1-3FLAG expressing cells confirms the Rad9 and Chk1 interaction. As in panel C, except that anti-MYC antibody was used for the IP. Rad9 binding to Rad53 was used as a further control. (F) ATP-dependent release of Rad53, but not Chk1 from Rad9 IPs. Assays were performed as described (Gilbert et al 2001) except Rad9-9MYC was immunoprecipitated using an anti-MYC monoclonal antibody. The amount of Rad9-9MYC, Chk1-3FLAG or Rad53 remaining on the beads (Beads) or released (Elution) after incubation with ATP (+), γS-ATP (γS), a non-hydrolysable analogue, or mock treatment without any nucleotide (-) was determined by western blotting. See also Figure S3.4.

### 3.4.8. CDK sites 1, 4, 5, 6 and 7 are required for activation of Chk1 signalling

To identify the key sites required for Chk1 activation, we initially took advantage of a collection of mutants, containing different combinations of mutated CDK sites and covering the CAD region, generated during "pop-out' recombination on 5-FOA counterselection for the *rad9*$^{CDK1\text{-}9A}$ mutant. These mutants ranged from single site mutants to mutants with up to five mutated sites (Figure 3.6A). In addition, given that CDK5 (T110) is conserved in MCPH1, a checkpoint mediator known to interact with Chk1 in human cells (Figure S3.5A), we generated an additional mutant, *rad9*$^{CDK4,5,6,7A}$, where CDK5 and the surrounding sites were mutated to alanine (S83A, T110A, T125A and T143A). We then performed G2/M checkpoint activation analysis with 8 different N-teminal CDK mutants (Figure 3.6B). Western blotting of protein samples from mock- or IR-treated cells showed that *rad9*$^{CDK1,3,4,6,9A}$, *rad9*$^{CDK4,5,6,7A}$ and *rad9*$^{CDK1A}$ have defects in Chk1 phosphorylation, being *rad9*$^{CDK4,5,6,7A}$ the most defective, although not to the same extent as *rad9*$^{CDK1\text{-}9A}$. Importantly to notice is that the two other defective mutants contain CDK1 mutated to alanine. Therefore, CDK1 site in combination with CDK sites 4, 5, 6 and 7 (S83, T110, T125 and T143 respectively) might be important for damage-induced Chk1 activation signaling. To test this hypothesis we generated the *rad9*$^{CDK1,4,5,6,7A}$ mutant and performed G2/M checkpoint activation analysis as previously. Interestingly, unlike wild type, Chk1 phosphorylation is completely abolished in *rad9*$^{CDK1,4,5,6,7A}$ cells comparable to *rad9*$^{CDK1\text{-}9A}$ mutant (Figure 3.6C). Note that in this mutant Rad9 is hyperphosphorylated after bleocin treatment comparable to wild type cells but Rad53 hyperphosphorylation is slightly defective. Altogether, these data suggest that the CDK sites 4, 5, 6 and 7 (S83, T110, T125 and T143 respectively) in combination with CDK 1 site (S11) are required for efficient damage induced activation of Chk1 signaling.

We recently have reported that CDK1 (S11) in CAD of Rad9 is involved in mediating the interaction between Rad9 and Dbp11 in G2/M, suggesting that this site should not be required for Rad9-Chk1 interaction, despite clearly being needed for Chk1 phosphorylation. Alternatively, the Rad9-Chk1 interaction via at least one of the CDK4-7 sites might be dependent on a prior Rad9-Dpb11 interaction through CDK1 site. To test this hypothesis we have performed co-immunoprecipitation experiments as previously in G2-arrested *rad9*$^{CDK1A}$, *rad9*$^{CDK4,5,6,7A}$ and *rad9*$^{CDK1,4,5,6,7A}$ cells in undamaged conditions and compared with wild type and *rad9*$^{CDK1-9A}$ cells (Figure 3.6D). Interestingly, Rad9-Chk1 interaction was completely abolished in *rad9*$^{CDK4,5,6,7A}$ and *rad9*$^{CDK1,4,5,6,7A}$, like in *rad9*$^{CDK1-9A}$ cells, but not in the *rad9*$^{CDK1A}$ mutant although to a less extend as wild type cells. However, surprisingly, the levels of Rad9 protein are lower in *rad9*$^{CDK4,5,6,7A}$ whereas Rad9 is clearly undetectable in *rad9*$^{CDK1,4,5,6,7A}$ cells. Notably, this decrease in Rad9 protein levels is not observed in western blotting analysis using total denaturing cell extracts, excluding the possibility of protein degradation when CDK1,4-7 sites are unphosphorylatable residues (Figure 3.6C). This suggests that Rad9 soluble levels might be altered in the native cell crude extracts from *rad9*$^{CDK4,5,6,7A}$ and *rad9*$^{CDK1,4,5,6,7A}$ cells comparative to wild type cells, difference that is masked in the denaturing whole cell extracts. These data resemble our previous results from immunoprecipitation experiments in *cdc28-as1* extracts with Cdc28 inactive (Figure S3.4F), suggesting that the phosphorylation of these sites by Cdc28 might regulate soluble Rad9 levels. In addition, CDK1 seems to be required for the stabilization of Rad9-Chk1 interaction.

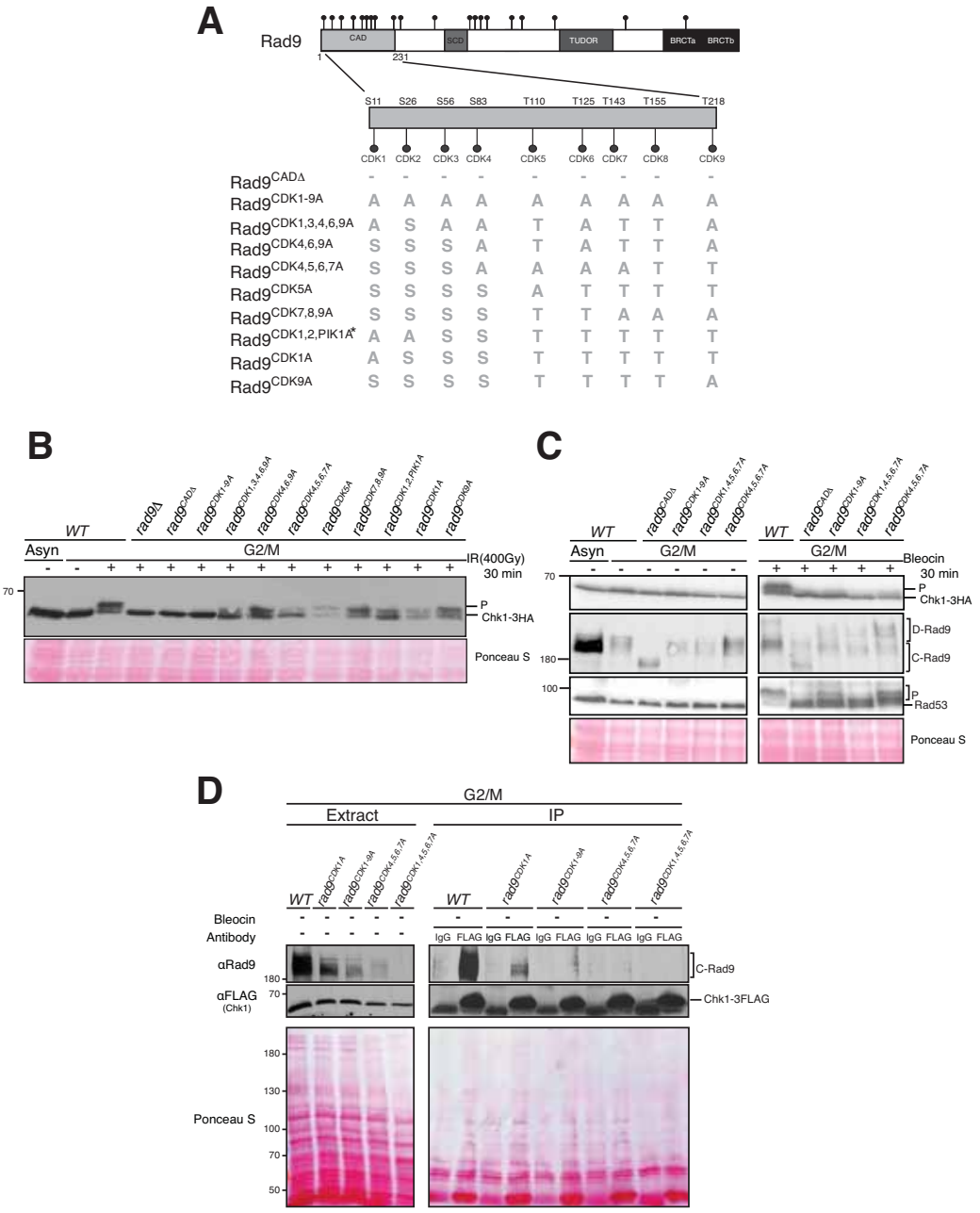


**Figure 3.6: CDK sites 4, 5, 6 and 7 are important for activation of Chk1 signaling.** (A) Schematic representation of the different combinations of mutated CDK sites in the CAD region of Rad9. (B) IR-induced Chk1 phosphorylation analysis in *rad9*$^{CDK}$ intermediate mutants shown in A. The single consensus PIKK phosphorylation site (T16) in the CAD region was also tested (in *rad9*$^{CDK1,2,PIK1}$ mutant) for IR-induced Chk1 phosphorylation, but had no effect. G2/M-arrested wild type and mutants were treated with IR and cells were collected after 30 min for western blot analysis. (C) Damage-induced Chk1 phosphorylation analysis in mentioned cells after treatment with 5µg/ml of Bleocin for 30 min. Like *rad9*$^{CDK1-9A}$ mutant, Chk1 phosphorylation is completely defective in *rad9*$^{CDK1,4,5,6,7A}$ mutant. The *rad9*$^{CDK}$ mutants are able to hyperphosphorylation Rad9 in response to DNA damage, whereas *rad9*$^{CDK4,5,6,7A}$ mutant is slightly defective for Rad53 activation like *rad9*$^{CADΔ}$. Experiments A, B and C done in collaboration with Ramesh Kumar. (D) Chk1 interaction with Rad9 is dependent on CDK sites 4,5,6 and 7. IPs were performed as indicated on extracts prepared from nocodazole-arrested cells, expressing Chk1-3FLAG, and mock treated. Mock (IgG) was performed as control. Rad9 and Chk1-3FLAG specific bands were detected in western blots. Lower exposures of the extracts are shown to facilitate their visualization. See Figure S3.5.

### 3.4.9. Ccdc28-dependent phosphorylated CDK7 is the main site regulating Rad9-Chk1 interaction

It is possible that in the generated *CDK* mutants described above, sites that have not been mutated can compensate for the sites mutated to alanine. Therefore, we sough out to perform complementary Y2H *add back* experiments to examine if any of the nine CDK sites in the CAD is sufficient to mediate the Rad9-Chk1 interaction. For this, we generated thirteen *add back* mutants using merely the CAD region of Rad9 since it is sufficient to mediate the interaction with Chk1 (Figure 3.7A and D). In each mutant, we reverted each CDK site to its wild type residue separately in the $CAD^{1\text{-}9A}$ mutant (Figure 3.7A). As previously, we detected a strong interaction between $CAD^{WT}$ and Chk1 proteins that is lost when all the CDK1-9 sites are mutated to alanine (Figure 3.7B). Interestingly, in the *add back* mutants we also detected a strong Y2H interaction when only CDK 7 site was reverted into its wild type residue ($CAD^{1\text{-}9A+7T}$). Wild type CDK 6 site ($CAD^{1\text{-}9A+6T}$) is the following site most important for CAD-Rad9 interaction. We also tested if these CDK sites mediate CAD-Rad9 interaction in a Cdc28-dependent manner (Figure 3.7C). In the presence of 1-NMPP1, the interaction between Chk1 with either $CAD^{1\text{-}9A+7T}$ or $CAD^{1\text{-}9A+6T}$ was lost. These data indicate that the Cdc28-dependent phosphorylation of mainly CDK7 wild type site, but also CDK6 wild type residue, is required for the interaction between CAD and Chk1.

We also tested if the combination of CDK1 wild type site with CDK 6 or 7 wild type residues affected CAD-Rad9 interaction (Figure 3.7D and E). Interestingly, when cells expressed CAD protein with either wild type CDK site 6 or 7 combined with wild type CDK1 ($CAD^{CDK1\text{-}9A+1S/6T}$ and $CAD^{CDK1\text{-}9A+1S/7T}$), a significant increase of the interaction was observed, reaching full length Rad9-Chk1 interaction levels for the later case (Figure 3.7E). A partial interaction signal was also observed with the CAD protein expressing CDK4 or 5 wild type residues when in combination with CDK1 wild type site but comparatively lower than CDK1 wild type residue combined with either CDK6 or 7 wild type residues. Together our data clearly suggests that, out of the 9 sites at the N-terminus of Rad9, CDK7 is the major site that, when phosphorylated by Cdc28, mediates the interaction between Rad9 CAD and Chk1. In addition, CDK1 in combination with CDK7 rather than alone improves this interaction.

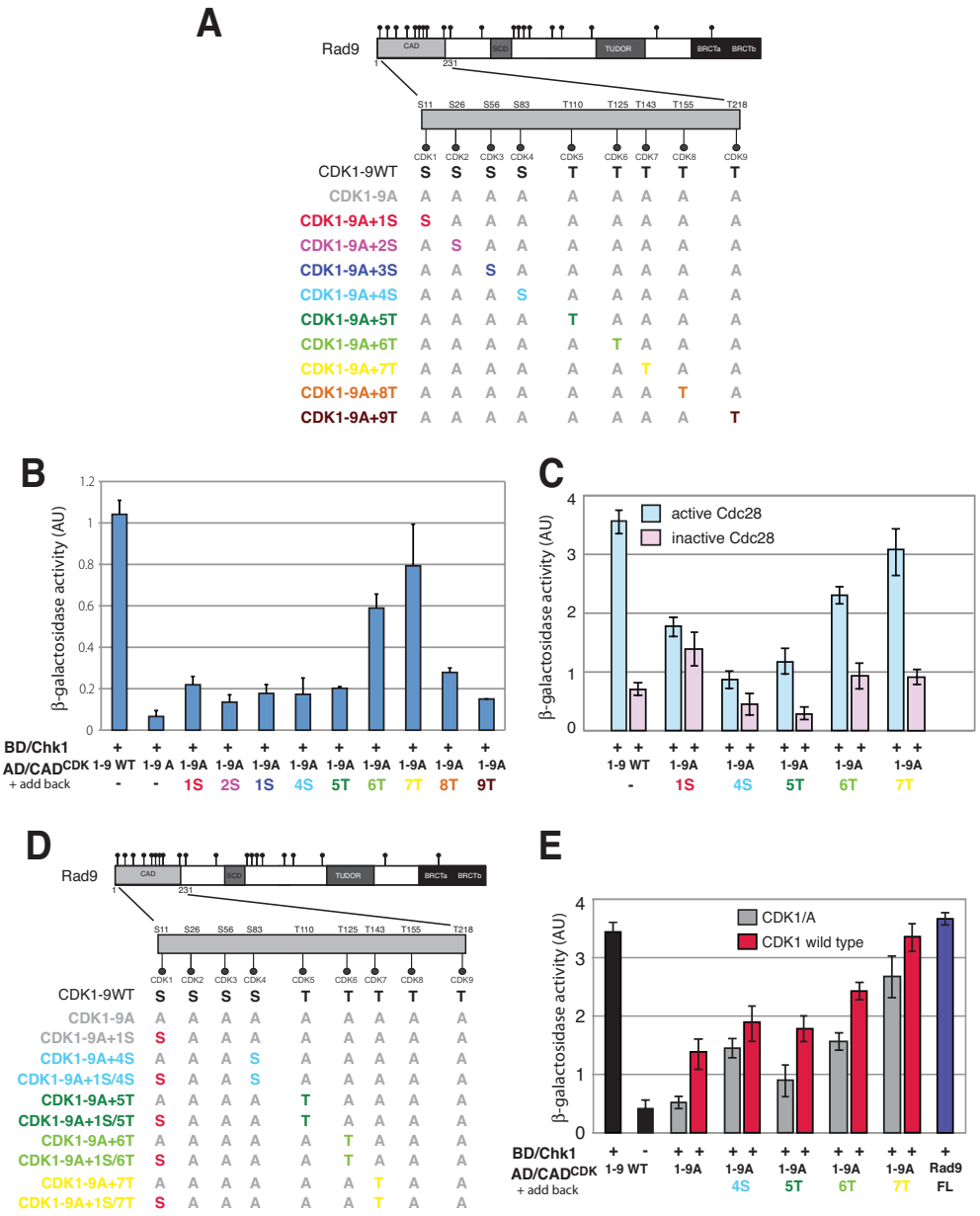


**Figure 3.7: CDK-dependent phosphorylation of the CDK site number 7 in Rad9 regulates the Rad9-Chk1 interaction.** (A) Schematic representation of the different combinations of added back CDK sites in the CAD$^{CDK1\text{-}9A}$ used for yeast two hybrid experiments in B. Black residues indicate wild type residue; Grey residues indicate alanine residue; Red, purple, dark and light blue, dark and light green, yellow, orange and brown indicate wild type CDK1, 2, 3, 4, 5, 6, 7, 8 and 9 residues, respectively. (B) and (C) Rad9 and Chk1 interaction measured using a yeast two-hybrid assay is dependent mainly on the integrity of CDK7 site and its dependent-phosphorylation by Ccd28 in G2/M cells. The indicated bait and prey plasmids were introduced into *cdc28-as1* cells treated or not with 1-NMPP1 1h after synchronization of cells with nocodazole and prior to induction of bait expression. Colors as in A. (D) Schematic representation of the different combinations of added back CDK sites in the CAD$^{CDK1\text{-}9A}$ used for yeast two hybrid experiments in D. Colors as in A. (E) Rad9 and Chk1 interaction measured *in vitro* using a yeast two-hybrid assay is rescued to wild type levels when wild type CDK7 site is combined with wild type CDK1 residue in G2/M cells; The indicated bait and prey plasmids were introduced into *cdc28-as1* cells treated or not with 1-NMPP1 1h after synchronization of cells with nocodazole and prior to induction of bait expression; Colors as in A and C; Blue bar indicate full length (FL) Rad9 is used as prey.

## 3.5. DISCUSSION

### 3.5.1. Complex cell cycle phosphorylation of Rad9 by Cdc28/Clb complexes

The DNA damage response mediator Rad9 is a peculiar protein in budding yeast since it comprises an unusual high number of putative CDK phosphorylation sites. The work presented here explores the phosphorylation and role of some of these sites in Rad9 functions. Firstly, we show that Rad9 exhibits a complex *in vivo* phosphorylation profile during a normal cell cycle which, as demonstrated by genetic evidences, is dependent on the activity of B-type cyclin (Clb1 to 6) forms of Cdc28 (also termed Cdk1). Our data is consistent with *in vitro* studies demonstrating phosphorylation of Rad9 by purified Cdc28/Clb5 and Cdc28/Clb2 complexes (Loog and Morgan, 2005). However, using merely the Rad9 CAD we demonstrate that this region is preferently phosphorylated *in vitro* by Cdc28/Clb2 complexes. Importantly, this is still in agreement with the cell cycle phosphorylation profile of Rad9 as cells progress through the S, G2 and M phases of the cell cycle given that Cdc28/Clb3 and Cdc28/Clb2 complexes regulate the cells entry into G2 and Mitosis respectively (Enserink and Kolodner, 2010). Notably, the fact that Rad9-related DDR mediators in higher cells (53BP1, BRCA1 and MDC1) are also highly composed by putative CDK phosphorylation sites, suggests that the CDK-dependent phosphorylation of mediator proteins is an evolutionarily conserved mechanism for the regulation of DDR. Consistent with this, some of these CDK sites have been shown to be phosphorylated *in vivo* by Cdk1, such as S379 of mouse 53Bp1, required for its binding to the mitotic kinase Plk1 (van Vugt et al., 2010), S1497 of BRCA1, needed for its subcellular localization (Ruffner et al., 1999), and S1189/S1191 together with S1497, required for efficient BRCA1 foci formation following cisplatin-induced DNA damage (Johnson et al., 2009).

### 3.5.2. Rad9 functions in the DDR are regulated by CDK-dependent phosphorylation

We hypothesized that specific DDR functions of Rad9 are modulated by the CDK-dependent phosphorylation of certain CDK sites. We show that a $Rad9^{12A}$ mutant, containing twelve mutated consensus CDK sites, displays a severe defect for its cell cycle phosphorylation. This indicates that at least some of these twelve CDK sites are phosphorylated *in vivo* during a normal cell cycle. Accordingly, mass spectrometric analyses have shown the *in vivo* phosphorylation of nine out of these

twelve sites (Albuquerque et al., 2008; Holt et al., 2009; Smolka et al., 2005). The possibility of a role for the CDK-dependent phosphorylation of these sites in preventing inappropriate checkpoint activation in response to DNA structures generated during a normal S phase is excluded by the fact that cell cycle proliferation or checkpoint activation were unaffected in the *rad9*$^{12A}$ cells. In fact, we have shown that S phase structures are not needed to drive Rad9 cell cycle phosphorylation under conditions in which the cell cycle proceeds to mitosis without initiating DNA replication. On the other hand, a *rad9-18A* mutant, containing mutation in eighteen out of the 20 consensus CDK sites, displays further defects in Rad9 DNA damage-induced phosphorylation (Bonilla et al., 2008), suggesting that the additional residues mutated in Rad9-18A, but not in Rad9$^{12A}$ (CDKs 2, 5, 7, 8, 10, 12, 13 and 15), are required for Rad9 DDR functions. Interestingly, four of these sites (CDKs 2, 5, 7 and 8) are comprised in the first N-terminal 250 amino acids of Rad9 (Chk1 Activation Domain), region that has been shown to be required for Chk1 phosphorylation upon DNA damage (Blankley and Lydall, 2004). The other four additional mutated sites (CDKs 10, 12, 13 and 15) might be required to control the damage-induced Rad53 activation either individually or in combination with the other sites. Accordingly, a recent study has shown that CDK12 and 13 sites (S462 and T474) are required to directly regulate the interaction between Rad9 and Dpb11 (Pfander and Diffley, 2011). This suggests that individual Rad9 CDK sites, or subsets of these sites, might regulate specific Rad9 functions. Consistent with this, we have observed specific phenotypes, including checkpoint recovery defects and specific sensitivity to DNA damaging agents, with specific CDK site mutants (*unpublished data*). In this report, we have investigated the role of the nine CDK sites comprised in the CAD region of Rad9 in regulating Chk1 activity.

### 3.5.3. Chk1 activation is dependent on Cdc28 phosphorylation of Rad9 in G2/M cells

In this study, we established that the CDK1-9 sites within the Rad9 CAD are specifically required for Chk1 activation in response to DNA damage, but not for Rad53 neither Rad9 damage-induced phosphorylation. Importantly, these sites or at least some of them are required for Rad9 cell cycle *in vivo* phosphorylation. Accordingly, data in our laboratory combined with mass spectrometry analyses from reported studies have shown that all of the consensus CDK sites located in the Rad9

CAD, with the exception of T143 (CDK7), are phosphorylated *in vivo* (Albuquerque et al., 2008; Holt et al., 2009; Smolka et al., 2005). In addition, we show that the damage-induced Chk1 phosphorylation is drastically abrogated in G2/M *rad9*$^{CDK1\text{-}9A}$ cells, contrasting with only a partial defect when arrested in G1 phase, indicating that the CDK1-9 sites are most important in the regulation of the Chk1 branch when cells have high Cdc28 activity.

The role of Cdc28 in DNA damage–induced checkpoint activation is not fully understood. Here, we established that Cdc28 activity is required for activation and maintenance of Chk1 phosphorylation, regardless of the type of DNA damage (DSBs, SSBs or bulky lesions repairable by nucleotide excision repair). This indicates that Chk1 activation is not simply a downstream consequence of the role of Cdk1 in DSBs resection (Huertas et al., 2008; Limbo et al., 2007) or the Cdc28-dependent role of Rad9 in inhibiting this process (Lazzaro et al., 2008), contrasting with Rad53 that is specifically activated in response to DSBs. Together, our data establish that CDK phosphorylation of one or more of the 9 sites within the Rad9 N-terminal region regulate Chk1 activation during periods of the cell cycle when Cdc28/Clb kinases are active.

### 3.5.4. CDK1-9 sites mediate Rad9 interaction with Chk1 in a Cdc28-dependent manner

The molecular mechanism of how Rad9 regulates Chk1 activity has not been identified to date. The only available evidence for a possible mechanism was obtained by Y2H approach showing an interaction between Rad9 and Chk1 under overexpressed conditions (Sanchez et al., 1999; Uetz et al., 2000). Here, we demonstrate by Y2H that the CAD region of Rad9 on its own is able to interact with Chk1. Importantly, we also show that the Rad9 CDK1-9 sites comprised in this region are absolutely required for this interaction in G2/M phase, being consistent with our Chk1 phosphorylation and *in vitro* Kinase assays data. In addition, the interaction between Rad9 and Chk1 was dependent on Cdc28 activity in G2/M phase of the cell cycle. Our data led us to conclude that the Cdc28-dependent phosphorylation of the nine putative CDK phosphorylation sites located in the CAD region of Rad9 regulate a physical interaction between Rad9 and Chk1 in G2/M phase of the cell cycle when CDK1 activity is high.

We also show that the Rad9 CDK1-9 sites comprised in the CAD are required for Rad9-Chk1 interaction in G1 phase, consistent with a slight defect in Chk1 phosphorylation in this cell cycle phase. However, the interaction between Rad9 and Chk1 was independent on Cdc28 activity in G1 phase of the cell cycle. Although our results indicate that the CDK1-9 sites are Cdc28 phosphorylation sites and are importantly required in G2/M cells when cells have high Cdc28 activity, it is possible that only particular residues require Cdc28 phosphorylation to drive the interaction while other residues are independent of Cdc28 activity. Therefore, the phosphorylation of the consensus CDK sites by kinases other than Cdc28 may be required for the Rad9-Chk1 interaction in G1 phase. In addition, we cannot exclude that the G1 interaction might be indirect. Taken together, our data suggest that the activation of Chk1 need a physical interaction between the nine putative CDK phosphorylation sites located in the CAD region of Rad9 and Chk1, process that is differentially regulated during G2/M and G1 phase of the cell cycle. It would be interesting to explore the role of Chk1 activation in G1 that remains unclear.

Consistent with our Y2H Rad9-Chk1 interaction findings we have validated the Rad9-Chk1 interaction and confirmed the requirement of the Rad9 sites CDK1-9 to mediate this interaction both in damaged and undamaged cells. Interestingly, Dpb11 (homologue of Cut5 in fission yeast and TOPBP1 in higher cells), like Chk1, was also bound to Rad9 both in the presence and in the absence of DNA damage (Granata et al., 2010). In contrast with the Chk1-Rad9 interaction, only the DNA damage-induced interaction between Dpb11 and Rad9 is dependent on the integrity of putative CDK phosphorylation sites in the Rad9 CAD (we have previously shown that S11 residue is required for this interaction, (Granata et al., 2010). It is possible that in undamaged cells, Dpb11-Rad9 interaction is dependent on additional CDK sites outside the CAD region of Rad9 as reported by others (Pfander and Diffley, 2011). In addition to this, a smaller fraction of Rad9 is bound to Dpb11 in contrast to the Chk1 bound Rad9 fraction. It is possible that the Rad9-Chk1 interaction is enriched in our extracts in contrast to the Rad9-Dpb11 interaction since the latter occurs on chromatin, fraction that is poorly represented in our extracts (*see Material and Methods*). To test this, it would be interesting to perform similar experiments in extracts that have been treated with benzonase in order to release the chromatin-

bound proteins. Our data clearly demonstrates that Rad9 forms two different complexes one with Chk1 and other with Dpb11. In our assays, simultaneous binding of Rad9, Chk1 and Dpb11 was not detected, whereas in fission yeast a Crb2-Chk1-Cut5 interaction has been reported (Mochida et al., 2004). It is possible that a Rad9-Chk1-Dpb11 interaction can occur *in vivo* but we were not able to detect in our assay perhaps because these complexes are too transient to detect in a Co-IP experiment or, alternatively, they occur in the chromatin context (*see Material and Methods*). To test this, it would be interesting to investigate Rad9-Chk1 and Rad9-Dpb11 interactions in the chromatin fraction of our protein extracts.

### 3.5.5. Novel Molecular mechanism of Chk1 activation in budding yeast

The work presented in this report clearly demonstrates a novel model for Chk1 activation illustrated in Figure 3.8 that is distinct from the previously reported model for Rad53 activation (Gilbert et al., 2001). This model is based on the regulation of a constitutive interaction between Chk1 and CDK-dependent modified Rad9 (C-Rad9) during S/G2/M phases. In the first step, C-Rad9 and Chk1 interact constitutively in the absence of DNA damage mainly dependent on the phosphorylation of CDK sites in Rad9 CAD by Cdc28/Clb2 complex [Figure 3.8, step 1]. This step might occur in the chromatin context because both proteins are believed to dynamically associate with chromatin even in the absence of DNA damage (Hammet et al., 2007). In this respect Chk1 activation is distinct from Rad53 activation, since the Rad53 kinase interacts specifically with Mec1/Tel1 phosphorylated Rad9 (D-Rad9) generated in response to DNA (Sweeney et al., 2005). Upon DNA damage, C-Rad9/Chk1 complex is further recruited and accumulated on the vicinity of damaged DNA, process mediated by Rad9 interaction with exposed or *de novo* generated specific histone marks (H3K79me and γH2A (Grenon et al., 2007; Hammet et al., 2007), as well as by Rad9 binding via CDK1 to Dpb11, protein recruited to the DNA lesions by the 9-1-1 complex (Granata et al., 2010; Navadgi-Patil and Burgers, 2009b; Puddu et al., 2008) [Figure 3.8, step 2]. Since we also observed an interaction between Dpb11 and Rad9 both before and after damage, the latter dependent on the integrity of CDK1-9 sites in Rad9 CAD, it is possible that the interaction between Rad9-Dpb11 after damage further promotes the interaction between Rad9 and Chk1 by recruiting and stabilizing Rad9 onto damaged chromatin via CDK1 (S11) (Granata et al., 2010).

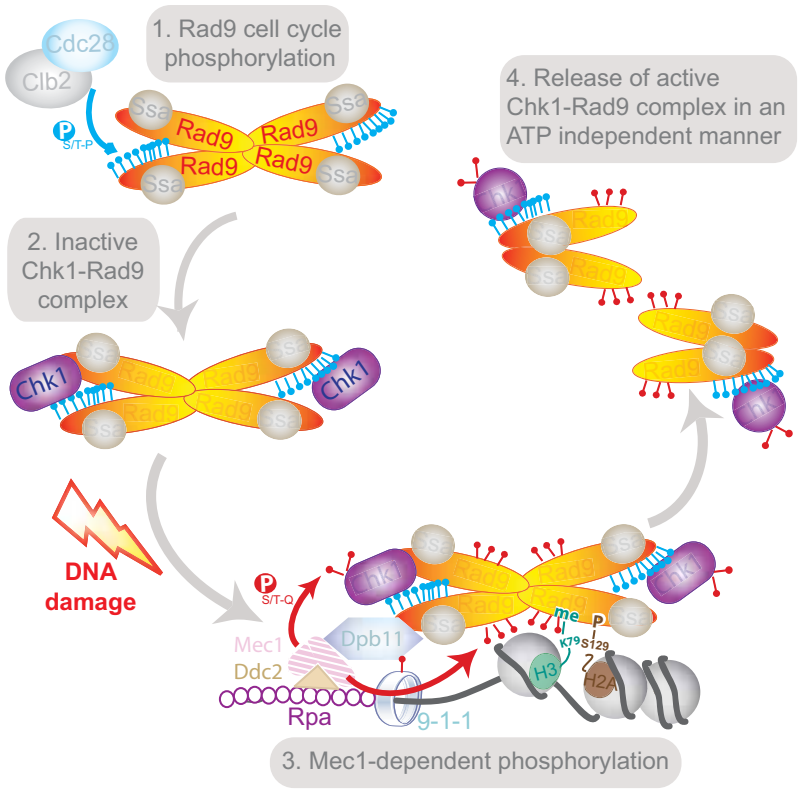


**Figure 3.8: Model for Chk1 activation mediated by Rad9 cell cycle phosphorylation.** (A) Model of Chk1 activation in response to DNA damage. Rad9 CAD region is phosphorylated by Clb-Cdc28 complexes during G2 phase and this process regulates a Rad9 constitutive interaction with Chk1. Upon DNA damage, Rad9-Chk1 complex is recruited to chromatin through several mechanisms to be in close proximity to the Mec1 kinase. After Rad9 hyperphosphorylation and Chk1 phosphorylation by Mec1, Rad9-Chk1 complex either stays on chromatin for Chk1 to phosphorylates local targets or the complex is released from chromatin through unknown mechanisms to phosphorylate the final targets in the nucleus; blue circles – cell cycle phosphorylation dependent on Cdc28 complexes; red circle – Mec1-dependent phosphorylation; see text for more details.

The 9-1-1/Dpb11 complex-dependent activation of Mec1 bound to RPA-coated ssDNA, process that is conserved from yeast to human (Majka and Burgers, 2007; Navadgi-Patil and Burgers, 2009a), results in DNA damage-dependent phosphorylation and remodeling of both Rad9 (Gilbert et al., 2003) and Chk1 (Tapia-Alveal et al., 2009). This would lead to *in cis* autophosphorylation of Chk1 (Chen et al., 2009) and the release of the D-Rad9/Chk1 complexes (possibly the ones detected in this study) in an ATP-independent manner [Figure 3.8, step 3]. In contrast, Rad53 full activation following its Mec1 (ATR)-dependent modification occurs by *in trans* autophosphorylation (Pellicioli and Foiani, 2005), which is then released from D-Rad9 in an ATP-dependent mechanism (Gilbert et al., 2001). It is

possible that the ATP-independent mechanism behind the release of activated Chk1 from Rad9 could allow the targeting of Chk1 substrates in conformity with an observed Rad9-independent activation of certain chk1 mutants in budding yeast (Chen et al., 2009). Alternatively, or perhaps in addition, a proportion of activated Chk1 could be kept in the proximity of damaged chromatin via its interaction with Rad9 to phosphorylate local targets.

### 3.5.6. Cdc28-dependent phosphorylation of CDK7 residue is the main contribution for Rad9-Chk1 interaction

We have also dissected the specific sites among the CDK1-9 sites in the CAD region of Rad9 required for Chk1 activation. We found that CDK sites 4 (S83), 5 (T110), 6 (T125) and 7 (T143) in combination with CDK1 (S11) site are required for damage-induced Chk1 phosphorylation. Interestingly, Rad9 CDK5 site (T110) and the surrounding sequence is highly conserved within the putative CAD of MCPH1 (~103-250 amino acids; *Steve Jackson, personal communication*; Figure S3.5), a checkpoint mediator protein in higher cells required for Chk1 activation through a physical between both proteins (Alderton et al., 2006).

We further refined the key residues in the CAD region required for Rad9-Chk1 interaction by Y2H *add back* experiments. We show that when wild type CDK6 (T125) or CDK7 (T143) residues are added back to $CAD^{CDK1\text{-}9A}$, a Cdc28-dependent increase in Rad9-Chk1 interaction is observed, being a stronger interaction with wild type CDK7 site. Surprisingly, when any of these sites are combined with wild type CDK1 the interaction between Rad9 and Chk1 is restored, reaching wild type levels for CDK7 site. Considering that we previously showed that CDK1 is involved in the interaction between Rad9 and Dpb11 (Granata et al., 2010), it is possible that this site might contribute to Rad9 recruitment and stabilization onto chromatin through binding to Dpb11, hence further promoting Rad9-Chk1 interaction via CDK7 residue. This data suggests that out of nine CDK sites needed for damage-induced Chk1 activation in G2/M phase, CDK7 site (T143) is the major residue interacting with Chk1 in a CDK-dependent manner. To reinforce these data it would be interesting to perform similar yeast two-hybrid interaction analysis as above adding back CDK site 7 mutated to a phospho-mimetic residue in the $CAD^{CDK1\text{-}9A}$ (i.e.

$CAD^{CDK1\text{-}9A+7D}$ or $CAD^{CDK1\text{-}9A+7E}$), as well as co-immunoprecipitation in the $rad9^{CDK1\text{-}9A+7T}$, $rad9^{CDK1\text{-}9A+1S+7T}$ and $rad9^{CDK1\text{-}9A+7D}$ or $rad9^{CDK1\text{-}9A+7E}$ mutants. Alternatively, or perhaps in addition, phospho-specific antibodies against the CDK1 (S11) and CDK7 (T143) residues should be generated and used to study these phosphorylation events in cell extracts.

Interestingly, alignment of the Rad9 CAD fragment with its fission homologue, Crb2, shows that the CDK7 residue of Rad9 is highly conserved (Figure S3.5B; Blankley and Lydall, 2004), suggesting a functional conservation between these proteins to drive its checkpoint functions, particularly in their interaction with Chk1. Therefore, it would be interesting to investigate whether the mechanism behind this process is regulated by CDK-dependent phosphorylation of the conserved CDK residues in a similar manner to scRad9.

### 3.5.7. Is Cdc28-dependent phosphorylation of CDK residues in Rad9 CAD required for Rad9 chromatin release?

We have also addressed the dependency on Cdc28 activity of the Rad9-Chk1 interaction by co-immunoprecipitations. Although the Rad9-Chk1 interaction was undetectable when Cdc28 was inactive, we cannot exclude completely the limitations in detecting Rad9 bound to Chk1 in these conditions, due to the lower Rad9 protein levels observed in the native cell crude extracts. Strikingly, this was not observed when protein denaturating extracts were analysed by western blotting, excluding the possibility of Rad9 degradation in these conditions. A possible explanation for these results is that in the absence of Cdc28-dependent phosphorylation Rad9 is retained on the chromatin. This is consistent with the fact that in native cell crude extracts the majority of the protein analysed is from the soluble fraction (most of the chromatin fraction is lost in the high speed centrifugation, s*ee Material and Methods*), while all the protein content in the cell is analysed when using total cell denaturing extracts. To test this hypothesis it would be interesting to perform similar immunoprecipitation experiments as shown in Figure 3.5F using extracts from mock- or bleocin-treated G2-arrested *cdc28as1* cells in the absence or presence of 1-NMPP1 after treatment with benzonase which releases the protein bound on chromatin.

We have also dissected by co-immunoprecipitations the involvement of specific sites among the CDK1-9 sites in the CAD region of Rad9 required for Rad9-Chk1 activation. Based on the Chk1 phosphorylation data, we focused in the CDK sites 4, 5, 6 and 7 either alone or in combination with CDK1 site. Interestingly, although no interaction was detected in both *rad9*$^{CDK4,5,6,7A}$ and *rad9*$^{CDK1,4,5,6,7A}$ cells, like *rad9*$^{CDK1-9A}$ cells, we observed lower Rad9 protein levels in these cells, resembling the previous results obtained when Cdc28 was inactive. Again, the decrease in Rad9 protein levels was only observed in native cell crude extracts but not in total cell denaturing extracts. These data suggest that in these cells Rad9 might be retained on the chromatin comparable when Cd28 is inactive. However, it is stinking that Rad9 levels are not altered as well in *rad9*$^{CDK1-9A}$ cells. It is possible that CDK sites mutated in *rad9*$^{CDK1-9A}$ but not in *rad9*$^{CDK4,5,6,7}$ contribute somehow for Rad9 retention onto chromatin. The Ccd28-dependent phosphorylation of Rad9 at the CDK sites 4, 5, 6 and 7 could then be required for Rad9 release from the chromatin in order to mediate the fully activation of the checkpoint kinases Rad53 and Chk1. Consistent with this hypothesis is the fact that *rad9*$^{CDK4,5,6,7A}$ cells are not only defective for Chk1 phosphorylation but also for Rad53 phosphorylation both after DNA damage, in contrast with *rad9*$^{CDK1-9A}$ cells that are only defective for damage-induced Chk1 phosphorylation.

In higher cells, the role played by DDR mediator proteins is more complex than in yeasts as multiple mediators are known and whose molecular mechanisms in checkpoint activation remain largely uncharacterised (Smits et al., 2010; Stracker et al., 2009a). Among the mediators, Claspin-dependent activation of CHK1 is best characterized, however, MCPH1, BRCA1 and MDC1 also play an undefined role in this activation. Our work suggests that activation of human CHK1 by mediator proteins, possibly those related to budding yeast Rad9, may also be integrated into cell cycle stage by their prior CDK-dependent phosphorylation and dynamic interaction with CHK1. Additionally, the extensive cell cycle phosphorylation of these proteins is likely to fine-tune their DNA damage functions, as we have observed with their budding yeast homologue, Rad9.

## 3.6. MATERIAL AND METHODS:

### 3.6.1. Yeast Strains:

All of the strains used in this work, except CG378 used in Figure 3.1A, are in the W303 background and are listed in Table S3.1. All mutant and tagged alleles used were integrated on the chromosome apart from the yeast two-hybrid experiment. Yeast Strain and plasmid constructions are described below. Plasmids and oligonucleotides used in this study are listed in Tables S3.2 and S3.3. The *cdc28-as1* strain was generated by integrating the pVF6 plasmid as described (Diani et al., 2009).

#### *3.6.1.1. Rad9 mutants:*

Mutations were targeted to the *RAD9* locus using integrative vectors and the final mutant strains generated differed from wild type cells only at the specific *rad9* mutation.

Integrative vectors containing *rad9*$^{CDK1\text{-}9A}$, *rad9*$^{CDK1,3,4,6,9A}$, *rad9*$^{CDK5A}$, *rad9*$^{CDK1A}$ *and* *rad9*$^{CAD\Delta}$ mutations, respectively, termed pRS306-*rad9*$^{CDK1\text{-}9A}$, pRS306-*rad9*$^{CDK1,3,4,6,9A}$, pRS306-$^{rad9CDK5A}$, pRS306-*rad9*$^{CDK1A}$ and pRS306-*rad9*$^{CAD\Delta}$, were linearised with MscI and transformed into W303-1a *RAD5*$^{+}$ cells. Putative integrants were selected for integration at *RAD9* locus by positive selection on plates lacking uracil. 'Pop-out' recombination of the *URA3* marker was achieved by negative selection on 5-fluoroorotic acid (5-FOA). Colonies were screened for the presence of the specific *rad9* mutations by amplifying *RAD9* DNA fragment with Rad9seq2 and Rad9 cdkwtm2 primers and finally sequenced with N1 Mut and other Rad9 sequencing primers (listed in Table S3.3).

To generate the *rad9*$^{CDK12A}$ mutant, W303 *RAD5*$^{+}$ cells were firstly transformed with PshAI-digested plasmid pRS306-*rad9*$^{CDK14,16\text{-}20A}$, lacking the first 1350 bp of the *RAD9* gene. Plasmid 'pop-out' events were selected on 5-FOA plates and clones containing the *rad9*$^{CDK14,16\text{-}20A}$ mutant allele were confirmed by PCR sequencing. The resultant *rad9*$^{CDK14,16\text{-}20A}$ mutant strain was subsequently transformed with MscI-digested plasmid pRS306-*rad9*$^{CDK1,11A}$, lacking the last 2456 bp of the *RAD9* gene. Plasmid excisions were then selected on 5-FOA plates, and clones containing the *rad9*$^{CDK11,14,16\text{-}20A}$ mutant allele were confirmed by PCR sequencing. Finally, BmgBI-

directed integration of pRS306-*rad9*$^{CDK1,3,4,6,9A}$, lacking the last 2456 bp of the *RAD9* gene, into *rad9*$^{CDK11,14,16-20A}$ cells yielded the strain encoding the *rad9*$^{CDK12A}$ mutant allele. Plasmid 'pop-out' events selected on 5-FOA plates, and clones containing the rad9CDK12A mutant allele were confirmed by PCR sequencing.

Strains used in Figure 3.3E for epistasis analysis were generated by crossing *MAT*a *rad9*$^{CDK1-9A}$ with *MAT*α *sml1::KANMX6 rad53::HIS3 chk1::URA3* (strain DLY2242 in (Blankley and Lydall, 2004).

***3.6.1.2. Chk1 tagged strains:***

To C-terminally tag Chk1 with 3HA, Chk1-DiaF and Chk1-DiaR primers were used to amplify 1.5Kb of *CHK1-3HA-KlURA3* DNA cassette from genomic DNA of strain YNL1144 (Clerici et al., 2004). Wild type and mutant yeast strains were transformed with the *CHK1-3HA-KlURA3* DNA cassette and selected for growth on plates lacking uracil. The putative transformants were screened for the expression of Chk1-3HA by western blot analysis and the correct integration of the *CHK1-3HA* allele at the *CHK1* locus was verified by diagnostic PCR.

To C-terminally tag Chk1 with 3-FLAG, Chk1-Flag-5' and Chk1-Flag-3' primers were used to amplify a *CHK1-3FLAG-KANMX* DNA cassette from p3FLAG-KanMX plasmid DNA (Gelbart et al., 2001). After positive selection on G418 plates, the putative integrants were screened for the presence of the 3FLAG tag by diagnostic PCR using primers Chk1-DiaF and Chk1-2, and Chk1-3FLAG expression was detected by western blot analysis.

***3.6.1.3. Dpb11 tagged strains:***

To C-terminally tag Dpb11 with 13MYC, strains were transformed with a *DPB1-13MYC-HIS3* PCR fragment amplified with DPB11-myc-5' and DPB11-myc-3' primers from the genomic DNA of strain YNL1426 (strain YFP38 in (Puddu et al., 2008). The *histidine*$^{+}$ integrants were screened for the presence of the 13MYC tag by diagnostic PCR using primers DPB11-testF and DPB11-testR, and Dpb11-13MYC expression was detected by western blot analysis.

### 3.6.2. Plasmids:

All constructs were sequenced to confirm the presence and absence of the specific mutations.

#### *3.6.2.1. RAD9 integrative plasmids:*

pRS306-*rad9*$^{CDK1\text{-}9A}$, pRS306-*rad9*$^{CDK1,3,4,6,9A}$, pRS306-*rad9*$^{CDK1,11A}$ and pRS306-*rad9*$^{CDK1A}$, and pRS306-*rad9*$^{CDK5A}$ constructs carrying the specific point mutations were introduced by site--directed mutagenesis (Stratagene) on pGEM-Teasy-NT*RAD9*, containing 2547 bp fragment of *RAD9* coding for the Rad9 N-terminus, from position -445 to position +2102 within the *RAD9* ORF. Mutations were introduced by successive round of mutagenesis using specific set of primers: Rad9N1F + Rad9N1R; Rad9N2F + Rad9N1R; Rad9N3F + Rad9N3R; Rad9N4F + Rad9N4R; Rad9N5F + Rad9N5R, as well as single primers R9T110A; R9S26A; R9N1T16A; R6T155A and R9T143A.

The pRS306-*rad9*$^{CAD\Delta}$ deletion construct containing a *RAD9* fragment deleted for the sequence coding for the CAD region (from +1 to +693 within the *RAD9* ORF) was generated as follows. A 430 bp Fragment named CADA, from position -445 to position -1 from the *RAD9* ORF, was amplified with CADP1 and CADP2 primers. A second 630 bp Fragment named CADB, from position +694 to position +2102 within the *RAD9* ORF, was amplified with CADP3 and CADP4 primers. CADA and CADB were fused in a 1.107 Kb fragment using CADP1 and CADP4 primers and ligated into pGEMTeasy vector by TA cloning (PROMEGA).

The 1.8kb (point mutations) and 1.107Kb (CAD deletion) BamHI-MscI fragments of the resulting pGEM-Teasy-NT*rad9*$^{CDK1\text{-}9A}$, pGEM-Teasy-NT*rad9*$^{CDK1,3,4,6,9A}$, pGEM-Teasy-NT*rad9*$^{CDK1A}$, pGEM-Teasy-NT*rad9*$^{CDK5A}$, pGEM-Teasy-NT*rad9*$^{CDK1,11A}$ and pGEM-Teasy-NT*rad9*$^{CAD\Delta}$ vectors were cloned into the equivalent sites of the pRS306-NT*rad9*$^{CDK1A}$ integrative vector.

For pRS306-*rad9*$^{CDK14,16\text{-}20A}$, the desired mutations were introduced by site--directed mutagenesis of pGEM-Teasy-CT*RAD9* containing a 3300bp fragment of *RAD9* coding for Rad9 C-terminus, from position +1214 within the *RAD9* ORF to position +584 downstream of the *RAD9* ORF. The presence of the desired mutations was

verified by sequencing. The 2.7kb MscI-BstEII fragment from the resulting pGEM-Teasy-*rad9*$^{CDK14,16\text{-}20A}$ vector was cloned into the equivalent sites of the pRS306-CT*RAD9* integrative vector.

***3.6.2.2. Generation of Y2H constructs:***

The Gal4 binding domain ('Bait') vectors pGBKT7-BD-*RAD9*, pGBKT7-BD-*CAD*, pGBKT7-BD-*rad9*$^{CDK1\text{-}9A}$ and pGBKT7-BD-*CHK1* were generated in two steps. In the first step 3930 bp of *RAD9*, 693 bp coding for *CAD*, 1584 bp from *CHK1* and 3930bp *rad9*$^{CDK1\text{-}9A}$ DNA fragments were amplified of the wild type and *rad9*$^{CDK\text{-}9A}$ mutant yeast strains by using specific set of primers (pGBKT7+pGADT7-AD-RAD9F and pGBKT7+pGADT7-AD-RAD9R for RAD9 and rad9CDK1-9A, pGBKT7+pGADT7-AD-RAD9F and pGBKT7+pGADT7-AD-RAD9CADR for CAD region, pGBKT7+pGADT7-AD-CHK1F and pGBKT7+pGADT7-AD-CHK1R for *CHK1*) containing restriction sites NdeI-BamHI (for *RAD9*) or NdeI-EcoRI (for *CHK1*). PCR amplified DNA fragments were cloned into pGBKT7 vector. A similar cloning strategy was used to generate the activation domain ('Prey') vectors pGADT7-AD-*RAD9*, pGADT7-AD-*rad9*$^{CDK1\text{-}9A}$, pGADT7-AD-*CAD* and pGADT7-AD-*CHK1*.

The Bait plasmid used in the triple plasmid based yeast two hybrid assay expresses a LexA-Chk1 fusion protein and was made as follows. The 1584 bp *CHK1* ORF was amplified from wild type yeast genomic DNA using pEG202CHK1F and pEG202CHK1R primers containg the XhoI and NcoI restriction sites. The XhoI/NcoI fragment was ligated into pEG202 vector cut with the same restriciton enzymes. To generated the pJG4-5-*RAD9*, the full length *RAD9* was cloned into pJG4-5 at XhoI cloning site. The pEG202-*CHK1* plasmid DNA was cotransformed with pJG4-5-*RAD9* (Granata et al., 2010) and pSH18-34 plasmid (Gyuris et al., 1993) and the interaction was analysed as described below. The Y2H *RAD9* constructs were sequenced to confirm the desired sequence using specific primers (T7 promoter, Rad9 Seq4, Rad9 Seq6, Rad9 Seq8, Rad9 Seq10, Rad9 Seq12, pGAD-AD-R and pGBK-BD-R). The Y2H *CHK1* constructs were sequenced with primers: T7 promotor, Chk1CD+600NtsF, pGAD-AD-R (for AD-CHK1) and pGBK-BD-R (for BD-CHK1).

#### *3.6.2.3. $CAD^{WT}$ and $CAD^{CDK1-9A}$ expression vectors:*

The pET-$CAD^{WT}$ and pET-$CAD^{CDK1-9A}$ were generated by amplifying a 717bp PCR fragment coding for $CAD^{WT}$ or $CAD^{CDK1-9A}$ (Rad9 residues 1 to 231) from wild-type genomic DNA and pRS306CDK1-9A, respectively, using primers AFG476 and pGBKT7/pGADT7-AD-RAD9CADR. The fragment was digested with NdeI? and BamHI and cloned into pET-15b (Novagen, cat. No. 69661-3) predigested with same restriction enzymes. The pET-$CAD^{WT}$ and pET-$CAD^{CDK1-9A}$ plasmids were transformed in the *E. coli* strain Rosetta2 (Novagen). A 50ml cell culture (O.D=0.8) was treated with 0.4mM IPTG for 4 hours to induce expression of the 10HIS-$CAD^{WT}$ or 10HIS-$CAD^{CDK1-9A}$, and collected by centrifugation. The cell pellet was resuspended in 10 ml of 50mM Tris pH7.5 100mM NaCl and sonicated for one minute at 40% amplitude with 5 seconds pulses and 10 seconds intervals with the Branson Sonifier. The lysed samples were loaded for purification on a 1mL His Trap HP column (GE Healthcare) performed in an ÄKTApurifier machine and eluted by gradually adding 50mM Tris, 100mM NaCl, 500mM Imidazole. 1ml fractions were collected and 15µls of each fraction were loaded onto a 12% SDS-PAGE gel for Coomassie staining analysis. Peak fractions were pulled and glycerol was added to a final concentration of 20%. 10µls aliquots of the 10HIS-CADs (approx. 0.35mg/ml) were frozen down to be used in kinase assay.

### 3.6.3. Cell cycle and checkpoint experiments

#### *3.6.3.1. G1 arrest and release experiment:*

Asynchronous, exponentially growing cells ($5x10^6$ cells/ml) were arrested in G1 by addition of α-factor (5 µg/ml final concentration) for 105 minutes. Following arrest, cells were washed with pre-warmed 0.9% saline, followed by YPD, and then resuspended in fresh YPD without α-factor. $2.5x10^7$ cells were taken at the indicated times for western blot, FACS and budding index analyses as previously described (O'Shaughnessy et al., 2006).

#### *3.6.3.2. CDC mutant experiments:*

Asynchronous, exponentially growing *cdc4-1*, *cdc7-1* and *cdc4-1 sic1Δ* cells were grown at permissive temperature (25°C) and arrested in G1 as above. 1 hour before removal of α-factor the cells were shifted to the restrictive temperature (37°C) and

α-factor removed as above. $2.5x10^7$ cells were taken at the indicated times for western blot and FACS analyses, as previously described (O'Shaughnessy et al., 2006).

***3.6.3.3. Cdc6 experiment:***

Cells in which Cdc6 was either present or absent were released from a late mitotic block (*cdc15-22* cells were grown at 36°C as described in (Cocker et al., 1996). Cells were then examined for Rad9 cell cycle phosphorylation and progression through the cell cycle.

***3.6.3.4. Alpha factor and nocodazole arrest experiments:***

Asynchronous exponentially growing cells ($5x10^6$ cells/ml) were arrested either in G1 with 5μg/ml of α-factor or in G2/M with 10μg/ml of nocodazole (Sigma) for 95 minutes. Cells were kept in α-factor or nocodazole for the duration of the experiment. Cells were divided into two and were either mock treated or treated with the indicated DNA damaging agents. For the IR experiment, both treated and untreated samples were resuspended in fresh media containing nocodazole or α-factor after irradiation. Samples were collected at indicated time points for budding index and checkpoint activation analysis (O'Shaughnessy et al., 2006).

***3.6.3.5. G2/M checkpoint analysis:***

G2/M checkpoint activation analysis was performed as reported (O'Shaughnessy et al., 2006). G2/M synchronised cells were either mock treated or treated with 400Gy, released into medium free of nocodazole but containing α-factor to trap cycling cells in the subsequent G1 phase. Progression through mitosis was then followed by budding index analysis.

***3.6.3.6. Cdc28 dependency of checkpoint initiation and maintenance:***

The role of Cdc28 in the initiation of Chk1 phosphorylation was analysed by arresting cdc28-as1 (analogue sensitive mutant) cells in G2/M with nocodazole. Once arrested, 1-NMPP1 (5μM) was added to half of the culture to inhibit Cdc28 activity. After one cell cycle (90 minutes) cells were split into three and were mock treated or damaged with either bleocin (5μg/ml) or 4-NQO (5μM). Cell samples

were collected at different time points for budding index and western blot analysis.
The role of Cdc28 in the maintenance of Chk1 phosphorylation was analysed by arresting *cdc28-as1* cells with nocodazole. These G2/M arrested cells were mock treated and treated either with bleocin (5µg/ml) or IR (200Gy). After 30 minutes (time 0), 1-NMPP1 (5µM) was added to half of the damaged or undamaged cells to inhibit the Cdc28 activity. Cells were collected at indicated time points after addition of NMPP1 for the budding index and protein profile analysis.

#### *3.6.3.7. CDC phenotype analysis:*

Overnight cultures were grown to a concentration of $5x10^6$ cells/ml. Cultures were divided into two and either mock-treated or irradiated with 200 Gy. Cells were allowed to recover for 3 hours before fixation with 3.7% formaldehyde for 1 hour at room temperature. Cells were subsequently washed with 0.9% saline before imaging. Images were taken with an Axioskop 2 plus microscope (Carl Zeiss MicroImaging, Inc.) coupled to a SPOT Idea 3.0 megapixel digital camera (Diagnostic Instruments, Inc.) and the SPOT software version 4.6.1.3 (Diagnostic Instruments, Inc.). Images were processed using Photoshop and Illustrator software (both Adobe).

### 3.6.4. DNA damaging agents

γ-irradiation (200 or 400 Gy) was carried out using a 137 Cs source at a dose--rate of 12.10 Gy/min (Mainance Engineering, UK). Bleocin (Calbiochem) was used at 0.25 µg/ml for DNA damage sensitivity, 5 µg/ml for checkpoint analyses and 20 µg/ml in the generation of yeast native extracts. 4-NQO (Sigma) was used either at 1.25 µM for DNA damage sensitivity or 5 µM for checkpoint analyses respectively.

DNA damage sensitivity analysis was performed by spotting five-fold serial dilutions ($5x10^6$ to $1x10^4$ cells/ml) of exponentially growing cultures of the indicated strains on plates containing the indicated genotoxic agents or treated as indicated. To analyse the DNA damage sensitivity in G2/M arrested cells, exponentially growing cells were arrested in G2/M (for 95 minutes) and spotted as described on YPD agar media containing 1.25µg/ml of nocodazole with and without DNA damaging agents.

### 3.6.5. Western blotting and Antibodies

Sodium hydroxide protein extracts (Kushnirov, 2000) were separated by sodium

dodecyl sulphate-polyacrylamide gel electrophoresis (SDS-PAGE). Western blotting was performed as previously described (O'Shaughnessy et al., 2006; Vialard et al., 1998). Rad9, Rad53, Swi6, Dpb11-13MYC, Rad9-9MYC and Chk1-3FLAG were resolved in 6.5%, 80/1 acrylamide/bis-acrylamide, SDS-PAGE gel and probed with NLO5 (O'Shaughnessy et al., 2006; Vialard et al., 1998), NLO16 (O'Shaughnessy et al., 2006; Vialard et al., 1998), NLO2 (D. Lee & N. Lowndes, *unpublished*) antibodies at 1:10000 dilution, whereas anti-MYC (9E11, Abcam) and anti-FLAG (M2, Sigma) antibodies were used at 1:1000 dilution in PBS containing 0.1% Tween-20.

Sic1, Clb2, Chk1-3HA and Orc6 were resolved in 10%, 80/1 acrylamide/bis-acrylamide, SDS-PAGE gel and probed with anti-Sic1 (JD156 from J. Diffley), anti-Clb2 (sc9071 from Santa Crutz), anti-HA (12CA5) and anti-Orc6 (SB49 from B. Stillman) antibodies at 1:5000, 1:2000, 1:1000, 1:3000 dilutions respectively, in PBS containing 0.1% Tween-20. HRP conjugated anti-mouse secondary antibody (from Pierce) or anti-rabbit secondary antibody (from Pierce) and Super Signal WestPico chemiluminescent substrate from Thermo Scientific (Product no. 34080) was used to detect the proteins.

### 3.6.6. Yeast two-hybrid analysis:

#### *3.6.6.1. Growth analysis:*

Two-hybrid interactions were assessed by using the Clontech MatchmakerTM Gold Yeast Two-hybrid system (Catalog no 630489). Activation domain vectors (derived from pGADT7-AD) were co-transformed with DNA binding domain vectors (derived from pGBKT7-BD) into the Y2H Gold cells. As a positive control for interaction, co-transformation with pGBKT7-53 and pGADT7-T vectors was performed in Y2H Gold cells. In addition, co-transformation with pGBKT7-Lam and pGADT7-T vectors was performed as a negative control. pGADT7-AD and pGBKT7-BD were also co-transformed either empty or carrying different combinations of bait and prey proteins to discriminate auto--activation events. Protein-protein interaction analysis between different bait and prey proteins was tested by drop test on the SD/-Leu-Trp agar media containing X-alpha-Gal (40mg/ml) and aureobasidin A (125ng/ml) according to the manufacturer's instructions using six independent clones for each vectors combination.

***3.6.6.2. Cdc28-dependent Rad9-Chk1 Y2H interaction analysis:***

A triple plasmids based assay was used to study the Cdc28-dependent interaction between Rad9 and Chk1 protein as described (Granata et al., 2010). Briefly, *cdc28-as1* cells expressing RAD9 prey (pJG4-5-RAD9), CHK1 bait (pEG202-Chk1) as well as having the reporter (pSH18-34) were grown overnight in yeast synthetic media (-Ura, -His, -Trp) with 2% (w/v) raffinose to a concentration of $5x10^6$cells/ml. Cells were arrested either in G1 or in G2/M phase as described above. Cells were divided into two, one half was mock treated and the other half was treated with 5µM 1-NMPP1 for 1.25 hours to inhibit Cdc28. Galactose (2% w/v) was added into the media to induce *RAD9* expression. After 3 hours, a 15ml sample was taken, centrifuged and resuspended in 250 µl of breaking buffer (100mM Tris HCl at pH 8.0, Glycerol 10%; DTT 1mM, 1 tablet of complete Roche antiproteolytic cocktail). Cells were harvested and ß-galactosidase activity assayed. Cells were lysed by using a Fast--Prep cell disruptor; the optical density (OD) of protein extract at 600nm was determined by using the Bio-Rad protein assay reagent. 1ml of Z buffer (60mM $Na_2HPO_4$, 40mM $NaH_2PO_4$, 10mM KCl, 1mM MgSO4, and 50mM ß-mercaptoethanol at pH 7.0) plus ONPG (Ortho 2-Nitrophenyl-ß-D-galactopyranoside) at 4mg/ml was aliquoted in a small glass tube for each sample. 20µl of protein extract was added to each tube and incubated at 37°C until a yellow color developed. The reaction was stopped by adding 400ml of 1M $Na_2CO_3$ and the OD at 420nm of each sample was measured. ß-galactosidase activity was calculated using the formula units = $1x10^3$ $OD_{420}/(OD_{600}$ x reaction time in minutes).

***3.6.6.3. G1 and G2 Yeast Two Hybrid analysis:***

Yeast two hybrid interaction between $Rad9^{CDK1-9}$ and Chk1 was analysed in G2/M or in G1 using the Clontech MatchmakerTM Gold Yeast Two Hybrid System (Catalog no. 630489). Y2H gold cells harboring pGBKT7-$rad9^{CDK1-9A}$ (DNA binding domain vector) and pGADT7-*CHK1* (activation domain vector) plasmid DNA were grown in minimal media (SD/-Leu-Trp). Overnight grown cells (corresponding to OD value 1) were arrested in either G2/M or G1 as described earlier. One ml of cells was centrifuged at 14000 rpm for 3 minutes and supernatant was collected in a fresh tube. The PNP (Para-Nitrophenyl α-D-Galactopyranoside, Sigma Cat no. N0877) assay was performed with the supernatant and α-galactosidase activity was measured according to Clontech Y2H instruction manual.

### 3.6.7. Yeast native extracts and Immunoprecipitations

1.5 liter cultures of yeast strains expressing both tagged Chk1-3FLAG and Dpb11-13MYC proteins under the control of their own endogenous promoters either in a wild type or in *rad9*$^{CDK1\text{-}9A}$ mutant background were grown in YPD medium at a cell density of $1x10^7$ cells/ml. Cells were then arrested in G2/M phase by addition of 20μg/ml of nocodazole (Sigma) and were either mock treated or treated with 20μg/ml of Bleocin (Calbiochem) for 45 minutes. Cells were washed twice with pre-cooled dd$H_2O$ and once in 2x lysis buffer (300 mM KCl, 100mM Hepes pH 7.5, 20% glycerol, 8mM β-mercaptoethanol, 2 mM EDTA, 0.1% Tween20, 0.01% NP-40). Cells were extruded into liquid nitrogen through a syringe and the frozen 'noodles' stored at -80ºC until required. Noodles were manually ground in a mortar in liquid nitrogen. One volume (relative to cells) of 2x lysis buffer, containing a protein inhibitor cocktail (2.8 μM leupeptin, 8 μM pepstatin A, 4 mM PMSF, 8 mM benzamidine, 8 μM antipain, 4 μM chymostatin in ethanol) and phosphatase inhibitors (2 mM sodium fluoride, 1.2mM β-glycerophosphate, 0.04 μM sodium vanadate, 2 mM EGTA, 10 mM sodium pyrophosphate), was added. Cell extract was clarified by a low speed centrifugation followed by additional centrifugation for 1 hour at 42000 rpm in a Beckman Sw55Ti rotor. The clarified crude extract (CCE) was adjusted to 10 mg/ml with 1x lysis buffer in the various immunoprecipitation experiments. 1 ml of CCE was precleared by incubation with 40 μl of 50% (v/v beads/1x lysis buffer) Protein G slurry (GE Healthcare) for 1 hour at 4ºC on a rotating wheel. Pre-cleared supernatants were incubated with either 20 μg of the anti-FLAG Mab M2 (Sigma), 20 μg of the anti-MYC Mab 9E11 (Abcam) or 20 μg of unspecific mouse IgG (Sigma). Samples were incubated for 2 hours at 4ºC on a rotating wheel and centrifuged at 14000 rpm for 15 minutes at 4ºC. 40 μl of 50% protein G slurry (GE Healthcare) were added to the supernatants, incubated on a rotating wheel for 2 hours at 4ºC and recovered by centrifugation. Immunoprecipitated samples were washed four times with 1 ml of lysis buffer containing protease and phosphatase inhibitors. Beads were finally resuspended in 40μl of 3x Laemmli buffer (IP), boiled for 5 minutes and released proteins were separated on 6.5% (80/1 acrylamide/bis-acrylamide) SDS-PAGE gels. Rad9, Chk1-3FLAG and Dpb11-13MYC were analysed as described above.

### 3.6.8. ATP-dependent Release Assay

Yeast cell crude extracts from G2-arrested and bleocin treated YNL1500 cells were prepared as described above. One ml of CCE at 10mg/ml were used to immunoprecipitate Rad9-9MYC with the anti-MYC monoclonal antibody (9E11 from Abcam) as described (Granata et al., 2010). The Rad9-9MYC beads were subjected to an ATP-dependent release assay as detailed (Gilbert et al., 2001), with the following modifications: beads were washed four times with 1ml of 1x lysis buffer containing protease and phosphatase inhibitors (see above) and subsequently washed twice with 1 ml of kinase buffer (25mM HEPES pH7.5, 5mM EGTA, 15mM $MgCl_2$, 15mM KAc, 1x protease and 1x phosphatase inhibitors). The beads were resuspended in 60µl of kinase buffer alone or kinase buffer containing either 10mM ATP (BioLabs) or non-hydrolysable γS-ATP (Sigma). After 45 minutes of incubation at 25oC, the elution fractions (containing released proteins) were carefully removed from the beads. Elutions and boiled beads were analysed on a 6.5%, 80/1 acrylamide/bisacrylamide SDS-PAGE gel. Rad9-9MYC, Chk1-3FLAG and Rad53 were analysed by western blotting as described above.

### 3.6.9. Rad9 dephosphorylation Assay

Yeast cell crude extracts from asynchronous W303 cells were prepared as described above and diluted to 1mg/ml total protein concentration. 500µg of total protein were subjected to immunoprecipitation as described above with the following modifications. Ten microliters of 50% (v/v beads/1x lysis buffer) Protein A slurry (GE Healthcare) were used to pre-clear the cell crude extracts and added to the supernatants after incubation with 2.5µg of NLO5 polyclonal antibody (O'Shaughnessy et al., 2006; Vialard et al., 1998) to immunoprecipitate Rad9. Immunoprecipitated samples were washed four times with 1 ml of lysis buffer containing protease inhibitors as above. Beads containing Rad9 were incubated in 1x λ-protein phosphatase buffer (New England Biolabs) and 2 mM $MnCl_2$ (New England Biolabs) containing 200 U of protein phosphatase (New England Biolabs) for 20 minutes at 30°C. The phosphatase inhibitor sodium orthovanadate (Sigma) was added to one reaction at the final concentration of 2.5mM. Phosphatase reactions were stopped by adding 20µl of 3x Laemmli sample buffer (125 mM Tris pH 6.8, 4% SDS, 10% β-mercaptoethanol, 20% glycerol, 0.002% bromophenol

blue) and incubation at 95°C for 5 minutes. Rad9 profile was analysed by western blot as described above.

### 3.6.10. Tandem Affinity Purification (TAP)

The TAP method was applied for purification of cyclin-Cdk1 complexes (Clb5-TAP-Cdk1, Clb3-TAP-Cdk1 and Clb2-TAP-Cdk1) as described previously (Puig et al., 2001; Ubersax et al., 2003). All steps were performed at 4°C, unless otherwise stated. TAP-Clb purification was performed on 2-4 liters of yeast culture. Large Scale Native (LSN) yeast extract were poured into a 50ml tube containing 200-400µl of pre-equilibrated IgG Sepharose 50% beads slurry (Amersham) and rotated 30 min at 4°C. The beads were centrifuged at 1000g for 3 min and were transferred to a 5 ml gravity flow column (Pierce). Once the bead bed was formed, the supernatant (lysate) was loaded over the column and the Flow Through (FT) fraction collected for western blot analysis. The beads were first washed with 30ml of IPP150 buffer (25mM HEPES-HCl pH8.0, 150mM NaCl, 0.1% NP-40) followed by a second wash with 10ml of TEV cleavage buffer (25mM HEPES-HCl pH8.0, 150mM NaCl, 0.1% NP-40, 0.5mM EDTA, 1mM DTT). The column was rotated for 15min at 23°C in 1ml TEV cleavage buffer. The column was drained and cleavage of the TEV site was performed by adding 1ml of TEV buffer containing 100 units of AcTEV protease (Invitrogen) by rotating the column for 30min at 23°C. The elution fraction was then recovered by gravity flow. 1mM MgAc, 1mM imidazole and 5mM $CaCl_2$ was added to the 1ml eluation fraction. This was then transferred into a new column containing 100-200µls of calmodulin binding beads (CBB, Stratagene) pre-equilibrated with 10ml of IPP150 calmodulin binding buffer (10mM β-mercaptoethanol, 25mM HEPES-HCl PH8.0, 150mM NaCl, 1mM MgAc, 1mM imidazole, 2mM $CaCl_2$, 0.1% NP-40) and rotated for 1h at 4°C. The entire content of column was then poured into a 5 ml by gravity flow column and the FT fraction collected for western blot analysis. The beads were washed with 30ml of IPP150 calmodulin binding buffer. Ten fractions of 200µls were then eluted with IPP150 calmodulin elution buffer (10mM β-mercaptoethanol, 25mM HEPES-HCl PH8.0, 150mM NaCl, 1mM MgAc, 1mM imidazole, 2mM EGTA, 0.1% NP-40). 10µls of each fraction and 40µls of FT samples were loaded onto a 12% SDS-PAGE gel and analysed by Silver and Coomassie staining. Peak fractions were pulled and 15µls aliquots were frozen down to be used in kinase assay.

### 3.6.11. HA Purification

3HA-Cln2-Cdk1 was purified according to published protocols (McCusker et al., 2007) using the 12CA5 Monoclonal antibody. Large Scale Native yeast extract were prepared from a 3L of 3HA-Cln2-Cdk1 cell culture and gently rotated with 500µls of anti-HA beads, prepared as described (McCusker et al., 2007), for 2 hr at 4°C. The beads were pelleted by brief centrifugation, washed twice with 15ml of lysis buffer (50mM HEPES pH7.4, 175mM KCl, 1mM EGTA, 1mM $MgCl_2$, 0.45% Tween, 5% Glycerol) and then transferred to a 5 ml gravity flow column (Pierce). The column was washed with 5ml of lysis buffer and then with 1ml of elution buffer (50mM HEPES pH7.4, 150mM KCl, 1mM EGTA, 1mM MgCl2, 0.05% Tween, 5% Glycerol). The column was transferred to room temperature and 250µl of elution buffer containing 1mg/ml HA tripeptide (Sigma) was added. After 15 min incubation, the elution fraction was collected. This step was repeated for a total of 8 fractions. 10µls of each fraction was loaded onto a 12% SDS-PAGE gel and analysed by Silver and Coomassie stainings. Peak fractions were pulled and 15µls aliquots were frozen down to be used in kinase assay.

### 3.6.12. Cdc28 Kinase assays

Kinase assays were performed as previously described (Koivomagi et al., 2011). For the steady-state kinetics, the initial velocity conditions were defined as an initial substrate turnover ranging up to 10% of the total turnover. This was estimated by a long-term incubation (30 and 60 minutes) with excess amounts of cyclin-Cdc28 (13nM) in the standard reaction mixture given below. Amounts of active cyclin-Cdc28 complexes were normalized and equalized considering the specificity constants of each cyclin-Cdc28 for H1 phosphorylation, model substrate for Cdc28 (values are: Cln2 1.394; Clb5 0.605; Clb3 2.237; Clb2 4.9; Koivomagi et al., 2011). The final adjusted kinase assay was performed in 20µls volume containing 2µM of H1 (Sigma), $CAD^{WT}$ or $CAD^{CDK1\text{-}9A}$ and about 0.1-1 nM of purified cyclin-Cdc28 complex. The basal composition of the assay mixture contained 50 mM Hepes pH 7.4, 100 mM NaCl, 0.2 mg/ml BSA, 1mM DTT, 500nM Cks1, and 100 µM ATP, 0.5µCi $^{32}$P-γ-ATP (6000Ci/mmol, Perkin Elmer). The reactions were incubated at room temperature and reaction aliquots were taken at two time points (8 and 16 min). In Figure 3.2E it is shown the 16min time point. The reactions were stopped by adding 5µls of 4x SDS-PAGE sample buffer and loaded on a 12% SDS-PAGE gel.

The gel was stained with Coomassie and then air dried over night.

## 3.7. REFERENCES


Albuquerque, C.P., Smolka, M.B., Payne, S.H., Bafna, V., Eng, J., and Zhou, H. (2008). A multidimensional chromatography technology for in-depth phosphoproteome analysis. Mol Cell Proteomics *7*, 1389-1396.

Alderton, G.K., Galbiati, L., Griffith, E., Surinya, K.H., Neitzel, H., Jackson, A.P., Jeggo, P.A., and O'Driscoll, M. (2006). Regulation of mitotic entry by microcephalin and its overlap with ATR signalling. Nat Cell Biol *8*, 725-733.

Barbour, L., Ball, L.G., Zhang, K., and Xiao, W. (2006). DNA damage checkpoints are involved in postreplication repair. Genetics *174*, 1789-1800.

Barlow, J.H., Lisby, M., and Rothstein, R. (2008). Differential regulation of the cellular response to DNA double-strand breaks in G1. Mol Cell *30*, 73-85.

Bishop, A.C., Ubersax, J.A., Petsch, D.T., Matheos, D.P., Gray, N.S., Blethrow, J., Shimizu, E., Tsien, J.Z., Schultz, P.G., Rose, M.D*., et al.* (2000). A chemical switch for inhibitor-sensitive alleles of any protein kinase. Nature *407*, 395-401.

Blankley, R.T., and Lydall, D. (2004). A domain of Rad9 specifically required for activation of Chk1 in budding yeast. J Cell Sci *117*, 601-608.

Bonilla, C.Y., Melo, J.A., and Toczyski, D.P. (2008). Colocalization of sensors is sufficient to activate the DNA damage checkpoint in the absence of damage. Mol Cell *30*, 267-276.

Chen, Y., Caldwell, J.M., Pereira, E., Baker, R.W., and Sanchez, Y. (2009). ATRMec1 phosphorylation-independent activation of Chk1 in vivo. J Biol Chem *284*, 182-190.

Clerici, M., Baldo, V., Mantiero, D., Lottersberger, F., Lucchini, G., and Longhese, M.P. (2004). A Tel1/MRX-dependent checkpoint inhibits the metaphase-to-anaphase transition after UV irradiation in the absence of Mec1. Mol Cell Biol *24*, 10126-10144.

Cobb, J.A., Shimada, K., and Gasser, S.M. (2004). Redundancy, insult-specific sensors and thresholds: unlocking the S-phase checkpoint response. Curr Opin Genet Dev *14*, 292-300.

Cocker, J.H., Piatti, S., Santocanale, C., Nasmyth, K., and Diffley, J.F. (1996). An essential role for the Cdc6 protein in forming the pre-replicative complexes of budding yeast. Nature *379*, 180-182.

Cortez, D., Wang, Y., Qin, J., and Elledge, S.J. (1999). Requirement of ATM-dependent phosphorylation of brca1 in the DNA damage response to double-strand breaks. Science *286*, 1162-1166.

Critchlow, S.E., and Jackson, S.P. (1998). DNA end-joining: from yeast to man. Trends Biochem Sci *23*, 394-398.

de la Torre-Ruiz, M., and Lowndes, N.F. (2000). The Saccharomyces cerevisiae DNA damage checkpoint is required for efficient repair of double strand breaks by non-homologous end joining. FEBS Lett *467*, 311-315.

Diani, L., Colombelli, C., Nachimuthu, B.T., Donnianni, R., Plevani, P., Muzi-Falconi, M., and Pellicioli, A. (2009). Saccharomyces CDK1 phosphorylates Rad53 kinase in metaphase, influencing cellular morphogenesis. J Biol Chem *284*, 32627-32634.

Emili, A. (1998). MEC1-dependent phosphorylation of Rad9p in response to DNA damage. Mol Cell *2*, 183-189.

Enserink, J.M., and Kolodner, R.D. (2010). An overview of Cdk1-controlled targets and processes. Cell Div *5*, 11.

Esashi, F., and Yanagida, M. (1999). Cdc2 phosphorylation of Crb2 is required for reestablishing cell cycle progression after the damage checkpoint. Mol Cell *4*, 167-174.

Finn, K., Lowndes, N.F., and Grenon, M. (2011). Eukaryotic DNA damage checkpoint activation in response to double-strand breaks. Cell Mol Life Sci.

FitzGerald, J.E., Grenon, M., and Lowndes, N.F. (2009). 53BP1: function and mechanisms of focal recruitment. Biochem Soc Trans *37*, 897-904.

Gardner, R., Putnam, C.W., and Weinert, T. (1999). RAD53, DUN1 and PDS1 define two parallel G2/M checkpoint pathways in budding yeast. EMBO J *18*, 3173-3185.

Gelbart, M.E., Rechsteiner, T., Richmond, T.J., and Tsukiyama, T. (2001). Interactions of Isw2 chromatin remodeling complex with nucleosomal arrays: analyses using recombinant yeast histones and immobilized templates. Mol Cell Biol *21*, 2098-2106.

Giannattasio, M., Sommariva, E., Vercillo, R., Lippi-Boncambi, F., Liberi, G., Foiani, M., Plevani, P., and Muzi-Falconi, M. (2002). A dominant-negative MEC3 mutant uncovers new functions for the Rad17 complex and Tel1. Proc Natl Acad Sci U S A *99*, 12997-13002.

Gilbert, C.S., Green, C.M., and Lowndes, N.F. (2001). Budding yeast Rad9 is an ATP-dependent Rad53 activating machine. Mol Cell *8*, 129-136.

Gilbert, C.S., van den Bosch, M., Green, C.M., Vialard, J.E., Grenon, M., Erdjument-Bromage, H., Tempst, P., and Lowndes, N.F. (2003). The budding yeast Rad9 checkpoint complex: chaperone proteins are required for its function. EMBO Rep *4*, 953-958.

Goldberg, M., Stucki, M., Falck, J., D'Amours, D., Rahman, D., Pappin, D., Bartek, J., and Jackson, S.P. (2003). MDC1 is required for the intra-S-phase DNA damage checkpoint. Nature *421*, 952-956.

Granata, M., Lazzaro, F., Novarina, D., Panigada, D., Puddu, F., Abreu, C.M., Kumar, R., Grenon, M., Lowndes, N.F., Plevani, P.*, et al.* (2010). Dynamics of Rad9 chromatin binding and checkpoint function are mediated by its dimerization and are cell cycle-regulated by CDK1 activity. PLoS Genet *6*.

Grenon, M., Costelloe, T., Jimeno, S., O'Shaughnessy, A., Fitzgerald, J., Zgheib, O., Degerth, L., and Lowndes, N.F. (2007). Docking onto chromatin via the Saccharomyces cerevisiae Rad9 Tudor domain. Yeast *24*, 105-119.

Grenon, M., Gilbert, C., and Lowndes, N.F. (2001). Checkpoint activation in response to double-strand breaks requires the Mre11/Rad50/Xrs2 complex. Nat Cell Biol *3*, 844-847.

Gyuris, J., Golemis, E., Chertkov, H., and Brent, R. (1993). Cdi1, a human G1 and S phase protein phosphatase that associates with Cdk2. Cell *75*, 791-803.

Halazonetis, T.D., Gorgoulis, V.G., and Bartek, J. (2008). An oncogene-induced DNA damage model for cancer development. Science *319*, 1352-1355.

Hammet, A., Magill, C., Heierhorst, J., and Jackson, S.P. (2007). Rad9 BRCT domain interaction with phosphorylated H2AX regulates the G1 checkpoint in budding yeast. EMBO Rep *8*, 851-857.

Harper, J.W., and Elledge, S.J. (2007). The DNA damage response: ten years after. Mol Cell *28*, 739-745.

Holt, L.J., Tuch, B.B., Villen, J., Johnson, A.D., Gygi, S.P., and Morgan, D.O. (2009). Global analysis of Cdk1 substrate phosphorylation sites provides insights into evolution. Science *325*, 1682-1686.

Huertas, P., Cortes-Ledesma, F., Sartori, A.A., Aguilera, A., and Jackson, S.P. (2008). CDK targets Sae2 to control DNA-end resection and homologous recombination. Nature *455*, 689-692.

Ira, G., Pellicioli, A., Balijja, A., Wang, X., Fiorani, S., Carotenuto, W., Liberi, G., Bressan, D., Wan, L., Hollingsworth, N.M.*, et al.* (2004). DNA end resection, homologous recombination and DNA damage checkpoint activation require CDK1. Nature *431*, 1011-1017.

Johnson, N., Cai, D., Kennedy, R.D., Pathania, S., Arora, M., Li, Y.C., D'Andrea, A.D., Parvin, J.D., and Shapiro, G.I. (2009). Cdk1 participates in BRCA1-dependent S phase checkpoint control in response to DNA damage. Mol Cell *35*, 327-339.

Jullien, D., Vagnarelli, P., Earnshaw, W.C., and Adachi, Y. (2002). Kinetochore localisation of the DNA damage response component 53BP1 during mitosis. J Cell Sci *115*, 71-79.

Jungmichel, S., and Stucki, M. (2010). MDC1: The art of keeping things in focus. Chromosoma *119*, 337-349.

Koivomagi, M., Valk, E., Venta, R., Iofik, A., Lepiku, M., Morgan, D.O., and Loog, M. (2011). Dynamics of Cdk1 substrate specificity during the cell cycle. Mol Cell *42*, 610-623.

Kushnirov, V.V. (2000). Rapid and reliable protein extraction from yeast. Yeast *16*, 857-860.

Lazzaro, F., Sapountzi, V., Granata, M., Pellicioli, A., Vaze, M., Haber, J.E., Plevani, P., Lydall, D., and Muzi-Falconi, M. (2008). Histone methyltransferase Dot1 and Rad9 inhibit single-stranded DNA accumulation at DSBs and uncapped telomeres. EMBO J *27*, 1502-1512.

Li, X., and Cai, M. (1997). Inactivation of the cyclin-dependent kinase Cdc28 abrogates cell cycle arrest induced by DNA damage and disassembly of mitotic spindles in Saccharomyces cerevisiae. Mol Cell Biol *17*, 2723-2734.

Liang, C., and Stillman, B. (1997). Persistent initiation of DNA replication and chromatin-bound MCM proteins during the cell cycle in cdc6 mutants. Genes Dev *11*, 3375-3386.

Limbo, O., Chahwan, C., Yamada, Y., de Bruin, R.A., Wittenberg, C., and Russell, P. (2007). Ctp1 is a cell-cycle-regulated protein that functions with Mre11 complex to control double-strand break repair by homologous recombination. Mol Cell *28*, 134-146.

Lindsey-Boltz, L.A., Sercin, O., Choi, J.H., and Sancar, A. (2009). Reconstitution of human claspin-mediated phosphorylation of Chk1 by the ATR (ataxia telangiectasia-mutated and rad3-related) checkpoint kinase. J Biol Chem *284*, 33107-33114.

Loog, M., and Morgan, D.O. (2005). Cyclin specificity in the phosphorylation of cyclin-dependent kinase substrates. Nature *434*, 104-108.

Lou, Z., Minter-Dykhouse, K., Wu, X., and Chen, J. (2003). MDC1 is coupled to activated CHK2 in mammalian DNA damage response pathways. Nature *421*, 957-961.

Lovejoy, C.A., and Cortez, D. (2009). Common mechanisms of PIKK regulation. DNA Repair (Amst) *8*, 1004-1008.

Lydall, D., and Weinert, T. (1997). Use of cdc13-1-induced DNA damage to study effects of checkpoint genes on DNA damage processing. Methods Enzymol *283*, 410-424.

Majka, J., and Burgers, P.M. (2007). Clamping the Mec1/ATR checkpoint kinase into action. Cell Cycle *6*, 1157-1160.

McCusker, D., Denison, C., Anderson, S., Egelhofer, T.A., Yates, J.R., 3rd, Gygi, S.P., and Kellogg, D.R. (2007). Cdk1 coordinates cell-surface growth with the cell cycle. Nat Cell Biol *9*, 506-515.

Mochida, S., Esashi, F., Aono, N., Tamai, K., O'Connell, M.J., and Yanagida, M. (2004). Regulation of checkpoint kinases through dynamic interaction with Crb2. EMBO J *23*, 418-428.

Moses, A.M., Liku, M.E., Li, J.J., and Durbin, R. (2007). Regulatory evolution in proteins by turnover and lineage-specific changes of cyclin-dependent kinase consensus sites. Proc Natl Acad Sci U S A *104*, 17713-17718.

Murakami-Sekimata, A., Huang, D., Piening, B.D., Bangur, C., and Paulovich, A.G. (2010). The Saccharomyces cerevisiae RAD9, RAD17 and RAD24 genes are required for suppression of mutagenic post-replicative repair during chronic DNA damage. DNA Repair (Amst) *9*, 824-834.

Nash, P., Tang, X., Orlicky, S., Chen, Q., Gertler, F.B., Mendenhall, M.D., Sicheri, F., Pawson, T., and Tyers, M. (2001). Multisite phosphorylation of a CDK inhibitor sets a threshold for the onset of DNA replication. Nature *414*, 514-521.

Navadgi-Patil, V.M., and Burgers, P.M. (2009a). A tale of two tails: activation of DNA damage checkpoint kinase Mec1/ATR by the 9-1-1 clamp and by Dpb11/TopBP1. DNA Repair (Amst) *8*, 996-1003.

Navadgi-Patil, V.M., and Burgers, P.M. (2009b). The unstructured C-terminal tail of the 9-1-1 clamp subunit Ddc1 activates Mec1/ATR via two distinct mechanisms. Mol Cell *36*, 743-753.

O'Donovan, P.J., and Livingston, D.M. (2010). BRCA1 and BRCA2: breast/ovarian cancer susceptibility gene products and participants in DNA double-strand break repair. Carcinogenesis *31*, 961-967.

O'Shaughnessy, A.M., Grenon, M., Gilbert, C., Toh, G.W., Green, C.M., and Lowndes, N.F. (2006). Multiple approaches to study S. cerevisiae Rad9, a prototypical checkpoint protein. Methods Enzymol *409*, 131-150.

Pellicioli, A., and Foiani, M. (2005). Signal transduction: how rad53 kinase is activated. Curr Biol *15*, R769-771.

Pfander, B., and Diffley, J.F. (2011). Dpb11 coordinates Mec1 kinase activation with cell cycle-regulated Rad9 recruitment. EMBO J *30*, 4897-4907.

Piatti, S., Bohm, T., Cocker, J.H., Diffley, J.F., and Nasmyth, K. (1996). Activation of S-phase-promoting CDKs in late G1 defines a "point of no return" after which Cdc6 synthesis cannot promote DNA replication in yeast. Genes Dev *10*, 1516-1531.

Puddu, F., Granata, M., Di Nola, L., Balestrini, A., Piergiovanni, G., Lazzaro, F., Giannattasio, M., Plevani, P., and Muzi-Falconi, M. (2008). Phosphorylation of the budding yeast 9-1-1 complex is required for Dpb11 function in the full activation of the UV-induced DNA damage checkpoint. Mol Cell Biol *28*, 4782-4793.

Puig, O., Caspary, F., Rigaut, G., Rutz, B., Bouveret, E., Bragado-Nilsson, E., Wilm, M., and Seraphin, B. (2001). The tandem affinity purification (TAP) method: a general procedure of protein complex purification. Methods *24*, 218-229.

Rappold, I., Iwabuchi, K., Date, T., and Chen, J. (2001). Tumor suppressor p53 binding protein 1 (53BP1) is involved in DNA damage-signaling pathways. J Cell Biol *153*, 613-620.

Ruffner, H., Jiang, W., Craig, A.G., Hunter, T., and Verma, I.M. (1999). BRCA1 is phosphorylated at serine 1497 in vivo at a cyclin-dependent kinase 2 phosphorylation site. Mol Cell Biol *19*, 4843-4854.

Ruffner, H., and Verma, I.M. (1997). BRCA1 is a cell cycle-regulated nuclear phosphoprotein. Proc Natl Acad Sci U S A *94*, 7138-7143.

Saka, Y., Esashi, F., Matsusaka, T., Mochida, S., and Yanagida, M. (1997). Damage and replication checkpoint control in fission yeast is ensured by interactions of Crb2, a protein with BRCT motif, with Cut5 and Chk1. Genes Dev *11*, 3387-3400.

Sanchez, Y., Bachant, J., Wang, H., Hu, F., Liu, D., Tetzlaff, M., and Elledge, S.J. (1999). Control of the DNA damage checkpoint by chk1 and rad53 protein kinases through distinct mechanisms. Science *286*, 1166-1171.

Sanchez, Y., Desany, B.A., Jones, W.J., Liu, Q., Wang, B., and Elledge, S.J. (1996). Regulation of RAD53 by the ATM-like kinases MEC1 and TEL1 in yeast cell cycle checkpoint pathways. Science *271*, 357-360.

Schwartz, M.F., Duong, J.K., Sun, Z., Morrow, J.S., Pradhan, D., and Stern, D.F. (2002). Rad9 phosphorylation sites couple Rad53 to the Saccharomyces cerevisiae DNA damage checkpoint. Mol Cell *9*, 1055-1065.

Schwob, E., Bohm, T., Mendenhall, M.D., and Nasmyth, K. (1994). The B-type cyclin kinase inhibitor p40SIC1 controls the G1 to S transition in S. cerevisiae. Cell *79*, 233-244.

Shimada, K., Pasero, P., and Gasser, S.M. (2002). ORC and the intra-S-phase checkpoint: a threshold regulates Rad53p activation in S phase. Genes Dev *16*, 3236-3252.

Smits, V.A., Warmerdam, D.O., Martin, Y., and Freire, R. (2010). Mechanisms of ATR-mediated checkpoint signalling. Front Biosci *15*, 840-853.

Smolka, M.B., Albuquerque, C.P., Chen, S.H., Schmidt, K.H., Wei, X.X., Kolodner, R.D., and Zhou, H. (2005). Dynamic changes in protein-protein interaction and protein phosphorylation probed with amine-reactive isotope tag. Mol Cell Proteomics *4*, 1358-1369.

Stracker, T.H., Usui, T., and Petrini, J.H. (2009a). Taking the time to make important decisions: the checkpoint effector kinases Chk1 and Chk2 and the DNA damage response. DNA Repair (Amst) *8*, 1047-1054.

Stracker, T.H., Williams, B.R., Deriano, L., Theunissen, J.W., Adelman, C.A., Roth, D.B., and Petrini, J.H. (2009b). Artemis and nonhomologous end joining-independent influence of DNA-dependent protein kinase catalytic subunit on chromosome stability. Mol Cell Biol *29*, 503-514.

Sun, Z., Fay, D.S., Marini, F., Foiani, M., and Stern, D.F. (1996). Spk1/Rad53 is regulated by Mec1-dependent protein phosphorylation in DNA replication and damage checkpoint pathways. Genes Dev *10*, 395-406.

Sweeney, F.D., Yang, F., Chi, A., Shabanowitz, J., Hunt, D.F., and Durocher, D. (2005). Saccharomyces cerevisiae Rad9 acts as a Mec1 adaptor to allow Rad53 activation. Curr Biol *15*, 1364-1375.

Tanaka, K. (2010). Multiple functions of the S-phase checkpoint mediator. Biosci Biotechnol Biochem *74*, 2367-2373.

Tapia-Alveal, C., Calonge, T.M., and O'Connell, M.J. (2009). Regulation of chk1. Cell Div *4*, 8.

Toh, G.W., and Lowndes, N.F. (2003). Role of the Saccharomyces cerevisiae Rad9 protein in sensing and responding to DNA damage. Biochem Soc Trans *31*, 242-246.

Toh, G.W., O'Shaughnessy, A.M., Jimeno, S., Dobbie, I.M., Grenon, M., Maffini, S., O'Rorke, A., and Lowndes, N.F. (2006). Histone H2A phosphorylation and H3 methylation are required for a novel Rad9 DSB repair function following checkpoint activation. DNA Repair (Amst) *5*, 693-703.

Ubersax, J.A., Woodbury, E.L., Quang, P.N., Paraz, M., Blethrow, J.D., Shah, K., Shokat, K.M., and Morgan, D.O. (2003). Targets of the cyclin-dependent kinase Cdk1. Nature *425*, 859-864.

Uetz, P., Giot, L., Cagney, G., Mansfield, T.A., Judson, R.S., Knight, J.R., Lockshon, D., Narayan, V., Srinivasan, M., Pochart, P*., et al.* (2000). A comprehensive analysis of protein-protein interactions in Saccharomyces cerevisiae. Nature *403*, 623-627.

Usui, T., Foster, S.S., and Petrini, J.H. (2009). Maintenance of the DNA-damage checkpoint requires DNA-damage-induced mediator protein oligomerization. Mol Cell *33*, 147-159.

van Vugt, M.A., Gardino, A.K., Linding, R., Ostheimer, G.J., Reinhardt, H.C., Ong, S.E., Tan, C.S., Miao, H., Keezer, S.M., Li, J*., et al.* (2010). A mitotic phosphorylation feedback network connects Cdk1, Plk1, 53BP1, and Chk2 to inactivate the G(2)/M DNA damage checkpoint. PLoS Biol *8*, e1000287.

Vialard, J.E., Gilbert, C.S., Green, C.M., and Lowndes, N.F. (1998). The budding yeast Rad9 checkpoint protein is subjected to Mec1/Tel1-dependent hyperphosphorylation and interacts with Rad53 after DNA damage. EMBO J *17*, 5679-5688.

Weinert, T.A., and Hartwell, L.H. (1988). The RAD9 gene controls the cell cycle response to DNA damage in Saccharomyces cerevisiae. Science *241*, 317-322.

Wohlbold, L., and Fisher, R.P. (2009). Behind the wheel and under the hood: functions of cyclin-dependent kinases in response to DNA damage. DNA Repair (Amst) *8*, 1018-1024.

Xia, Z., Morales, J.C., Dunphy, W.G., and Carpenter, P.B. (2001). Negative cell cycle regulation and DNA damage-inducible phosphorylation of the BRCT protein 53BP1. J Biol Chem *276*, 2708-2718.

Xu, N., Libertini, S., Black, E.J., Lao, Y., Hegarat, N., Walker, M., and Gillespie, D.A. (2012). Cdk-mediated phosphorylation of Chk1 is required for efficient activation and full checkpoint proficiency in response to DNA damage. Oncogene *31*, 1086-1094.

Xu, N., Libertini, S., Zhang, Y., and Gillespie, D.A. (2011). Cdk phosphorylation of Chk1 regulates efficient Chk1 activation and multiple checkpoint proficiency. Biochem Biophys Res Commun *413*, 465-470.

Xu, X., and Stern, D.F. (2003). NFBD1/MDC1 regulates ionizing radiation-induced focus formation by DNA checkpoint signaling and repair factors. FASEB J *17*, 1842-1848.

Zhou, B.B., and Elledge, S.J. (2000). The DNA damage response: putting checkpoints in perspective. Nature *408*, 433-439.

## 3.8. SUPPLEMENTAL INFORMATION

### 3.8.1. Inventory

**Supplemental Figures (pages 157 to 162)**

**Figure S3.1**, related to Figure 3.1: Cell cycle phosphorylation of Rad9 is not dependent on DNA replication structures but on multiple potential CDK phosphorylation sites in Rad9.

**Figure S3.2**, related to Figure 3.3: The CDK1-9 sites or multiple combinations of these sites within the CAD region of Rad9 are specifically required for DNA damage-induced Chk1 activation in the G2/M phase; but not for damage-induced Rad9 and Rad53 phosphorylations.

**Figure S3.3**, related to Figure 3.4: Cdc28 activity is required for initiation and maintenance of IR-induced Chk1 activation in G2/M cells.

**Figure S3.4**, related to Figure 3.5: Yeast-two hybrid interaction analysis in G1 and G2/M cells and protein expression in respective Y2H clones. DNA damage sensitivity analysis in clones used for co-imunoprecipitation experiments.

**Figure S3.5,** related to Figure 3.6: Cross-species Rad9 alignments suggest conserved consensus CDK phospho-sites within the CAD domains.

**Supplemental Tables (pages 163-167)**

### 3.8.2. Supplemental Figures

***Figure S3.1***

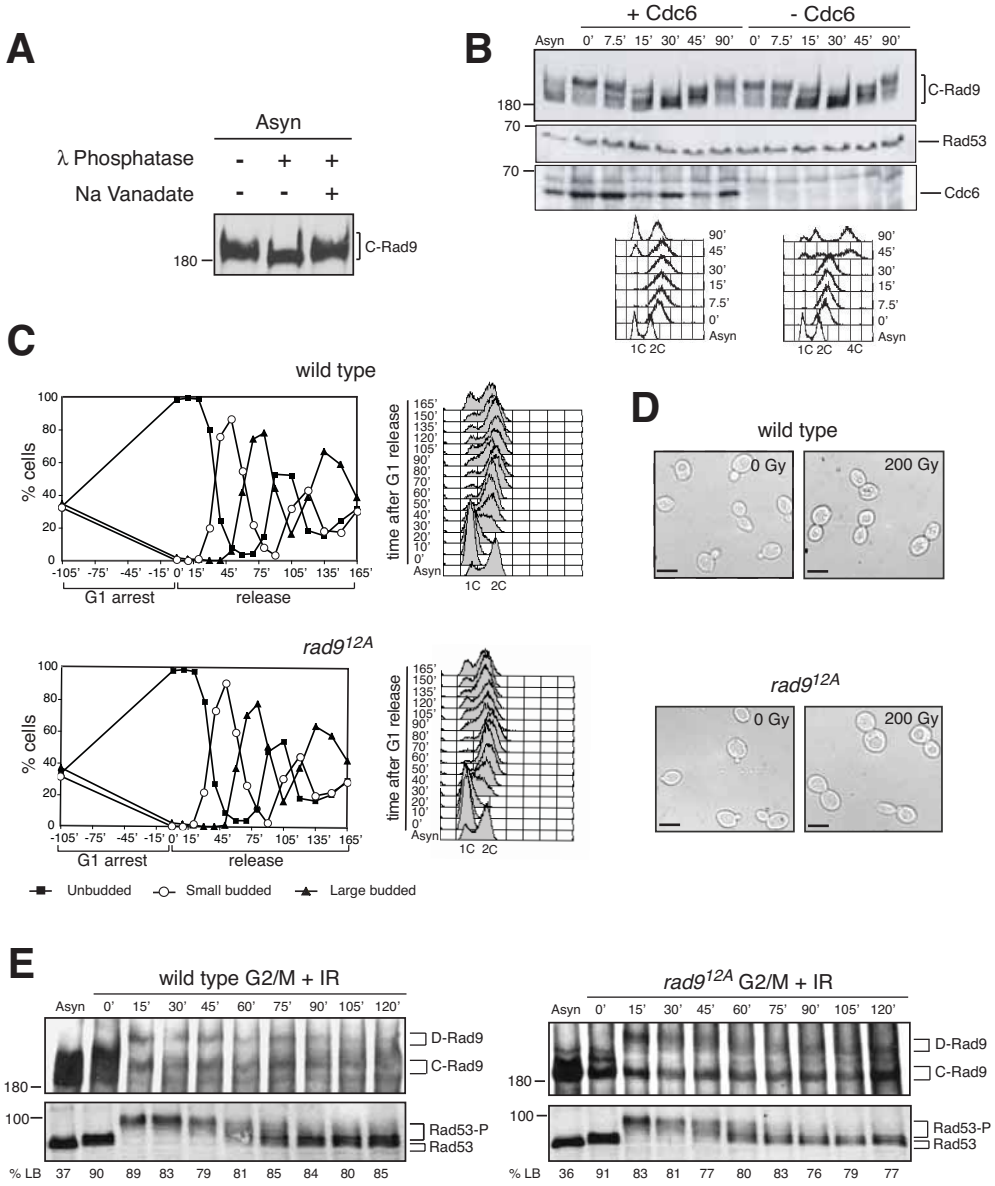


**Figure S3.1**, related to Figure 3.1. (A) Rad9 is phosphorylated in asynchronous cells in absence of DNA damage. The slow migrating forms of Rad9 caused by cell cycle phosphorylation disappear in response to λ phosphatase treatment. (B) Rad9 phosphorylation is independent from the initiation of DNA synthesis. Cell cycle phosphorylation of Rad9 was examined in a cell cycle engineered to bypass S phase, by manipulating the level of the Cdc6 replication protein. In the absence of Cdc6 cells undergo a haploid mitosis in which the monovalent chromosomes are randomly segregated to either pole. Cells in which Cdc6 was either present or absent were released from a late mitotic block (the *cdc15-2*2 mutation at 36°C) (Cocker et al., 1996) and examined for Rad9 cell cycle phosphorylation and progression through the cell cycle. Rad9 was normally phosphorylated irrespective of whether DNA synthesis took place or not. Thus, although Rad9 phosphorylation during cell cycle progression is dependent upon Clb-Cdc28, it is independent of DNA structures generated during a normal S phase. (C) Mutations of 12 putative CDK phosphorylation sites of Rad9 do not affect cell cycle progression as indicated by budding index and FACS analyses. (D) Lack of Rad9 cell cycle phosphorylation in *rad9*$^{12A}$ cells does not result in checkpoint arrest in the absence of exogenous DNA damage. Representative images are shown. Scale bar is 10 μm. The percentage large

budded cells were as follows: wild type + 0 Gy = 35%; wild type +200 Gy = 73%; *rad9*$^{CDK1\text{-}9}$ + 0 Gy = 37%; *rad9*$^{CDK1\text{-}9}$ +200 Gy = 74%. (E) G2/M arrested *rad9*$^{12A}$ cells are proficient for DNA damage induced phosphoryation of Rad9 and Rad53 in response to IR.

## *Figure S3.2*

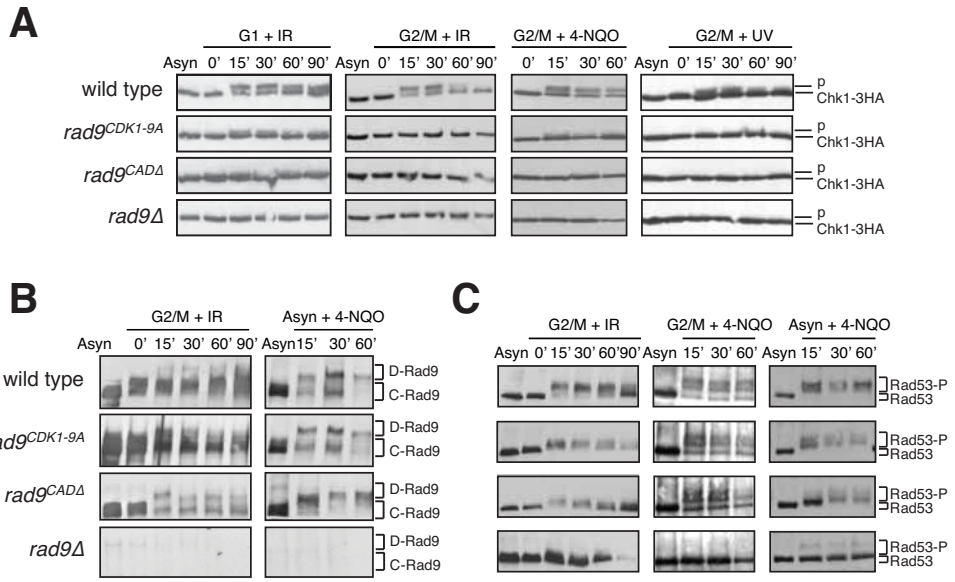


**Figure S3.2**, related to Figure 3.3**.** (A) IR, 4NQO or UV induced Chk1 phosphorylation is abolished in nocodazole arrested *rad9*$^{CDK1\text{-}9A}$, *rad9*$^{CAD}$ and *rad9Δ* cells, but there is residual Chk1 activation partially dependent on the CDK1-9 sites in G1-arrested cells. (B) Rad9 DNA damage induced phosphorylation is not dependent on the CDK1-9 sites in G2/M-arrested cells after IR and in asynchronously growing cells after 4-NQO. (C) Rad53 DNA damage induced phosphorylation is not dependent on the CDK1-9 sites in G2-arrested cells after IR or 4-NQO and in asynchronous cells after 4-NQO.

***Figure S3.3***

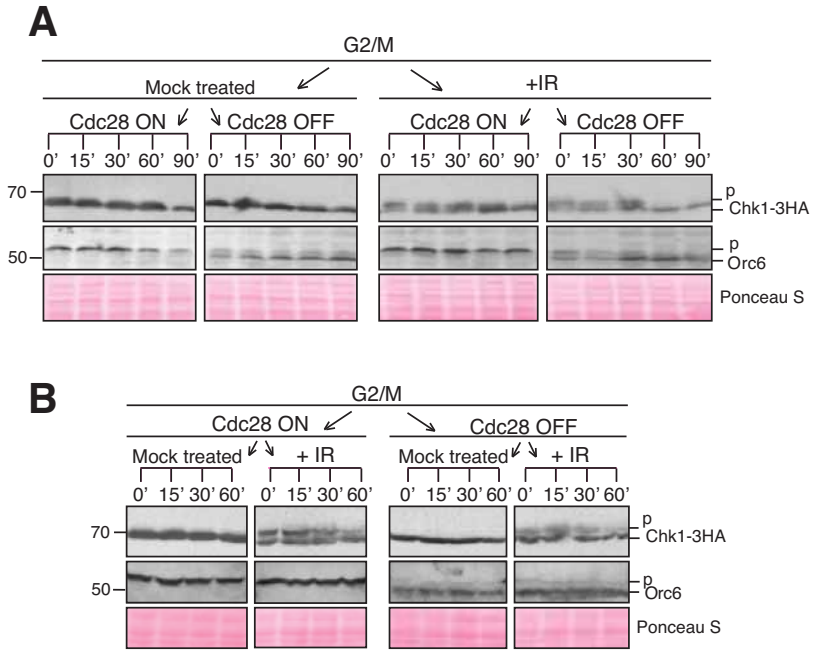


**Figure S3.3**, related to Figure 3.4**.** (A) CDK-dependency of the maintenance of IR (+400Gy) induced Chk1 phosphorylation. 1-NMPP1 was added into half of the G2 arrested and IR-treated cells to inactivate Cdk1 activity. Chk1 phosphorylation analysis was performed from protein extracts collected at the indicated time points. (B) CDK-dependency of the initial IR (+400Gy) induced phosphorylation of Chk1. Cdc28 was inactivated in half of the G2 arrested cells and treated with IR to initiate the checkpoint in populations with and without Cdc28 activity. Protein samples were collected at the indicated time points and Chk1 phosphorylation analysis was performed. Orc6 phosphorylation is used as a control for Cdc28 inactivation in both experiments.

## *Figure S3.4*

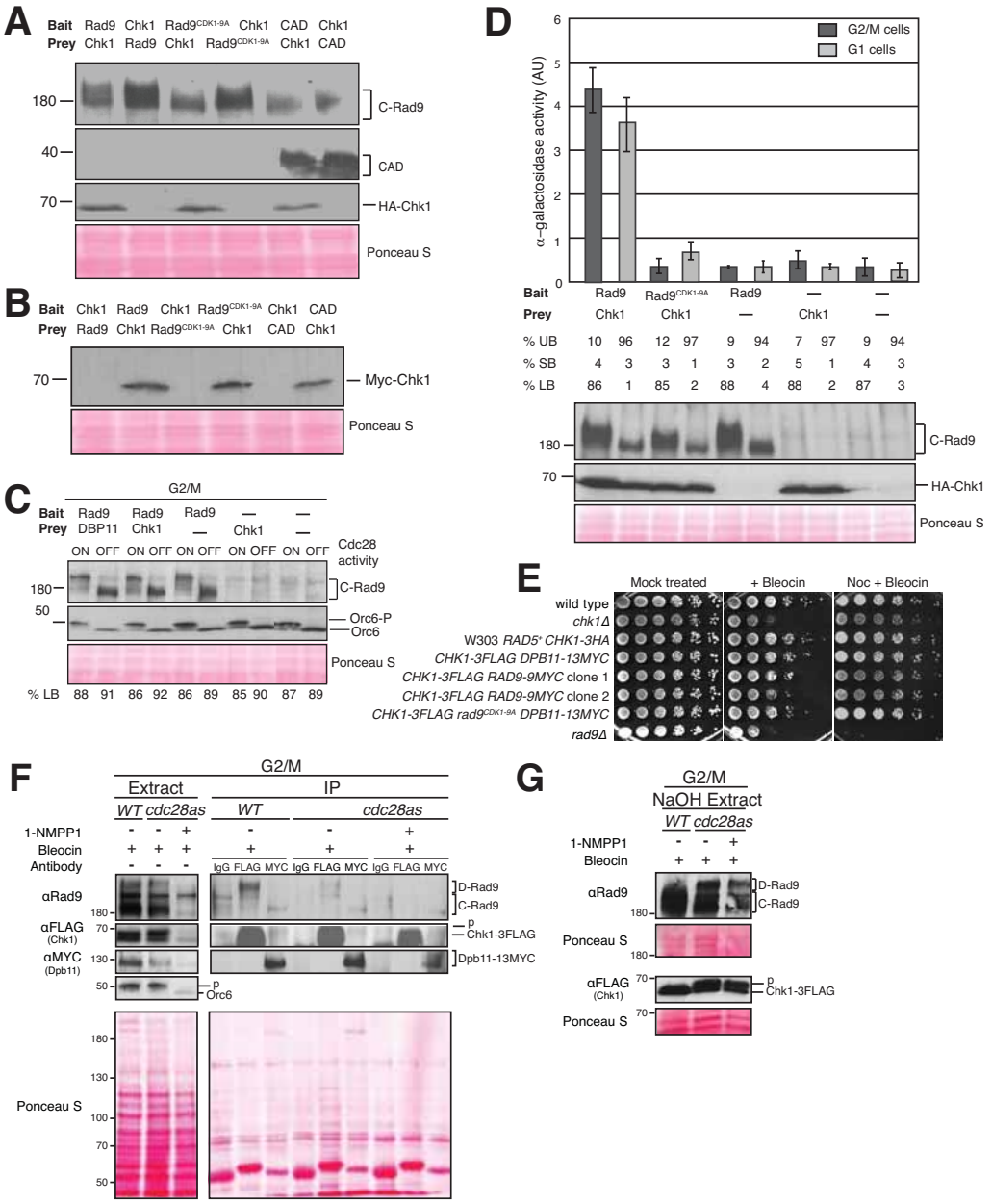


**Figure S3.4**, related to Figure 3.5. Western blotting of Rad9 and Chk1 over-expressing yeast two-hybrid cells shown in Figure 3.5. (A) Rad9 western of all bait and prey combinations shown in Figure 3.5A. HA western for cells expressing Chk1 as prey is also shown (B). (B) Anti-MYC western blot demonstrating expression of MYC-tagged Chk1 expressed as a bait in Y2H cells. (C) Anti-Rad9 western blot demonstrating expression of Rad9 in G2/M arrested Y2H cells used in Figure 3.5B. Orc6 was probed as marker for Cdc28 activity. The same clones were used in the G1 experiment presented in Figure 3.5B. (D) The Y2H interaction between Rad9 and Chk1 is dependent on the CDK1-9 sites in both G1 and G2/M cells. The indicated bait and prey plasmids introduced into Y2H cells (identical to clones shown in S5A) were grown, divided into two flasks and arrested in G2/M and G1 phase of cell cycle. 1 ml of cells corresponding to one OD value were used to perform the PNP assay (see supplementary information). The α-galactosidase activity was measured according to Clontech Yeast Two Hybrid instructions. (E) Drop test analysis of the indicated tagged strains used for immunoprecipitation experiments shown in Figure 3.5. Note that these strains are not sensitive to Nocodazole and bleocin treatments, conditions also used in Figure 3.5E and F. (F) Chk1 interaction with Rad9 is dependent on Cdc28 activity. IPs were performed as indicated on extracts prepared from

nocodazole-arrested wild type and *cdc28as1* cells, expressing both Chk1-3FLAG and Dpb11-13MYC, and either mock treated or treated with 20μM of 1-NMPP1 for 1h45min before adding 20μg/ml of bleocin for 45 min. Mock (IgG) or MYC IPs were performed as controls. Rad9, Chk1-3FLAG and Dpb11-13MYC specific bands were detected in western blots. Lower exposures of the extracts are shown to facilitate their visualization. (G) Whole cell extracts (NaOH extracts) prepared from nocodazole-arrested wild type and *cdc28as1* cells and treated as indicated in F.

***Figure S3.5***

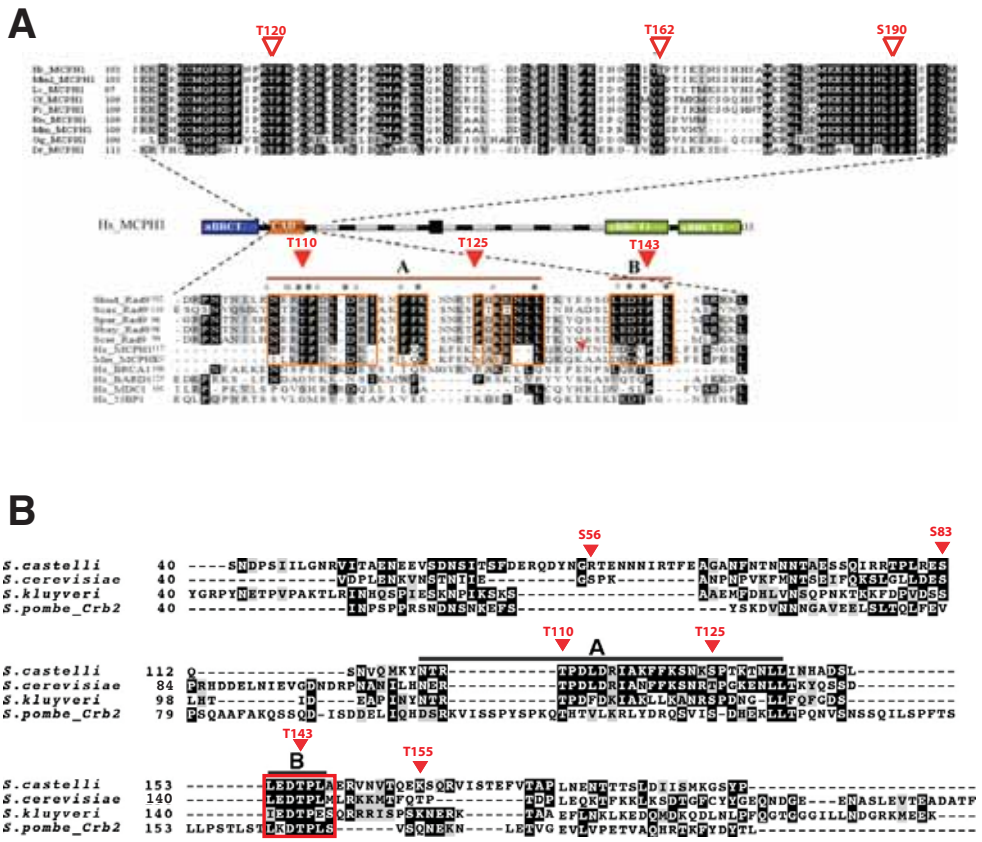


**Figure S3.5**, related to Figure 3.6. Cross-species Rad9 alignments suggest conserved consensus CDK phospho-sites within the CAD domains. (A) Cross-species Mcph1-Rad9 alignments. In *sc*Rad9: T110 (TPDL, CDK5); T125 (TPGK, CDK6); and T143 (TPLM, CDK7); In hMCPH1: T120 (TPED); T162 (TPTI); and S190 (SPTS); T110 (CDK7) of Rad9 is conserved with T120 of Mcph1 (Steve Jackson, personal communication). (B) N-terminal domains of Rad9 are comparatively well conserved in other yeast species. Alignment adapted from Blankley and Lydall, 2004. Amino acids 40-200 of the three Rad9 orthologues were aligned with amino acids 40-200 from *S. pombe* Crb2 using the ClustalW algorithm. In *sc*Rad9: S56 (SPKA, CDK4); S83 (SPRH, CDK5), T110 (TPDL, CDK5); T125 (TPGK, CDK6); T143 (TPLM, CDK7) and T155 (TPTD, CDK8); *sc*Rad9 T143 is conserved in the shown yeast species (red square). Perfectly conserved residues are highlighted in black, structurally similar residues are highlighted in grey. Domains A and B show patches of sequence with high identity.

### 3.8.3. Supplemental Tables

### Table S3.1: Strains used in this study.

| Collection Number | Strain name | Relevant Genotype | Source | Figure |
|---|---|---|---|---|
| **YNL0420** | CG378 | ***MAT*a** *ade5-7 can1-1 leu2-3,112, trp1-289 ura3-52* | L. Johnston | 3.1A |
| **YNL0220** | W303-1a | ***MAT*a** *ade2-1 trp1-1 leu2-3,112, his3-11,15 ura3-1 can1-100 rad5-535* | K. Nasmyth | S3.1A |
| **YNL1312** | *cdc28-as1* | W303-1a *cdc28-as1 (*JAU01) | (Bishop et al., 2000) | 3.1B; 3.2C; S3.5C |
| **YNL0620** | *cdc4-1* | W303-1a *cdc4-1* | J. Diffley | 3.1C |
| **YNL0264** | *cdc7-1* | W303-1a *cdc7-1* | J. Diffley | 3.1C |
| **YNL0742** | YLD1 | ***MAT*a** *cdc15-2 cdc6::hisG trp1::TRP1:MET3-CDC6* | J Diffley | S3.1B |
| **YNL1287** | W303-1a *RAD5*$^{+}$ | ***MAT*a** *ade2-1 trp1-1 leu2-3,112, his3-11,15 ura3-1 can1-100 RAD5*$^{+}$ | This study | 3.1E; 3.2; S3.1C-E; S3.5E |
| **YNL1341** | *rad9*$^{12A}$ | W303-1a *RAD5*$^{+}$ *rad9*$^{12A}$ | This study | 3.1D,E;S3.1C-E |
| **YNL1350** | *rad9*$^{CAD\Delta}$ | W303-1a *RAD5*$^{+}$ *rad9*$^{CAD\Delta}$ | This study | 3.2A-C |
| **YNL1347** | *rad9*$^{CDK1-9A}$ | W303-1a *RAD5*$^{+}$ *rad9*$^{S11A,S26A,S56A,S83A,T110A,T125A,T143A,T155A,T218A}$ | This study | 3.2A-C |
| **YNL1016** | *rad9Δ* | W303-1a *rad9::URA3* | (Grenon et al., 2007) | 3.2B,C; S3.5E |
| **YNL1145** | *sml1Δ chk1Δ* | W303-1a *RAD5*$^{+}$ *sml1::KanMX6 chk1::URA3* | This study | 3.2B; 3.3E; S3.3E |
| **YNL1280** | *CHK1-3HA* | W303-1a *CHK1-3HA::KlURA3* | (Clerici et al., 2004) | |
| **YNL1144** | *CHK1-3HA RAD5*$^{+}$ | W303-1a *RAD5*$^{+}$ *CHK1-3HA::KlURA3* | This study | 3.2D; 3.3A-D; S3.2;S3.3; S3.5E |
| **YNL1431** | *rad9*$^{CDK1-9A}$ *CHK1-3HA* | W303-1a *RAD5*$^{+}$ *rad9*$^{Cdk1-9A}$ *CHK1-3HA::KlURA3* | This study | 3.2D; 3.3A-D; S3.2; S3.3 |
| **YNL1432** | *rad9*$^{CAD\Delta}$ *CHK1-3HA* | W303-1a *RAD5*$^{+}$ *rad9*$^{CAD\Delta}$ *CHK1-3HA::KlURA3* | This study | 3.2D; 3.3A-D; S3.2; S3.3 |
| **YNL1433** | *rad9Δ CHK1-3HA* | W303-1a *RAD5*$^{+}$ *rad9::LEU2 CHK1-3HA::KlURA3* | This study | 3.2D; 3.3A-D; S3.2; S3.3 |
| **YNL1445** | *sml1Δ rad53Δ chk1Δ* | ***MAT*α** *sml1:: kanMX6 rad53::HIS3 chk1::URA3 RAD5*$^{+}$ *ade2-1 trp1-1 can1-100 ura3* | (Blankley and Lydall, 2004) | |
| **YNL1143** | *sml1Δ* | W303-1a *RAD5*$^{+}$ *sml1::KanMX6* | This study | 3.3E |
| **YNL1447** | *sml1Δ rad53Δ* | W303-1a *RAD5*$^{+}$ *sml1::KanMX6 rad53::HIS3* | This study | 3.3E |
| **YNL1142** | *sml1Δ rad53Δ chk1Δ* | W303-1a *RAD5*$^{+}$ *sml1::KanMX6 rad53::HIS3 chk1::URA3* | This study | 3.3E |
| **YNL1146** | *sml1Δ rad9*$^{CDK1-9A}$ | W303-1a *RAD5*$^{+}$ *sml1::KanMX6 rad9*$^{CDK1-9A}$ | This study | 3.3E |
| **YNL1147** | *sml1Δ rad9*$^{CDK1-9A}$ *chk1Δ* | W303-1a *RAD5*$^{+}$ *sml1::KanMX6 rad9*$^{CDK1-9A}$ *chk1::URA3* | This study | 3.3E |
| **YNL1240** | *sml1Δ rad9*$^{CDK1-9A}$ *rad53Δ* | W303-1a *RAD5*$^{+}$ *sml1::KanMX6 rad9*$^{CDK1-9A}$ *rad53::HIS3* | This study | 3.3E |
| **YNL1239** | *sml1Δ rad9*$^{CDK1-9A}$ *rad53Δ chk1Δ* | W303-1a *RAD5*$^{+}$ *sml1::KanMX6 rad9*$^{CDK1-9A}$ *rad53::HIS3 chk1::URA3* | This study | 3.3E |
| **YNL1441** | *rad9*$^{CDK1,3,4,6,9A}$ *CHK1-3HA* | W303-1a *RAD5*$^{+}$ *rad9*$^{S11A,S56A,S83A,T125A,T218A}$ *CHK1-3HA::KlURA3* | This study | S3.2 |
| **YNL1440** | *rad9*$^{CDK4,6,9A}$ *CHK1-3HA* | W303-1a *RAD5*$^{+}$ *rad9*$^{S83A,T125A,T218A}$ *CHK1-3HA::KlURA3* | This study | S3.2 |
| **YNL1421** | *rad9*$^{CDK4,5,6,7A}$ *CHK1-3HA* | W303-1a *RAD5*$^{+}$ *rad9*$^{S83A,T110A,T125A,T143A}$ *CHK1-3HA::KlURA3* | This study | S3.2 |
| **YNL1419** | *rad9*$^{CDK5A}$ *CHK1-3HA* | W303-1a *RAD5*$^{+}$ *rad9*$^{T110A}$ *CHK1-3HA::KlURA3* | This study | S3.2 |

| | | | | |
|---|---|---|---|---|
| **YNL1439** | *rad9$^{CDK7,8,9A}$ CHK1-3HA* | W303-1a *RAD5$^{+}$ rad9$^{T143A,T155A,T218A}$ CHK1-3HA::KlURA3* | This study | S3.2 |
| **YNL1443** | *rad9$^{CDK1,2,PIK1A}$ CHK1-3HA* | W303-1a *RAD5$^{+}$ rad9$^{S11A,S26A,T16A}$ CHK1-3HA::KlURA3* | This study | S3.2 |
| **YNL1435** | *rad9$^{CDK1A}$ CHK1-3HA* | W303-1a *RAD5$^{+}$ rad9$^{S11A}$ CHK1-3HA::KlURA3* | This study | S3.2 |
| **YNL1437** | *rad9$^{CDK9A}$ CHK1-3HA* | W303-1a *RAD5$^{+}$ rad9$^{T218A}$ CHK1-3HA::KlURA3* | This study | S3.2 |
| **YNL1424** | *cdc28-as1 CHK1-3HA* | W303-1a *cdc28-as1 CHK1-3HA::KlURA3* | This study | 3.4; S3.3 |
| **YNL1425** | Y2HGold | *MATa, trp1-901, leu2-3, 112, ura3-52, his3-200, gal4Δ, gal80Δ, LYS2::GAL1UAS–Gal1TATA–His3, GAL2UAS–Gal2TATA–Ade2 URA3::MEL1UAS–Mel1TATA AUR1-C MEL1* | Clontech | 3.5A,B; S3.4A,B, D |
| **YNL1426** | *DBP11-13MYC* | W303-1a *DPB11-13MYC::HIS3* | (Puddu *et al*., 2008) | |
| **YNL1427** | *CHK1-3FLAG DBP11-13MYC* | W303-1a *RAD5$^{+}$ CHK1-3FLAG::KANMX DPB11-13MYC::HIS3* | This study | 3.5C,D; S3.4E |
| **YNL1428** | *rad9$^{CDK1-9A}$* CHK1-3FLAG DBP11-13MYC | W303-1a *RAD5$^{+}$ rad9$^{CDK1-9A}$ CHK1-3FLAG::KANMX DPB11-13MYC::HIS3* | This study | 3.5C,D; S3.4E |
| **YNL1430** | *RAD9-9MYC* | W303-1a *RAD9-9MYC::TRP1* | (Giannattasio et al., 2002) | |
| **YNL1500** | *RAD9-9MYC CHK1-3FLAG* | W303-1a *RAD9-9MYC::TRP1 CHK1-3FLAG::KANMX* | This study | 3.5E,F; S3.4E |

**Table S3.2: Plasmids used in this study.**

| Collection Number | Plasmid | Usage | Source |
|---|---|---|---|
| **ENL0757** | pVF6 | *cdc28-as1* mutation | (Diani et al., 2009) |
| **ENL0749** | pRS306-*rad9*$^{CDK1\text{-}9A}$ | Integrative vector | This study |
| **ENL0026** | pRS306-*rad9*$^{CDK1,3,4,6,9A}$ | Integrative vector | This study |
| **ENL0758** | pRS306-*rad9*$^{CDK5A}$ | Integrative vector | This study |
| **ENL0746** | pRS306-*rad9*$^{CDK1A}$ | Integrative vector | This study |
| **ENL0750** | pRS306-*rad9*$^{CADΔ}$ | Integrative vector | This study |
| **ENL0029** | pRS306-*rad9*$^{CDK14,16\text{-}20A}$ | Integrative vector | This study |
| **ENL0031** | pRS306-*rad9*$^{CDK1,11A}$ | Integrative vector | This study |
| **ENL0186** | pRS306-CTRAD9 | Integrative vector | This study |
| **ENL0760** | p3FLAG-KANMX | Tagging vector | (Gelbart et al., 2001) |
| **ENL0759** | pGEM-Teasy-NTRAD9 | Mutagenesis vector | This study |
| **ENL0747** | pGEM-Teasy-NT*rad9*$^{CDK1\text{-}9A}$ | Mutagenesis vector | This study |
| **ENL0011** | pGEM-Teasy-NT*rad9*$^{CDK1,3,4,6,9A}$ | Mutagenesis vector | This study |
| **ENL746** | pGEM-Teasy-NT*rad9*$^{CDK1A}$ | Mutagenesis vector | This study |
| **ENL0025** | pGEM-Teasy-NT*rad9*$^{CDK1,11A}$ | Mutagenesis vector | This study |
| **ENL0748** | pGEM-Teasy-NT*rad9*$^{CADΔ}$ | Mutagenesis vector | This study |
| **ENL0706** | pGEM-Teasy-CTRAD9 | Mutagenesis vector | This study |
| **ENL0022** | pGEM-Teasy-*rad9*$^{CDK14,16\text{-}20A}$ | Mutagenesis vector | This study |
| **ENL0733** | pGBKT7-BD | Y2H vector | Clontech |
| **ENL0755** | pGBKT7-Lam | Y2H vector | Clontech |
| **ENL0753** | pGBKT7-53 | Y2H vector | Clontech |
| **ENL0737** | pGBKT7-BD-RAD9 | Y2H vector | This study |
| **ENL0741** | pGBKT7-BD-CAD | Y2H vector | This study |
| **ENL0744** | pGBKT7-BD-*rad9*$^{CDK1\text{-}9A}$ | Y2H vector | This study |
| **ENL0739** | pGBKT7-BD-CHK1 | Y2H vector | This study |
| **ENL0734** | pGADT7-T | Y2H vector | Clontech |
| **ENL0754** | pGADT7-AD | Y2H vector | Clontech |
| **ENL0736** | pGADT7-AD-RAD9 | Y2H vector | This study |
| **ENL0756** | pGADT7-AD-*rad9*$^{CDK1\text{-}9A}$ | Y2H vector | This study |
| **ENL0740** | pGADT7-AD-CAD | Y2H vector | This study |
| **ENL0738** | pGADT7-AD-CHK1 | Y2H vector | This study |
| **ENL0752** | pEG202 | Y2H vector | (Granata et al., 2010) |
| **ENL0735** | pEG202-CHK1 | Y2H vector | This study |
| **ENL0721** | pJG4-5 | Y2H vector | (Granata et al., 2010) |
| **ENL0725** | pJG4-5-RAD9 | Y2H vector | This study |
| **ENL0751** | pSH18-34 | Y2H vector | (Granata et al., 2010) |

**Table S3.3: Primers used in this study.**

| Name | *5'→ 3' Sequence* | Usage |
|---|---|---|
| Rad9seq2 | CGGCCTTGTTAGCGTTAGAT | To amplify *CAD* region of *RAD9* from genomic DNA |
| Rad9 cdkwtm2 | GCAAGATAGAGAAACGCCATAG | To amplify *CAD* region of *RAD9* from genomic DNA |
| N1 Mut | GCAAGATAGAGAAACGCCATAG | *CAD* mutants sequencing |
| Chk1-Dia F | CACGTTGCAACCTATGGATG | To amplify *CHK1-3HA::KlURA3* cassette; *CHK1-3FLAG* diagnosis PCR |
| Chk1-Dia R | GAACGGAATATCTGTGGAAG | To amplify *CHK1-3HA::KlURA3* cassette |
| Chk1-Flag-5' | AATTTCAACTATCTGTAGGGATATTATCCTAATTCCCA ACAGGGAACAAA AGCTGGAG | To amplify *CHK1-3FLAG::KANMX* |
| Chk1-Flag-3' | TGATCAGTGCATCTTAACCCTTCTTTTGTCTCCATTTTT TCTATAGGGCGAATTGGGT | To amplify *CHK1-3FLAG::KANMX* |
| Chk1-2 | GTTACGATGACACACTAG | *CHK1-3FLAG* diagnosis PCR |
| DPB11-myc-5' | GAAAAACCTATGAGACGACAGACAAGAAATCAGACA AAGGAATTAGATTCTCGGATCCCCGGGTTAATTAA | To amplify *DPB11-13MYC::HIS3* |
| DPB11-myc-3' | GCTGTAGATGGCGTATGTAAATGAATATCTTATAAAA TTACGGACTACATTTCAGAATTCGAGCTCGTTTAAAC | To amplify *DPB11-13MYC::HIS3* |
| DPB11-testF | AGCTTGAACTCGTGGTTCCT | *DPB11-13MYC* diagnosis PCR |
| DPB11-testR | ATGCCAGGAGGCATAAGGTT | *DPB11-13MYC* diagnosis PCR |
| Rad9N1F | GTTCAATGGAAAAGCGCTCCAGATCGAGTC | Mutagenesis of S11 to Ala |
| Rad9N1R | GACTCGATCTGGAGCGCTTTTCCATTGAAC | Mutagenesis of S11 to Ala |
| Rad9N2F | CATAATCGAAGGAGCTCCCAAAGCAAATCC | Mutagenesis of S56 to Ala |
| Rad9N2R | GGATTTGCTTTGGGAGCTCCTTCGATTATG | Mutagenesis of S56 to Ala |
| Rad9N3F | GGATTACTTGACGAGGCTCCAAGACATGATG | Mutagenesis of S83 to Ala |
| Rad9N3R | CATCATGTCTTGGAGCCTCGTCAAGTAATCC | Mutagenesis of S83 to Ala |
| Rad9N4F | CAAAAGCAATCGAGCCCCTGGTAAAG | Mutagenesis of T125 to Ala |
| Rad9N4R | CTTTACCAGGGGCTCGATTGCTTTTG | Mutagenesis of T125 to Ala |
| Rad9N5F | GCATTGGAAGGAATTGTTGCACCTAAAAG | Mutagenesis of T218 to Ala |
| Rad9N5R | CTTTTAGGTGCAACAATTCCTTCCAATGC | Mutagenesis of T218 to Ala |
| R9T110A | TAACATATTGCATAATGAAAGGGCTCCTGACCTTGAC CGAATTG | Mutagenesis of T110 to Ala |
| R9S26A | TATAAAGGAAGCACTGCATGCTCCCTTGGCTGATGGC GAC | Mutagenesis of S26 to Ala |
| R9N1T16A | AAGCGCTCCAGATCGAGTCGCCCAAAGCGCTATAAAG GAAG | Mutagenesis of T16 to Ala |
| R9T155A | GAAAAAAAATGACTTTTCAAGCTCCAACTGATCCATT GGAAC | Mutagenesis of T155 to Ala |
| R9T143A | CAAAGCTCCGATCTGGAAGACGCTCCTCTGATGTTAA GAAAAAAAATG | Mutagenesis of T143 to Ala |
| CADP1 | CGCGGATCCAGTAGAACACTTGGGAATCC | To generate pGEMTeasy-NT*rad9*$^{CAD\Delta}$ |
| CADP2 | CTCGTATCACTCTTTTAGAAGTTGTAGTCCCGATACGT TCTACTTGCTCAAG | To generate pGEMTeasy-NT*rad9*$^{CAD\Delta}$ |
| CADP3 | GAAAATCTTCAACATCAGGG*CT*ATGCAAGATGAACGA GTTCAAAAAACTCAAATC | To generate pGEMTeasy-NT*rad9*$^{CAD\Delta}$ |
| CADP4 | CTTCTGTCTGGCCAGTAGAATGAAAAACAGG | To generate pGEMTeasy-NT*rad9*$^{CAD\Delta}$ |
| pGBKT7/pGADT7-AD-RAD9F | CATGCACATATGTCAGGCCAGTTAGTTCAATGGAAAA GC | Y2H *RAD9* constructs |

| | | |
|---|---|---|
| pGBKT7/pGADT7-AD-RAD9R | CATGACGGATCCCTCATCTAACCTCAGAAATAGTGTTG | Y2H *RAD9* constructs |
| pGBKT7/pGADT7-AD-CHK1F | CATGCACATATGAGTCTCTCGCAGGTGTCACCTTTACC | Y2H *CHK1* constructs |
| pGBKT7/pGADT7-AD-CHK1R | CATGACGAATTCTCAGTTGGGAATTAGGATAATATCC | Y2H *CHK1* constructs |
| pGBKT7/pGADT7-AD-RAD9CADR | CATGACGGATCCTCATCCTCCACTTTTACTTAATTCGTC | Y2H *CAD* constructs |
| pEG202CHK1F | CATGCAGAATTCATGAGTCTCTCGCAGGTGTCACCTTTACC | To amplify *CHK1* in Y2H constructs |
| pEG202CHK1R | CATGACCTCGAGTCAGTTGGGAATTAGGATAATATCC | To amplify *CHK1* in Y2H constructs |
| T7 Promoter | GTAATACGACTCACTATAGGGCGA | To sequence Y2H constructs |
| Rad9 Seq4 | GTTGAAGTCAGATACTGGG | *RAD9* sequencing |
| Rad9 Seq6 | TTTCCCAAGGCATATCTGC | *RAD9* sequencing |
| Rad9 Seq8 | CGAAAGCAAAGGACAGAGC | *RAD9* sequencing |
| Rad9 Seq10 | GGATTCTAGAGACGCATTAGC | *RAD9* sequencing |
| Rad9 Seq12 | GGTAAATCTCAGATGAAGC | *RAD9* sequencing |
| Chk1CD+600NtsF | ATGGATCAAAGGGGTTCTCCAC | *CHK1* sequencing |
| pGAD-AD-R | AGATGGTGCACGATGCACAG | *RAD9*/*CHK1* Y2H vector sequencing |
| pGBK-BD-R | TTTTCGTTTTAAAACCTAAGAGTC | *RAD9*/*CHK1* Y2H vector sequencing |

# CHAPTER 4

## Conclusions and Future Directions

Carla Manuela Abreu[1], Muriel Grenon[1] & Noel Francis Lowndes[1]

[1]Centre for Chromosome Biology, School of Natural Science, National University of Ireland Galway, University Road, Galway, Ireland

## 4.1. STRUCTURE-FUNCTION RELATIONSHIP OF MEC1

The structure, function and regulation of the checkpoint protein Mec1 have been the subject of intense investigation in the past decade. While significant knowledge has been generated regarding the regulation of its activity in the cellular response to DNA damage and replication stress, there still remains much to learn. One of the aims of this project (Chapter 2) has been to further characterise the structure-function relationship of Mec1 using the genetic tractable *S. cerevisiae* as a model system.

To do so, we developed a strategy based on the break-mediated version of the *delitto perfetto* approach developed by Storici and colleagues (Storici et al., 2003; Storici et al., 2001; Storici and Resnick, 2003, 2006) and fusion PCR methodology. With this strategy, we created a unique set of genetically engineered *mec1* strains (*mec1::CORE1*, *mec1::CORE2*, *mec1::CORE3* and *mec1::CORE4*) that can be used for the easy generation of any structure-function mutant of Mec1 in a haploid *sml1Δ* background. In fact, these parental *mec1* strains can be transformed with the appropriate fusion DNA fragments to generate, in one-step, any mutation (deletions, integrations, replacements or point mutations) at any position within the *MEC1* ORF.

Mec1, the homologue of human ATR, is a member of the PIKK family due to the presence of its conserved kinase, FAT and FATC domains in its C-terminus. In addition, just as in other PIKKs, tandem helical motifs, called HEAT repeats, make up most of the non-kinase portion of Mec1. However, the role of the HEAT repeats in PIKK function is currently ill understood. In this study, we hypothesised that HEAT repeats mediate specific interactions with other biomolecules and commenced a structure-function analysis of their essential and DDR-specific role(s). We predicted that we would be able to assign specific functions to specific HEAT repeat regions of Mec1. However, we showed that six sequential *mec1* window deletion mutants, spanning the entire HEAT repeat regions of the proteins and corresponding to loss of either multiple or a single HEAT repeat, all had null phenotypes indistinguishable from a *mec1* deleted strain. The phenotypes we studied included sensitivity to different to DNA damaging agents, replication stress and dNTPs homeostasis. The null phenotype of these mutations is not due protein destabilisation as all the mutants were expressed similarly to wild type Mec1. In support of these unexpected results, null phenotypes were also obtained in chicken DT40 cells

expressing equivalent window deletion mutants of ATR (Eykelenboom J and Agost LM, *unpublished data*).

One possibility to explain these results is that all the Mec1 (and also ATR) HEAT repeats deletion mutants included in the deleted region at least one HEAT repeat required for an essential function. This would be consistent with protein-protein interactions required for Mec1 essential function being distributed throughout the entire protein length of the HEAT repeat region. Furthermore, as similar results were obtained with ATR, this would also indicate that the distribution of essential function(s) throughout the HEAT repeat region is evolutionarily conserved. This possibility could be further tested by deletion of the individual HEAT repeats that make up the region deleted within the Mec1/ATR window deletions already made. Possibly, loss of some individual HEAT repeats might not result in a null phenotype.

On the other hand, loss of even a single HEAT repeats could affect a structural property of Mec1/ATR required for their function. However, when we tested this by generating replacement mutants using the equivalent HEAT repeats from the orthologous and related PIKKs, ATR and Tel1 respectively, the Mec1-ATR and Mec1-Tel1 hybrids still displayed null phenotypes. However, as our results with the replacement mutations are negative, they cannot be used to support the hypothesis that HEAT repeats are required for a crucial structural property. If the replaced region of Mec1 is required for an essential function and this function is not conserved within the HEAT repeats taken from ATR or Tel1, then the null phenotype of the replacement mutants can be explained, just as in the window mutants, by loss of an essential function.

In order to control our results properly it would be interesting to generate a *mec1* hybrid mutant where the two most conserved HEATs within the FAT domain are replaced by the equivalent region from a closely related budding yeast species such as *Saccharomyces paradoxus*. The FAT domain is common to all PIKKs and has been implicated in regulating their kinase activity (Bosotti et al., 2000). Therefore, not only would such a conservative substitution be expected to be functional, but it would provide the positive control our Mec1 structure-functions results are thus far lacking.

Additional biochemical and molecular analyses could also be carried out in the *mec1* mutants already generated in order to understand the consequences of the window deletions or replacements on Mec1 activity and functions. In particular, it would be interesting to test the *in vitro* kinase activity of Mec1. *In vivo*, the kinase activity of Mec1 is known to be required for all its functions (Mallory and Petes, 2000; Paciotti et al., 2000; Wakayama et al., 2001). It is possible that the null mutants generated in this study may still have appreciable *in vitro* kinase activity. Alternatively, the Mec1 mutant proteins could be defective *in vitro* kinases indicating that HEAT repeats distributed along the entire length of the HEAT repeat region are required for this activity. Alternatively, or perhaps in addition, given that Ddc2 is required for all Mec1 functions (Mallory and Petes, 2000; Paciotti et al., 2000; Wakayama et al., 2001), it is possible that the compromised structure of all the Mec1 mutant proteins does not allow an efficient binding of Mec1 to the Ddc2 cofactor protein and therefore results in the null phenotype.

The determination of the molecular architecture of the Mec1 and/or ATR mutant proteins relative to their wild type would be interesting with respect to the hypothesis that the mutant proteins all have structural abnormalities. On going work in our laboratory is currently investigating the architecture of wild type ATR from DT40 cells using cryo-EM analysis (*John Eykelenboom* and *Marta Llorens-Agost* in collaboration with *Eva Nogales*, Berkeley). Interestingly, in preliminary images the WT ATR protein can be observed as “diamond ring-like” structures similar to those reported for DNA-PK (Sibanda et al., 2010).

An aspect of the Mec1 primary amino acid structure that has not been explored to date is the presence of concensus PIKK and CDK phosphorylation sites distributed throughout the protein. There is some evidence suggesting that Mec1 undergoes autophosphorylation *in vitro*, resulting in a four-fold increase in the phosphate content of the protein (Zhu et al., 2000). However, a molecular mechanism role for this process remains to be uncharacterised. It is possible that Mec1 autophosphorylation is involved in engaging Dpb11 to allow its full activation at sites of DNA damage, analogously to ATR in mammalian cells (Liu et al., 2011). Unpublished data from our laboratory also suggest that Mec1 is phosphorylated during a normal cell cycle and further phosphorylated in response to DNA damage

(Steffano Maffini, *unpublished results*). The essential role of Mec1 during cellular proliferation is to maintenance of dNTPs homeostasis, which is critical for efficient DNA replication and repair (Zhao et al., 1998). This observation also suggests that Mec1 activity might be regulated during the cell cycle. The phosphorylation of Mec1 by Cdc28, the unique CDK in yeast, could be involved in this process. A testable hypothesis using our four *mec1::CORE* strains to introduce phospho-site mutations in the concensus PIKK and CDK phosphorylation sites, is that the phosphorylation status of Mec1/ATR is an important factor in the regulation of its kinase activity *in vivo*.

Our results clearly show that Mec1/ATR functions are tightly dependent on its HEAT repeats. Importantly, although the separation of discrete functions could not be achieved by the structure function studies conducted in this work, it is remarkable that Mec1 and ATR, and possibly all other PIKKs, are very sensitive to changes in their primary amino structure. This perhaps indicates that Mec1 and ATR have structures that are exquisitely sensitive to even subtle perturbations, constituting a challenge for structure-function studies. Therefore, the development of new strategies might be needed to elucidate the structure and function of Mec1/ATR protein. For instance, to investigate if specific HEAT repeats from Mec1/ATR mediate specific protein-protein interactions, pull down experiments using purified, recombinant HEAT repeat-containing fragments could be performed.

### 4.2. THE RAD9 CHECKPOINT MEDIATOR: LINKING CELL CYCLE REGULATION AND DNA DAMAGE RESPONSE

In this study we also elucidated a role for the CDK-dependent phosphorylation of Rad9 (Chapter 3). Using a genetic approach we showed that phosphorylation of Rad9 during the S, G2 and M phases of the cell cycle depends on B-type cyclin (Clbs) forms of Cdc28 in budding yeast. This is in agreement with studies demonstrating that Rad9 is an *in vitro* substrate of Cdc28/Clb2 and Cdc28/Clb5 complexes (Loog and Morgan, 2005). We proposed that the cell cycle phosphorylation of Rad9 is not required for its checkpoint activity in response to normal replication structures generated during S-phase, but rather it modulates the activity of the various Rad9 functions during the DDR. In particular we focussed upon the role of Rad9 in the activation of the Chk1 checkpoint kinase.

The Rad9 checkpoint protein plays a pivotal role in the DNA damage response as a mediator of the PIKK-dependent activation of the effector checkpoint kinases Rad53 and Chk1 (Gilbert et al., 2001; Blankley and Lydall, 2004; Sweeney et al., 2005). Although the PIKK- and Rad9-dependent mechanism of Rad53 activation has been well described (Gilbert et al., 2001; Schwartz et al., 2002; Sweeney et al., 2005), the mechanism of activation of Chk1 is not well understood. The experimental work presented in chapter 3 has been built upon the initial observations of Blankely and Lydall who demonstrated that truncation of the N-terminal region of Rad9 results in defective DNA damage-induced Chk1 phosphorylation (Blankley and Lydall, 2004). We have determined that the multiple consensus CDK phosphorylation sites located within this Chk1 Activation Domain, or CAD, region of Rad9 are required for damage-induced Chk1 activation. Similarly to deletion of *CHK1*, a mutant of Rad9 in which the nine consensus CDK sites in the CAD region were mutated to alanine (*rad9*$^{CDK1\text{-}9A}$) is not sensitive to many forms of DNA damage. Interestingly, we did notice that *chk1Δ* cells are sensitive to low doses of bleocin, a treatment that results in sensitivity particularly during DNA synthesis. The sensitivity of *chk1Δ* cells to bleocin was rescued by extended arrest in G2/M. This suggests that Chk1 might have a role in surviving bleocin-induced lesions during S phase. It would be interesting to further investigate the role of Chk1 in the S-phase checkpoint in response to bleocin-induced DNA damage.

Cell cycle phosphorylation of Rad9 was partially defective in *rad9*$^{CDK1\text{-}9A}$ mutants. When compared with *rad9*$^{12A}$ mutants, Rad9$^{CDK1\text{-}9A}$ migrated faster than Rad9 in blots using extracts prepared from both asynchronous and G2/M cells. In both cases the faster migrating forms of Rad9 were lost in the absence of Cdc28 activity. Thus, at least some of the CDK sites mutated in Rad9$^{CDK1\text{-}9A}$ are phosphorylated *in vivo* in a Cdc28-dependent fashion. Although our data combined with other reported studies have shown that all the consensus CDK sites located in the Rad9 CAD, with the exception of T110 (CDK5), are phosphorylated *in vivo*, it is not directly demonstrated if the phosphorylation of all these sites or only some of them is Cdc28-dependent. Using *in vitro* kinase assays we determined that the CAD region of Rad9 is preferentially phosphorylated by the Cdc28/Clb3 complex, followed by the Cdc28/Clb2 complex. CAD phosphorylation by Cdc28/Clb3 and Clb2 is abolished

when the CDK1-9 sites are mutated to alanine. Thus, at least some of the nine Cdc28 phosphorylation sites mutated in Rad9$^{CDK1\text{-}9A}$ are phosphorylated *in vitro* by Cdc28. It would be interesting to investigate if Cdc28/Clb3 complexes preferentially phosphorylate specific CDK sites within Rad9 CAD region. This could be addressed by *in vitro* phosphorylation of a peptide array containing peptides spanning the entire Rad9 CAD region using recombinant Cdc28/Cdlb3 complexes. A mass spectrometry approach using endogenous Rad9 from *cdc28-as1* cells in which Cdc28 activity can be easily manipulated would be also useful for examining the *in vivo* Cdc28-dependency of the CDK sites in Rad9 CAD.

We also determined the role of nine putative CDK phosphorylation sites in the CAD region. Western blot analysis of Rad9$^{CDK1\text{-}9A}$ relative to wild type Rad9 clearly suggested that the nine putative CDK phosphorylation sites of the CAD region are specifically involved in mediating the damage-induced phosphorylation of Chk1, but not in Rad53, nor the DNA damage-induced phosphorylation of Rad9. Furthermore, this function seems to be particularly important in the G2/M phase of the cell cycle. We also supported this data with epistasis analysis using the G2/M checkpoint activation assay (O'Shaughnessy et al., 2006). In this assay, the epistatic relationship between *rad9*$^{CDK1\text{-}9A}$ and *chk1*Δ, as well as the additive relationship between *rad9*$^{CDK1\text{-}9A}$ and *rad53*Δ, strongly indicate that the CDK1-9 sites of Rad9 function specifically to regulate Chk1 activation in response to DNA damage. Thus, the activation of Chk1 activation requires high Cdc28-Clb activity, which targets the N-terminal region of Rad9 for cell cycle-dependent phosphorylation during the G2 and early M phases of the cell cycle.

We have also elucidated the role of Cdc28 in DNA damage–induced checkpoint activation. Cdc28 activity plays a key role in DSB resection (Enserink and Kolodner, 2010; Ira et al., 2004). We have found that Cdc28 activity is absolutely required for the initial activation of Chk1 and the maintenance of Chk1 in its active state. This is irrespective of whether DNA damaging agents resulting in DSBs, SSBs or bulky lesions were used. This indicated that Chk1 activation is not simply a downstream consequence of the role of Cdc28 in DSBs resection (Huertas et al., 2008; Limbo et al., 2007) or the Cdc28-dependent role of Rad9 in inhibiting this process (Lazzaro et al., 2008). Together, our data established that CDK phosphorylation of one or more

of the 9 sites within the Rad9 N-terminal region regulate Chk1 activation during periods of the cell cycle when Cdc28/Clb kinases are active.

The molecular mechanisms of how the nine consensus CDK sites of the CAD region regulate Chk1 activation have also been partially elucidated in this study. Using an Y2H-based assay we have obtained evidence for a direct physical interaction between Rad9 and Chk1 protein that is absolutely dependent on the nine CDK sites in the Rad9 CAD. This data is consistent with our Chk1 activation and *in vitro* kinase assays. In addition, the interaction between Rad9 and Chk1 was dependent on Cdc28 activity in G2/M phase of the cell cycle. Our data led us to conclude that the Cdc28-dependent phosphorylation of the nine putative CDK phosphorylation sites located in the CAD region of Rad9 regulate a physical interaction between Rad9 and Chk1 in G2/M phase of the cell cycle when Cdc28 kinase activity is high.

Surprisingly, we also showed that the Rad9 CDK1-9 sites in the CAD are required for a Rad9-Chk1 interaction in the G1 phase of the cell cycle. This interaction is consistent with some Chk1 activation, albeit less than in G2/M, in the G1 phase of the cell cycle. Importantly, the Rad9-Chk1 interaction is not Cdc28 dependent as it was not abolished when the activity of Cdc28 was inhibited in G1 arrested cells. In this respect, the phosphorylation of either the consensus CDK sites or alternative sites by kinases other than Cdc28 may be required for the Rad9-Chk1 interaction in G1 phase. However, we also cannot exclude the possibility that the G1 interaction might be indirect. Nevertheless, this data suggested that there are two distinct mechanisms that take place either in the G1 or G2/M phases of the cell cycle by which Chk1 functions in the damage response are regulated, but only the G2/M mechanism requires Cdc28 activity. Phosphomimetic mutants might be useful to determine which of the nine sites is important for Chk1 interaction in G1 cells. Further experiments are also required to elucidate the role of Chk1 phosphorylation and, presumably activation, in G1 phase of the cell cycle.

Importantly, we extended the Y2H Rad9-Chk1 interaction data by using co-immunoprecipitation experiments to confirm the Rad9-Chk1 interaction in G2/M phase. The Rad9-Chk1 G2/M interaction does not appear to be damage-specific as it occurs in both undamaged cells and in bleocin-treated cells. Notably, we

reproducibly observed two different forms of Rad9 in a Chk1 IP, the cell cycle modified form (C-Rad9) in undamaged cells and the DNA-damaged form (D-Rad9) in bleocin-treated cells. Both forms of Rad9 were not detected in IPs performed with extracts from *rad9*$^{CDK1\text{-}9A}$ cells. Thus one or more of the nine-consensus CDK phosphorylation sites is/are also required to mediate the Rad9 interaction with Chk1 *in vivo*.

We also observed that the Rad9-Chk1 complex is a distinct, independent complex from the Rad9-Dpb11 complex, which we previously identified (Granata et al., 2010). Although we detected less Rad9 bound to Dpb11 relative to the amount of Rad9 bound to Chk1, different antibodies with different sensitivities were used and no conclusion can be taken from these experiments relative to the fraction of Rad9 either bound to Dpb11 or Chk1. It would be interesting to perform gel filtration analysis in these two complexes to clarify this matter. Note that in fission yeast evidence for a Crb2-Chk1-Cut5 complex has been reported (Mochida et al., 2004). It is possible that the Rad9-Chk1 interaction is enriched in our extracts in contrast to the Rad9-Dpb11 interaction since the latter occurs on chromatin, a fraction that is poorly represented in our soluble crude cell extracts. Similarly, a Rad9-Chk1-Dpb11 interaction might occur *in vivo* but only in the context of chromatin. To test these possibilities, it would be interesting to perform IP experiments in extracts treated with a nuclease, to the release of the chromatin-bound proteins into the soluble extracts, and investigate the Rad9-Chk1 and Rad9-Dpb11 interactions.

We also showed by immunoprecipitation experiments in *cdc28-as1* cells that the Rad9-Chk1 interaction detected in the IPs is dependent on the activity of Cdc28. Moreover, these experiments suggested that the soluble levels of Rad9 in our native cell crude extracts are lower when Cdc28 is inactivated. One explanation for lower levels of soluble Rad9 in the absence of Cdc28 activity is that Cdc28-dependent phosphorylation of Rad9 might be important for Rad9 release from damaged chromatin following its activation. IP experiments in nuclease-treated extracts from *cdc28-as1* cells in which Cdc28 activity is either active or inactive would be also useful to address if Rad9 levels are increased in the chromatin fraction when Cdc28 is inactivated and if this process also occurs in unperturbed conditions.

To identify the most important sites for Rad9-Chk1 interaction in G2/M phase of the cell cycle we first found that CDK sites 4 (S83), 5 (T110), 6 (T125) and 7 (T143) in combination with CDK1 (S11) site are required for damage-induced Chk1 phosphorylation (although not appreciably in any of the individual mutants). Interestingly, Rad9 CDK5 site (T110) and the surrounding sequence is highly conserved within the putative CAD of MCPH1 (~103-250 amino acids; Steve Jackson, *personal communication*), a checkpoint mediator protein in higher cells required for Chk1 activation through a physical between both proteins (Alderton et al., 2006). We have also dissected by co-immunoprecipitations the involvement of the specific CDK sites 4, 5, 6 and 7 either alone or in combination with CDK1 site required for Rad9-Chk1 activation. Interestingly, although no interaction was detected in both *rad9*$^{CDK4,5,6,7A}$ and *rad9*$^{CDK1,4,5,6,7A}$ cells, we observed lower Rad9 protein levels in these cells, resembling the previous results obtained when Cdc28 was inactive. Thus, Cdc28-dependent phosphorylation of Rad9 at the CDK sites 1, 4, 5, 6 and 7 might be required for Rad9 release from the chromatin in order to mediate full activation of the checkpoint kinases Rad53 and Chk1. Again, similar IP experiments in nuclease treated protein extracts would be useful to examine if the Cdc28-dependent phosphorylation CDK sites 1, 4, 5, 6 and/or 7 in Rad9 CAD region is required to release Rad9 from damaged chromatin following its PIKK-dependent hyper-phosphorylation. It would also be interesting to see if the Cdc28-dependent phosphorylation of Rad9 also regulates its chromatin recruitment/release in undamaged conditions.

To further refine the key residues in Rad9 CAD responsible for Rad9-Chk1 interaction we adopted a different strategy. Using CAD$^{CDK1\text{-}9A}$ as a starting point we individually reverted candidate residues back to the wild type residue (i.e. the other residues remained as alanine mutations). This analysis strongly implicated CDK7 (T143) as the most important Cdc28-dependent residue required for Rad9-Chk1 interaction, followed by CDK6 site. The interaction is further enhanced when wild type CDK6 or CDK7 is combined with wild type CDK1 site. Note that Dbp11 is known to mediate Rad9 recruitment to chromatin during the G2/M and this requires CDK1 site (S11). We then proposed that CDK1 site might contribute to Rad9 recruitment and stabilization onto chromatin through binding to Dpb11, hence further promoting Rad9-Chk1 interaction via CDK7 residue. Although it has not

been reported that CDK7 site is phosphorylated *in vivo*, mass spectrometry data from our laboratory has identified this residue to be phosphorylated during an unperturbed cell cycle (Finn K., *unpublished data*). It would be interesting to repeat the Y2H interaction analysis using $CAD^{CDK1\text{-}9A}$ in which CDK site 7 was mutated to a phosphomimetic residue (i.e. $CAD^{CDK1\text{-}9A+7D}$ or $CAD^{CDK1\text{-}9A+7E}$) in order to demonstrate that the phosphorylation status of CDK7 is important to mediate Rad9-Chk1 interaction. Alternatively, or perhaps in addition, the generation of a phospho-specific antibody against CDK7 should be generated and used to study this phosphorylation event in cell extracts. On going immunoprecipitation experiments in our laboratory are also being performed to confirm that the wild type CDK7 alone or in combination with wild type CDK1 site is sufficient to mediate the Rad9-Chk1 interaction *in vivo*.

Interestingly, alignment of the Rad9 CAD fragment with its fission homologue, Crb2, shows that the CDK6 and CDK7 residues of Rad9 are highly conserved (Blankley and Lydall, 2004), suggesting a functional conservation between these proteins to drive its checkpoint functions, particularly in their interaction with Chk1. Therefore, it would be interesting to investigate whether the mechanism behind this process is regulated by CDK-dependent phosphorylation of the conserved CDK residues in a similar manner to Rad9.

Increasing information of the different checkpoint roles of the budding yeast mediator protein Rad9 has provided further insight into the DNA damage response. Even after extensive work by several laboratories only small regions of the protein (just $1/3^{rd}$ of the protein in total) have been assigned specific functions. It would be interesting to conduct detailed structure function studies of the remainder of Rad9 protein with unassigned functions. For example, towards the middle of the protein we have identified a 32 amino acid stretch with significant homology to 53BP1 (*data not shown*). This region contains one consensus PIKK and two consensus CDK phosphorylation sites. Deletion of this region followed by detailed phenotypic characterization might uncover a novel role for Rad9 that is conserved with 53BP1, its orthologue in higher cells.

In higher cells, the role played by DDR mediator proteins is more complex than in

yeasts as multiple mediators are known and whose molecular mechanisms in checkpoint activation remain largely uncharacterised (Smits et al., 2010; Stracker et al., 2009). Among the mediators, Claspin-dependent activation of CHK1 is best characterized, however, MCPH1, BRCA1 and MDC1 also play an undefined role in this activation. Our work suggests that activation of human CHK1 by mediator proteins, possibly those related to budding yeast Rad9, may also be integrated into cell cycle stage by their prior CDK-dependent phosphorylation and dynamic interaction with CHK1. Additionally, the extensive cell cycle phosphorylation of these proteins is likely to fine-tune their DNA damage functions, as we have observed with their budding yeast homologue, Rad9.

## 4.3. REFERENCES

Alderton, G.K., Galbiati, L., Griffith, E., Surinya, K.H., Neitzel, H., Jackson, A.P., Jeggo, P.A., and O'Driscoll, M. (2006). Regulation of mitotic entry by microcephalin and its overlap with ATR signalling. Nat Cell Biol *8*, 725-733.

Blankley, R.T., and Lydall, D. (2004). A domain of Rad9 specifically required for activation of Chk1 in budding yeast. J Cell Sci *117*, 601-608.

Bosotti, R., Isacchi, A., and Sonnhammer, E.L. (2000). FAT: a novel domain in PIK-related kinases. Trends Biochem Sci *25*, 225-227.

Enserink, J.M., and Kolodner, R.D. (2010). An overview of Cdk1-controlled targets and processes. Cell Div *5*, 11.

Gilbert, C.S., Green, C.M., and Lowndes, N.F. (2001). Budding yeast Rad9 is an ATP-dependent Rad53 activating machine. Mol Cell *8*, 129-136.

Granata, M., Lazzaro, F., Novarina, D., Panigada, D., Puddu, F., Abreu, C.M., Kumar, R., Grenon, M., Lowndes, N.F., Plevani, P.*, et al.* (2010). Dynamics of Rad9 chromatin binding and checkpoint function are mediated by its dimerization and are cell cycle-regulated by CDK1 activity. PLoS Genet *6*.

Huertas, P., Cortes-Ledesma, F., Sartori, A.A., Aguilera, A., and Jackson, S.P. (2008). CDK targets Sae2 to control DNA-end resection and homologous recombination. Nature *455*, 689-692.

Ira, G., Pellicioli, A., Balijja, A., Wang, X., Fiorani, S., Carotenuto, W., Liberi, G., Bressan, D., Wan, L., Hollingsworth, N.M.*, et al.* (2004). DNA end resection, homologous recombination and DNA damage checkpoint activation require CDK1. Nature *431*, 1011-1017.

Lazzaro, F., Sapountzi, V., Granata, M., Pellicioli, A., Vaze, M., Haber, J.E., Plevani, P., Lydall, D., and Muzi-Falconi, M. (2008). Histone methyltransferase Dot1 and Rad9 inhibit single-stranded DNA accumulation at DSBs and uncapped telomeres. EMBO J *27*, 1502-1512.

Limbo, O., Chahwan, C., Yamada, Y., de Bruin, R.A., Wittenberg, C., and Russell, P. (2007). Ctp1 is a cell-cycle-regulated protein that functions with Mre11 complex to control double-strand break repair by homologous recombination. Mol Cell *28*, 134-146.

Liu, S., Shiotani, B., Lahiri, M., Marechal, A., Tse, A., Leung, C.C., Glover, J.N., Yang, X.H., and Zou, L. (2011). ATR autophosphorylation as a molecular switch for checkpoint activation. Mol Cell *43*, 192-202.

Mallory, J.C., and Petes, T.D. (2000). Protein kinase activity of Tel1p and Mec1p, two Saccharomyces cerevisiae proteins related to the human ATM protein kinase. Proc Natl Acad Sci U S A *97*, 13749-13754.

Mochida, S., Esashi, F., Aono, N., Tamai, K., O'Connell, M.J., and Yanagida, M. (2004). Regulation of checkpoint kinases through dynamic interaction with Crb2. EMBO J *23*, 418-428.

O'Shaughnessy, A.M., Grenon, M., Gilbert, C., Toh, G.W., Green, C.M., and Lowndes, N.F. (2006). Multiple approaches to study S. cerevisiae Rad9, a prototypical checkpoint protein. Methods Enzymol *409*, 131-150.

Paciotti, V., Clerici, M., Lucchini, G., and Longhese, M.P. (2000). The checkpoint protein Ddc2, functionally related to S. pombe Rad26, interacts with Mec1 and is regulated by Mec1-dependent phosphorylation in budding yeast. Genes Dev *14*, 2046-2059.

Schwartz, M.F., Duong, J.K., Sun, Z., Morrow, J.S., Pradhan, D., and Stern, D.F. (2002). Rad9 phosphorylation sites couple Rad53 to the Saccharomyces cerevisiae DNA damage checkpoint. Mol Cell *9*, 1055-1065.

Sibanda, B.L., Chirgadze, D.Y., and Blundell, T.L. (2010). Crystal structure of DNA-PKcs reveals a large open-ring cradle comprised of HEAT repeats. Nature *463*, 118-121.

Smits, V.A., Warmerdam, D.O., Martin, Y., and Freire, R. (2010). Mechanisms of ATR-mediated checkpoint signalling. Front Biosci *15*, 840-853.

Storici, F., Durham, C.L., Gordenin, D.A., and Resnick, M.A. (2003). Chromosomal site-specific double-strand breaks are efficiently targeted for repair by oligonucleotides in yeast. Proc Natl Acad Sci U S A *100*, 14994-14999.

Storici, F., Lewis, L.K., and Resnick, M.A. (2001). In vivo site-directed mutagenesis using oligonucleotides. Nat Biotechnol *19*, 773-776.

Storici, F., and Resnick, M.A. (2003). Delitto perfetto targeted mutagenesis in yeast with oligonucleotides. Genet Eng (N Y) *25*, 189-207.

Storici, F., and Resnick, M.A. (2006). The delitto perfetto approach to in vivo site-directed mutagenesis and chromosome rearrangements with synthetic oligonucleotides in yeast. Methods Enzymol *409*, 329-345.

Stracker, T.H., Usui, T., and Petrini, J.H. (2009). Taking the time to make important decisions: the checkpoint effector kinases Chk1 and Chk2 and the DNA damage response. DNA Repair (Amst) *8*, 1047-1054.

Sweeney, F.D., Yang, F., Chi, A., Shabanowitz, J., Hunt, D.F., and Durocher, D. (2005). Saccharomyces cerevisiae Rad9 acts as a Mec1 adaptor to allow Rad53 activation. Curr Biol *15*, 1364-1375.

Wakayama, T., Kondo, T., Ando, S., Matsumoto, K., and Sugimoto, K. (2001). Pie1, a protein interacting with Mec1, controls cell growth and checkpoint responses in Saccharomyces cerevisiae. Mol Cell Biol *21*, 755-764.

Zhao, X., Muller, E.G., and Rothstein, R. (1998). A suppressor of two essential checkpoint genes identifies a novel protein that negatively affects dNTP pools. Mol Cell *2*, 329-340.

Zhu, H., Klemic, J.F., Chang, S., Bertone, P., Casamayor, A., Klemic, K.G., Smith, D., Gerstein, M., Reed, M.A., and Snyder, M. (2000). Analysis of yeast protein kinases using protein chips. Nat Genet *26*, 283-289.

# APPENDIX A: AUTHORS PUBLICATION

## Dynamics of Rad9 chromatin binding and checkpoint function are mediated by its dimerization and are cell cycle-regulated by Cdk1 activity

Magda Granata[1•], Federico Lazzaro[1•], Daniele Novarina[1], Davide Panigada[1], Fabio Puddu[1], Carla Manuela Abreu[2], Ramesh Kumar[2], Muriel Grenon[2], Noel F. Lowndes[2], Paolo Plevani[1*], Marco Muzi-Falconi[1*]

[1] Dipartimento di Scienze Biomolecolari e Biotecnologie, Università degli Studi di Milano, Milano, Italy,

[2] Centre for Chromosome Biology, School of Natural Science, National University of Ireland Galway, Galway, Ireland

OPEN ACCESS Freely available online PLoS GENETICS

# Dynamics of Rad9 Chromatin Binding and Checkpoint Function Are Mediated by Its Dimerization and Are Cell Cycle–Regulated by CDK1 Activity

**Magda Granata[1☯], Federico Lazzaro[1☯], Daniele Novarina[1], Davide Panigada[1], Fabio Puddu[1], Carla Manuela Abreu[2], Ramesh Kumar[2], Muriel Grenon[2], Noel F. Lowndes[2], Paolo Plevani[1]*, Marco Muzi-Falconi[1]***

**1** Dipartimento di Scienze Biomolecolari e Biotecnologie, Università degli Studi di Milano, Milano, Italy, **2** Centre for Chromosome Biology, School of Natural Science, National University of Ireland Galway, Galway, Ireland

## Abstract

*Saccharomyces cerevisiae* Rad9 is required for an effective DNA damage response throughout the cell cycle. Assembly of Rad9 on chromatin after DNA damage is promoted by histone modifications that create docking sites for Rad9 recruitment, allowing checkpoint activation. Rad53 phosphorylation is also dependent upon BRCT-directed Rad9 oligomerization; however, the crosstalk between these molecular determinants and their functional significance are poorly understood. Here we report that, in the G1 and M phases of the cell cycle, both constitutive and DNA damage-dependent Rad9 chromatin association require its BRCT domains. In G1 cells, GST or FKBP dimerization motifs can substitute to the BRCT domains for Rad9 chromatin binding and checkpoint function. Conversely, forced Rad9 dimerization in M phase fails to promote its recruitment onto DNA, although it supports Rad9 checkpoint function. In fact, a parallel pathway, independent on histone modifications and governed by CDK1 activity, allows checkpoint activation in the absence of Rad9 chromatin binding. CDK1-dependent phosphorylation of Rad9 on Ser11 leads to specific interaction with Dpb11, allowing Rad53 activation and bypassing the requirement for the histone branch.

**Citation:** Granata M, Lazzaro F, Novarina D, Panigada D, Puddu F, et al. (2010) Dynamics of Rad9 Chromatin Binding and Checkpoint Function Are Mediated by Its Dimerization and Are Cell Cycle–Regulated by CDK1 Activity. PLoS Genet 6(8): e1001047. doi:10.1371/journal.pgen.1001047

**Editor:** Gregory P. Copenhaver, The University of North Carolina at Chapel Hill, United States of America

**Received** December 24, 2009; **Accepted** July 2, 2010; **Published** August 5, 2010



**Funding:** This work was supported by grants from AIRC and Fondazione Cariplo to PP and MM-F, the European Union FP6 Integrated Project DNA repair contract number 512113 to PP and NFL, a NUIG college fellowship to RK, and a Science Foundation Ireland Principal Investigator award 07/IN1/B958 to NFL. CMA was supported by Fundação para a Ciência e a Tecnologia (SFRH/BD/42128/2007, Portugal). The funders had no role in study design, data collection and analysis, decision to publish or preparation of the manuscript.

**Competing Interests:** The authors have declared that no competing interests exist.

* E-mail: marco.muzifalconi@unimi.it (MM-F); paolo.plevani@unimi.it (PP)

☯ These authors contributed equally to this work.

## Introduction

The DNA damage checkpoint coordinates cell cycle progression, DNA repair, replication, recombination, apoptosis and senescence in response to genotoxic stress. Defects in this surveillance mechanism lead to increased genomic instability, cancer susceptibility, ageing and several human pathologies [1,2]. The checkpoint is organized as a signal transduction cascade, whose players have been conserved throughout evolution [3,4]. When DNA is damaged, cells are able to sense and process the lesions generating a series of phosphorylation events, which are then amplified and propagated to specific targets [3,4]. Critical checkpoint factors are phosphorylated in response to DNA damage and their order of functions in the cascade has been mainly inferred by monitoring their phosphorylation state [5]. The apical kinases in the pathway are members of a family of phosphatidylinositol 3′ kinase-like kinases (PIKKs), which includes Mec1 and Tel1 from budding yeast, as well as mammalian ATM, ATR and DNA-PK [6]. In the yeast *Saccharomyces cerevisiae* the first biochemical event in response to checkpoint activation is the Mec1-dependent phosphorylation of its interacting subunit Ddc2 [7–9]. Other critical Mec1 targets are histone H2A, the 9-1-1 complex and the Rad9 mediator which is necessary for the recruitment and activation of the main effector kinase Rad53 [10–16]. Rad53 phosphorylation is a key step in the signal transduction cascade and it is generally used as a marker to monitor full checkpoint activation [17].

In a pioneering study, *RAD9* was the first DNA damage checkpoint gene identified in yeast and it is required for proper DNA damage response in all cell cycle phases and in response to a variety of genotoxins [18–20]. Rad9 is a large protein of 148 kDa containing a tandem repeat of the BRCT (BRCA1 C-terminus) motif, which is required for Rad9 oligomerization and function [21–23]. Until recently the biochemical role of the *RAD9* gene product remained obscure. Gilbert et al., were the first to purify Rad9 complexes from undamaged and UV-treated cells; structural characterization of such complexes led to the proposal that Rad9 recruits and catalyzes the activation of Rad53, by acting as a scaffold protein bringing Rad53 molecules in close proximity, thus facilitating the Rad53 autophosphorylation reaction [14].

The Rad9 protein contains several potential target sites for CDK1/Cdc28 kinase and PIKK-directed phosphorylation [24].

## Author Summary

In response to DNA damage all eukaryotic cells activate a surveillance mechanism, known as the DNA damage checkpoint, which delays cell cycle progression and modulates DNA repair. Yeast *RAD9* was the first DNA damage checkpoint gene identified. The genetic tools available in this model system allow to address relevant questions to understand the molecular mechanisms underlying the Rad9 biological function. By chromatin-binding and domain-swapping experiments, we found that Rad9 is recruited into DNA both in unperturbed and in DNA–damaging conditions, and we identified the molecular determinants required for such interaction. Moreover, the extent of chromatin-bound Rad9 is regulated during the cell cycle and influences its role in checkpoint activation. In fact, the checkpoint function of Rad9 in G1 cells is solely mediated by its interaction with modified histones, while in M phase it occurs through an additional scaffold protein, named Dpb11. Productive Rad9-Dpb11 interaction in M phase requires Rad9 phosphorylation by CDK1, and we identified the Ser11 residue as the major CDK1 target. The model of Rad9 action that we are presenting can be extended to other eukaryotic organisms, since Rad9 and Dpb11 have been conserved through evolution from yeast to mammalian cells.


Rad9 is phosphorylated in an unperturbed cell cycle and it is hyper-phosphorylated in a Mec1- and/or Tel1-dependent manner after genotoxic treatments [12,13]. This hyper-phosphorylation is a pre-requisite for Rad9-Rad53 association, which is mediated by the two forkhead associated (FHA) Rad53 domains and specific Rad9 amino acid residues that are modified in the hyper-phosphorylated Rad9 form [12,13,15,16,25–27]. Recent data confirmed that the Rad9 BRCT domains mediate Rad9 oligomerization, and these interactions are also modulated by Mec1/Tel1-dependent phosphorylation of a SQ/TQ cluster domain (SCD) in Rad9. Rad9 oligomerization is required to maintain checkpoint signaling through a feedback loop involving Rad53-dependent phosphorylation of the Rad9 BRCT domains, which attenuates BRCT-SCD interactions [27].

Despite the fundamental nature of the cellular response to DNA damage, Rad9 and its *Schizosaccharomyces pombe* and metazoan orthologs Crb2 and 53BP1 show a modest level of amino acid sequence conservation. Dimerization mediated by the BRCT domains has been shown to be essential for the biological function of both Rad9 and Crb2 [21,28], however, 53BP1 oligomerization occurs in a BRCT-independent manner [29,30]. Recent structural analysis showed that an equivalent surface is conserved to a certain degree also in 53BP1 and it provides the binding site for p53. It was thus suggested that a functional requirement for dimerization of a checkpoint mediator may have been conserved in the evolution, but in metazoan organisms it may be delivered via a second protein rather than through homotypic interactions [31].

In the last few years it became evident that chromatin remodelling activities and post-translational modifications of chromatin components, including histones, influence DNA damage checkpoint signalling and repair in all eukaryotic cells (see [32] for a recent review). Moreover, it has been recently suggested that Rad9 may also be chromatin-bound in the absence of DNA damage [22]. This dynamic interaction with chromatin appears to require the Tudor domain of Rad9 and methylated lysine 79 of histone H3 (H3-K79me). Furthermore, this interaction modulates Rad9 functions after DNA damage [22,23,33–35]. However, the Crb2 and 53BP1 orthologues of Rad9 both recognize H4 methylated at lysine 20 (H4-K20me), although human 53BP1 may also be recruited to chromatin through interactions with H3-K79me [34,36–39].

For the Rad9/Crb2/53BP1 mediator proteins, efficient recruitment seems to require additional molecular interactions. Rad9 and Crb2 interact via their BRCT domains with H2A phosphorylated at serine 129 (γH2A) at sites of DNA damage [22,31,37,40–42]. 53BP1 binding to DSBs is facilitated by phosphorylation of serine 139 of the histone variant H2AX (γH2AX) [29,43–45]. It has been reported that various oligomerization domains in 53BP1 facilitate its recruitment to damaged DNA sites [30]. Moreover, 53BP1 recruitment to chromatin is facilitated by ubiquitination of H2A and H2AX by RNF8 through a yet unidentified mechanism [46–48].

Recently, it has been shown that Dpb11 in *S. cerevisiae* and its *S. pombe* and metazoan orthologs, termed Rad4/Cut5 and TopBP1, respectively, are required for full PIKK-dependent checkpoint activation in response to DNA damage [49,50]. Moreover it has been suggested that Dpb11 orthologs may modulate checkpoint activation through interaction with mediator/adaptor proteins [37,51]. To explore the functional role and the relationship between the BRCT domains and Rad9 ability to bind chromatin, we have analyzed both Rad9 chromatin recruitment and checkpoint activation in cells engineered to express various forms of Rad9 harboring mutated BRCT domains, including point mutations, deletion and substitutions with heterologous dimerization domains. We found that the requirements for Rad9 binding to chromatin are different in G1 or in M phase cells and in damaging versus unperturbed conditions. Moreover, we tested the requirements for Rad9 chromatin binding in yeast mutants defective in either the histone-dependent and/or histone-independent pathways essential for full checkpoint activation in M phase. Importantly, we found that CDK1-dependent Rad9 phosphorylation on Ser11 modulates the Dpb11-dependent branch in the M phase of the cell cycle in a chromatin-independent manner.

## Results

### Rad9 BRCT domains are required for its binding to chromatin in unperturbed and DNA damaging conditions

The Rad9 checkpoint mediator protein contains a tandem repeat of the BRCT motif at its C-terminus. Previous experiments have shown that the BRCT domains are critical for the activation of the DNA damage checkpoint and two-hybrid and GST pull-down analysis indicated that the BRCT domains modulate Rad9-Rad9 interactions [21]. More recently, it has been shown that Rad9 mutations in a conserved region of the first BRCT motif affect binding to γH2A, thus altering the G1 checkpoint signaling in response to DSBs [22,40] and the G2/M response to uncapped telomeres [23]. However, the mutations analyzed did not influence Rad9 chromatin binding in unperturbed conditions [22].

The *rad9-F1104L* or the *rad9-W1280L* mutations substitute the most highly conserved amino acid residues in the two BRCT motifs and each mutation affects productive Rad9-Rad9 interactions [21]. We tested whether such *rad9* mutations impair Rad9 recruitment to chromatin both in unperturbed and DNA damaging conditions. As expected, a proportion of wild-type Rad9 migrated much more slowly under our gel running conditions after UV treatment, consistent with hyper-phosphorylation of Rad9 (Figure 1A). A relevant fraction of Rad9 was found associated to chromatin in the absence of DNA damage, both in G1- and in M-arrested cells, confirming previous observations [22]. Control experiments were routinely performed to verify the distribution of standard protein markers in the soluble and

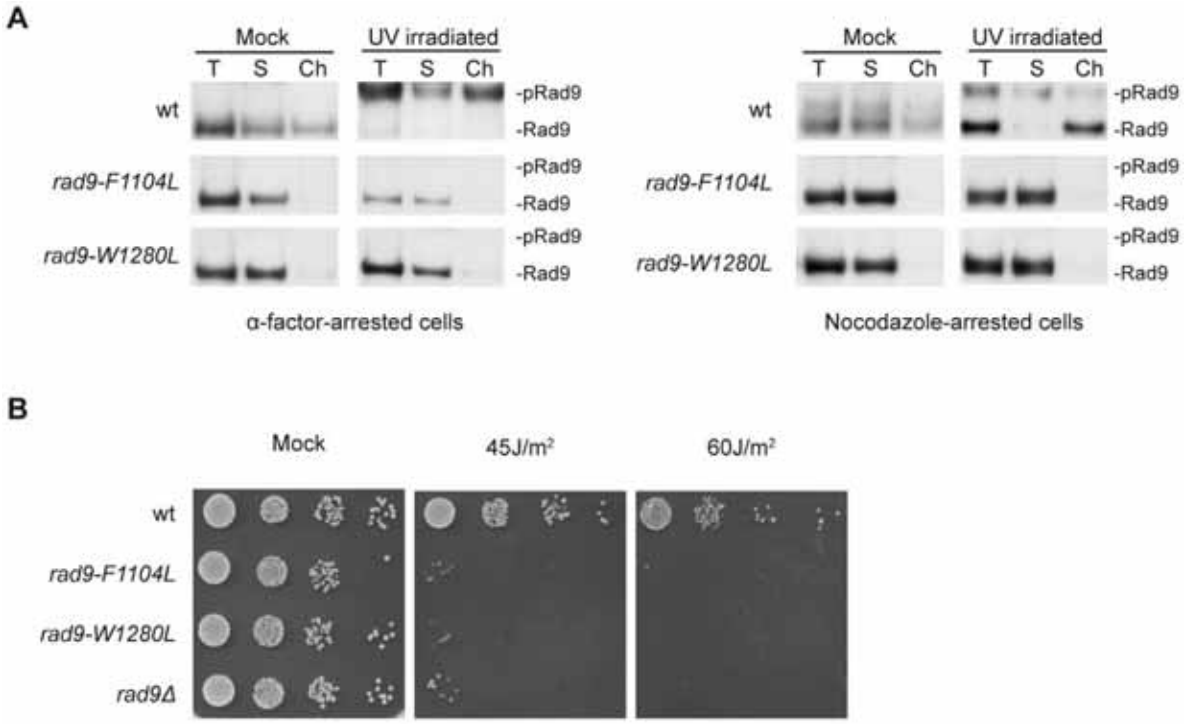


**Figure 1. Rad9 chromatin binding requires an intact BRCT domains in UV–treated and in unperturbed conditions.** (A) wt (K699), *rad9-F1104L* (YNOV15), *rad9-W1280L* (YNOV31) strains were arrested in G1 with α-factor or in M with nocodazole and either mock or UV irradiated (75 J/m$^2$). 10 min after irradiation, samples were collected and analyzed in their total (T), soluble (S) and chromatin-enriched (Ch) fractions. Blots were probed with anti-Rad9 antibodies and, after staining, the blots were cut to eliminate the Rad9-unrelated protein species migrating adjacent to the hyper-phosphorylated Rad9 isoform (Figure S1A). The positions of Rad9 and its hyper-phosphorylated isoform (pRad9) are indicated. (B) The same yeast strains analyzed in A and a *rad9Δ* strain (YMAG88) were grown overnight to log phase and serial dilutions were spotted onto YPD plates, which were then irradiated at the indicated UV doses and incubated for 3 days.
doi:10.1371/journal.pgen.1001047.g001

chromatin fractions (Figure S1B). In various experiments we consistently found that the ratio of hyper- to hypo-phosphorylated Rad9 was approximately constant in both the soluble and chromatin fractions in G1 cells. Interestingly, in M phase cells, hyper-phosphorylated Rad9 was mostly present in the soluble fraction, while chromatin was enriched in the hypo-phosphorylated form (Western blot quantitation are shown in Figure S1C). As shown in Figure 1A, any of the two BRCT mutations abolished Rad9 phosphorylation and recruitment to chromatin in G1- or M-arrested cells. As expected [21], *rad9-F1104L* and *rad9-W1280L* mutant cells were highly sensitive to UV treatments (Figure 1B).

These results indicate that BRCT domains influence not only Rad9 binding to chromatin by modulating its interaction with γH2A after DNA damage [22], but they also control Rad9 recruitment to chromatin in unperturbed conditions.

## A heterologous dimerization domain restores Rad9 binding to chromatin in G1-arrested, but not M-arrested, cells

To further evaluate the relevance of Rad9-Rad9 interactions in chromatin binding, we generated a set of yeast strains in which the C-terminal region of Rad9, containing the BRCT motifs, was substituted with either a 13-MYC epitope or a GST tag (see Materials and Methods). The latter has been shown to act as a heterologous constitutive dimerization domain [28,52,53].

As shown in Figure 2A, the GST tag was capable of driving, albeit somewhat less efficiently, Rad9 chromatin binding in G1-arrested cells, both in the absence or presence of DNA damage. Importantly, Rad9ΔBRCT::GST recruitment to chromatin still occurs through its interaction with H3-K79me, as it was drastically reduced in a *dot1Δ* background, lacking the specific H3-K79 histone methyl-transferase. Rad9 dimerization through the GST tag also significantly recovered Rad9 hyper-phosphorylation after UV irradiation and full checkpoint function (Figure 2A and data not shown).

It must be underlined that addition of the GST tag to Rad9ΔBRCT, allowing Rad9 dimerization, reconstitutes chromatin binding even though Rad9ΔBRCT::GST lacks the BRCT tandem repeats and is, therefore, unable to interact with γH2A [22]. These authors suggested that, after DNA damage, Rad9 shifts from H3-K79me to phosphorylated H2A-S129, and this translocation would be deficient in *rad9ΔBRCT::GST* cells. As a consequence of its defective interaction with γH2A, binding of Rad9ΔBRCT::GST to chromatin is probably much less stable. This hypothesis may explain the finding that in the *rad9ΔBRCT::GST* strain the majority of phosphorylated Rad9 after UV irradiation in G1 is found in the soluble fraction (Figure 2A).

To further support the role of Rad9 dimerization in its chromatin binding in G1-arrested cells solely by inducing Rad9-Rad9 interactions, we tested the possibility to direct a Rad9ΔBRCT isoform to chromatin by adding to the truncated protein a FKBP

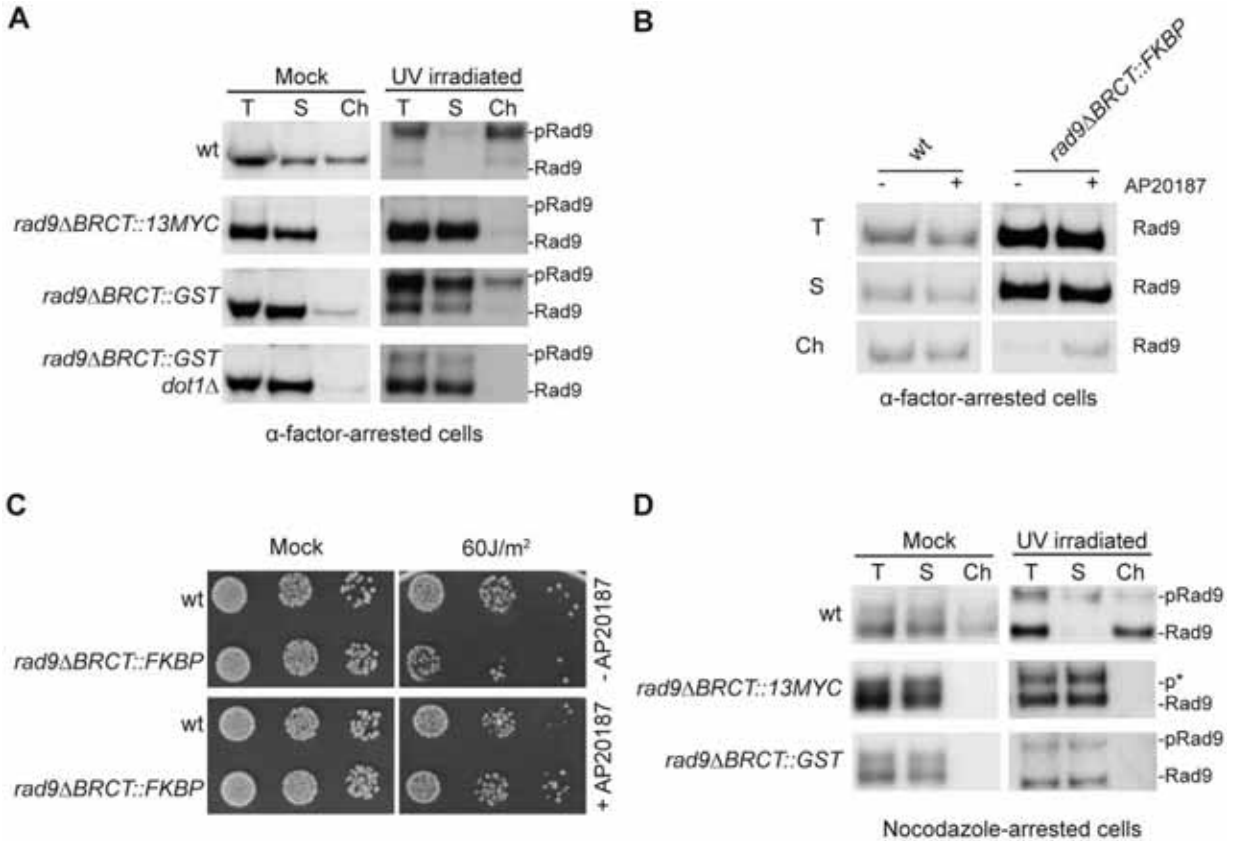


**Figure 2. GST-driven Rad9 dimerization recovers its binding to chromatin in G1, but not in M phase.** (A) wt (K699), *rad9ΔBRCT::13MYC* (YFL696/1b), *rad9ΔBRCT::GST* (YMAG74) and *rad9ΔBRCT::GST dot1Δ* (YFL773/2c) cells were arrested in G1 with α-factor and either mock or UV irradiated (75 J/m$^2$). After 10 min, samples were collected and analyzed in their total (T), soluble (S) and chromatin-enriched (Ch) fractions. Blots were probed with anti Rad9 antibodies as in the legend to Figure 1A. (B) wt (K699) and *rad9ΔBRCT::FKBP* (YFL901) cells were incubated for 6 h in the presence or in the absence of the dimerization-inducing molecule AP20187, blocked in G1 with α-factor and analyzed in their total (T), soluble (S) and chromatin-enriched (Ch) fractions. Blots were probed with anti Rad9 antibodies. (C) The same strains as in B were grown overnight to log phase and incubated for 6 h in the presence or in the absence of the dimerization-inducing molecule AP20187. Serial dilutions were spotted onto YPD plates, which were then irradiated at the indicated UV doses and incubated for 3 days. (D) Western blot analysis of the total, soluble and chromatin-enriched fractions from wt (K699), *rad9ΔBRCT::13MYC* (YFL696/1b) and *rad9ΔBRCT::GST* (YMAG74) cells arrested in M phase and either mock or UV irradiated (75 J/m$^2$). In all panels, the positions of Rad9 and its hyper-phosphorylated isoform (pRad9) are indicated. p* marks a partially phosphorylated Rad9 species.
doi:10.1371/journal.pgen.1001047.g002

tag, which can dimerize only in the presence of the small inducing molecule AP20187 [54]. Indeed, the presence of the FKBP tag partially rescued Rad9 chromatin binding in G1-arrested cells, but only in the presence of inducing AP20187 (Figure 2B). Importantly, addition of the dimerization inducing molecule fully recovered the UV sensitivity of *rad9DBRCT* cells (Figure 2C).

Contrary to our observations in G1-arrested cells, the heterologous GST dimerization domain did not rescue Rad9 binding to chromatin in nocodazole-arrested cells, although it restored checkpoint activation after DNA damage (Figure 2D, Figure 3A). Rad9 missing the BRCT domains only exhibits partial phosphorylation; this form can be distinguished from the hyper-phosphorylated isoform due to different electrophoretic mobility and its incapacity to activate Rad53 (see Figure 3A).

Altogether, the findings reported above indicate that dimerization is required for Rad9 to bind H3-K79me in G1-arrested cells, both with and without an exogenous DNA damaging agent. However, this is not the case in M phase-arrested cells, where GST-directed Rad9 dimerization partially recovers genotoxin-induced Rad9 hyper-phosphorylation, but fails to rescue its binding to chromatin. This may suggest that, at least in M phase, Rad9 chromatin binding is not directly linked to Rad9 hyper-phosphorylation.

## GST-driven Rad9 dimerization rescues checkpoint activation and UV–sensitivity, despite undetectable chromatin binding

Although the addition of a heterologous dimerization domain to truncated Rad9ΔBRCT was not able to allow Rad9 chromatin binding in M phase-arrested cells, it rescues Rad53 activation after UV irradiation. In fact, as shown in Figure 3A, the phosphorylation state of the effector checkpoint kinase, Rad53, was found to be very different after UV-irradiation of *rad9ΔBRCT::GST* or *rad9ΔBRCT::13MYC* cells arrested with nocodazole. The hyper-phosphorylated form of Rad53 is absent in UV treated *rad9ΔBRCT::13MYC* cells, while it is clearly detectable in *rad9ΔBRCT::GST* cells. Although the extent of

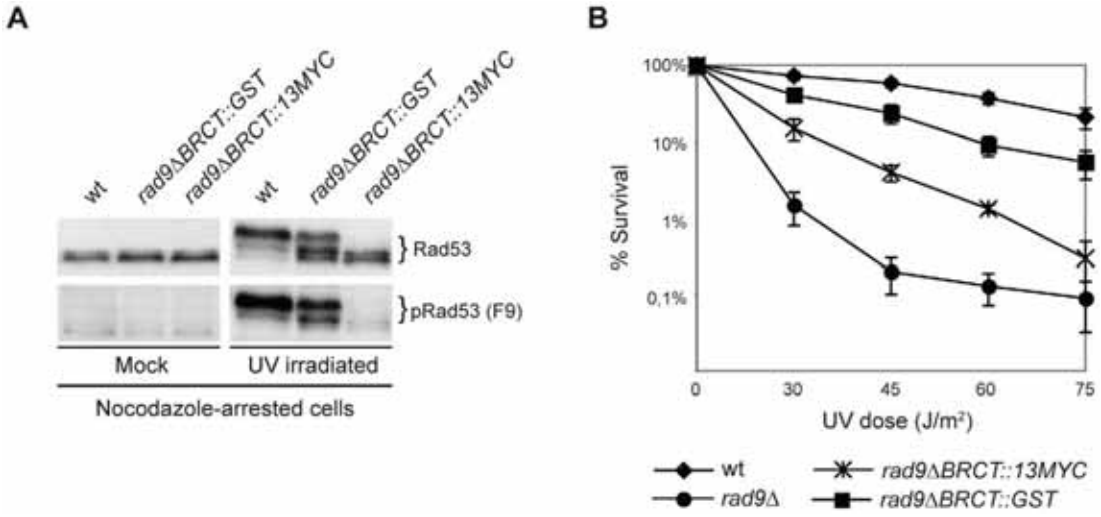


**Figure 3. GST-driven Rad9 dimerization allows M checkpoint function regardless of Rad9 chromatin binding.** (A) wt (K699), *rad9ΔBRCT::13MYC* (YFL696/1b), *rad9ΔBRCT::GST* (YMAG74) cells were cultured to mid-log phase, arrested in M with nocodazole, and either mock or UV irradiated (75 J/m$^2$); 10 min after irradiation, Rad53 phosphorylation was analyzed by SDS-PAGE and Western blotting with polyclonal Rad53 antibodies and with the F9 monoclonal antibody (Mab) recognizing only the hyper-phosphorylated active form of Rad53 to monitor checkpoint activation. (B) The same cells analyzed in A and a *rad9Δ* control strain (YMAG88) were cultured overnight, diluted and plated on YPD plates, which were irradiated with the indicated UV doses. Cell survival was assayed by determining the number of colonies grown on plates after 2 days; error bars were obtained from 3 independent experiments.
doi:10.1371/journal.pgen.1001047.g003

Rad53 phosphorylation was reduced in *rad9ΔBRCT::GST* relative to wild-type cells, the presence of the heterologous GST dimerization domain recovers the Rad9 checkpoint function, as confirmed by a direct checkpoint assay (data not shown). This conclusion is also supported by the observation that addition of the GST tag significantly rescued, although not completely, the UV sensitivity of the *rad9ΔBRCT::13MYC* strain (Figure 3B), and these findings are in agreement with previous experiments in *S.pombe* [28].

Thus far our data indicate that dimerization of Rad9 directed by an heterologous domain confers activation of the DNA damage checkpoint cascade, as well as significant resistance to UV in M phase-arrested cells, despite undetectable binding of Rad9 to chromatin (see Figure 2D).

## Checkpoint activation in M phase requires CDK1 activity and is driven by Rad9–Dpb11 interaction

We have recently demonstrated that in the M phase of the cell cycle, full activation of the DNA damage checkpoint in response to various genotoxic stress is dependent upon Dpb11 [50]. Our data suggested that Dpb11 facilitates the recruitment of Rad9 proximally to DNA lesions through a mechanism independent of histone modifications. Indeed, as shown in Figure 4A, checkpoint activation after UV irradiation of nocodazole-arrested cells is only partially affected either in *dot1Δ* or in *dpb11ΔCT* cells. On the other hand, *dot1Δ dpb11ΔCT* double mutant cells are dramatically deficient in Rad53 phosphorylation since both the histone-dependent and histone-independent pathways for checkpoint activation are not functional. This finding can be interpreted by hypothesizing that when Rad9 cannot bind to chromatin via histone marks, Dpb11 may act as a platform for Rad9 recruitment in a histone-independent manner. Moreover, because the Dpb11-dependent pathway is particularly relevant in the G2 to M phases of the cell cycle [50], it was tempting to hypothesize that the proposed interaction between Rad9 and Dpb11 might be regulated by cell cycle-dependent control mechanisms [55]. Initially, we monitored this interaction using two-hybrid analysis performed at different cell cycle stages (see Materials and Methods). As shown in Figure 4B, a strong Rad9-Dpb11 interaction was observed in nocodazole-arrested cells. Several independent two-hybrid experiments showed that Rad9-Dpb11 interaction was more evident in M- rather than in G1-arrested cells. Experiments performed with a bait and a prey already known to interact by two-hybrid, indicate that the M/G1 ratio of Rad9-Dpb11 interaction was significantly higher than that found in the controls, suggesting a cell cycle-specific effect (Figure S2A). The Rad9-Dpb11 interaction was further confirmed biochemically (see below).

Since the interaction between Rad9 and Dpb11 appears to be induced in M phase, we reasoned that the Dpb11-dependent branch of the DNA damage checkpoint in M phase might be related to the increasing level of CDK1 kinase activity as cells move through the S, G2 and M phases of the cell cycle. To address this issue, we took advantage of the *cdc28-as1* mutant (in which only the Cdc28 kinase is specifically sensitive to bulky ATP analogues, such as 1NMPP1 [56]) to conditionally inactivate CDK1 in nocodazole-treated cells. Cdc28 kinase activity was inhibited or not with 1NMPP1 in nocodazole arrested cells and mitotic cells were then mock- or UV irradiated to induce DNA damage. Western blot analysis of Rad53 revealed that CDK1 inhibition abolished phosphorylation of Rad53 in the absence of the histone-dependent pathway, while no effect was observed in *DOT1* cells (Figure 4C). A similar experiment was performed by tethering checkpoint factors to DNA in the absence of damage [57]. The difference between our result and that reported by Bonilla, may be explained if, in their experimental conditions, without the addition of genotoxic agents, checkpoint activation is independent upon the Dpb11 branch.

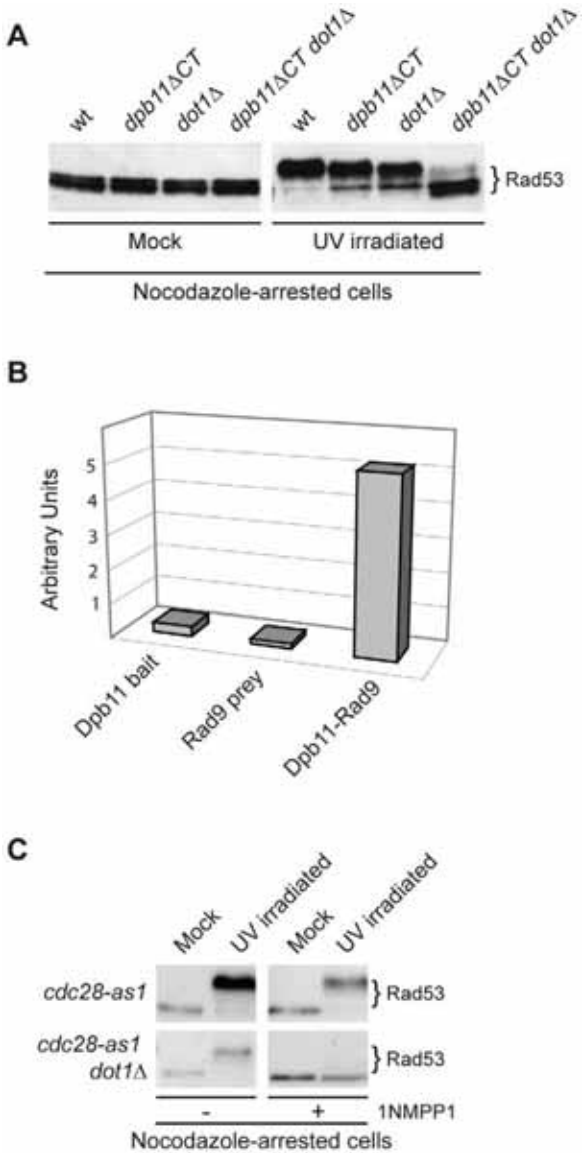


**Figure 4. A cell cycle–dependent interaction between Dpb11 and Rad9 may regulate the Dpb11-dependent pathway.** (A) wt (YMAG149/7B), *dpb11ΔCT* (YMAG145/20C), *dot1Δ* (YMAG150/4A) and *dpb11ΔCT dot1Δ* (YMAG148) strains were arrested in M with nocodazole and mock or UV irradiated (75 J/m$^2$). 10 min after irradiation, samples were taken and protein extracts were separated by SDS-PAGE. Blots were analyzed with anti Rad53 antibodies. (B) EGY42 cells, containing the pSH18-34 β-galactosidase reporter plasmid, were transformed with the Rad9 prey plasmid pMAG11.1 (pJG4-5-*RAD9*) and/or with the Dpb11 bait plasmid pFP15 (pEG202-*DPB11*). Strains were cultured overnight in -His, -Trp, -Ura medium plus raffinose and arrested in M phase by nocodazole treatment. Galactose was then added to the medium to induce bait expression. A modified version of ONPG yeast two-hybrid assay was used to determine the β-galactosidase activity in each strain, expressed in relative units. (C) *cdc28-as1* (JAU01) and *cdc28-as1 dot1Δ* (YNOV4) strains were arrested in M with nocodazole and, after incubation for 2 h in the absence or in the presence of 5 μM 1NMPP1, were either mock or UV irradiated (75 J/m$^2$). After 10 min, samples were collected and protein extracts were separated by SDS-PAGE. Blots were analyzed with anti-Rad53 antibodies.
doi:10.1371/journal.pgen.1001047.g004

Altogether, our results indicate that CDK1 activity is required for the function of the histone-independent branch necessary for Rad53 phosphorylation in cells arrested in mitosis.

## CDK1-dependent phosphorylation of serine 11 of Rad9 modulates the Dpb11-dependent branch in M phase cells

Rad9 contains 20 potential (SP or TP) target sites for CDK-dependent phosphorylation, 9 of which conform to the canonical CDK phosphorylation site (S/T-P-x-K/R) (Figure S2B). We hypothesized that Rad9 could be a relevant CDK1 target in the histone-independent branch of the DNA damage checkpoint in M phase cells. Initially, we tested a *rad9ΔNT* mutant strain, in which the first 231 amino acids, including 9 S/T-P sites, of Rad9 are missing (Materials and Methods and [58]). As shown in Figure 5A, Rad53 phosphorylation was partially defective in both *dot1D* and *rad9DNT* mutants and essentially abolished in a *rad9ΔNT dot1Δ* double mutant strain.

All 9 potential Cdc28 phosphorylation sites in the Rad9 N-terminal region were individually mutagenized and different mutant combinations tested (Materials and Methods and data not shown). *rad9-S11A* cells displayed a detectable defect in cell cycle-regulated Rad9 phosphorylation (Figure S2C). Moreover, the *rad9-S11A* mutation recapitulates the phenotype we observed in *rad9ΔNT* cells, namely, severe loss of DNA damage-dependent Rad53 phosphorylation when combined with *dot1D* (Figure 5B). Consistently, the *rad9-S11A* mutation alone did not confer a strong sensitivity to UV irradiation (Figure 5C), while a *rad9-S11A dot1Δ* double mutant strain was synthetically sensitive to genotoxic treatment. On the other hand, a *rad9-S11A dpb11ΔCT* double mutant strain did not exhibit an increased sensitivity to UV irradiation when compared to strains harboring the single mutations, indicating that Dpb11 and Rad9-S11 phosphorylation act in the same pathway (data not shown). Phosphorylation of Rad9S11 has been reported *in vivo* [59]. In order to verify the relevance of S11 phosphorylation in our experimental conditions, we reverted the S11A mutation to Thr, another phosphorylatable residue. Figure 5D shows that Rad9 carrying a Thr at position 11 rescues the phenotype imparted by the S11A mutation, since checkpoint activation in the *rad9-S11T dot1Δ* strain is identical to that found in *dot1Δ* cells.

Interestingly, Rad9-Dpb11 interaction by two-hybrid analysis was reduced when the Rad9NT isoform, lacking the 9 potential CDK1 phosphorylation sites, was used as a prey in a wild-type background, or when Cdc28 activity was inhibited by 1NMPP1 addition in the *cdc28-as1* strain (Figure 6A). The *in vivo* interaction between Rad9 and Dpb11 was also confirmed by co-immunoprecipitation of the endogenous proteins after genotoxic treatment. As shown in Figure 6B, immunoprecipitation of MYC-tagged Dpb11 recovers the hyper-phosphorylated isoform of Rad9, and this interaction is virtually lost in the *rad9-S11A* mutant strain (Figure 6C). We also noticed that the Rad9-S11A mutant protein has slighlty less gel-mobility than its wild type counterpart, as shown in Figure 6C. This observation can be explained by either a mild defect in Mec1/Tel1-dependent hyperphosphorylation of the Rad9-S11A protein, due to the loss of Rad9-Dpb11 interaction, or a direct effect of the S11A mutation which, affecting CDK1-dependent phosphorylation of Rad9, may directly modify its migration in SDS PAGE.

Altogether, the above findings indicate that the Ser11 CDK1-consensus site on Rad9 is a relevant target to modulate Rad9-Dpb11 interaction and the CDK1-dependent checkpoint response in M phase cells.

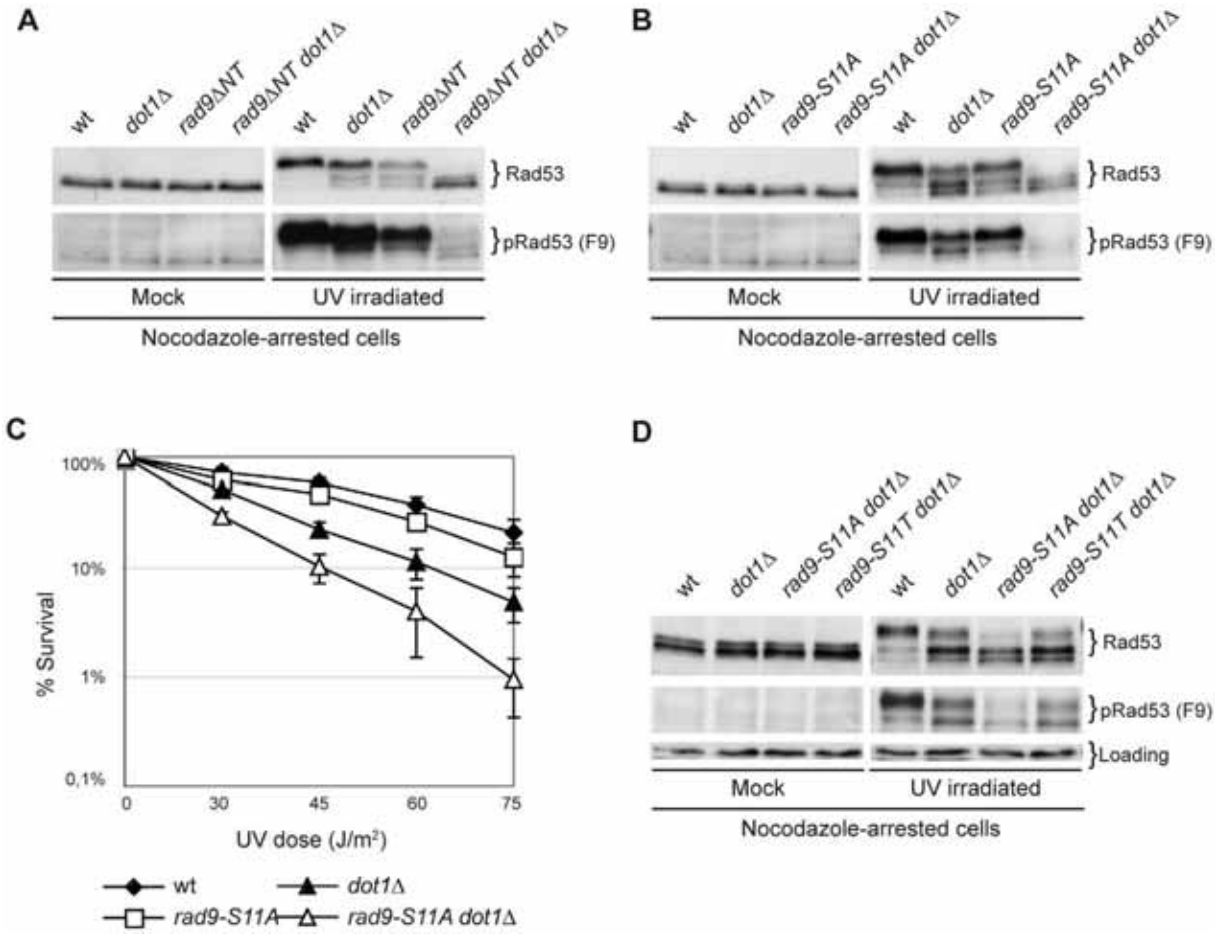


**Figure 5. Phosphorylation of Rad9S11 by CDK1 is required for the establishment of an effective UV response in the absence of Dot1.** (A) wt (K699), *dot1Δ* (YFL234), *rad9ΔNT* (DLY2236) and *rad9ΔNT dot1Δ* (YFP91) strains were arrested with nocodazole and either mock or UV irradiated (75 J/m$^2$). After 10 min samples were collected and protein extracts were separated by SDS-PAGE. Blots were analyzed with anti-Rad53 or with the F9 Mab to monitor checkpoint activation. (B) wt (K699), *dot1Δ* (YFL234), *rad9-S11A* (YMAG162) and *rad9-S11A dot1Δ* (YMAG164) strains were arrested in M, irradiated and Rad53 was detected by Western blotting as describe in panel A. (C) The same strains analyzed in B were cultured overnight, diluted and plated on YPD plates, which were irradiated with the indicated UV doses. Cell survival was assayed as described in the legend of Figure 3. (D) wt (K699), *dot1Δ* (YFL234), *rad9-S11A dot1Δ* (YMAG164) and *rad9-S11T dot1Δ* (YNOV52) strains were arrested with nocodazole and either mock or UV irradiated (75 J/m$^2$). After 10 min samples were collected and protein extracts were separated by SDS-PAGE. Blots were analyzed with anti-Rad53 or with the F9 Mab to monitor checkpoint activation.
doi:10.1371/journal.pgen.1001047.g005

## The Dpb11-dependent branch in M phase modulates checkpoint activation in a chromatin-independent manner

To gain further insights into the mechanisms involving Rad9 and the Dpb11-dependent branch of the DNA damage checkpoint operating in nocodazole-arrested cultures, cell extracts were fractionated into soluble and chromatin fractions. Specifically, we monitored Rad9 chromatin binding and Rad53 phosphorylation in strains harbouring defects in the different branches known to regulate Rad9 checkpoint functions during M phase.

As shown in Figure 7, following DNA damage, the Dpb11 C-terminal region carrying the BRCT domain does not appear to be required for Rad9 binding to chromatin, as *dpb11DCT* cells behave as wild type. However, as expected, Rad9 chromatin recruitment is defective in *dot1Δ* and *H2A-S129A* mutant cells, as binding of Rad9 is dependent upon H3-K79me and γH2A, via its Tudor and BRCT domains respectively [22,34,60]. Checkpoint activation, as determined by Rad53 phosphorylation, was abolished in any double or triple mutant combinations carrying the *dpb11ΔCT* mutation (Figure 7). Intriguingly, even when detectable Rad9 binding to chromatin is abrogated (as in the single *dot1Δ* and *H2A-S129A* or in the double *dot1Δ H2A-S129A* mutant strains) Rad53 can be fully phosphorylated. Similar genetic dependencies were found when the various single, double and triple mutant strains were tested for checkpoint activation in response to zeocin treatment, which is known to cause DSBs (Figure S3 and data not shown).

## Dpb11 is responsible for checkpoint activation in M phase cells when the Rad9 BRCT domains are replaced with a heterologous dimerization domain

We have determined (Figure 3A) that in nocodazole-arrested cells defective checkpoint activation due to the absence of the Rad9 BRCT domain can be partially rescued by adding the GST

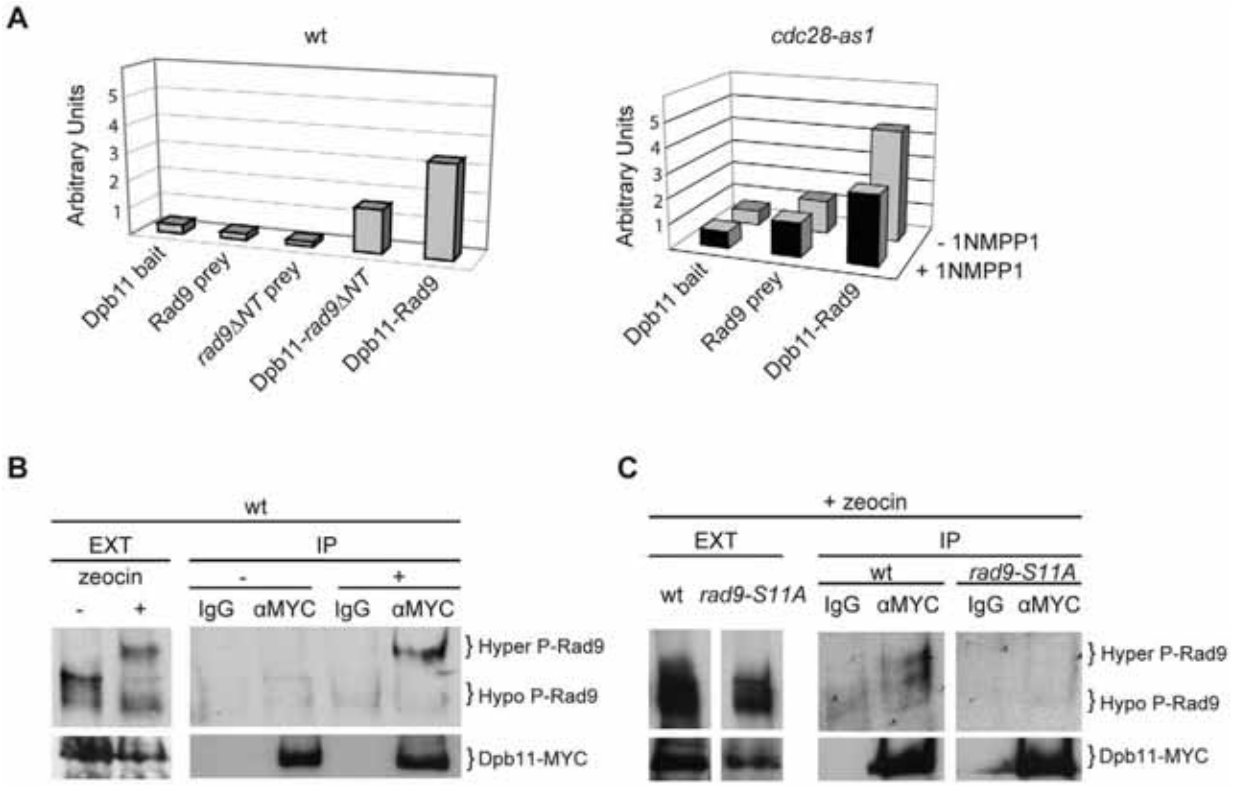


**Figure 6. CDK1-dependent phosphorylation of S11-Rad9 modulates Rad9-Dpb11 interaction.** (A) Two-hybrid interaction between Dpb11 and Rad9 was tested in a wt (K699) (left) or in a *cdc28-as1* (JAU01) (right) genetic background with the indicated bait and prey plasmids. Where specified 5 μM 1NMPP1 was added to the media for 1 h before bait induction and extracts preparation. (B) The *Dpb11-myc* (YFP38) strain was arrested with nocodazole and either mock treated or treated with 150 μg/ml of zeocin for 30 min. Whole cell protein extract was prepared and tagged Dpb11-MYC was immunoprecipitated either with anti-MYC antibodies or unspecific mouse IgG as described in Materials and Methods. The presence of Rad9 in the IPs was detected by Western blot analysis of the immunoprecipitates with specific anti-Rad9 antibodies. (C) Immunoprecipitations with anti-MYC antibodies were performed on extracts from nocodazole arrested cells, treated with 150 μg/ml of zeocin for 30 min, expressing Dpb11-MYC in a *RAD9* (YFP38) or *rad9S11A* (YMAG281) background. The presence of Rad9 was detected by Western blot analysis of the immunoprecipitates with specific anti-Rad9 antibodies. Lower exposure of the crude extracts lanes are shown to allow visualization of both Rad9 and Dpb11 specific bands.
doi:10.1371/journal.pgen.1001047.g006

dimerization domain. Moreover, we demonstrated that the M phase-specific DNA damage checkpoint contains a pathway based on Rad9-Dpb11 interactions and modulated via phosphorylation of the Ser11 residue of Rad9 by CDK1 (Figure 4, Figure 5, and Figure 6). As a consequence, we tested whether, in nocodazole-arrested cells, checkpoint activation supported by the heterologous dimerization motif in the *rad9ΔBRCT::GST* mutant strain was dependent upon Dpb11. To address this question, we introduced the *S11A* point mutation in the *rad9ΔBRCT::GST* strain (*rad9-S11AΔBRCT::GST)*. Whilst either single mutant strain was only partially defective in Rad53 phosphorylation, in *rad9-S11AΔBRCT::GST* cells, checkpoint activation was severely impaired (Figure 8A). This result indicates that in *rad9ΔBRCT::GST* cells residual checkpoint activation depends upon an active Dpb11 branch acting through a potential CDK1 site (S11) in the amino terminus of Rad9. As expected, *rad9-S11ADBRCT::GST* cells, in which the sole Rad9 expressed contains both the point mutation and the domain swap, are more sensitive to UV irradiation than either single mutant (Figure 8B).

In conclusion, our data are consistent with the hypothesis that Rad9 plays two independent roles in checkpoint activation: the first mediated by its dimerization and binding to modified histones, the second, which involves its phosphorylation by CDK1 and interaction with Dpb11 (Figure 9).

## Discussion

*RAD9* was the first DNA damage checkpoint gene identified in yeast [18]; however, the precise molecular details regarding the role of the corresponding gene product, its function and regulation remain far from being fully understood. In budding yeast, Rad9 seems to act as an adaptor protein in the signal transduction checkpoint cascade, mediating the transmission of the signal from the apical PIKKs to the main primary transducer kinase, Rad53 [27,61]. Rad9 phosphorylation, mediated by Mec1, is an early event in the signal transduction cascade and this modification in G1 is mainly influenced by histone H3 methylation [22,33,60,62]. In M phase, Rad9 phosphorylation also requires Dpb11, whose role as an alternative scaffold for Rad9 activation has been unveiled only recently [50]. The dynamics of Rad9 recruitment at various cell cycle stages and the genetic dependencies controlling Rad9 interaction with DNA/chromatin and other proteins are largely unknown.

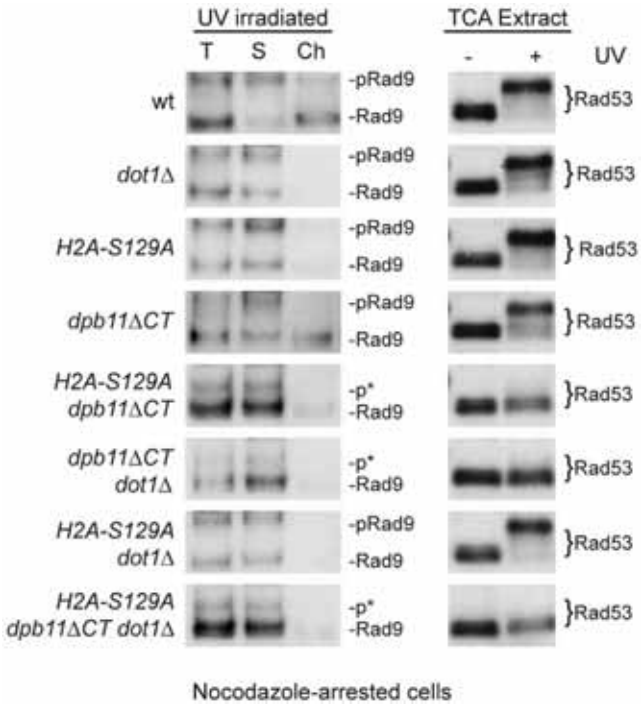


**Figure 7. The Dpb11-dependent pathway in M phase modulates Rad53 activation in a chromatin-independent manner.** wt (YMAG149/7B), *H2A-S129A* (YMAG168), *dpb11ΔCT* (YMAG145/20C), *dot1Δ* (YMAG150/4A), *H2A-S129A dpb11ΔCT* (YMAG155), *H2A-S129A dot1Δ* (YMAG170), *dpb11ΔCT dot1Δ* (YMAG148) and *H2A-S129A dpb11ΔCT dot1Δ* (YMAG157) strains were arrested in M with nocodazole and UV irradiated (75 J/m$^2$). After 10 min, samples were collected and analyzed in their total (T), soluble (S) and chromatin-enriched (Ch) fractions; blots were probed with anti-Rad9 antibodies (left panel). Protein extracts were also prepared from mock and UV treated samples and analyzed by SDS-PAGE and Western blotting with anti-Rad53 antibodies to monitor checkpoint activation (right panel). The positions of Rad9 and its hyper-phosphorylated isoform (pRad9) are indicated. p* marks partially phosphorylated Rad9 species.
doi:10.1371/journal.pgen.1001047.g007

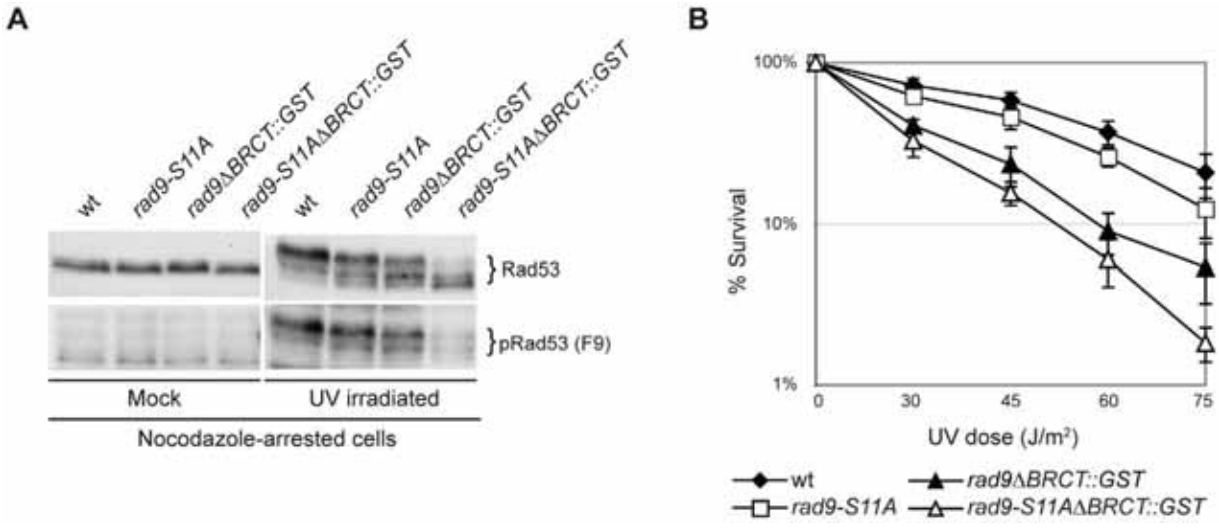


**Figure 8. Partial checkpoint activation after forced Rad9 dimerization in M phase acts through the Dpb11-dependent checkpoint pathway.** (A) wt (K699), *rad9-S11A* (YMAG162), *rad9ΔBRCT::GST* (YMAG74) and *rad9-S11AΔBRCT::GST* (YFL1177) strains were arrested with nocodazole and mock or UV irradiated (75 J/m$^2$). After 10 min, samples were collected and protein extracts were separated by SDS-PAGE. Blots were analyzed either with anti-Rad53 antibodies or with the F9 Mab to monitor checkpoint activation. (B) UV survival assay. The same strains as in A were cultured overnight and then diluted and plated on YPD plates, which were irradiated with the indicated UV doses. Cell survival was assayed as described in the legend to Figure 3.
doi:10.1371/journal.pgen.1001047.g008

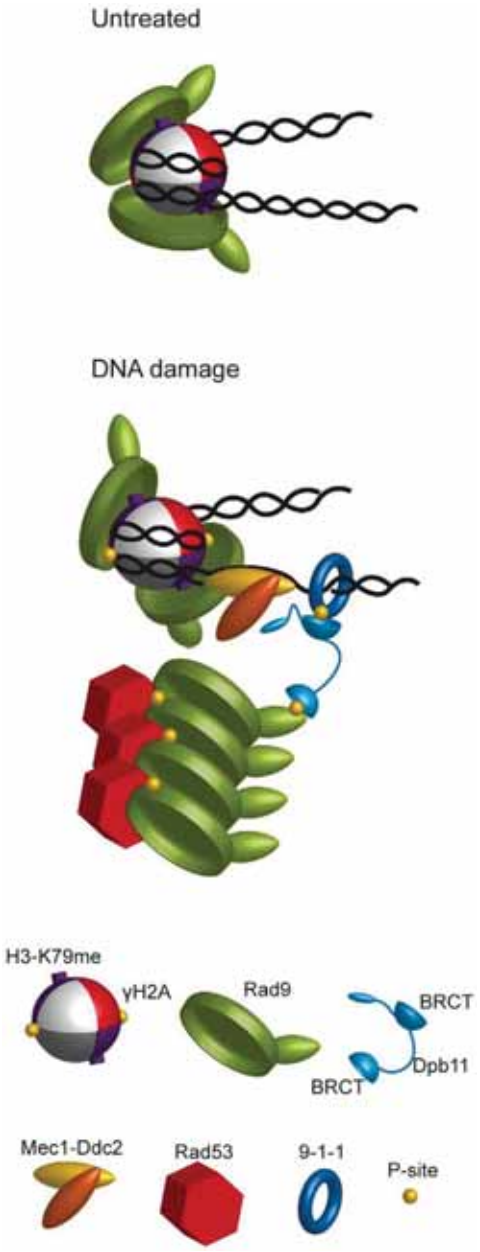


**Figure 9. Possible model of the dynamics of Rad9 chromatin binding and its interaction with Dpb11 to modulate checkpoint activation in M phase.** Under untreated conditions, Rad9 is chromatin bound through the interaction of its Tudor domain with H3-K79me and its BRCT-mediated dimerization. After DNA damage, activated Rad9 may change its conformation, interacting also with γ-H2A. In M-phase an alternative means of Rad9 recruitment near DNA lesions involves its interaction with Dpb11. This factor is brought near the Mec1-Ddc2 complex via its interaction with the 9-1-1 clamp, and it binds the phosphorylated N-terminal portion of Rad9 leading to full checkpoint activation.
doi:10.1371/journal.pgen.1001047.g009

Here, we show that a significant proportion of Rad9 is already chromatin-bound in unperturbed conditions throughout the cell cycle, confirming previous suggestions [22] and supporting our earlier model [14]. According to the current view, Rad9-chromatin association is controlled by interaction between its Tudor domain and H3-K79me. Constitutive, dynamic recruitment of Rad9 to chromatin may facilitate the efficiency and speed of the Rad9-dependent response to genotoxins. After DNA damage, Rad9 binding to chromatin is further strengthened through its BRCT domain, which is required to productively interact with γH2A [22,23]. In this study we found that the BRCT domain of Rad9, in addition to promoting interaction with γH2A, has a more general function in modulating Rad9 recruitment. In fact, the *rad9-F1104L* and *rad9-W1280L* mutations, affecting the folding of the whole BRCT domain [21], alter binding to chromatin also in the absence of any genotoxic treatment. The observation that *rad9-K1088M* cells are defective in Rad9 chromatin recruitment only after γ-irradiation may be explained if such mutation only prevents Rad9-γH2A interaction [22].

In G1 cells, Rad9 binding to chromatin can be achieved by substituting the BRCT repeats with a heterologous dimerization domain; such recruitment requires the activity of Dot1 histone methyl-transferase, indicating that BRCT-mediated dimerization may be a pre-requisite for constitutive interaction between the Rad9 Tudor domain and H3-K79me. Given the symmetrical structure of the histone octamer within the nucleosome core, dimerization might facilitate the correct orientation and positioning of two Rad9 molecules on the nucleosome, allowing productive interactions with modified histones (Figure 9). Such hypothesis is supported by structural modeling of a dimeric *S. pombe* Crb2 complex on a single nucleosome, where all the interactions with H4-K20me and γH2A are satisfied without changing the conformation of the histone core [31].

It is worth noting that dimerization forced by replacement of the Rad9 BRCT domains with the heterologous GST tag only restores Rad9 binding to chromatin in G1-, and not in M-arrested cells. In fact, in cells arrested with nocodazole, we observed that GST-induced dimerization can rescue Rad9 hyper-phosphorylation and DNA damage checkpoint activation, but not its stable recruitment to chromatin. It is possible that in mitosis cell cycle-dependent phosphorylation of Rad9 may interfere with the chromatin association of this artificial Rad9 dimer. Alternatively, in nocodazole-arrested cells the Rad9 BRCT motifs may play additional roles in modulating Rad9-chromatin interactions.

Several findings indicate that the cellular response to DNA damage, including the repair mechanisms themselves, are regulated differently in distinct cell cycle stages. Multiple layers of cell cycle regulation may modulate the recruitment of critical checkpoint and repair factors to damaged DNA, as well as facilitate their reciprocal cross-talk [63–67]. We have previously shown that Dpb11 is essential for full DNA damage checkpoint activation in M-arrested cells [50]. Dpb11 is held in proximity to damaged DNA through its interaction with phosphorylated 9-1-1 complex, leading to Mec1-dependent Rad9 phosphorylation. Taking advantage of the *cdc28-as1* mutation, which allows conditional turn off of CDK1 kinase activity, we have demonstrated that CDK1, targeting Rad9, is required for the function of the Dpb11-dependent branch of the checkpoint response. Indeed, yeast cells carrying a truncated Rad9 version lacking 9 putative Cdc28 phosphorylation sites in the N-terminal region, are checkpoint-defective in M phase, in the absence of the histone-dependent branch. The Ser11 residue in the Rad9 N-terminal region is the most relevant Cdc28 target site, since a *rad9-S11A* mutation recapitulates the phenotypes observed in *rad9ΔNT* cells.

By two-hybrid analysis we showed that Rad9 and Dpb11 specifically interact in M-phase arrested cells, even in the absence of DNA damage, and this interaction is stimulated by CDK1-dependent Rad9 phosphorylation. Co-immunoprecipitation exper-

iments confirmed that Rad9-Dpb11 interaction requires phosphorylation of Rad9-S11 and revealed that it depends upon genotoxic treatment, although we cannot exclude a weak/transient interaction in untreated conditions. This finding can be explained if activation of Mec1 by DNA damage facilitates or controls this interaction, e.g phosphorylating Dpb11 [50], exposing phospho-S11 or stimulating Rad9-S11 modification by CDK1. The overexpression conditions typical of the two hybrid system can easily explain why a weak interaction can be detected also in the absence of DNA damage. Interestingly, the functional interactions between Dpb11 and Rad9 in budding yeast are reminiscent of similar findings in the distantly related *S. pombe*, where histone-independent checkpoint activation is also modulated by CDK1 [37].

The Dpb11-dependent pathway does not require the histone modifications modulating Rad9 recruitment to chromatin. We found that a truncated C-terminal version of Dpb11 does not affect Rad9 recruitment to chromatin, which is instead abolished when the histone-dependent pathway is defective. Surprisingly, in a *dot1Δ H2A-S129A* double mutant strain checkpoint activation in M phase is virtually undistinguishable from that found in wild type cells, although Rad9 is not stably bound to chromatin. Only when the *dpb11ΔCT* mutation is combined with the *dot1Δ* or *H2A-S129A* mutation the checkpoint response is turned off. The working model presented in Figure 9, suggests that Dpb11 may act in M-phase as an alternative means of Rad9 recruitment. Dpb11 is located close to sites of DNA damage through its interaction with the Mec1-phosphorylated 9-1-1 complex; DNA damage leads to Mec1-dependent phosphorylation of Dpb11 [50], which interacts with S11-phosphorylated Rad9 (Figure 9). This Dpb11-dependent localization of Rad9 to sites of DNA damage allows rapid Rad9 hyper-phosphorylation by PIKKs, as suggested by the observation that the interaction between Rad9 and Dpb11 is induced by genotoxic agents and hyper-phosphorylated Rad9 is enriched in the Dpb11-bound population. Subsequently, Rad53 recruitment via its FHA domains leads to full activation of the checkpoint response. Unlike Rad9 bound via histone marks, Rad9 complexed with Dpb11 does not appear to be tightly linked to chromatin, explaining why the Dpb11-dependent branch for checkpoint activation seems to act in a chromatin-independent manner. However, we cannot rule out the possibility that the Rad9-Dpb11 complex can transiently or weakly bind to chromatin.

The model suggested here is in agreement with similar findings in the distantly related *S.pombe* fission yeast [37] as well as with recent *in vitro* data describing Dpb11 role in checkpoint activation [68], suggesting that the proposed mechanism can be extended to other eukaryotic organisms.

## Materials and Methods

### Strains and plasmids

All of the strains used in this work are derivatives of W303 [*MAT*a *ade2-1 trp1-1 can1-100 leu2-3,12 his3-11,15 ura3 rad5-535*]; only strains YFP91 and DLY2236 (provided by D. Lydall), are *RAD5*$^{+}$. All the strains used in this study are listed in Table S1 and further information regarding strains and plasmids is available upon request.

Plasmids pMAG11.1 and pFP15 are, respectively, the Rad9 prey and Dpb11 bait plasmids used for the yeast two-hybrid analysis. They were obtained by amplifying the relevant coding sequences from genomic DNA and by ligating the resulting fragments into pJG4-5 and pEG202 [69], respectively.

The plasmid pMAG9, which encodes the Rad9ΔNT prey, was obtained cloning the *rad9ΔNT* sequence, amplified from the yeast strain DLY2236, into pJG4-5.

Gene deletions were obtained by PCR-mediated gene replacement [70].

The YNOV15 (*rad9-F1140L*) and YNOV31 (*rad9-W1280L*) strains were obtained from YFL871. The *kanMX4* and *klURA3* CORE cassettes, amplified from pCORE [71], were integrated in a K699 strain at position 1941 of the *RAD9* gene. Subsequently, the CORE cassette was replaced with the C-terminus of the *rad9-F1104L* or *rad9-W1280L* alleles, amplified respectively from pFL75.5 or pFL69.1, thus restoring the full-length *RAD9* open reading frame bearing the intended mutation. *RAD9* site-specific mutations on plasmids pFL75.5 and pFL69.1 were obtained by PCR with mutagenic oligonucleotides on the pFL36.1 plasmid [50]. Recombination events were selected on 5-fluoroorotic acid plates, and the strains were verified by sequencing.

The *rad9ΔBRCT::13MYC* and the *rad9ΔBRCT::GST* mutant alleles were obtained by introducing the 13-MYC or GST tags at the 984 aa, using the one-step PCR method [70], thus eliminating the whole Rad9 BRCT domain.

The *cdc28-as1* mutant allele was obtained by ClaI-directed integration of plasmid pVF6 [72] at the *CDC28* locus into the desired background. Plasmid pop-out events were selected on 5-fluoroorotic acid plates, and the presence of the *cdc28-as1* mutation was verified by assessing sensitivity to 1NMPP1 on plate.

Strains encoding the *rad9-S11A* mutant allele were obtained by MscI-directed integration of pRS306-NTRAD9$^{cdk1}$ into the desired background. The transversion TCT-GCT causing the *rad9-S11A* mutation and the reversion GCT to ACT generating the *rad9-S11T* allele were produced by site- directed mutagenesis (Stratagene) of pGEMTeasyRAD9, containing a 2547 bp fragment from position -445 to position +2102 within the *RAD9* ORF. The 1.8 Kb BamHI-MscI fragment from the pGEMTeasyRAD9 vector was swapped with the equivalent fragment from an existing 6.3 Kb pRS306-NTRAD9 integrative vector, containing a BamHI-SpeI *RAD9* fragment from position −445 to position 1478 within the *RAD9* ORF and the presence of the mutation verified by sequencing. Plasmid pop-out events were selected on 5-fluoroorotic acid plates, and the *rad9-S11A* mutation was confirmed by PCR sequencing.

The *dpb11ΔCT* mutant allele was obtained by introducing a premature stop codon at the 583 aa and the *HPH* cassette after the codon with the one step PCR method previously described [73], thus mimicking the *dpb11-1* mutation [74].

Strain YFL921 was obtained by using the one-step PCR strategy described in Longtine 1998, using pFA6-*FKBP2x-13MYC-KanMX6*, as template. This plasmid was generated by cloning in PacI-linearized pFA6-*13MYC-KanMX6* the *FKBP2x* sequence amplified from pC4M-FV2E (ARGENT Regulated Homodimerization kit, ARIAD Pharmaceutical).

The yeast two hybrid was performed using the B42/lexA system with strain EGY42 (*MATa his3 ura3 trp1 6lexAOP-LEU2*; *lex- AOP-lacZ* reporter on plasmid pBH18-34) as the host strain [69].

### Chromatin binding

To analyze chromatin binding of proteins, yeast extracts were prepared from G1- or M-arrested cells following published procedures [22].

### Cell cycle blocks and DNA damage treatments

Cells were grown in YPD medium at 28°C (25°C in the experiments with strains harboring the *dpb11ΔCT* mutation) to a concentration of $6\times10^{6}$ cells/ml and arrested in G1 or M with α-factor (20 μg/ml) or nocodazole (20 μg/ml), respectively. 50 ml of cultures were centrifuged, resuspended in 500 μl of fresh YPD and plated on a Petri dish (14 cm diameter). Plates were quickly

irradiated with a Stratalinker at 75 J/m$^2$ and cells resuspended in 50 ml of YPD plus α-factor or nocodazole. A 25 ml sample was taken 10 min after the treatment and processed for protein extraction with trichloroacetic acid (TCA) [75]. For analysis of the double-strand breaks (DSBs) checkpoint response, cells arrested at the proper cell cycle phase were treated with 150 μg/ml of zeocin. Samples were taken 45 min after treatment and processed for protein extraction.

### FKBP dimerization

To analyze FKBP-driven (FK506 binding protein) dimerization, overnight cell cultures were diluted at a concentration of $1\times10^6$ cells/ml and treated for 6 h with 1 μM AP20187 (ARGENT Regulated Homodimerization kit, ARIAD Pharmaceutical). UV sensitivity assays or chromatin binding analysis were performed as described elsewhere in this section.

### Inactivation of the Cdc28 kinase activity

Exponentially growing cells in a *cdc28-as1* background were harvested at a concentration of $4\times10^6$ cells/ml and blocked in M phase as described above. To selectively inhibit Cdc28 activity [56], the ATP analogue 1NMPP1 was then added to a concentration of 5 μM to half of the cultures; after 2 h of incubation at 28°C, cells were either mock- or UV-irradiated and protein extracts were prepared.

### SDS-PAGE and western blotting

TCA protein extracts or chromatin binding samples were separated by sodium dodecyl sulfate-polyacrylamide gel electrophoresis (SDS-PAGE) in 10% acrylamide gels. For the analysis of Rad9 phosphorylation, NuPAGE Tris-acetate 3% to 8% gels were used following the manufacturer's instructions. Western blotting was performed with anti-Rad9 (D. Stern), anti-Rad53 (C. Santocanale), with anti-phosphorylated Rad53 F9 Mab antibodies [76] anti-ORC2 (Abcam) and anti-tubulin (ML. Carbone), using standard techniques.

### UV–sensitivity assay

To assess cell survival after UV irradiation, serials dilutions of overnight cultures were spotted onto YPD plates, which were either irradiated with different UV doses or mock-treated. For survival curves, yeast strains were cultured overnight to exponentially growing phase. Cells were diluted and approximately 500 cells/plate were plated, and then either irradiated with various UV doses or mock-treated. After 3 days, the total number of colonies formed on each plate was counted.

### Yeast two-hybrid analysis

Protein interaction between Rad9 and Dpb11 in the G1 and M phase of the cell cycle was assessed by measuring β-galactosidase activity with ortho-Nitrophenyl-β-galactoside (ONPG) assay. Briefly, cells expressing Rad9 bait and/or Dpb11 prey were cultured overnight in yeast synthetic media (-Ura, -His, -Trp) with 2% (w/v) raffinose to a concentration of $5\times10^6$ cells/ml. Cultures were centrifuged and cells resuspended in YP plus raffinose and arrested in G1 or M phases, as described above. Galactose to a 2% w/v final concentration was added to the medium to induce prey expression. A 15 ml sample was taken after 1 h of galactose induction, centrifuged and resuspended in 250 μl of breaking buffer (100 mM Tris HCl at pH 8.0, Glycerol 10%; DTT 1 mM, 1 tablet of complete Roche antiproteolytic cocktail. Cells were lysed by using a FastPrep cell disruptor; the optical density (OD) of protein extract at 600 nm was determined using the Bio-Rad protein assay reagent. 1 ml of Z buffer (60 mM $Na_2HPO_4$, 40 mM $NaH_2PO_4$, 10 mM KCl, 1 mM $MgSO_4$, and 50 mM β-mercaptoethanol at pH 7.0) plus ONPG 4 mg/ml was aliquoted in a small glass tube for each sample. 20 μl of protein extract was added to each tube and incubated at 37°C until a yellow color developed. The reaction was stopped by adding 400 ml of 1 M $NaCO_3$ and the OD at 420 nm of each sample was measured. β - Galactosidase activity was calculated by using the formula units $= 10^3$ $OD_{420}/(OD_{600}$ x reaction time in min).

### Rad9-Dpb11-MYC immunoprecipitation

1.5 l cultures of strains YFP38 and YMAG281 expressing, respectively, the tagged Dpb11-MYC fusion protein under the control of the endogenous *DPB11* promoter in a wild-type or *rad9S11A* mutant background were grown in YPD medium at a cell density of $1\times10^7$ cells/ml. Cells were then arrested in M phase by addition of 10 μg/ml of nocodazole and were either mock treated or treated with 150 μg/ml of zeocin for 30 min. Cells were washed twice with pre-cooled $ddH_2O$ and once in 2× lysis buffer (300 mM KCl, 100 mM Hepes (pH 7.5), 20% glycerol, 8 mM β-mercaptethanol, 2 mM EDTA, 0.1% Tween20, 0.01% NP-40). Resuspended cells were frozen as droplets in liquid nitrogen. Aliquots of frozen cells were manually ground in a mortar in liquid nitrogen. One volume of 2× lysis buffer, containing a protein inhibitor cocktail (2.8 μM leupeptin, 8 μM pepstatin A, 4 mM PMSF, 50 mM benzamidine, 25 μM antipain, 4 μM chymostatin in ethanol) and phosphatase inhibitors (2 mM sodium fluoride, 1.2 mM β-glycerophosphate, 0.04 mM sodium vanadate, 2 mM EGTA, 10 mM sodium pyrophosphate), was added. Cell extract was clarified by a low speed centrifugation followed by additional centrifugation for 1 h at 42.000 rpm in a Beckman Sw55Ti rotor. The clarified crude extract (Ext) was adjusted to 10 mg/ml in the various immunoprecipitation experiments. 1 ml of Ext was precleared by incubation with 40 μl of 50% (v/v beads/1× lysis buffer) Protein G slurry for 1 hour at 4°C on a rotating wheel. Precleared supernatants were incubated with either 20 μg of the anti-myc Mab 9E11 or 20 μg of unspecific mouse IgG. Samples were incubated for 2 h at 4°C on a rotating wheel and centrifuged at 14.000 rpm for 15 min at 4°C. 40 μl of 50% protein G slurry were added to the supernatants, incubated on a rotating wheel for 2 h at 4°C and recovered by centrifugation. Immunoprecipitated Dpb11-MYC samples were washed four times with 1 ml of lysis buffer containing protease and phosphatase inhibitors. Beads were finally resuspended in 40 μl of 3× Laemmli buffer (IP), boiled for 5 min and released proteins separated on 6.5% (80/1 acrylamide/bisacrylamide) SDS-PAGE gels. After blotting, Rad9 was visualized with the NLO5 Rad9 polyclonal antibody [13] or the 9E11 Mab (Abcam).

## Supporting Information

**Figure S1** (A) wt (K699) cells were arrested in G1 with α-factor and either mock or UV irradiated (75 J/m$^2$). 10 min after irradiation, samples were collected and analyzed in their total (T), soluble (S) and chromatin-enriched (Ch) fractions. Blots were probed with anti Rad9 polyclonal antibodies. After UV irradiation the hyper-phosphorylated Rad9 isoform migrates and it is detected on Western blots probed with anti-Rad9 antibodies near to an aspecific protein species (mostly present in the supernatant fraction) [50]. Such band was omitted in the Western blots shown in Figure 1, Figure 2, and Figure 7 for clarity. The positions of Rad9 and its hyper-phosphorylated isoform (pRad9) are indicated; * marks the background protein species unrelated to Rad9. (B) The Western blots in which the presence of Rad9 was analyzed in

the total (T), soluble (S) and chromatin-enriched (Ch) fractions were controlled for proper fractionation of control proteins, known to remain in the soluble fraction (Tubulin) or to bind to chromatin (Orc2). The blots in S1 Panel B show the results obtained with the same protein samples analyzed in Figure 1A. (C) Quantitative analysis of the percentage of hyper-phosphorylated and hypo-phosphorylated Rad9 isoforms in the total (T), soluble (S) and chromatin-enriched (Ch) fractions in α-factor and nocodazole arrested wild-type cells. Quantification was obtained with a Versadoc (Biorad) after incubation with fluorescent secondary antibodies, and error bars were obtained from 4 independent experiments. The percentages of hyper- and hypo- phosphorylated isoforms were calculated respectively to the total amount of Rad9.
Found at: doi:10.1371/journal.pgen.1001047.s001 (1.16 MB TIF)

**Figure S2** (A) The histograms show the M/G1 ratio increase in β-galactosidase activity, when the interaction between Dpb11/Rad9 or the positive controls p53 and SV40-TAg was measured by two-hybrid analysis in nocodazole (M) or α-factor (G1) arrested cells. Error bars were obtained from three independent two-hybrid experiments. (B) Amino acid sequence of the Rad9 ORF; the basic CDK1 (S/T-P) and PIKK (S/T-Q) consensus phosphorylation sites are shown in black or gray, respectively. (C) wt (K699) and *rad9-S11A* (YMAG162) strains were arrested in M with nocodazole and samples were collected to prepare protein extracts. Rad9 phosphorylation was analyzed by SDS-PAGE and Western blotting with anti-Rad9 antibodies.
Found at: doi:10.1371/journal.pgen.1001047.s002 (0.77 MB TIF)

**Figure S3** wt (YMAG149/7B), *H2A-S129A* (YMAG168), *dpb11ΔCT* (YMAG145/20C), *H2A-S129A dpb11ΔCT* (YMAG155), *dot1Δ* (YMAG150/4A), *H2A-S129A dot1Δ* (YMAG170), *dpb11ΔCT dot1Δ* (YMAG148) and *H2A-S129A dpb11ΔCT dot1Δ* (YMAG157) strains were arrested in M with nocodazole and treated with zeocin (150 μg/ml). After 45 min, samples were collected and protein extracts were analyzed by SDS-PAGE and Western blotting with anti Rad53 antibodies to monitor checkpoint activation.
Found at: doi:10.1371/journal.pgen.1001047.s003 (0.76 MB TIF)

**Table S1** Strains used in this study. All of the strains used in this work are derivatives of W303 [*MAT*a *ade2-1 trp1-1 can1-100 leu2-3,12 his3-11,15 ura3 rad5-535*]; only strains YFP91 and DLY2236 (provided by D. Lydall), are *RAD5*$^{+}$.
Found at: doi:10.1371/journal.pgen.1001047.s004 (0.06 MB DOC)

## Acknowledgments

We thank C. Santocanale, D. Lydall, D. Stern, F. Vanoli, A. Pellicioli for the gift of antibodies, strains, and plasmids. T. Weinert and the members of our labs are acknowledged for stimulating discussions. ARIAD (www.ariad.com/regulationkits) provided the FKBP regulated homodimerization kit.

## Author Contributions

Conceived and designed the experiments: M Granata, F Lazzaro, R Kumar, M Grenon, NF Lowndes, P Plevani, M Muzi-Falconi. Performed the experiments: M Granata, F Lazzaro, D Novarina, D Panigada, F Puddu, CM Abreu. Analyzed the data: M Granata, F Lazzaro, D Novarina, D Panigada, F Puddu, M Grenon, NF Lowndes, P Plevani, M Muzi-Fal. Contributed reagents/materials/analysis tools: M Granata, F Lazzaro, D Novarina, D Panigada, F Puddu. Wrote the paper: NF Lowndes, P Plevani, M Muzi-Falconi.

## References

1. Lazzaro F, Giannattasio M, Puddu F, Granata M, Pellicioli A, et al. (2009) Checkpoint mechanisms at the intersection between DNA damage and repair. DNA Repair (Amst) 8: 1055–1067.
2. Kerzendorfer C, O'Driscoll M (2009) Human DNA damage response and repair deficiency syndromes: linking genomic instability and cell cycle checkpoint proficiency. DNA Repair (Amst) 8: 1139–1152.
3. Melo J, Toczyski D (2002) A unified view of the DNA-damage checkpoint. Curr Opin Cell Biol 14: 237–245.
4. Harrison JC, Haber JE (2006) Surviving the breakup: the DNA damage checkpoint. Annu Rev Genet 40: 209–235.
5. Longhese MP, Foiani M, Muzi-Falconi M, Lucchini G, Plevani P (1998) DNA damage checkpoint in budding yeast. EMBO J 17: 5525–5528.
6. Durocher D, Jackson SP (2001) DNA-PK, ATM and ATR as sensors of DNA damage: variations on a theme? Curr Opin Cell Biol 13: 225–231.
7. Paciotti V, Clerici M, Lucchini G, Longhese MP (2000) The checkpoint protein Ddc2, functionally related to S. pombe Rad26, interacts with Mec1 and is regulated by Mec1-dependent phosphorylation in budding yeast. Genes Dev 14: 2046–2059.
8. Rouse J, Jackson SP (2000) LCD1: an essential gene involved in checkpoint control and regulation of the MEC1 signalling pathway in Saccharomyces cerevisiae. EMBO J 19: 5801–5812.
9. Wakayama T, Kondo T, Ando S, Matsumoto K, Sugimoto K (2001) Pie1, a protein interacting with Mec1, controls cell growth and checkpoint responses in Saccharomyces cerevisiae. Mol Cell Biol 21: 755–764.
10. Downs JA, Lowndes NF, Jackson SP (2000) A role for Saccharomyces cerevisiae histone H2A in DNA repair. Nature 408: 1001–1004.
11. Paciotti V, Lucchini G, Plevani P, Longhese MP (1998) Mec1p is essential for phosphorylation of the yeast DNA damage checkpoint protein Ddc1p, which physically interacts with Mec3p. EMBO J 17: 4199–4209.
12. Emili A (1998) MEC1-dependent phosphorylation of Rad9p in response to DNA damage. Mol Cell 2: 183–189.
13. Vialard JE, Gilbert CS, Green CM, Lowndes NF (1998) The budding yeast Rad9 checkpoint protein is subjected to Mec1/Tel1-dependent hyperphosphorylation and interacts with Rad53 after DNA damage. EMBO J 17: 5679–5688.
14. Gilbert CS, Green CM, Lowndes NF (2001) Budding yeast Rad9 is an ATP-dependent Rad53 activating machine. Mol Cell 8: 129–136.
15. Schwartz MF, Duong JK, Sun Z, Morrow JS, Pradhan D, et al. (2002) Rad9 phosphorylation sites couple Rad53 to the Saccharomyces cerevisiae DNA damage checkpoint. Mol Cell 9: 1055–1065.
16. Sweeney FD, Yang F, Chi A, Shabanowitz J, Hunt DF, et al. (2005) Saccharomyces cerevisiae Rad9 acts as a Mec1 adaptor to allow Rad53 activation. Curr Biol 15: 1364–1375.
17. Pellicioli A, Lucca C, Liberi G, Marini F, Lopes M, et al. (1999) Activation of Rad53 kinase in response to DNA damage and its effect in modulating phosphorylation of the lagging strand DNA polymerase. EMBO J 18: 6561–6572.
18. Weinert TA, Hartwell LH (1988) The RAD9 gene controls the cell cycle response to DNA damage in Saccharomyces cerevisiae. Science 241: 317–322.
19. Weinert TA, Hartwell LH (1990) Characterization of RAD9 of Saccharomyces cerevisiae and evidence that its function acts posttranslationally in cell cycle arrest after DNA damage. Mol Cell Biol 10: 6554–6564.
20. Siede W, Friedberg AS, Friedberg EC (1993) RAD9-dependent G1 arrest defines a second checkpoint for damaged DNA in the cell cycle of Saccharomyces cerevisiae. Proc Natl Acad Sci U S A 90: 7985–7989.
21. Soulier J, Lowndes NF (1999) The BRCT domain of the S. cerevisiae checkpoint protein Rad9 mediates a Rad9-Rad9 interaction after DNA damage. Curr Biol 9: 551–554.
22. Hammet A, Magill C, Heierhorst J, Jackson SP (2007) Rad9 BRCT domain interaction with phosphorylated H2AX regulates the G1 checkpoint in budding yeast. EMBO Rep 8: 851–857.
23. Nnakwe CC, Altaf M, Cote J, Kron SJ (2009) Dissection of Rad9 BRCT domain function in the mitotic checkpoint response to telomere uncapping. DNA Repair (Amst) 8: 1452–1461.
24. Toh GW-L, Lowndes NF (2003) Role of the Saccharomyces cerevisiae Rad9 protein in sensing and responding to DNA damage. Biochem Soc Trans 31: 242–246.
25. Sun Z, Hsiao J, Fay DS, Stern DF (1998) Rad53 FHA domain associated with phosphorylated Rad9 in the DNA damage checkpoint. Science 281: 272–274.
26. Durocher D, Henckel J, Fersht AR, Jackson SP (1999) The FHA domain is a modular phosphopeptide recognition motif. Mol Cell 4: 387–394.
27. Usui T, Foster SS, Petrini JHJ (2009) Maintenance of the DNA-damage checkpoint requires DNA-damage-induced mediator protein oligomerization. Mol Cell 33: 147–159.
28. Du L-L, Moser BA, Russell P (2004) Homo-oligomerization is the essential function of the tandem BRCT domains in the checkpoint protein Crb2. J Biol Chem 279: 38409–38414.
29. Ward I, Kim J-E, Minn K, Chini CC, Mer G, et al. (2006) The tandem BRCT domain of 53BP1 is not required for its repair function. J Biol Chem 281: 38472–38477.

30. Zgheib O, Pataky K, Brugger J, Halazonetis TD (2009) An oligomerized 53BP1 tudor domain suffices for recognition of DNA double-strand breaks. Mol Cell Biol 29: 1050–1058.
31. Kilkenny ML, Doré AS, Roe SM, Nestoras K, Ho JCY, et al. (2008) Structural and functional analysis of the Crb2-BRCT2 domain reveals distinct roles in checkpoint signaling and DNA damage repair. Genes Dev 22: 2034–2047.
32. van Attikum H, Gasser SM (2009) Crosstalk between histone modifications during the DNA damage response. Trends Cell Biol 19: 207–217.
33. Giannattasio M, Lazzaro F, Plevani P, Muzi-Falconi M (2005) The DNA damage checkpoint response requires histone H2B ubiquitination by Rad6-Bre1 and H3 methylation by Dot1. J Biol Chem 280: 9879–9886.
34. Huyen Y, Zgheib O, Ditullio RA, Gorgoulis VG, Zacharatos P, et al. (2004) Methylated lysine 79 of histone H3 targets 53BP1 to DNA double-strand breaks. Nature 432: 406–411.
35. Grenon M, Magill CP, Lowndes NF, Jackson SP (2006) Double-strand breaks trigger MRX- and Mec1-dependent, but Tel1-independent, checkpoint activation. FEMS Yeast Res 6: 836–847.
36. Sanders SL, Portoso M, Mata J, Bähler J, Allshire RC, et al. (2004) Methylation of histone H4 lysine 20 controls recruitment of Crb2 to sites of DNA damage. Cell 119: 603–614.
37. Du L-L, Nakamura TM, Russell P (2006) Histone modification-dependent and -independent pathways for recruitment of checkpoint protein Crb2 to double-strand breaks. Genes Dev 20: 1583–1596.
38. Botuyan MV, Lee J, Ward IM, Kim J-E, Thompson JR, et al. (2006) Structural basis for the methylation state-specific recognition of histone H4-K20 by 53BP1 and Crb2 in DNA repair. Cell 127: 1361–1373.
39. Schotta G, Sengupta R, Kubicek S, Malin S, Kauer M, et al. (2008) A chromatin-wide transition to H4K20 monomethylation impairs genome integrity and programmed DNA rearrangements in the mouse. Genes Dev 22: 2048–2061.
40. Javaheri A, Wysocki R, Jobin-Robitaille O, Altaf M, Cote J, et al. (2006) Yeast G1 DNA damage checkpoint regulation by H2A phosphorylation is independent of chromatin remodeling. Proc Natl Acad Sci U S A 103: 13771–13776.
41. Toh GW-L, O'shaughnessy AM, Jimeno S, Dobbie IM, Grenon M, et al. (2006) Histone H2A phosphorylation and H3 methylation are required for a novel Rad9 DSB repair function following checkpoint activation. DNA Repair (Amst) 5: 693–703.
42. Nakamura TM, Du L-L, Redon C, Russell P (2004) Histone H2A phosphorylation controls Crb2 recruitment at DNA breaks, maintains checkpoint arrest, and influences DNA repair in fission yeast. Mol Cell Biol 24: 6215–6230.
43. Iwabuchi K, Basu BP, Kysela B, Kurihara T, Shibata M, et al. (2003) Potential role for 53BP1 in DNA end-joining repair through direct interaction with DNA. J Biol Chem 278: 36487–36495.
44. Pryde F, Khalili S, Robertson K, Selfridge J, Ritchie A-M, et al. (2005) 53BP1 exchanges slowly at the sites of DNA damage and appears to require RNA for its association with chromatin. J Cell Sci 118: 2043–2055.
45. Ward IM, Minn K, Jorda KG, Chen J (2003) Accumulation of checkpoint protein 53BP1 at DNA breaks involves its binding to phosphorylated histone H2AX. J Biol Chem 278: 19579–19582.
46. Huen MSY, Grant R, Manke I, Minn K, Yu X, et al. (2007) RNF8 transduces the DNA-damage signal via histone ubiquitylation and checkpoint protein assembly. Cell 131: 901–914.
47. Kolas NK, Chapman JR, Nakada S, Ylanko J, Chahwan R, et al. (2007) Orchestration of the DNA-damage response by the RNF8 ubiquitin ligase. Science 318: 1637–1640.
48. Mailand N, Bekker-Jensen S, Faustrup H, Melander F, Bartek J, et al. (2007) RNF8 ubiquitylates histones at DNA double-strand breaks and promotes assembly of repair proteins. Cell 131: 887–900.
49. Furuya K, Poitelea M, Guo L, Caspari T, Carr AM (2004) Chk1 activation requires Rad9 S/TQ-site phosphorylation to promote association with C-terminal BRCT domains of Rad4TOPBP1. Genes Dev 18: 1154–1164.
50. Puddu F, Granata M, Nola LD, Balestrini A, Piergiovanni G, et al. (2008) Phosphorylation of the budding yeast 9-1-1 complex is required for Dpb11 function in the full activation of the UV-induced DNA damage checkpoint. Mol Cell Biol 28: 4782–4793.
51. Liu S, Bekker-Jensen S, Mailand N, Lukas C, Bartek J, et al. (2006) Claspin operates downstream of TopBP1 to direct ATR signaling towards Chk1 activation. Mol Cell Biol 26: 6056–6064.
52. Walker J, Crowley P, Moreman AD, Barrett J (1993) Biochemical properties of cloned glutathione S-transferases from Schistosoma mansoni and Schistosoma japonicum. Mol Biochem Parasitol 61: 255–264.
53. Inouye C, Dhillon N, Thorner J (1997) Ste5 RING-H2 domain: role in Ste4-promoted oligomerization for yeast pheromone signaling. Science 278: 103–106.
54. Clackson T, Yang W, Rozamus LW, Hatada M, Amara JF, et al. (1998) Redesigning an FKBP-ligand interface to generate chemical dimerizers with novel specificity. Proc Natl Acad Sci U S A 95: 10437–10442.
55. Saka Y, Esashi F, Matsusaka T, Mochida S, Yanagida M (1997) Damage and replication checkpoint control in fission yeast is ensured by interactions of Crb2, a protein with BRCT motif, with Cut5 and Chk1. Genes Dev 11: 3387–3400.
56. Bishop AC, Ubersax JA, Petsch DT, Matheos DP, Gray NS, et al. (2000) A chemical switch for inhibitor-sensitive alleles of any protein kinase. Nature 407: 395–401.
57. Bonilla CY, Melo JA, Toczyski DP (2008) Colocalization of sensors is sufficient to activate the DNA damage checkpoint in the absence of damage. Mol Cell 30: 267–276.
58. Blankley RT, Lydall D (2004) A domain of Rad9 specifically required for activation of Chk1 in budding yeast. J Cell Sci 117: 601–608.
59. Smolka MB, Albuquerque CP, Chen SH, Schmidt KH, Wei XX, et al. (2005) Dynamic changes in protein-protein interaction and protein phosphorylation probed with amine-reactive isotope tag. Mol Cell Proteomics 4: 1358–1369.
60. Grenon M, Costelloe T, Jimeno S, O'shaughnessy A, Fitzgerald J, et al. (2007) Docking onto chromatin via the Saccharomyces cerevisiae Rad9 Tudor domain. Yeast 24: 105–119.
61. Pellicioli A, Foiani M (2005) Signal transduction: how rad53 kinase is activated. Curr Biol 15: R769–771.
62. Wysocki R, Javaheri A, Allard S, Sha F, Côté J, et al. (2005) Role of Dot1-dependent histone H3 methylation in G1 and S phase DNA damage checkpoint functions of Rad9. Mol Cell Biol 25: 8430–8443.
63. Ira G, Pellicioli A, Balijja A, Wang X, Fiorani S, et al. (2004) DNA end resection, homologous recombination and DNA damage checkpoint activation require CDK1. Nature 431: 1011–1017.
64. Aylon Y, Liefshitz B, Kupiec M (2004) The CDK regulates repair of double-strand breaks by homologous recombination during the cell cycle. EMBO J 23: 4868–4875.
65. Barlow JH, Lisby M, Rothstein R (2008) Differential regulation of the cellular response to DNA double-strand breaks in G1. Mol Cell 30: 73–85.
66. Branzei D, Foiani M (2008) Regulation of DNA repair throughout the cell cycle. Nat Rev Mol Cell Biol 9: 297–308.
67. Lazzaro F, Sapountzi V, Granata M, Pellicioli A, Vaze M, et al. (2008) Histone methyltransferase Dot1 and Rad9 inhibit single-stranded DNA accumulation at DSBs and uncapped telomeres. EMBO J 27: 1502–1512.
68. Navadgi-Patil VM, Burgers PM (2009) A tale of two tails: activation of DNA damage checkpoint kinase Mec1/ATR by the 9-1-1 clamp and by Dpb11/TopBP1. DNA Repair (Amst) 8: 996–1003.
69. Gyuris J, Golemis E, Chertkov H, Brent R (1993) Cdi1, a human G1 and S phase protein phosphatase that associates with Cdk2. Cell 75: 791–803.
70. Longtine MS, McKenzie A, Demarini DJ, Shah NG, Wach A, et al. (1998) Additional modules for versatile and economical PCR-based gene deletion and modification in Saccharomyces cerevisiae. Yeast 14: 953–961.
71. Storici F, Lewis LK, Resnick MA (2001) In vivo site-directed mutagenesis using oligonucleotides. Nat Biotechnol 19: 773–776.
72. Diani L, Colombelli C, Nachimuthu BT, Donnianni R, Plevani P, et al. (2009) Saccharomyces CDK1 phosphorylates Rad53 kinase in metaphase, influencing cellular morphogenesis. J Biol Chem 284: 32627–32634.
73. Goldstein AL, McCusker JH (1999) Three new dominant drug resistance cassettes for gene disruption in Saccharomyces cerevisiae. Yeast 15: 1541–1553.
74. Araki H, Leem SH, Phongdara A, Sugino A (1995) Dpb11, which interacts with DNA polymerase II(epsilon) in Saccharomyces cerevisiae, has a dual role in S-phase progression and at a cell cycle checkpoint. Proc Natl Acad Sci U S A 92: 11791–11795.
75. Muzi Falconi M, Piseri A, Ferrari M, Lucchini G, Plevani P, et al. (1993) De novo synthesis of budding yeast DNA polymerase alpha and POL1 transcription at the G1/S boundary are not required for entrance into S phase. Proc Natl Acad Sci U S A 90: 10519–10523.
76. Fiorani S, Mimun G, Caleca L, Piccini D, Pellicioli A (2008) Characterization of the activation domain of the Rad53 checkpoint kinase. Cell Cycle 7: 493–499.

# APPENDIX B: AUTHORS FUNDING AND CONTRIBUTIONS

## FUNDING

**Personal doctoral grant award** from the FCT (Fundação para a Ciência e a Tecnologia) of Portugal in 2008;

**Erasmus scholarship award** from the University of Minho, Portugal (European Commission funding) in 2007.

## ORAL PRESENTATIONS

**Selected for Oral Presentation in the Irish Radiation Research Society Scientific (IRRSS) Meeting 2009**, National University of Ireland, Galway Ireland, 16th-17th October 2009, "*Biochemical characterisation of Mec1, homologue of human ATR Kinase*"

**Selected for Oral Presentation in the 2nd EU – IP DNA Repair: Workshop for Young Scientists & Career Event**, Porto, Portugal, 23rd-27th June 2008, "*A novel regulation model for Saccharomyces cerevisiae Mec1, homologue of ATR Kinase*"

## SCIENTIFIC COMMUNICATIONS

Magda Granata*, Federico Lazzaro*, Daniele Novarina, Davide Panigada, Fabio Puddu, **Carla Manuela Abreu**, Ramesh Kumar, Muriel Grenon, Noel F. Lowndes, Paolo Plevani, Marco Muzi-Falconi (2010) *Dynamics of Rad9 Chromatin Binding and Checkpoint Function Are Mediated by Its Dimerization and Are Cell Cycle–Regulated by CDK1 Activity*, PLoS Genetics 6(8): e1001047. doi:10.1371/journal.pgen.1001047

Ramesh Kumar*, **Carla Manuela Abreu***, Karen Finn, Kevin Creavin, Muriel Grenon & Noel Francis Lowndes, *Phosphorylation of the DNA damage mediator Rad9 by cyclin-dependent kinases (CDKs) regulates activation of Checkpoint kinase 1 (Chk1)*, In preparation

## POSTER PRESENTATIONS

Genome Instability and Cancer, Biochemical Society Meeting, NUI Galway, Ireland, 4th December 2008
Stefano Maffini, Muriel Grenon, **Carla Abreu**, Noel Lowndes "*A novel regulation model for Saccharomyces cerevisiae Mec1, homologue of ATR Kinase"*;

British Yeast Group Meeting, NUI Maynooth, Ireland, 18th-20th March 2008
Stefano Maffini, Muriel Grenon, **Carla Abreu**, Noel Lowndes "*A novel regulation model for Saccharomyces cerevisiae Mec1, homologue of ATR Kinase"*;

Irish Fungal Meeting, NUI Galway, Ireland, 13rd June 2008
Stefano Maffini, Muriel Grenon, **Carla Abreu**, Noel Lowndes "*A novel regulation model for Saccharomyces cerevisiae Mec1, homologue of ATR Kinase"*;

Research Day of the National Centre for Biomedical Engineering Science (NCBS), NUI Galway, Ireland, 26th June 2008

Stefano Maffini, Muriel Grenon, **Carla Abreu**, Noel Lowndes "*A novel regulation model for Saccharomyces cerevisiae Mec1, homologue of ATR Kinase"*;

Irish Fungal Meeting, University College of Dublin, Ireland, 8th January 2009
Stefano Maffini, Muriel Grenon, **Carla Abreu**, Noel Lowndes "*A novel regulation model for Saccharomyces cerevisiae Mec1, homologue of ATR Kinase"*;
(and) Ramesh Kumar, Karen Finn, Mary Walsh, Aisling O'Shaugnessy, **Carla Abreu**, Noel Lowndes and Muriel Grenon, "*Budding yeast Rad9 is regulated by Cdc28-dependent phosphorylation*".

Irish Association for Cancer Research, Galway, Ireland, 3rd – 5th March 2010
**Carla M. Abreu**, Clara Nogues, Muriel Grenon, Noel F. Lowndes "*Structure-Function analysis os Saccharomyces cereviseae Mec1, homologue of human ATR Kinase*";
(*and*) Ramesh Kumar, Karen Finn, Mary Walsh, Aisling O'Shaugnessy, **Carla Abreu**, Noel Lowndes and Muriel Grenon, "*Budding yeast Rad9 is regulated by Cdc28-dependent phosphorylation*".

Irish Fungal Meeting, University College Cork, Ireland, 17-18th June, 2010
**Carla M. Abreu**, Clara Nogues, Muriel Grenon, Noel F. Lowndes "*Structure-Function analysis os Saccharomyces cereviseae Mec1, homologue of human ATR Kinase*";

British Yeast Group Meeting, Oxford, UK, 17-19th March, 2010
Ramesh Kumar, **Carla Abreu**, Kevin Creavin, Karen Finn, Aisling O'Shaugnessy, Noel F Lowndes and Muriel Grenon "*Budding yeast Rad9 is regulated by Cdc28 dependent phosphorylation: Multiple potential Cdk phosphorylation sites are required for Chk1 activation*".

Yeast Genetics and Molecular Biology Meeting, University of British Columbia, Vancouver, BC Canada, 27th July – 1st August 2010
Ramesh Kumar, **Carla Abreu**, Kevin Creavin, Karen Finn, Aisling O'Shaugnessy, Noel F Lowndes and Muriel Grenon "*Budding yeast Rad9 is regulated by Cdc28 dependent phosphorylation: Multiple potential Cdk phosphorylation sites are required for Chk1 activation*".

British Yeast Group Meeting, University of Sussex, Birmingham, UK, 23-25th March 2011
Ramesh Kumar, **Carla Abreu**, Kevin Creavin, Karen Finn, Aisling O'Shaugnessy, Noel F Lowndes and Muriel Grenon "*Budding yeast Rad9 is regulated by Cdc28 dependent phosphorylation: Multiple potential Cdk phosphorylation sites are required for Chk1 activation*".

Genome Stability Network Meeting: "Responses to DNA damage: from molecular mechanism to human disease", Egmond aan Zee, The Netherlands, 3rd – 8th April 2011
Ramesh Kumar, **Carla Abreu**, Kevin Creavin, Karen Finn, Aisling O'Shaugnessy, Noel F Lowndes and Muriel Grenon "*Budding yeast Rad9 is regulated by Cdc28 dependent phosphorylation: Multiple potential Cdk phosphorylation sites are required for Chk1 activation*".

# APPENDIX C: PROTOCOLS

## Transformation to delete/replace a specific number of HEAT repeats in *MEC1*

1. 1.5mls O/N culture → 50mls DropOut –LEU medium + 2% Galactose
2. 4hrs growing
3. 2x washes in dd$H_2O$
4. +250uls 1xLiAc-TE → 7-8 transformations
   eppendorf: 2ugs DNA + 300uls LiAc/TE/PEG50% + 50uls cells (1ml LiAc/TE/PEG50% = 100µls LiAc 1M + 100µls TE 10x + 800µls PEG50%)
5. 30' @ 30°C, 800rpm
6. 15' @ 42°C, 800rpm
7. spin 4' @ 5000rpm
8. + 100uls saline
9. plate 10% and 90% cells

| | |
|---|---|
| **CLONE** | |
| **DELETION** | |
| **CELL CONCENTRATION (cells/ml)** | |
| **TOTAL CELL NUMBER (in 50mls)** | |
| **CELL NUMBER/TRANSF.** | |

| **SRAINS** / **CONDITIONS** | YPD | **DNA FRAGMENT(S)** | **DATE** | **[DNA] (ng/ul)** | **DNA AMOUNT TRANSFORMED (uls/ngs)** |
|---|---|---|---|---|---|
| A | 1 | | | | |
| | 2 | | | | |
| B | 1 | | | | |
| | 2 | | | | |
| C | 1 | | | | |
| | 2 | | | | |
| C | 1 | | | | |
| | 2 | | | | |
| D | 1 | | | | |
| | 2 | | | | |

| | | | | | | | |
|---|---|---|---|---|---|---|---|
| **PLATED CELLS** | 10% | | | | | | |
| | 90% | | | | | | |
| **NO. COLONIES** | | **%** | **B** | **B** | **C** | **C** | **D** |
| | 1 | 10% | | | | | |
| | | 90% | | | | | |
| | 2 | 10% | | | | | |
| | | 90% | | | | | |

**SPAGHETTI OF CELLS (LIQUID NITROGEN YEAST EXTRACT PREPARATION)**

**A. Two days before:**

1. Make a fresh culture of the respective strain on a YPD plate.

**B. One day before:**

1. Make 150 ml of 200mM HEPES and then use it to make 250ml of 2x Native Lyses Buffer adding the rest of the reagents.
2. Fill up a sterile glass bottle of 250ml and store it in the cold room (-4ºC).

**2x Native Lysis Buffer (V=250 ml)**

| Reagents | Initial concentration (*stock*) | Volume to add | Final concentration |
|---|---|---|---|
| **HEPES (pH 7.5)*** | 200mM | 125ml | 100mM |
| **KCl** *(lab shelf)* | 1M | 75ml | 300mM |
| **Glycerol** *(lab shelf)* | 100% | 50ml | 20% |
| **EDTA** *(Karen)* | 500mM | 1ml | 2mM |
| **Tween20** *(lab shelf)* | 100% | 250µl | 0,1% |
| **NP-40** *(Karen)* | 100% | 250µl | 0,01% |
| **B-mercaptethanol** *(last to add - hote)* | 14mM | 155µl | 8mM |

***200mM HEPES (V=150 ml)**

| Reagents | Initial concentration (*stock*) | Amount | Final concentration |
|---|---|---|---|
| **HEPES (99,5% minimum titration)** *(lab shelf)* | 100% | 7,1493g | 100mM |
| **Milli-Q** *(lab shelf)* | 100% | 150ml | 20% |
| **KOH** *(lab shelf)* **(potassium hydroxide)** *(add at last single pills to correct the pH)* | 100% | 0,675g | 300mM |

3. Set up two cultures of the respective strain (2x5ml) into special tubes for 2DT at least.
4. Count the cells and watch them at the microscope to see if there is any contamination.
5. Set up a the big cultures O/N strain. Calculate the volume of the old culture needed to add to obtain $1x10^7$cells/ml in the morning, using the following formula:

$V_o$ = Volume to be added (ml)
$V_t$ = Volume of media (ml)
$C_t$ = $1x10^7$cells/ml
$C_o$ = Origin Concentration
$x$ = how long (hours)
$y$ = 1.45hrs (DT)

$$V_o = \frac{V_t \times C_t}{2^{x/y} \times C_o}$$

6. Reserve the big centrifuge for next morning.

**C. The day:** The protocol should be done as fast as you can.

1. Prepare all the material and solutions that are needed to do the protocol
   - Reserve the centrifuge for falcon tubes.
   - Centrifuge conical tubes
   - Weight an empty centrifuge tube. (without lid)
   - sterile $H_2O$ → Keep on ice
   - 2xLB → Keep on ice.
   - 20mls syringes, melt the tip of the syringes and put them inside of falcon tubes with some paper at the bottom of the tubes.
2. Count the cells (should be no more than ~1-2x$10^7$cells/ml)
3. Spin them down in the big yeast centrifuge for 5minutes at 2800rpm.
4. Discard the S/N and wash 2x with dd$H_2O$
5. Resuspend cells in 2xLB (no need for inhibitors) and tranfer into a serynge
6. Take a container of liquid $N_3$ *(down stairs)* and pour some of it into a clean ice boxes and into the labelled falcon tubes placed on dry ice.
7. Discard the S/N, cut tip of syringe and extrude cells into liquid $N_3$.
8. Store at -80C in the falcon tube pre-cooled.

## FLAG/MYC/HA-IP Example Protocol

**NOTES:**

- Eppendorf tubes used during experiment are low adhesion tubes
- Buffers are prepared fresh (or done within 1-2 weeks maximum) and are kept at 4C (B-Mercaptoethanol and inhibitors are added just before the respective step of the protocol)
- Experiment done on ice always and cold room when appropriate
- Loading tips are used to remove any extra buffer in the beads (but never touching them)

### 1. 1x LB Preparation:

8 mls

4000 uls 2xLB
3677.7 uls filtered MilliQ $H_2O$
160uls 100xPis (2xfinal)
160uls 50xPpis (1xfinal)
2.3uls B-mercaptoethanol

### 2. Beads Preparation:

**Per sample → 20uls beads$_{100\%}$ / 10mgs Protein**

| Antibody | Beads | |
|---|---|---|
| **MONOCLONAL** | **Protein G** | |
| ~~**POLYCLONAL**~~ | ~~**Protein A**~~ | |

**N.o of IPs:** 40uls beads$_{100\%}$/IP → 40 x 10 = 400uls

**BEADS STOCK:**

**100uls beads 80% ----------→ 80uls beads 100%**
**X ----------→ 400 uls**

**X = 400 x 100 / 80 = 500 uls**

Washes (3xfiltered MilliQH2O + 3x $_{1x}$LB)
(spins at 2000rpm for 30sec, cold table centrifuge, swing rotor, 4°C)

**+ 400 uls 1xLB**

### 3. Preparation of the Extracts for IP (Protein/IP = 10 mgs)

| G2-arrested untreated |
|---|
| **rad9Δ**<br>**Chk1-Flag**<br>**Dpb11-MYC** |

| | **13.08.12** |
|---|---|
| | |
| **[P] (mg/ml)** | 18.29 |
| $V_{aliquot}$ | 600 |
| **$V_{1xLB\ to\ add}$** | 497.4 |
| $V_T$ | 1097.4 |
| **$V_{to\ take\ for\ IP}$** | **1000** (10mgs) |

**CCE Sample preparation:**

- For IP gel: 60uls 1xLB + 10uls $CCE_{@10mg/ml}$ + 30uls 3xSB → dry ice → -80°C

4. **PRE-CLEARING:** Extracts + 40 uls 50% pre-washed beads → **rolling, 1hr @ 4°C**

5. **Spin at 2000rpm for 3min (cold table centrifuge, swing rotor, 4°C)**

6. **Ab BINDING**: Pre-cleared extracts + ab → **rolling, 2hrs @ 4°C**

**Ab amount/IP**

**MYC/FLAG ab: 1mg Protein ----------→ 2ugs ab** (abcam advised conditions and successfully tested)

**HA (12CA5) ab** (@ ± 2.5-3µg/µl)**: 10mg Protein/20µl $beads_{100\%}$ ----------→ 10ug ab** (successfully tested)

7. **Spin at 14000rpm for 10min (cold table centrifuge, fix rotor, 4°C) → change S/N to new tube containing pre-washed beads**

8. **+2xPis & +1xPpis** = 20uls $_{100x}$Pis + 20uls $_{50x}$Ppis

9. **IP:** Extract-Ab + pre-washed 40uls $_{50\%}$ beads → **rolling, 2hrs @ 4°C**

10. **Spin at 2000rpm for 3min (cold table centrifuge, swing rotor, 4°C)**

11. **4x washes with 1xLB (spin at 2000rpm for 1' each, cold table centrifuge, swing rotor, 4°C)**

**NOTE: first S/N = FT fraction** (Keep it and prepare to load on a gel as shown below)

**1x LB Preparation:**

34 mls
- 17 000 uls 2xLB
- 15630.3 uls filtered MilliQ $H_2O$
- 680 uls 100xPis (2xfinal)
- 680 uls 50xPpis (1xfinal)
- 9.7 uls B-mercaptoethanol

**FT Sample preparation:** 10uls 3x Sample Buffer + 20uls FT → dry ice → -80°C

**Washes Sample preparation:** 10uls 3x Sample Buffer + 20uls washes → dry ice → -80°C

**NOTE**: in last wash remove most of the S/N carefully with loading tips (but without touching beads)

## 12. Preparation of the extracts for western blot

**IP Sample preparation:** 20uls beads + 37uls 3x Sample Buffer → dry ice → -80°C

**13. Western blot:** take samples direct from dry ice and boil them at 95C for 5min. Give a quick spin (10000rpm for 12sec) and load the proper amount.

| LOADING | 6.5% gel (Rad9 gel, 1mm) |
|---|---|
| **CCE** | 27 uls |
| **FT** | 27 , uls |
| **IP** | **40 uls** |

Run conditions:

- Running Buffer: 1xTG+0.1%SDS

Transfer conditions:

- Transfer Buffer: 1xTG+0.01%SDS
- 70V for 1h50'

Antibodies conditions for WB:

- FLAG/MYC WB:
  - 1h blocking in 5% milk – 1xPBS-0.01%Tween, RT
  - 1:1000 M2 FLAG ab in 1% milk – 1xPBS-0.01%Tween, O/N, 4C
  - 3x 5' washes in 1xPSD-0.01%Tween, RT

  - 1:5000 anti-mouse secondary antibody in 1xPBS-0.01%Tween, 1h, RT
  - 3x 5’ washes in 1xPSD-0.01%Tween, RT
  - ECL for 3’
  - Expose

- HA WB:
  - 10’ blocking in 1% milk – 1xPBS-0.01%Tween, RT
  - 1:1000 12CA5 ab in 1% milk – 1xPBS-0.01%Tween, O/N, 4C
  - 3x 5’ washes in 1xPSD-0.01%Tween, RT
  - 1:5000 anti-mouse secondary antibody in 1xPBS-0.01%Tween, 1h, RT
  - 3x 5’ washes in 1xPSD-0.01%Tween, RT
  - ECL for 3’
  - Expose

## FLAG-IP and Phosphatase assay Example Protocol

**NOTES:**

- Eppendorf tubes used during experiment are low adhesion tubes
- Buffers are prepared fresh (or done within 1-2 weeks maximum) and are kept at 4C (B-Mercaptoethanol and inhibitors are added just before the respective step of the protocol)
- Experiment done on ice always and cold room when appropriate
- Loading tips are used to remove any extra buffer in the beads (but never touching them)

### 14. 1x LB Preparation:

7 mls

3500 uls 2xLB
3218 uls filtered MilliQ $H_2O$
140uls 100xPis (2xfinal)
140uls 50xPpis (1xfinal)
2uls B-mercaptoethanol

### 15. Beads Preparation:

**Per sample → 20uls beads$_{100\%}$ / 10mgs Protein**

| Antibody | Beads | |
|---|---|---|
| **MONOCLONAL** | **Protein G** | |
| ~~**POLYCLONAL**~~ | ~~**Protein A**~~ | |

**N.o of IPs:** 10uls beads$_{100\%}$/IP → 10x2 x 8 = 160uls

**BEADS STOCK:**

**100uls beads 80% ----------→ 80uls beads 100%**
**X ----------→ 160 uls**

**X = 360 x 100 / 80 = 200 uls**

Washes (3xfiltered MilliQH2O + 3x $_{1x}$LB)
(spins at 2000rpm for 30sec, cold table centrifuge, swing rotor, 4°C)
**+ 200 uls 1xLB**

### 16. Preparation of the Extracts for IP (Protein/IP = 10 mgs)

| | **WT Chk1-Flag Dpb11-Myc untreated** | **WT Chk1-Flag Dpb11-Myc ++Bleocin** |
|---|---|---|

| | **_02.02.11 (2x)** | **(20g/ml) _02.02.11 (2x)** |
|---|---|---|
| FLAG ab (M2) | **Mock/λPhosp/λ Phosp+Ppis** | **Mock/λPhosp/λP hosp+Ppis** |
| **[P] (mg/ml)** | 25.24 | 22.05 |
| $V_{aliquot}$ | 450 | 530 |
| **$V_{1xLB\ to\ add}$** | 685.8 | 638.65 |
| $V_T$ | 1135.8 | 1168.65 |
| **$V_{to\ take\ for\ IP}$** | **500** (5mgs) | **500** (5mgs) |

**CCE Sample preparation:**

- For IP gel: 60uls 1xLB + 10uls $CCE_{@10mg/ml}$ + 30uls 3xSB → dry ice → -80°C

17. **PRE-CLEARING:** Extracts + 40 uls 50% pre-washed beads → **rolling, 1hr @ 4°C**

18. **Spin at 2000rpm for 3min (cold table centrifuge, swing rotor, 4°C)**

19. **Ab BINDING**: Pre-cleared extracts + ab → **rolling, 2hrs @ 4°C**

**Per sample → 1mg Protein ----------→ 2ugs ab (M2 FLAG ab -**
abcam advised conditions and successfully tested)

20. **Spin at 14000rpm for 10min (cold table centrifuge, fix rotor, 4°C) → change S/N to new tube containing pre-washed beads**

21. **+2xPis** = 20uls $_{100x}$Pis

22. **IP:** Extract-Ab + pre-washed 40uls $_{50\%}$ beads → **rolling, 2hrs @ 4°C**

23. **Spin at 2000rpm for 3min (cold table centrifuge, swing rotor, 4°C)**

24. **4x washes with 1xLB without Ppis (spin at 2000rpm for 1' each, cold table centrifuge, swing rotor, 4°C)**

**NOTE: first S/N = FT fraction** (Keep it and prepare to load on a gel as shown below)

**1x LB Preparation:**

26 mls | 13 000 uls 2xLB
12 472.6 uls filtered MilliQ $H_2O$
520 uls 100xPis (2xfinal)
7.4 uls B-mercaptoethanol

**FT Sample preparation:** 10uls 3x Sample Buffer + 20uls FT → dry ice → -80°C

**Washes Sample preparation:** 10uls 3x Sample Buffer + 20uls washes → dry ice → -80°C

**NOTE**: in last wash remove most of the S/N carefully with loading tips (but without touching beads)

**25. Dry beads with loading tip and resuspend in**

| 1 Reaction | | Phosphatase / Inhibitor (µls) | | |
|---|---|---|---|---|
| REAGENTS | FINAL CONC./AMOUNT | Mock | λPhosp | λPhosp+Ppis |
| $QH_2O$ | Up to 20µls | 36 | 34 | 31 |
| 10xBuffer | 1x | 7 | 7 | 7 |
| 10mM $MnCl_2$ | 2 mM | 7 | 7 | 7 |
| | Prepare mixture above and add to beads | | | |
| Beads | 5 mgs protein | 20 | 20 | 20 |
| 50x Ppis | 1x | --- | --- | 3 |
| Lambda Phospatase | 0.2U/µg | --- | 2.5 | 2.5 |
| Total volume | --- | 70 µls | | |

**26. Incubate beads at 30$^{O}$C for 30 minutes using a heating block (mix occasionally)**

**27. Spin beads at 2000rpm for 3' and Remove the S/N with loading tip and transfer it into a new tube.**

**NOTE: DO NOT DRY the beads until the end. Avoid touching the beads with the tip, leaving ~25% of S/N behind. Then, with new loading tip remove the left S/N and discard it.**

28. **Spin the kept S/N at 2000rpm for 5' and transfer again the S/N with loading tip into a new tube to remove any contaminating beads. Add 15µls of 3xSB → dry ice**

29. **Add 20uls of 3xSB to the beads → Dry ice**

30. **Western blot:** take samples direct from dry ice and boil them at 95C for 5min. Give a quick spin (10000rpm for 12sec) and load the proper amount.

## Phosphatase treatment Example Protocol

1. Preparation of the reactions

| 1 Reaction | | Phosphatase / Inhibitor (µls) | | |
|---|---|---|---|---|
| **REAGENTS** | **FINAL CONC./AMOUNT** | **- / -** ($4^{o}$C or mock) | **+ / -** | **+ / +** |
| **$QH_2O$** | Up to 20µls | 2 | 1.8 | --- |
| **10xBuffer** | 1x | 2 | 2 | 2 |
| **10mM $MnCl_2$** | 2 mM | 4 | 4 | 4 |
| **WCE (@1mg/ml)** | 10ug (total protein) | 10 | 10 | 10 |
| **10mM Na Vanadate** | 2.5 mM | --- | --- | 5 |
| **Lambda Phospatase** | 80 Units | --- | 0.2 | 0.2 |

2. Incubate @ 30°C for 20min

3. Stop reaction adding 20µls 2x Sample buffer (or 10µls 4xSB)

4. Freeze on dry ice → -80°C

**MYC-IP and Release assay Example Protocol**

**NOTES:**

- Eppendorf tubes used during experiment are low adhesion tubes
- Buffers are prepared fresh (or done within 1-2 weeks maximum) and are kept at 4C (B-Mercaptoethanol and inhibitors are added just before the respective step of the protocol)
- Experiment done on ice always and cold room when appropriate
- Loading tips are used to remove any extra buffer in the beads (but never touching them)

**31.1x LB Preparation:**

7 mls
- 3500 uls 2xLB
- 3218 uls filtered MilliQ $H_2O$
- 140uls 100xPis (2xfinal)
- 140uls 50xPpis (1xfinal)
- 2uls B-mercaptoethanol

**32.Beads Preparation:**

**Per sample → 20uls beads$_{100\%}$ / 10mgs Protein**

| Antibody | Beads | |
|---|---|---|
| **MONOCLONAL** | **Protein G** | |
| ~~**POLYCLONAL**~~ | ~~**Protein A**~~ | |

**N.o of IPs:** 20uls beads$_{100\%}$/FlagIP (10mgsProtein) → (20x2) x 5 = 200uls **G BEADS**

**BEADS STOCK:**

**100uls beads 80% ----------→ 80uls beads 100%**
**X ----------→ 200 uls**

**X = 360 x 100 / 80 = 250 uls**

Washes (3xfiltered MilliQH2O + 3x $_{1x}$LB)
(spins at 2000rpm for 30sec, cold table centrifuge, swing rotor, 4°C)

**+ 200 uls 1xLB**

**33. Preparation of the Extracts for IP (Protein/IP = 10 mgs)**

| | **WT**<br>**Rad9-9Myc Chk1-3Flag**<br>**++Bleocin (20g/ml)**<br>**_27.04.11 (x3)** |
|---|---|
| MYC ab (ab56) | **Mock+ATP+γSATP** |
| **[P] (mg/ml)** | 18.75 |
| $V_{aliquot}$ | 590 |
| $V_{1xLB\ to\ add}$ | 516.25 |
| $V_T$ | 1106.25 |
| $V_{to\ take\ for\ IP}$ | **1000**<br>(10mgs) |

**CCE Sample preparation:**

- For IP gel: 60uls 1xLB + 10uls $CCE_{@10mg/ml}$ + 30uls 3xSB → dry ice → -80°C

**34. PRE-CLEARING:** Extracts + 40 uls 50% pre-washed beads → **rolling, 1hr @ 4°C**

**35. Spin at 2000rpm for 3min (cold table centrifuge, swing rotor, 4°C)**

36. **Ab BINDING**: Pre-cleared extracts + ab → **rolling, 2hrs @ 4°C**

- **FLAG IP: Ab amount/IP ( ab56 (anti- MYC ab))**

**Per sample → 1mg Protein ----------→ 2ugs ab** (abcam advised conditions and successfully tested)

**37. Spin at 14000rpm for 10min (cold table centrifuge, fix rotor, 4°C) → change S/N to new tube containing pre-washed beads**

38. **+2xPis & +1xPpis** = 20uls $_{100x}$Pis + 20uls $_{50xP}$pis

39. **IP:** Extract-Ab + pre-washed 40uls $_{50\%}$ beads → **rolling, 2hrs @ 4°C**

**40. 3x washes with 1xLB (spin at 2000rpm for 1' each, cold table centrifuge, swing rotor, 4°C)**
**NOTE: first S/N = FT fraction** (Keep it and prepare to load on a gel as shown below)

**1x LB Preparation:**

14 mls
- 7 000 uls 2xLB
- 6436 uls filtered MilliQ $H_2O$
- 280 uls 100xPis (2xfinal)
- 280 uls 50xPpis (1xfinal)
- 4 uls B-mercaptoethanol

**FT Sample preparation:** 10uls 3x Sample Buffer + 20uls FT → dry ice → -80°C

**Washes Sample preparation:** 10uls 3x Sample Buffer + 20uls washes → dry ice → -80°C

**NOTE**: in last wash remove most of the S/N carefully with loading tips (but without touching beads)

**41. Spin at 2000rpm for 3min (cold table centrifuge, swing rotor, 4°C)**

**42. 2x washes with 500µls of 1xKinase buffer**

| REAGENTS | STOCK CONCENTRATION | FINAL CONCENTRATION | FINAL VOLUME 5mls |
|---|---|---|---|
| Milli Q $H_2O$ | --- | --- | µls |
| HEPES (pH7.5) | 200 mM | 25 mM | 625 µls |
| EGTA | 50 mM | 5 mM | 500 µls |
| $MgCl_2$ | 500 mM | 15 mM | 150 µls |
| KAc | 500 mM | 15 mM | 150 µls |
| ATP / γS-ATP | 10 mM | 1 mM | ---- |
| Protease inhibitors | 100x | 1x | 50 µls |
| Phosphatase inhibitors | 50x | 0.5x | 50 µls |

**43. Dry beads with loading tip (don't touch them) and resuspend with 60uls of 1xKinaseBuffer without ATP/ with ATP / or with γS-ATP, respectively**

| | | | MOCK | + ATP | + γS-ATP |
|---|---|---|---|---|---|
| REAGENTS | STOCK CONCENTRATION | FINAL CONCENTRATION | FINAL VOLUME 100µls | FINAL VOLUME 100µls | FINAL VOLUME 100µls |
| Milli Q $H_2O$ | --- | --- | 68.5 µls | 58.5 µls | 58.5 µls |
| HEPES (pH7.5) | 200 mM | 25 mM | 12.5 µls | 12.5 µls | 12.5 µls |
| EGTA | 50 mM | 5 mM | 10 µls | 10 µls | 10 µls |
| $MgCl_2$ | 500 mM | 15 mM | 3 µls | 3 µls | 3 µls |

| | | | | | |
|---|---|---|---|---|---|
| **KAc** | 500 mM | 15 mM | **3 µls** | **3 µls** | **3 µls** |
| **ATP / γS-ATP** | 10 mM | 1 mM | **----** | **10 µls ATP** | **10 µls γS-ATP** |
| **Protease inhibitors** | 100x | 1x | **1 µls** | **1 µls** | **1 µls** |
| **Phosphatase inhibitors** | 50x | 1x | **2 µls** | **2 µls** | **2 µls** |

**44. Incubate beads at 25$^{O}$C for 30 minutes using a heating block (mix occasionally)**

**45. Spin beads at 2000rpm for 3' and Remove the S/N with loading tip and transfer it into a new tube (~55µls).**

**NOTE: DO NOT DRY the beads until the end. Avoid touching the beads with the tip, leaving ~25% of S/N behind. Then, with new loading tip remove the left S/N and discard it.**

**46. Spin the kept S/N at 2000rpm for 5' and transfer again the S/N with loading tip (~50µls) into a new tube to remove any contaminating beads. Add 15µls of 3xSB → dry ice**

**47. Add to the dried beads 40uls of 3xSB → dry ice → -80$^{0}$C**

48. **Western blot:** take samples direct from dry ice and boil them at 95C for 5min. Give a quick spin (10000rpm for 12sec) and load the proper amount.

**PullDown of semi-purified Chk1 with CDK6/7 peptides**
**Example Protocol**

**NOTES:**

- Eppendorf tubes used during experiment are low adhesion tubes
- Buffers are prepared fresh (or done within 1-2 weeks maximum) and are kept at 4C (B-Mercaptoethanol and inhibitors are added just before the respective step of the protocol)
- Experiment done on ice always and cold room when appropriate
- Loading tips are used to remove any extra buffer in the beads (but never touching them)

**49.1x LB Preparation:**

| | |
|---|---|
| 10 mls | 5000 uls 2xLB<br>3677.7 uls filtered MilliQ $H_2O$<br>200uls 100xPis (2xfinal)<br>200uls 50xPpis (1xfinal)<br>2.3uls B-mercaptoethanol |

**50.Beads Preparation:**

**Per sample → 50uls beads$_{100\%}$ / 20mgs Protein**

| Antibody | Beads | |
|---|---|---|
| **MONOCLONAL** | **Protein G** | |
| ~~**POLYCLONAL**~~ | ~~**Protein A**~~ | |

**N.o of IPs:** 50uls beads$_{100\%}$/IP → 50 x 6 = 300uls

**BEADS STOCK:**

**Protein G beads (80% slurry):**

**100uls beads 80% ----------→ 80uls beads 100%**
**X ----------→ 300 uls**

**X = 300 x 100 / 80 = 375 uls**

Washes (3xfiltered MilliQH2O + 3x $_{1x}$LB)
(spins at 2000rpm for 30sec, cold table centrifuge, swing rotor, 4°C)

**+ 300 uls 1xLB**

**M2 FLAG-affinity gel (50% slurry):**

**100uls beads 80% ----------→ 50uls beads 100%**
**X ----------→ 300 uls**

**X = 300 x 100 / 50 = 600 uls**

Washes (3xfiltered MilliQH2O + 3x $_{1x}$LB)
(spins at 2000rpm for 30sec, cold table centrifuge, swing rotor, 4°C)

**+ 300 uls 1xLB**

## 51. Preparation of the Extracts for IP (Protein/IP = 15 mgs)

| | **G2-arrested untreated** |
|---|---|
| | **rad9Δ Chk1-Flag Dpb11-MYC 28.08.12** |
| | **=6tubes** |
| **[P] (mg/ml)** | 20.28 |
| $V_{aliquot}$ | 540 + 270 = 810 |
| $V_T$ | 1095.12 |
| **$V_{to\ take\ for\ IP}$** | **1000** (20mgs) |

**CCE Sample preparation:**

- 60uls 1xLB + 10uls CCE$_{@10mg/ml}$ + 30uls 3xSB → dry ice → -80°C

**52. <u>PRE-CLEARING</u>:** Extracts + 100 uls 50% pre-washed beads → **rolling, 1hr @ 4°C**

**53. Spin at 2000rpm for 3min (cold table centrifuge, swing rotor, 4°C)**

54. **<u>FlagM2-beads BINDING</u>**: Pre-cleared extracts + 100µls pre-washed FlagM2-beads$_{50\%}$ slurry → **rolling, 2hrs @ 4°C**

**55. Spin at 2000rpm for 3min (cold table centrifuge, swing rotor, 4°C)**

**56. 4x washes with 1xLB**
**NOTE: first S/N = FT fraction** (Keep it and prepare to load on a gel as shown below)

**1x LB (no Ppis) Preparation:**

22 mls
- 11 000 uls 2xLB
- 10553.7 uls filtered MilliQ $H_2O$
- 440 uls 100xPis (2xfinal)
- 6.3 uls B-mercaptoethanol

**FT Sample preparation:** 60µls 1xLB+ 10µls FT + 30µls 4x Sample Buffer → dry ice → -80°C

**NOTE**: in last wash remove most of the S/N carefully with loading tips (but without touching beads)

**57.** Resuspend beads with 100µls 1xLB and add 6µls of 3xFLAG peptide (±1:20 dilution) → **rolling, 1hr @ 4°C**

58. Spin @ 2000rpm for 3'

59. Take S/N into new tube (=eluted Chk1±100µls) (add 40µls of 4xSB to dryed beads → load 1µl in gel) → Pull all elutions into a new tube → centrifuge again at 2rpm for 2' → change elution into another new tube (to remove contaminating beads)

NOTE: Keep a bit of Chk1 elution to load on a gel (1µl of elution + 69µls 1xLB + 30µls 4xSB → load 4.8µls)

60. Incubate purified Chk1 (±100µls of elution) with 80µls Peptide-Beads (prepared previously) → **rolling, 2hrs @ 4°C**

61. Spin pulldown samples (2000rpm for 3') and take S/N (=FT2)

**FT2 Sample preparation:**

69uls 1xLB + 1uls FT2 + 30uls 3xSB → dry ice → -80°C → load 4.8 µls

**62. 4x washes with 1xLB (use the magnetic rack to concentrate beads in tube wall)**

**1x LB (no Ppis) Preparation:**

22 mls
- 11 000 uls 2xLB
- 10553.7 uls filtered MilliQ $H_2O$
- 440 uls 100xPis (2xfinal)
- 6.3 uls B-mercaptoethanol

## 63. Preparation of the extracts for western blot

- Add 40 uls 4x Sample Buffer to the 80 uls of beads → load 3µls onto 20% gel (peptide) and the rest onto 6.5% gel (Rad9 gel to see Chk1)

**64. Western blot:** take samples direct from dry ice and boil them at 95C for 5min. Give a quick spin (10000rpm for 12sec) and load the proper amount.

| LOADING | 6.5% gel (Rad9 gel, 1mm) |
|---|---|
| **CCE** | 6 uls |
| **FT1** | 6 , uls |
| **FT2** | 4.8 µls |
| **Elution** | 4.8µls |
| **Beads from elution** | 1µl |
| **Pulldown samples** | **3 µls (peptides) /40 uls (Chk1)** |

Run conditions:

- Running Buffer: 1xTG+0.1%SDS

Transfer conditions:

- Transfer Buffer: 1xTG+0.01%SDS
- 70V for 1h50'

Antibodies conditions for WB:

- FLAG WB (Chk1):
  - 1h blocking in 5% milk – 1xPBS-0.01%Tween, RT
  - 1:1000 M2 FLAG ab in 1% milk – 1xPSD-0.01%Tween, O/N, 4C
  - 3x 5' washes in 1xPSD-0.01%Tween, RT
  - 1:5000 anti-mouse secondary antibody in 1xPBS-0.01%Tween, 1h, RT
  - 3x 5' washes in 1xPSD-0.01%Tween, RT
  - ECL for 3'
  - Expose

- Streptadivin WB (peptides):
  - 20min blocking in 5% BSA-1xTBS-0.01%Tween
  - 1:1000 Streptadivin-HRP ab (R&D systems) in 1% BSA-1xTBS-0.01%Tween, 1hr, RT (put foil covering because is light sensitive)
  - 3x 5' washes in 1xPSD-0.01%Tween, RT
  - ECL for 3'
  - Expose

## Clb3/Cdc28 100% KINASE REACTION

(turn on the 95°C incubator in the hot room before starting)

1. Prepare **20x Kinase buffer**:

| | Stock | Final | 20x (5mls) |
|---|---|---|---|
| **HEPES pH 7.4** | powder | 1M | 1.1915g |
| **$MgCl_2$** | 1M | 100mM | 500 µls |
| **NaCl** | powder | 1.8/3M | 0.526/0.877g |

2. Prepare **Pre-incubation mixture**:

**+ ATP**

| REACTION | STOCK | FINAL | 1X REACTION (20 µls) |
|---|---|---|---|
| **$QH_2O$ (high H1/high CAD/low H1/low CAD)** | | | 5.8/3.7/13.5/11.4 |
| **Substrate: H1 / $CAD^{WT}$** | 1 / 0.44 $_{mg/ml}$ | 2µM | 0.9 µl $^{H1}$ / 3 µls |
| **Kinase Buffer** | 20x | 1x | 1 µl |
| **BSA** | 5 mg/ml | 0.2 mg/ml | 0.8 µl |
| **Cks1** | 35.7 ng/µl | 500 nM | 1 µls of 1:2.5 |
| **Clb3** | 0.14 ng/µl | 2.4nM (0.08ng/µl) | 8 / 0.3 µls |
| **Cold ATP** | 20mM | 0.5mM | 0.5 µl |
| γ-32P-ATP | 10µCi/µl | 0.5 µCi/µl | 2µls of 1:20 |

3. Prepare eppendorf tubes with substrates for each reaction

4. Prepare master Pre-incubation mixture in another tube

| REACTION | STOCK | FINAL | 1X REACTION (+ATP) 20µls tube 1/2/3/4 |
|---|---|---|---|
| **H2O** | | | 5.8/3.7/13.5/11.4 |
| **Kinase Buffer+ coldATP** | 20x | 1x | 1 µl |
| **BSA** | 5 mg/ml | 0.2 mg/ml | 0.8 µl |
| **Cks1** | 35.7 ng/µl | 500 nM | 1 µls of 1:2.5 |
| **Clb3** | 0.14 ng/µl | 2.4nM (0.08ng/µl) | 8/8/0.3/0.3 µls |
| **Cold ATP** | 20mM | 0.5mM | 0.5 µl |
| **Total** | | | 17.1/15/17.1/15 |

HOT room…

5. Dilute 1:20 **γ-$^{32}$P-ATP** stock (need 8 µls → do 12 µls)

- **11.4 µls $QH_2O$ + 0.6 µl of γ-$^{32}$P-ATP stock** → mix
- add **2µls** of dilution in each +ATP tubes (x4)

6. Add substrate: 0.9/3/0.9/3 µls → start timer/reaction (at RT)

7. Take 10 µls from tubes 3 and 4 at 8' incubation and Take 10 µls from tubes 1 and 2 at 30' incubation transfer to a new tube containing 5µls of 4xSB to stop the reaction
8. Take tubes 3 and 4 at 16' incubation tubes 1 and 2 at 60' and add 5µls 4xSB to stop the reaction
9. Boil 5' at 95°C.

10. Load everything (14µls in case of no ATP reactions) on a 12% SDS-PAGE gel for 1h30' (don't let the radioactivity run off from the gel)

11. Cut the end of the gels with radioactivity and discard

12. Stain with Coomassie blue for 30-45min

13. Destain until gel is transparent and bands are visible.

14. Air dry in the frame under the hood.

## Cyclin/Cdc28 KINASE REACTION: 10% phosphorylation of substrates

(turn on the 95°C incubator in the hot room before starting)

1. Prepare **20x Kinase buffer**:

| | Stock | Final | 20x (5mls) |
|---|---|---|---|
| **HEPES pH 7.4** | powder | 1M | 1.1915g |
| **$MgCl_2$** | 1M | 100mM | 500 µls |
| **NaCl** | powder | 3M | 0.877g |

2. Prepare **Pre-incubation mixture**:

**+ ATP**

| REACTION | STOCK | FINAL | 1X REACTION (20 µls) |
|---|---|---|---|
| **$QH_2O$ (H1/ CAD)** | | | H1: 13.42/12.4/12.1/12.9<br>CAD:<br>11.35/10.5/10.1/10.9 |
| **Substrate: H1 / $CAD^{WT}$** | 1 / 0.44 mg/ml | 2µM | 0.9 µl H1 / 3 µls |
| **Kinase Buffer** | 20x | 1x | 1 µl |
| **BSA** | 5 mg/ml | 0.2 mg/ml | 0.8 µl |
| **Cks1** | 35.7 ng/µl | 500 nM | 1 µls of 1:2.5 |
| **Cln2/Clb5/Clb3/Clb2** | 0.5/0.14/1.1*/0.21 ng/µl<br>*NOTE: dilute 10x | (8.625ng/ml) | H1:<br>0.38/1.4/1.7*/0.9µls<br>CAD:<br>0.35/1.2/1.6*/0.8µls<br>*from 1:10 dilution |
| **Cold ATP** | 20mM | 0.5mM | 0.5 µl |
| γ-32P-ATP | 10µCi/µl | 0.5 µCi/µl | 2µls of 1:20 |

3. Prepare eppendorf tubes with $H_2O$+enzymes for each reaction

| REACTION | STOCK | FINAL | 1X REACTION (20 µls) |
|---|---|---|---|
| **$QH_2O$ (H1/ CAD)** | | | H1: 13.42/12.4/12.1/12.9<br>CAD:<br>11.35/10.5/10.1/10.9 |
| **Cln2/Clb5/Clb3/Clb2** | 0.5/0.14/1.1*/0.21 ng/µl<br>*NOTE: dilute 10x | (8.625ng/ml) | H1:<br>0.38/1.4/1.7*/0.9µls<br>CAD:<br>0.35/1.2/1.6*/0.8µls<br>*from 1:10 dilution |

4. Prepare 2 master Pre-incubation mixtures in two other tubes (one for H1 and other for CAD)

| REACTION | STOCK | FINAL | 5X REACTION (+ATP) 20µls tube 1/2/3/4 | |
|---|---|---|---|---|
| **Kinase Buffer** | 20x | 1x | 5 µl | |
| **BSA** | 5 mg/ml | 0.2 mg/ml | 4 µl | |
| **Cks1** | 35.7 ng/µl | 500 nM | 5 µls of 1:2.5 | |
| **H1/CAD** | 1 / 0.44 mg/ml | 2µM | 4.5/15 µls | |
| **Cold ATP** | 20mM | 0.5mM | 2.5 µl | |
| γ-$^{32}$P-ATP | | | 10 µl | HOT ROOM* |
| **Total** | | | 31/41.5 µls **Divide $6.2^{H1}$/$8.3^{CAD}$ µls by 4 tubes** (with H2O+enzyme) | |

HOT room*…

5. Dilute 1:20 **γ-$^{32}$P-ATP** stock (need 20 µls → do 26 µls)

- **24.7 µls $QH_2O$ + 1.3 µl of γ-$^{32}$P-ATP stock** → mix
- add **10µls** of dilution in H1/CAD master mix tubes (x2)

6. Add H1/CAD mastermixes to enzyme tubes (as indicated in tables) → start timer/reaction (at RT)

7. Take 10 µls from tubes at 8'incubation and transfer to a new tube containing 5µls of 4xSB to stop the reaction
8. At 16' incubation add 5µls of 4xSB to the remaining reaction in tubes
9. Boil 5' at 95°C.

10. Load everything (14µls reactions) on a 12% SDS-PAGE gel for 1h30' (don't let the radioactivity run off from the gel)

11. Cut the end of the gels with radioactivity and discard

12. Stain with Coomassie blue for 30-45min

13. Destain until gel is transparent and bands are visible.

14. Air dry in the frame under the hood.

**Adjusted final Cyclin/Cdc28 KINASE REACTION**
(turn on the 95°C incubator in the hot room before starting)

1. Prepare **20x Kinase buffer**:

| | Stock | Final | 20x (5mls) |
|---|---|---|---|
| **HEPES pH 7.4** | powder | 1M | 1.1915g |
| **$MgCl_2$** | 1M | 100mM | 500 µls |
| **NaCl** | powder | 3M | 0.877g |

2. Prepare **Pre-incubation mixture**:

**+ ATP**

| REACTION | STOCK | FINAL | 1X REACTION (20 µls) |
|---|---|---|---|
| **$QH_2O$ (H1/ CAD)** | | | H1: 11.3/12.73/11.6/11.44<br>CAD:<br>9.2/10.63/9.5/9.34 |
| **Substrate: H1 / $CAD^{WT}$** | 1 / 0.44 mg/ml | 2µM | 0.9 µl $^{H1}$ / 3 µls |
| **Kinase Buffer** | 20x | 1x | 1 µl |
| **BSA** | 5 mg/ml | 0.2 mg/ml | 0.8 µl |
| **Cks1** | 35.7 ng/µl | 500 nM | 1 µls of 1:2.5 |
| **Cln2/Clb5/Clb3/Clb2** | 0.5/0.14/1.1/0.21 ng/µl | | H1/CAD:<br>2*/0.57/1.7*/1.86µls<br>*from 1:10 dilution |
| **Cold ATP** | 10mM | 0.5mM | 1 µl |
| γ-32P-ATP | 10µCi/µl | 0.5 µCi/µl | 2µls of 1:20 |

3. Prepare eppendorf tubes with $H_2O$+enzymes for each reaction

| REACTION | STOCK | FINAL | 1X REACTION (20 µls) |
|---|---|---|---|
| **$QH_2O$ (H1/ CAD)** | | | H1: 11.3/12.73/11.6/11.44<br>CAD:<br>9.2/10.63/9.5/9.34 |
| **Cln2/Clb5/Clb3/Clb2** | 0.5/0.14/1.1*/0.21 ng/µl<br>*NOTE: dilute 10x | | H1/CAD:<br>2*/0.57/1.7*/1.86µls<br>*from 1:10 dilution |

4. Prepare 2 master Pre-incubation mixtures in two other tubes (one for H1 and other for CAD)

| REACTION | STOCK | FINAL | 5X REACTION (+ATP) 20µls tube 1and2 | |
|---|---|---|---|---|

| | | | | |
|---|---|---|---|---|
| **Kinase Buffer** | 20x | 1x | 5 µl | |
| **BSA** | 5 mg/ml | 0.2 mg/ml | 4 µl | |
| **Cks1** | 35.7 ng/µl | 500 nM | 5 µls of 1:2.5 | |
| **H1/CAD** | 1 / 0.44 mg/ml | 2µM | 4.5/15 µls | |
| **Cold ATP** | 10mM | 0.5mM | 5 µl | |
| γ-$^{32}$P-ATP | | | 10 µl | HOT ROOM* |
| **Total** | | | 33.5/44 µls **Divide $6.7^{H1}/8.8^{CAD}$ µls by 4 tubes** (with H2O+enzyme) | |

HOT room*…

5. Dilute 1:20 **γ-$^{32}$P-ATP** stock (need 20 µls → do 26 µls)

- **24.7 µls $QH_2O$ + 1.3 µl of γ-$^{32}$P-ATP stock** → mix
- add **10µls** of dilution in H1/CAD master mix tubes (x2)

6. Add H1/CAD mastermixes to enzyme tubes (as indicated in tables) → start timer/reaction (at RT)

7. Take 10 µls from tubes at 8'incubation and transfer to a new tube containing 5µls of 4xSB to stop the reaction
8. At 16' incubation add 5µls of 4xSB to the remaining reaction in tubes
9. Boil 5' at 95°C.

10. Load everything (14µls reactions) on a 12% SDS-PAGE gel for 1h30' (don't let the radioactivity run off from the gel)

11. Cut the end of the gels with radioactivity and discard

12. Stain with Coomassie blue for 30-45min

13. Destain until gel is transparent and bands are visible.

14. Air dry in the frame under the hood.